

Vol. 10 No. 3 December 2023



Jurnal Farmasi dan Ilmu Kefarmasian Indonesia

E-ISSN: 2580-8303

P-ISSN: 2406-9388



PUBLISHED BY:
FACULTY OF PHARMACY UNIVERSITAS AIRLANGGA in collaboration with
INDONESIAN PHARMACISTS ASSOCIATION (IAI) OF EAST JAVA



Accredited SINTA 2
No: B/1796/E5.2/KI.02.00/2020

Jurnal Farmasi dan Ilmu Kefarmasian Indonesia

Chief Editor:

apt. Elida Zairina, S.Si, MPH., Ph.D.

Editorial Boards:

Prof. apt. Dewi Melani Hariyadi, S.Si, M.Phil., PhD.

Prof. Dr. Alfi Khatib

Prof. Dr. apt. Wiwied Ekasari, M.Si.

Dr. Ariyanti Suhita Dewi, S.Si., M.Sc.

Dr. Adliah Mhd. Ali

Dr. Long Chiau Ming

Dr.rer.nat apt. Maria Lucia Ardhani D. L., S.Si., M.Pharm

Dr. apt. Susi Ari Kristina, M.Kes.

Dr. apt. Yunita Nita, S.Si., M.Pharm.

Asst. Prof. Dr. Nungruthai Suphrom

Assist. Prof. Dr.rer.nat. Nuttakorn Baisaeng

apt. Chrismawan Ardianto, S.Farm., M.Sc., Ph.D.

apt. Suciati, S.Si., M.Phil, PhD.

apt. Tutik Sri Wahyuni, S.Si., M.Si., Ph.D.

apt. Helmy Yusuf, S.Si., MSc., Ph.D.

apt. Didik Setiawan, Ph.D.

Debra Dorotea, Ph.D.

Deby Fapyane, Ph.D.

Tina Tran, PharmD

Administrative Editor:

Susmiandri, S.Kom.

Peer Reviewers

Prof. Dr. apt. Djoko Agus Purwanto, M.Si.

Prof. Dr. apt. Retno Sari., M.Sc.

Prof. Dr. apt. Noorma Rosita, M.Si.

Prof. apt. Dr. Dyah Aryani Perwitasari, M.Si., Ph.D.

Dr. apt. Tri Widiandani, S.Si., Sp.FRS.

Dr. apt. Idha Kusumawati, S.Si, M.Si.

Dr. apt. Wenny Putri Nilamsari, S.Farm., Sp. FRS.

Dr. apt. Agriana Rosmalina Hidayati, M.Farm.

Dr. apt. Dhadhang Wahyu Kurniawan, S.Si., M.Sc.

Dr. apt. Andri Prasetyo, M.Farm.

Dr. apt. Fahrauk Faramayuda, M.Sc.

Dr. apt. Gunawan Pamuji Widodo, S.Si., M.Si.

apt. Pinus Jumaryatno, S.Si., M.Phil., Ph.D.

apt. Suci Hanifah, M.Si., Ph.D.

apt. Anna Wahyuni Widayanti, MPH., Ph.D.

Irda Safni, SP., MCP., Ph.D.

apt. Andang Miatmoko, S.Farm., M.Pharm.Sci., Ph.D.

apt. Muhammad Faris Adrianto, M.Farm., Ph.D.

apt. Neny Purwitasari, S.Farm., M.Sc.

apt. Lili Fitriani, S.Si, M.Pharm.SC.

apt. Fauna Herawati S.Si., M.Farm-Klin.

apt. Fenita Shoviantari, M.Farm.

Faculty of Pharmacy, Universitas Airlangga
Jl. Dr. Ir. H. Soekarno, Mulyorejo, Surabaya,
East Java – 60115, Indonesia

Phone. (6231) 5933150, Fax. (6231) 5932594

Website:

<http://e-journal.unair.ac.id/index.php/JFIKI>

Email: jfiki@ff.unair.ac.id

Informasi Bagi Penulis

Jurnal Farmasi dan Ilmu Kefarmasian Indonesia (Pharmacy and Pharmaceutical Sciences Journal) P-ISSN: 2406-9388; E-ISSN: 2580-8303 is an official journal published by the Faculty of Pharmacy, Universitas Airlangga in collaboration with Indonesian Pharmacists Association (IAI) of East Java and Center Patient Safety Research which the articles can be accessed and downloaded online by the public (open-access journal).

This journal is a peer-reviewed journal published three times a year on topics of excellence of research outcomes in the fields of pharmacy service and practise, community medicine, pharmaceutical technology, and health science disciplines that are closely related. This journal only accepts English-language submission. The following are the research areas that this journal focuses on

1. Clinical Pharmacy
2. Community Pharmacy
3. Pharmaceutics
4. Pharmaceutical Chemistry
5. Pharmacognosy
6. Phytochemistry

This journal receives a manuscript from the research results, systematic reviews and meta analyses that are closely related to the health sector, particularly the pharmaceutical field. Selected manuscripts for publication in this journal will be sent to two reviewers, experts in their field, who are not affiliated with the same institution as the author(s). Reviewers are chosen based on the consideration of the editorial team. Manuscripts accepted for publication are edited copies checked for the grammar, punctuation, print style, and format. The entire process of submitting manuscripts to make a final decision for publishing is conducted online.

Table of Content

No	Title	Page
1.	Resveratrol Reduce the Severity of Anemia and Thrombocytopenia in <i>Plasmodium berghei</i> ANKA-Infected Mice Faizal Hermanto, Fahmy Ahsanul Haq, Aqila Refiani	266-271
2.	Development of Colloidal Silver-based Mercury Sensors in Whitening Cream Muhammad Hilmi Afthoni, Sherly Yunita, Eva Monica	272-279
3.	Characterization of microencapsulated Saga Leaves Extract (<i>Abrus precatorius</i> L.) and Analgetic Activity Tests in Male Mice (<i>Mus musculus</i>) Nabilah Nauli Jehan, Titik Sunarni, Dian Marlina	280-289
4.	Fibrinolytic Protease Production: Impact of Initial pH and Temperature in Solid-State Fermentation Using <i>Rhizopus microsporus</i> var. <i>oligosporus</i> FNCC 6010 Rebhika Lusiana, Achmad Toto Poernomo, Achmad Syahrani	290-299
5.	Optimizing Gel Formulations Using Carbopol 940 and Sodium Alginate Containing <i>Andrographis paniculata</i> Extract for Burn-Wound Healing Elsa Fitria Apriani, Naisa Kornelia, Annisa Amriani	300-311
6.	Effect of CaCl₂ Crosslinker Concentration On The Characteristics, Release and Stability of Ciprofloxacin HCl-Alginate-Carrageenan Microspheres Amiruddin, Muh. Agus Syamsur Rijal, Dewi Melani Hariyadi	312-323
7.	Patient Satisfaction with Pharmaceutical Services at a Hospital Outpatient Pharmacy in West Sumatra, Indonesia Dian Ayu Juwita, Nurul Qalbi Desri, Dita Permatasari	324-330
8.	Formulation and Characterization of Instant Powder Combination of Ginger, Bangle, and Lemon Extract as an Antioxidant Nur Aji, Shandra Isasi Sutiswa	331-346

9. **Analysis of Molecular Docking and Dynamics Simulation of Mahogany (*Swietenia macrophylla* King) Compounds Against the PLpro Enzyme SARS-COV-2** 347-359
Lalu Sanik Wahyu Fadil Amrulloh, Nuraini Harmastuti, Andri Prasetyo, Rina Herowati
 10. **Five Years Outpatients Antibiotics Consumption at Public Tertiary Hospital in Bengkulu According to Access, Watch and Reserve Classification** 360-368
Yusna F. Apriyanti, Saepudin, Siti Maisharah S. Gadzi
 11. **The Development and Validation of The Indonesian Insulin Adherence Influence Factor Questionnaire (IIAIFQ)** 369-378
Yuniarti Suryatinah, Umi Athiyah, Adliah Binti Mohd. Ali, Elida Zairina
 12. **Protective Factor Evaluation of Purslane (*Portulaca grandiflora*) Magenta Flower Variety Herbs Extract Cream Formula** 379-385
Bida Cincin Kirana, Erlien Dwi Cahyani, Antonius Budiawan
 13. **Green Tea Dregs (*Camellia sinensis* (L.) Extraction Method Effect on *Cutibacterium acnes* and Development of Spot Cream** 386-394
Maria Odelia Vania Arief, Caroline Lieanto, Jessica Mei Sabani, Purwanto
-



Resveratrol Reduce the Severity of Anemia and Thrombocytopenia in *Plasmodium berghei* ANKA-Infected Mice

Faizal Hermanto^{1*}, Fahmy Ahsanul Haq¹, Aqila Refiani²

¹Department of Pharmacology and Toxicology, Faculty of Pharmacy, Universitas Jenderal Achmad Yani, Cimahi, Indonesia

²Bachelor program of Pharmacy, Faculty of Pharmacy, Universitas Jenderal Achmad Yani, Cimahi, Indonesia

*Corresponding author: faizal.hermanto@lecture.unjani.ac.id

Submitted: 6 March 2023

Revised: 16 October 2023

Accepted: 6 December 2023

Abstract

Background: Malaria is an infectious disease with a high mortality rate. One of the complications of malaria is blood disorders. Hematological disorders such as anemia and thrombocytopenia are common in malaria infection. Resveratrol has been reported to have antimalarial activity. **Objective:** This study aimed to evaluate the effect of resveratrol in reducing the severity of anemia and thrombocytopenia in *Plasmodium berghei*-infected mice. **Methods:** The study began with parasite inoculation in mice. After the mice were infected, and randomly grouped into negative control, chloroquine 20 mg/Kg (positive control), and resveratrol with doses 25, 50, and 100 mg/Kg. The mice's blood profile was measured on day 0 and day 4 using a hematology analyzer. **Results:** The results showed that after administration of resveratrol at various doses, the number of RBC, hemoglobin, hematocrit and platelets was higher than the control. **Conclusion:** It can be concluded that resveratrol can reduce the severity of anemia and thrombocytopenia in mice infected with *P. berghei*.

Keywords: anemia, malaria, *Plasmodium berghei*, resveratrol, thrombocytopenia

How to cite this article:

Hermanto, F., Haq, F. A. & Refiani, A. (2023). Resveratrol Reduce the Severity of Anemia and Thrombocytopenia in *Plasmodium berghei* ANKA-Infected Mice. *Jurnal Farmasi dan Ilmu Kefarmasian Indonesia*, 10(3), 266-271. <http://doi.org/10.20473/jfiki.v10i32023.266-271>.

INTRODUCTION

The prevalence of malaria continues to increase every year. Based on the World Health Organization report in 2021, there were 274 million malaria cases in the world (World Health Organization, 2022). Indonesia is one of the endemic malaria areas, especially in the eastern part of Indonesia. Malaria is an infectious disease caused by *Plasmodium* sp. The *Plasmodium* life cycle occurs in mosquitoes and humans. The human body is divided into two phases: the exoerythrocytic (in the liver) and erythrocytic (in the red blood cells). Parasite invasion and multiplication in red blood cells (RBC) are responsible for the onset of symptoms and pathogenesis of malaria. In infected red blood cells (iRBC), modifications occur on the surface of the erythrocyte membrane so that parasite-infected erythrocytes will be easily attached, especially to the surrounding uninfected RBC (rosetting), platelets and endothelial cells (cytoadherence) (Wickramasinghe & Abdalla, 2000). As a result of rosetting and cytoadherence, blood clots occur in the microvascular, which can cause multiorgan disorders such as the liver, spleen, kidney, and brain (Bhutani *et al.*, 2020).

Hematological abnormalities such as anemia and thrombocytopenia are common in malaria patients. During malaria, infected red blood cells lyse and release merozoites to complete their life cycle by infecting new red blood cells. This cyclical process repeatedly occurs, causing a reduction in red blood cells and anemia. Infected red blood cells during lysis will release Hb derivative products such as hemin, methemoglobin (MetHb), and hemozoin which are malaria pigments. The release of these products can cause oxidative stress, which triggers oxidative damage to RBC (Balaji *et al.*, 2020; Rifkind *et al.*, 2015). The pathogenesis of thrombocytopenia is associated with blood clotting disorders, sequestration and cytoadherence in the spleen, destruction of platelets by macrophages, and oxidative stress (Wassmer *et al.*, 2008).

Malaria infection needs to be treated quickly to prevent complications of severe malaria. Malaria treatment faces obstacles, including parasites resistant to the available antimalarials (Dondorp *et al.*, 2009; Gil & Krishna, 2017). The search for new antimalarial compounds has been developed both from natural and synthetic origins, and medicinal plants are a potential source for investigating and developing new antimalarials.

Resveratrol is a flavonoid compound that is found in the skin and seeds of grapes, nuts, jackfruit, and mulberries. Resveratrol has biological activities such as antioxidant, anti-inflammatory, anticancer, neuroprotective, anticancer, and antimalarial (Galiniak *et al.*, 2019; Moon & Sim, 2008). Based on the results of previous studies, resveratrol was reported to have antimalarial activity and can reduce the organ index liver, spleen, and kidney indices in mice infected with *P. berghei*, which is an indicator of inflammation (Hermanto *et al.*, 2022). Resveratrol's activity as an antimalarial can inhibit parasite growth, inhibiting parasite invasion of red blood cells, which can cause hemolysis. Oxidative stress caused by malaria infection can trigger tissue damage, including hemolysis (Gomes *et al.*, 2022). Resveratrol has antioxidant activity, allowing it to suppress free radicals caused by malaria infection to prevent hemolysis. Research on the effect of resveratrol on the blood profile of malaria-infected mice has not yet been studied. This study aimed to evaluate the effect of resveratrol in reducing malaria complications such as anemia and thrombocytopenia.

MATERIALS AND METHODS

Materials

The materials used in this study were resveratrol (Chengdu Biopurify Ltd.), chloroquine (Merck), anticoagulant (Inviclot[®]), Giemsa dye (Merck), methanol, carboxymethylcellulose (CMC), immersion oil.

Parasites and mice

The parasite culture used in this research was *P. berghei* ANKA obtained from the Malaria Laboratory, Faculty of Pharmacy, Universitas Jenderal Achmad Yani. The test animals used in this study were male Swiss Webster mice aged 7-8 weeks with a body weight of 20-35 g, obtained from PT Biomedical Technology Indonesia, Bogor. This research was conducted after receiving prior approval from the preclinical ethics committee of the Faculty of Pharmacy, Universitas Jenderal Achmad Yani, with number 8015/KEP-UNJANI/VI/2022.

Methods

The effect of resveratrol on the blood profile of mice infected with *Plasmodium berghei* was tested in February-November 2023. All mice were grouped into six groups: one normal group (uninfected) and five groups *P. berghei* infected-mice. The mouse was inoculated intraperitoneally with *P. berghei* ANKA as much as 200 μ L, which contained 1×10^6 parasites. After the mice were infected with a parasitemia level of

2%, the mice were randomized and divided into several groups (n = 5). Control (Na CMC 0.5%), chloroquine 20 mg/Kg, resveratrol (25, 50, and 100 mg/Kg). Chloroquine and resveratrol are suspended in 0.5% sodium carboxy cellulose (Na CMC) and given orally. The dose approach used is based on previous research that can inhibit the growth of *Plasmodium* (Hermanto *et al.*, 2022). Before being given the treatment (D0), all mice were examined for their blood profile (erythrocytes, hemoglobin, hematocrit, and platelets) by taking 200 µL of blood from the tails, measured using a hematology analyzer (Melet Schloesing®). The treatment was conducted for four days orally, and on the last day (D4), a blood test was carried out again.

RESULTS AND DISCUSSION

Hematological disorders such as anemia and thrombocytopenia are complications that often occur in malaria patients. This study evaluated resveratrol in reducing hematological disorders in *P. berghei* ANKA-infected mice with RBC, hemoglobin, hematocrit, and platelets. The findings on the number of RBC, hemoglobin, hematocrit, and platelets on day 0 in the control, chloroquine, and all resveratrol groups decreased compared to normal. This is because the mice in this group were infected with the parasite. The RBC profile of mice infected with *P. berghei* (Figure 1) showed that the control group had the lowest number of RBCs on day four compared to all the test groups. Meanwhile, the chloroquine and resveratrol groups had a higher RBC count than the control group. In the resveratrol group, the decrease in the number of red blood cells was not dose-dependent, especially at doses of 50 and 100 mg/Kg. However, the number of red blood cells was still higher than the control group, which correlated with the parasite density level. Previous research showed that resveratrol was reported to have antimalarial activity in *P. berghei*-infected mice with an effective dose 50 (ED₅₀) value of 27.25 mg/Kg (Hasugian *et al.*, 2014), so resveratrol can suppress parasites, preventing invasion and multiplication of parasites in RBC cause reducing hemolysis.

The pathogenesis of anemia in malaria infection is multifactorial, including destroying iRBC, impaired RBC production in the bone marrow, and parasite phagocytosis in iRBC (Awoke & Arota, 2019). The spleen is an organ that plays a role in cleaning red blood cells. In malaria infection, changes in blood cleaning are carried out by spleen macrophages. iRBC cells will express marker compounds such as rho-

associated protein-2 (RSP-2) and phosphatidylserine (PS) on the surface of the RBC membrane, which will be recognized by lymph macrophages and will then cause phagocytosis. Anemia is caused by the significant number of infected red blood cells cleansed by the spleen, and the burden on the spleen in cleaning parasites is more remarkable, which might interfere with the spleen organ. This is in line with previous research that *P. berghei*-infected mice that were not given treatment showed an increase in the spleen organ index, widening of the white pulp and depletion of the red pulp, which are indicators of spleen damage, while mice treated with resveratrol showed a decrease in the spleen organ index and improvement in histology spleen (Hasugian *et al.*, 2014; Intan *et al.*, 2017).

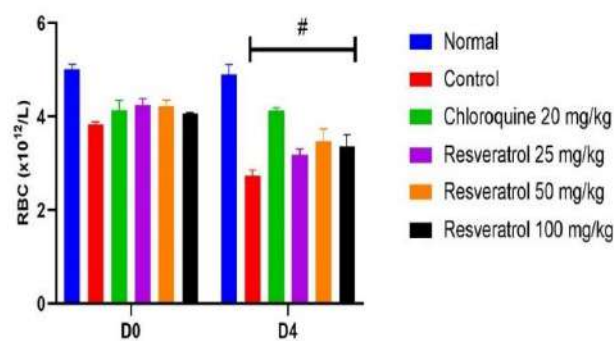


Figure 1. RBC profile of mice treated with resveratrol. The data shown are mean ± SEM. n = 5. * = p < 0.05 for the negative control group. # = P < 0.05 for the standard group

The hemoglobin profile in *P. berghei*-infected mice after being treated with resveratrol can be seen in Figure 2. The hemoglobin level of the control group on day 4 showed the lowest compared to the entire test group. The chloroquine and resveratrol groups had higher hemoglobin than the controls. In the erythrocytic cycle, the parasite will use hemoglobin as a source of nutrition.

Hemoglobin will be degraded into heme and then biomineralized into hemozoin. Compounds resulting from the degradation of hemoglobin, such as heme, methemoglobin, and hemozoin, are free radicals that can cause damage to the RBC membrane and increase the occurrence of hemolysis (Balaji & Trivedi, 2012). Resveratrol's antioxidant action is suggested to prevent hemolysis.

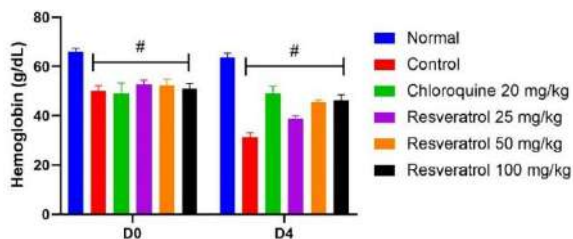


Figure 2. The hemoglobin profile of mice treated with resveratrol. The data shown are mean ± SEM. n= 5. *= $p < 0.05$ for the negative control group. #= $P < 0.05$ for the normal group

Hematocrit is the ratio of the number of red blood cells to whole blood. In malaria infection, the hematocrit will decrease. Changes in the hematocrit profile in *P. berghei*-infected mice are shown in Figure 3. In the control group, the number of hematocrites on day 4 decreased, while in the chloroquine and resveratrol groups, it was higher than the control group and not significantly different from the normal group. The decrease in the number of hematocrit correlated with the level of parasite density. In the erythrocytic phase, the parasite will multiply, resulting in many ruptured RBCs (Akinosoglou *et al.*, 2012). Chloroquine and resveratrol have been shown to inhibit parasite growth, reducing the decrease in hematocrit. The findings in this study showed that resveratrol could reduce malaria complications in the form of anemia with higher RBC, hemoglobin, and hematocrit profiles than the control group.

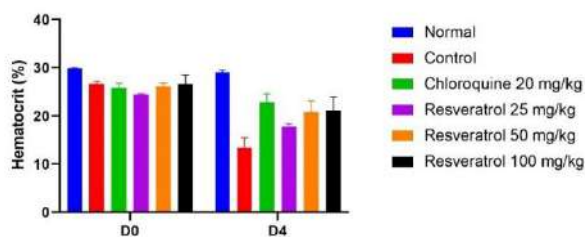


Figure 3. The hematocrit profile of mice treated with resveratrol. The data shown are mean ± SEM. n= 5. *= $p < 0.05$ for the negative control group. #= $P < 0.05$ for the normal group

A hematological disorder in severe malaria infection is thrombocytopenia, which is found to occur in around 50-80% of malaria cases. Figure 4 shows the blood profile of mice infected with *P. berghei* after resveratrol administration. The control group on day 4 showed the lowest platelet count compared to all test groups. In the chloroquine and resveratrol group, the decrease in platelets was not as common as in the

control group. Decreased platelets are associated with an increase in the number of parasites. High levels of parasites can trigger an increase in pro-inflammatory cytokines such as TNF- α , INF- γ , and IL12.

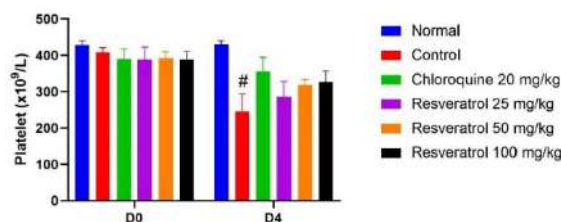


Figure 4. Platelet profile of mice treated with resveratrol. The data shown are mean ± SEM. n= 5. *= $p < 0.05$ for the negative control group. #= $P < 0.05$ for the normal group

This increase in pro-inflammatory cytokines impacts platelets trapped and used for inflammation in blood vessels. Besides that, the immune response increases macrophage activity to destroy platelets which can cause thrombocytopenia (Hasugian *et al.*, 2015; Lee *et al.*, 1997). Previous studies reported that on day 4, mice infected with *P. berghei* had lower parasitemia values than controls (Hermanto *et al.*, 2022), and these results were consistent with their platelet profiles. In addition, resveratrol is also reported to have anti-inflammatory activity by suppressing IL-6, TNF- α , and INF- γ (Galiniak *et al.*, 2019). The ability of resveratrol to suppress parasite growth and suppress pro-inflammatory cytokines proves that resveratrol can reduce malaria complications in the form of thrombocytopenia.

All blood parameters in mice infected with *P. berghei* after administration of resveratrol showed improvements in several factors that can cause this. Firstly, resveratrol can inhibit parasite growth, thereby preventing parasite invasion of red blood cells, which will cause hemolysis. Secondly, the antioxidant activity of resveratrol makes it possible to prevent tissue damage due to oxidative stress that occurs during the infection process. Thirdly, anti-inflammatory from resveratrol can prevent an increase in pro-inflammatory cytokines, which is one of the factors that worsens malaria. This study has limitations in not evaluating the effect of resveratrol on antioxidant activity and pro-inflammatory cytokines in mice infected with *Plasmodium*. So that in the future, it can be used as further research regarding the study of the mechanism of action of resveratrol in reducing blood disorders due to complications of malaria.

CONCLUSION

This study investigated the effect of resveratrol in reducing the severity of anemia and thrombocytopenia. The results show that resveratrol can reduce the severity of anemia and thrombocytopenia by reducing parasitemia levels and antioxidant activity and suppressing pro-inflammatory cytokines. However, further research is still needed.

ACKNOWLEDGMENT

The researcher would like to thank Lembaga Penelitian dan Pengabdian Masyarakat, Universitas Jenderal Achmad Yani, Cimahi, which has funded this research.

AUTHOR CONTRIBUTIONS

Conceptualization, F. H.; Methodology, F. H.; Software, F. H., F. A. H.; Validation, F. H.; Formal Analysis, F. H.; Investigation, F. H., A. R., F. A. H.; Resources, F. H.; Data Curation, A. R., F. A. H.; Writing - Original Draft, F. H., A. R., F. A. H.; Writing - Review & Editing, F. H., F. A. H.; Visualization, F. H., F. A. H.; Supervision, F. H.; Project Administration, F. A. H.; Funding Acquisition, F. H.

FUNDING STATEMENT

Lembaga Penelitian dan Pengabdian Masyarakat, Universitas Jenderal Achmad Yani, supported this study.

CONFLICT OF INTEREST

The authors declared no conflict of interest.

REFERENCES

- Akinosoglou, K. S., Solomou, E. E. & Gogos, C. A. (2012). Malaria: A Haematological Disease. *Hematology*; 17; 106–114. doi: 10.1179/102453312X13221316477336.
- Awoke, N. & Arota, A. (2019). Profiles of Hematological Parameters in *Plasmodium falciparum* and *Plasmodium vivax* Malaria Patients Attending Tercha General Hospital, Dawuro Zone, South Ethiopia. *Infection and Drug Resistance*; 12; 521–527. doi: 10.2147/IDR.S184489.
- Balaji, S., Deshmukh, R. & Trivedi, V. (2020). Severe Malaria: Biology, Clinical Manifestation, Pathogenesis and Consequences. *Journal of Vector Borne Diseases*; 57; 1–13. doi: 10.4103/0972-9062.308793.
- Balaji, S. N. & Trivedi, V. (2012). Extracellular Methemoglobin Mediated Early ROS Spike Triggers Osmotic Fragility and RBC Destruction: An Insight into the Enhanced Hemolysis During Malaria. *Indian Journal of Clinical Biochemistry (IJCB)*; 27; 178–185. doi: 10.1007/S12291-011-0176-5.
- Bhutani, A., Kaushik, R. M., & Kaushik, R. (2020). A Study on Multi-Organ Dysfunction Syndrome in Malaria Using Sequential Organ Failure Assessment Score. *Tropical Parasitology*; 10; 86–94. doi: 10.4103/tp.TP_12_19.
- Dondorp, A. M., Nosten, F., Yi, P., Das, D., Phyto, A. P., Tarning, J., Lwin, K. M., Arie, F., Hanpithakpong, W., Lee, S. J., Ringwald, P., Silamut, K., Imwong, M., Chotivanich, K., Lim, P., Herdman, T., An, S. S., Yeung, S., Singhasivanon, P. & White, N. J. (2009). Artemisinin Resistance in *Plasmodium falciparum* Malaria. *New England Journal of Medicine*; 361; 455–467. doi: 10.1056/nejmoa0808859.
- Galiniak, S., Aebischer, D., & Bartusik-Aebischer, D. (2019). Health Benefits of Resveratrol Administration. *Acta Biochimica Polonica*; 66; 13–21. doi: 10.18388/abp.2018_2749.
- Gil, J. P. & Krishna, S. (2017). Pfmdr1 (*Plasmodium falciparum* Multidrug Drug Resistance Gene 1): a Pivotal Factor in Malaria Resistance to Artemisinin Combination Therapies. *Expert Review of Anti-Infective Therapy*; 15; 527–543. doi: 10.1080/14787210.2017.1313703.
- Gomes, A. R. Q., Cunha, N., Varela, E. L. P., Brígido, H. P. C., Vale, V. V., Dolabela, M. F., De Carvalho, E. P. & Percário, S. (2022). Oxidative Stress in Malaria: Potential Benefits of Antioxidant Therapy. *International Journal of Molecular Sciences*; 23; 1–26. doi: 10.3390/ijms23115949.
- Hasugian, A., H. W., & Tjitra, E. (2014). In Vivo Antimalarial Efficacy of Acetogenins, Alkaloids and Flavonoids Enriched Fractions from *Annona crassiflora* Mart. *Natural Product Research*; 28; 1254–1259. doi: 10.1080/14786419.2014.900496.
- Hasugian, A., Wibowo, H. & Tjitra, E. (2015). Peranan Trombosit dalam Patogenesis Malaria. *Majalah Kedokteran Andalas*; 37; 219–225. doi: 10.22338/mka.v37.i3.p219-225.2014.
- Hermanto, F., Nur Anisa, I., Wahyuningsih, S., Alatas, F., Suryani, S., Rachmawan, R. L., Ahsanul Haq,

- F. & Adhary, F. (2022). Antiplasmodium Activity and the Effect of Resveratrol on Index Organs of Mice Infected with *Plasmodium berghei* ANKA. *PHARMACY: Jurnal Farmasi Indonesia (Pharmaceutical Journal of Indonesia)*; 19; 28-39. doi: 10.30595/pharmacy.v19i1.12693.
- Intan, P. R., Lestari, T. W. & Sani, Y. (2017). Histopathological Study After Delivery Mixed Extract of *Alstonia scholaris* Bark and *Phyllanthus niruri* Administration in *Plasmodium berghei* Infected mice. *Jurnal Kedokteran Yarsi*; 25; 10–22.
- Lee, S. H., Looareesuwan, S., Chan, J., Wilairatana, P., Vanijanonta, S., Chong, B. & Chong, H. (1997). Plasma Macrophage Colony-Stimulating Factor and P-selectin Levels in Malaria-Associated Thrombocytopenia. *Thromb Haemost*; 77; 289-293.
- Moon, H. I., & Sim, J. (2008). Antimalarial Activity in Mice of Resveratrol Derivative from *Pleuropterus ciliinervis*. *Annals of Tropical Medicine and Parasitology*; 102; 447–450. doi: 10.1179/136485908X300832.
- Rifkind, J. M., Mohanty, J. G. & Nagababu, E. (2015). The Pathophysiology of Extracellular Hemoglobin Associated with Enhanced Oxidative Reactions. *Frontiers in Physiology*; 5; 1-7. doi: 10.3389/FPHYS.2014.00500.
- Wassmer, S. C., Taylor, T., MacLennan, C. A., Kanjala, M., Mukaka, M., Molyneux, M. E. & Grau, G. E. (2008). Platelet-Induced Clumping of *Plasmodium falciparum*-Infected Erythrocytes from Malawian Patients with Cerebral Malaria-Possible Modulation In Vivo by Thrombocytopenia. *The Journal of Infectious Diseases*; 197; 72–78. doi: 10.1086/523761.
- Wickramasinghe, S. N. & Abdalla, S. H. (2000). Blood and Bone Marrow Changes in Malaria. *Bailliere's Best Practice and Research in Clinical Haematology*; 13; 277–299. doi: 10.1053/beha.1999.0072.
- World Health Organization. (2022). World Malaria Report 2022. In: *World Health* 12. Geneva: World Health Organization.



Development of Colloidal Silver-based Mercury Sensors in Whitening Cream

Muhammad Hilmi Afthoni^{1,2}, Sherly Yunita¹, Eva Monica^{1*}

¹Department of Pharmacy, Faculty of Science and Technology, Machung University, Malang, Indonesia

²Department of Clinical and Community Pharmacy, Faculty of Pharmacy, University of Jember, Jember, Indonesia

*Corresponding author: eva.monica@machung.ac.id

Submitted: 26 March 2023

Revised: 16 October 2023

Accepted: 18 December 2023

Abstract

Background: Mercury, a hazardous heavy metal known for its toxicity to the human body, finds application in cosmetics due to its capacity to inhibit melanin formation. Traditional mercury analysis relies on resource-intensive and time-consuming instrumentation. **Objective:** This study aims to devise cost-effective and practical sensors for mercury detection. **Methods:** The sensor development process involves immobilizing the sensor onto paper, reacting it with mercury, scanning the outcome using a scanner, and subsequently quantifying RGB values using the ImageJ software. **Results:** Optimization of reagent concentrations gave a ratio of methylene blue, AgNO₃, gallic acid, and ascorbic acid at 0.5:7:1.5:1 generating the best results. Additionally, pH optimization within the range of 5 to 9 demonstrates stability without necessitating the inclusion of a buffer solution. Notably, the blue variant exhibits superior responsiveness during concentration optimization. Characterization of the sensor reveals a response time of 3 minutes and minimal interference of 2.145% from other substances. The sensor exhibits a linearity range of 0.5-250 ppm, regression equation $y = 8.603x + 21.124$, an R-value of 0.994, and an exceedingly low p-value of $6.9924589548512 \times 10^{-9}$. The sensor boasts a limit of detection (LOD) of 0.206 and a limit of quantification (LOQ) of 0.265, indicative of its precision. Further assessments reveal a percent relative standard deviation (% RSD) precision of 2.017% and a recovery rate of 96.14%. **Conclusion:** The sensor has exhibited stability for over one month under room temperature storage conditions. A comparison between the UV-Vis spectrophotometer and the sensor signifies no significant difference between the two methods.

Keywords: AgNO₃, colloidal silver, mercury, methylene blue, sensor

How to cite this article:

Afthoni, M. H., Yunita, S. & Monica, E. (2023). Development of Colloidal Silver-based Mercury Sensors in Whitening Cream. *Jurnal Farmasi dan Ilmu Kefarmasian Indonesia*, 10(3), 272-279. <http://doi.org/10.20473/jfiki.v10i32023.272-279>

INTRODUCTION

Mercury, a chemical element, finds application in facial whitening creams owing to its capacity to impede the melanin formation process, known as melanogenesis. Melanogenesis represents a fundamental physiological pathway responsible for the generation of melanin, a pigment that absorbs light and plays a pivotal role in determining human skin colour and hair pigmentation. The melanin synthesis pathway is reliant on the enzymatic activity of tyrosinase, an enzyme with a copper-dependent mechanism responsible for converting tyrosine into melanin. Tyrosinase, being a glycoprotein, undergoes an essential N-glycosylation process to attain its active enzymatic state. Following cleavage by glucosidase, glycosylated tyrosinase assumes a properly folded conformation, rendering it amenable to active transport facilitated by Cu^{2+} within the Golgi apparatus before reaching melanosomes. Notably, inorganic forms of Mercury operate as solid inhibitors of melanin production by competing with or displacing copper ions, impairing the catalytic activity of the tyrosinase enzyme in melanin synthesis. Ultimately, this inhibition leads to the achievement of a brighter skin complexion (Haryanti et al., 2020).

Mercury can be analyzed using several instruments, including Inductively Coupled Plasma Mass Spectrometry (ICP-MS), Inductively Coupled Plasma Atomic Emission Spectrometry (ICP-AES), Gas Chromatography Coupled to Atomic Absorption Spectrometry (GC-AAS), Cold Vapor Atomic Absorption Spectrometry (CV-AAS), Atomic Fluorescence Spectrometry (AFS), and Anodic Stripping Voltammetry (ASV) (Kristianingrum, 2009). However, analysis with this technique is costly, and the process is quite complicated. Therefore, researchers have developed colloidal silver-based chemical sensors. Colloidal silver is a nanotechnology-based product that is currently being developed and can be applied as a catalyst and optical sensor detector. The reaction mechanism in colloidal silver is that when Hg^+ ions are added to the solution, an oxidation-reduction reaction will occur between Ag^0 and Hg^+ ions (Kumar et al., 2017). In manufacturing colloidal silver-based sensors, methylene blue is used as a marker to detect the presence of mercury, and gallic acid is used as a capping agent so that the particles become more stable by preventing aggregation. Based on this, this study developed a colloidal silver-based chemical sensor that can detect the presence of Mercury in cosmetic products quickly, simply, and economically.

MATERIALS AND METHODS

Materials

HgNO_3 (Loba Chemie), methylene blue (Merck), ascorbic acid (Merck), AgNO_3 , gallic acid (Merck), demineralized water (Hydrobatt), methanol (Merck), Whatman paper (paint No.1), phosphate buffer solution pH 5-9, dithizone (Merck), sodium hydroxide (Merck), hydrochloric acid (Merck), whitening cream samples, mica.

Tools

UV-Vis spectrophotometer (JASCO V-760), cuvette, scanner (canon LiDE 300), analytical balance (OHAUS), 50, 100, and 250 mL beakers glass (pyrex), 5, 10, 50, and 100 mL volumetric flasks (pyrex), 50 mL measuring glass (pyrex), ultrasonic (Mosinix USA), pH meter (OHAUS), drip plate, micropipette 100-1000 l and 1000-5000 l (socorex), dropper pipette, volume pipette (pyrex), ball filler, stir bar, tweezers, vial, punch hole, hairdryer, stopwatch, scissors.

Method

Sensor immobilization

The immobilization technique used is adsorption, which is done by soaking the paper in the reagent for 24 hours. The sensor paper was dried using a hairdryer. The dried paper is stored at room temperature (25°C) to maintain its stability. Paper that has been immobilized and dried is used for sensor optimization, sensor characterization, and testing on samples.

Strip test fabrication

The mercury detection strip test in cosmetic samples consists of two parts, namely the handle and the detection area as shown in Figure 1. The handle of the strip test is made of non-absorbent mica with a size of 7.5 cm x 1 cm. The detection area is made of paper glued to the bottom of the handle of the strip test.

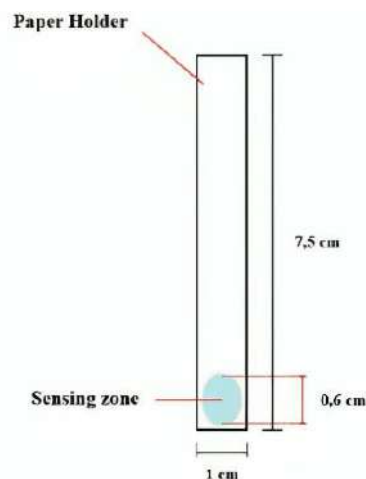


Figure 1. Strip test design

Table 1. Mercury detection reagent formula

Reagent	Volume (mL) pipetted in 10 mL							
	F1	F2	F3	F4	F5	F6	F7	F8
Methylene Blue ($3,127 \times 10^{-3}$ M)	-	0.5	-	0.5	-	0.5	-	0.5
AgNO ₃ ($5,887 \times 10^{-3}$ M)	5	5	6	6	7	7	8	8
Ascorbic Acid (0,1 M)	1	1	1	1	1	1	1	1
Gallic Acid (0,1 M)	4	3.5	3	2.5	2	1.5	1	0.5

Chemical sensor optimization

Optimization of reagent concentration

Optimization of reagent concentration was done by making reagents with variations of the formulas made in Table 1 using immobilization techniques. Each reagent that has been made was immersed in paper for 24 hours. After that, the immobilized paper was reacted with 250 ppm Mercury and then measured. All of the experiments were carried out in triplicate. Then, each formula was measured for its RGB value, and the highest RGB value was observed using the ImageJ program.

Optimization of pH

Optimization of pH was done by making a phosphate buffer solution with a pH of 5, 6, 7, 8, and 9. Furthermore, the sensor paper that had been immobilized was added with a buffer solution of various pH and drops of Mercury with a concentration of 250 ppm. Then the RGB value was measured, and the highest mean RGB value was observed using the ImageJ program (Hermanto *et al.*, 2019). All of the experiments were carried out in triplicate.

Optimization of test concentration

Optimization of test concentration was carried out by making mercury concentrations of 0.5, 1, 5, 10, 50, 100, and 250 ppm. Tests were carried out using sensor paper that had been immobilized and then dripped with various concentrations of Mercury that had been prepared. Then, the colour intensity was measured at each concentration using the ImageJ program to determine the RGB mean value and look for the most linear colour response. Optimal optimization can be done by seeing the colour change and giving the most linear colour response value; all the experiments were carried out in triplicate (Hidayat *et al.*, 2017).

Chemical sensor characterization

Response time

The timing of the sensor was done by measuring the time it takes for the reagent to react with Mercury. The response time was determined by dipping the test strip that had been immobilized. The measurements were carried out every minute for 30 minutes using a stopwatch and the RGB values were measured from the scan results using the ImageJ program and the mean

RGB values were obtained. The measurement results show that the most optimal time was generated from the mean RGB; all of the experiments were carried out in triplicate (Hermanto *et al.*, 2019).

Selectivity

The determination of selectivity was carried out using a mercury standard based on the results of optimization that had been added with interfering components (nipagin, nipasol, and triethanolamine). The selectivity was determined by measuring the Δ mean RGB value using the ImageJ program. Selectivity is good if it has a value of % interference < 5%.

Linearity

Determination of linearity was done by dipping the test strip into the reagent with a test concentration range of 0.5-250 ppm. After that, a linearity curve was made between concentration and Δ mean RGB. From this curve, the value of the regression equation was obtained. Furthermore, the ANOVA data processing was done using Microsoft Excel to determine the p-value (Hermanto *et al.*, 2019).

Limit of detection (LOD) dan limit of quantitation (LOQ)

Determination of LOD and LOQ values was done by making several mercury standard solutions with concentrations below the smallest concentration of the linearity test range. Then, the linearity curve between concentration and Δ mean RGB was determined (Hermanto *et al.*, 2019).

Precision

The precision value can be determined by calculating the relative standard deviation (RSD) of 6 measurements made using different test strips. Interday testing (repetition on various days) was performed using sample solutions of different concentrations; then, the colour change was measured using the ImageJ program so that the mean RGB value was obtained (Hermanto *et al.*, 2019).

Accuracy

Determination of accuracy was carried out by the standard addition method, namely by calculating the % recovery from three times the addition of analyte of 30%, 45%, and 60% of the sample concentration from the test concentration. Next, the cream sample was

prepared, and then the test strip was dipped in the solution, and the colour change was observed. The Δ mean RGB value of the measurement results is then entered into the regression equation to obtain the mercury concentration in the sample (Hermanto *et al.*, 2019).

Stability

Determination of stability was done by storing the sensor at room temperature (25°C). The sensor response was measured every day until it reached a 15% decrease from the original sensor response (Hermanto *et al.*, 2019).

Mercury testing using a UV-Vis spectrophotometer

The standard solution was made by weighing 10 mg of Mercury in a 10 mL volumetric flask and then diluting it to various concentrations. Next, a sample solution was made by weighing 100 mg of the cream sample and dissolving it in 100 mL of demineralized water, which resulted in a sample solution with a concentration of 1000 ppm. The sample solution was diluted to 10 ppm by means of a 100 μ L pipette dissolved in a 10 mL volumetric flask. After that, it was checked using a UV-Vis spectrophotometer in a way that each of the standard solution and sample was pipetted as much as 100 μ L and added with 100 μ L of 10 ppm dithizone solution (Jamaluddin & Reazul, 2003).

Sensor application

Tests using the test strip method were carried out by dipping the test strip in each sample that had been prepared by weighing 100 mg of cream and dissolving it in 100 mL of water. Then 0.1 mL of the solution was taken and dissolved in 10 mL of water. After dipping, the results of the color change can be compared with the color results of the mercury standard.

RESULTS AND DISCUSSION

Chemical sensor optimization

The reagent concentration optimization was carried out to obtain reagents that could detect Mercury optimally. In optimizing the reagent concentration, reagents were made with variations of 8 formulas using a combination of methylene blue, AgNO₃, ascorbic acid, and gallic acid. Determination of the reagent concentration was carried out on sensor paper that had been immobilized for 24 hours, which was then added with 250 ppm mercury. The results of the reagent concentration optimization experiment can be seen in Figure 2. This optimization experiment was conducted through three replication attempts. The results of reading the RGB values on ImageJ and observing color

changes directly by the eye, the optimal reagent concentration is formula 6, because it has the highest Δ mean blue value.

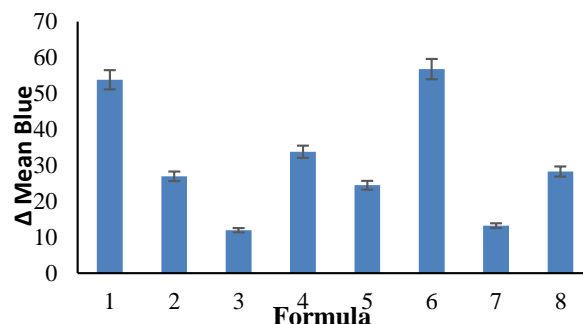


Figure 2. Comparison of reagent concentration to color change

The sensor's pH was optimized to know the optimal working pH on this sensor. The immobilized sensor paper was added with a buffer solution at pH 5, 6, 7, 8, and 9, and then reacted with 250 ppm mercury concentration. The results of reading RGB values using ImageJ and pH optimization data can be seen in Figure 3, where these results indicate that this sensor was not affected by pH because there was no significant change in the five pH values, so this sensor did not need additional buffer.

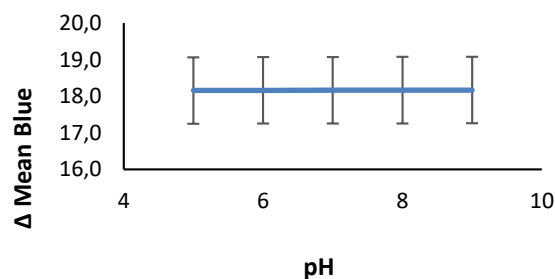


Figure 3. Sensor response at various pH to color change

The test concentration was optimized to know the most linear colour response produced by the sensor. The test concentration was optimized by making a serial solution of mercury concentration with levels of 0.5 ppm, 1 ppm, 5 ppm, 10 ppm, 50 ppm, 100 ppm, and 250 ppm. After that, the sensor paper that had been immobilized was reacted with a solution of various levels of Mercury. The results of reading RGB values using ImageJ as well as optimization test concentration data can be seen in Figure 4, where from these results, it can be seen that the blue colour response provides the most optimal response compared to other colours, with an R-value of 0.9923 so that the value of mean blue is used as a characterization reading and sensor testing.

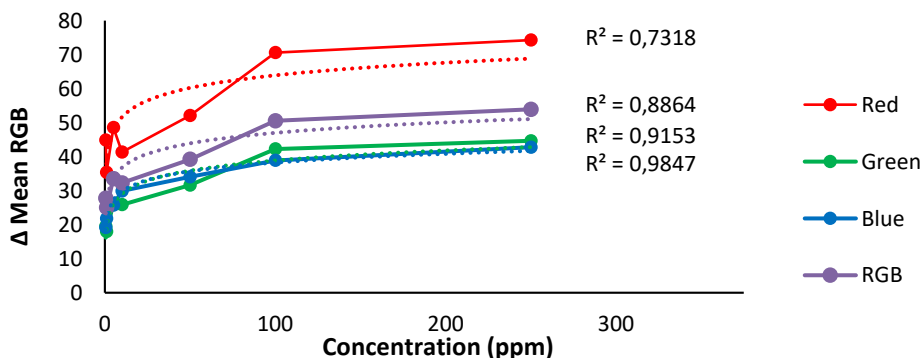


Figure 4. Response of color reading to test concentration

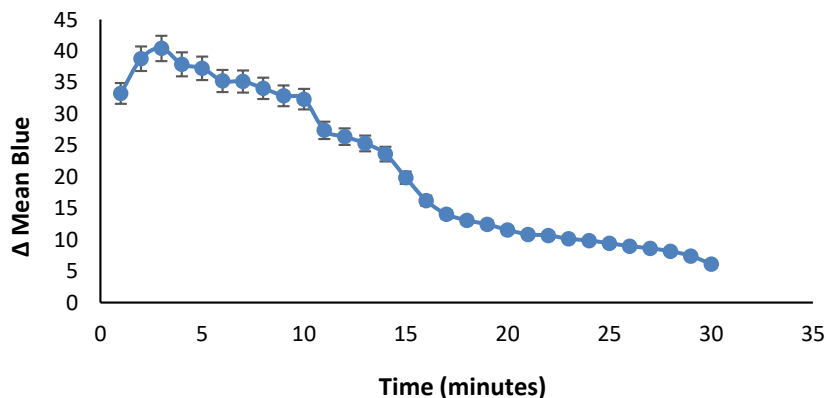


Figure 6. Sensor response time to color change (Δ mean blue)

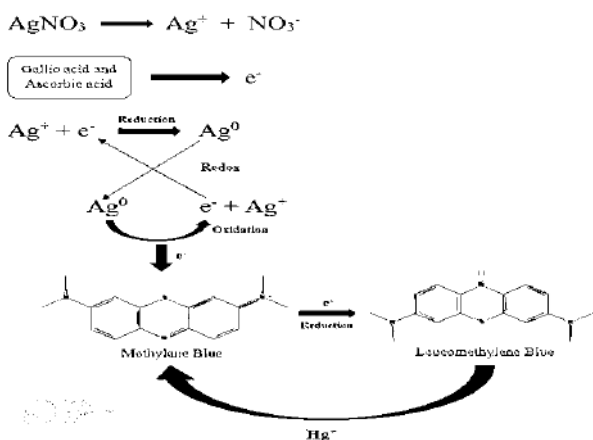


Figure 5. Reaction schematic of mercury with methylene blue, AgNO₃, gallic acid, and ascorbic acid

Sensing mechanism

In developing a colloidal silver-based mercury sensor, a reaction occurs between gallic acid and ascorbic acid with AgNO₃, which will then reduce methylene blue. The reduction of methylene blue is influenced by colloidal silver, which is formed as a result of the reduction of AgNO₃. In the electron transfer process, when there is a significant difference in redox potential between the acceptor and the donor, then there is a possibility of restriction in the electron transfer (Clayden & Greeves, 2012). However, electron transfer

will proceed easily if the effective catalyst has an intermediate redox potential between the acceptor and donor. In this case, colloidal silver acts as a mediator of electron transfer and contributes to methylene blue by acting as a redox catalyst. Gallic acid and ascorbic acid reduce Ag⁺ from AgNO₃ to Ag⁰, where colloidal silver acts as an electron transfer mediator and donates to methylene blue as a redox catalyst, also reducing methylene blue to leucomethylene blue (Mona *et al.*, 2018). This colourless leucomethylene blue, when it reacts with Hg⁺, an oxidation process will occur, which releases electrons, and methylene blue will capture electrons, thus making the blue colour of methylene blue reform, as shown in Figure 5.

Chemical sensor characterization

Response time testing was carried out to measure the time required for Mercury by optimizing the concentration to react with the reagents in the sensor to give the most optimal color response results. This measurement is carried out every minute for 30 minutes where the sensor reacts with a standard Mercury solution with a concentration of 250 ppm. The results of the response time testing can be seen in Figure 6, where the most optimal sensor response time is obtained, which is in the 3rd minute.

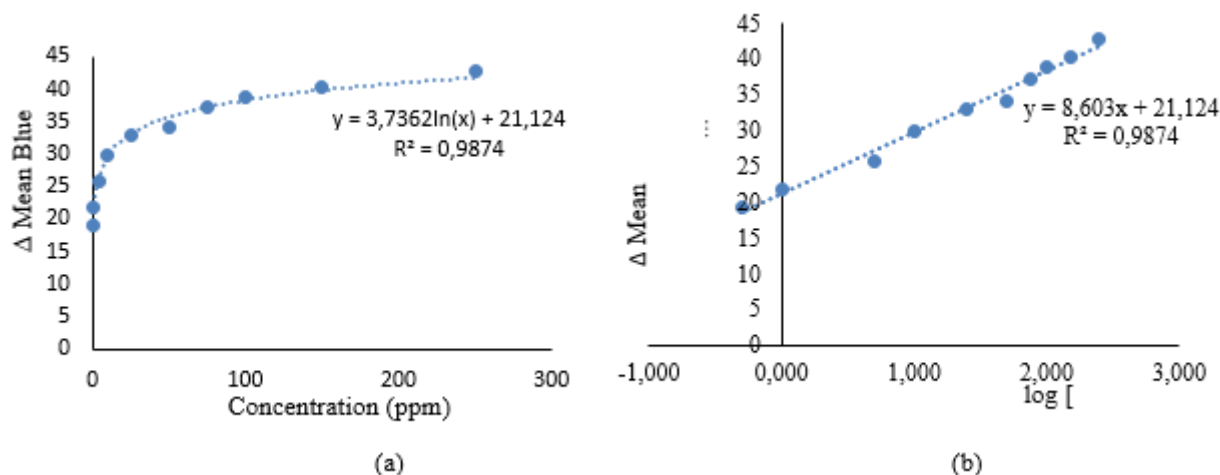


Figure 8. (a) Linearity test results in logarithmic equations; (b) linearity test results in linear equations

The selectivity test was carried out to determine the confounding component's effect. The nuisance components used in this test are usually found in cosmetics, such as methyl paraben, propylparaben, and triethanolamine (TEA). The preparation was done by mixing Mercury with the interfering component, in which 1:1, 1:10, and 1:100 ratios were used. The results of the selectivity test obtained from the presence of 3 interfering components can be seen in Table 2 and Figure 7. The % interference value is 2.145%, where this result is by the requirements of the selectivity test, which is <5%, so it can be said that the method used is not affected by the presence of a nuisance component (Nethercote & Ermer, 2012).

Table 2. Results of comparison of interference values

Comparison	Nipagin	Nipasol	TEA
1 : 1	3,639	0,706	4,193
1 : 10	2,899	1,087	3,176
1 : 100	1,200	1,384	1,017

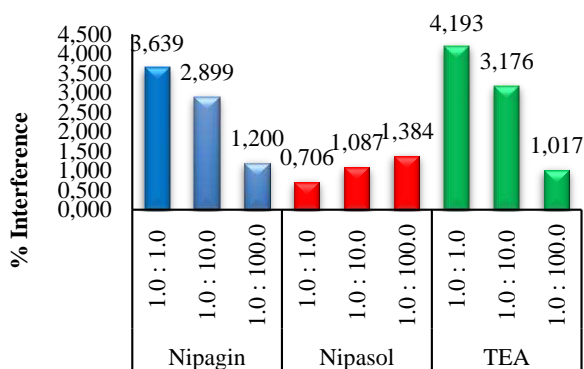


Figure 7. Results % interference selectivity test

The linearity test was carried out to determine the relationship between the detector response and changes in concentration. The concentration in the linearity test ranges from 0.5-250 ppm with 10 test points. Tested using the scanometry method, then measured RGB values in the ImageJ program. From these results, the regression equation $y = 3.7362\ln(x) + 21,124$ is obtained for the logarithmic curve, as shown in Figure 8(a). The regression equation formed becomes $y = 8.603x + 21,124$, and the R-value is 0.994, as shown in Figure 8(b). After that, the ANOVA test was carried out, which obtained a p-value of $6.9924589548512 \times 10^{-9}$. The results of the linearity test can be seen in Appendix F, where these results have met the requirements of good linearity, namely the correlation coefficient (r) 0.999, and the p-value of the ANOVA test is less than = 0.01(Nethercote & Ermer, 2012).

LOD is determined to know the smallest amount of analyte or sample in the sample that still gives a significant response to the sensor method. In contrast, the determination of LOQ aims to determine the most minor level or the smallest concentration of Mercury that can still be quantified for precision and accuracy determination. The results obtained from the determination of LOD and LOQ values were 0.206 ppm and 0.625 ppm, respectively.

The precision test was carried out to know the closeness of a series of measurements obtained from the sample. Test precision was determined by calculating the relative standard deviation (RSD). This test was carried out on 3 consecutive days using the same concentration (interday), each with six replications. % RSD resulting from the average precision test was 2.017%, so it can be concluded that this test has met the

requirement since the % RSD was less than 7.3 for a concentration of 10 ppm sample (Huber, 2007).

The accuracy test is carried out to determine the measurement method's accuracy. The accuracy test was carried out using the standard addition method with three replications. The value of % recovery obtained from the average accuracy test is 96.14%, so it can be said that this test meets the requirements % recovery is in the range of 80-110% for a concentration of 10 ppm sample (Huber, 2007).

The stability test was carried out to know the time at which the sensor gave the same and stable reaction to an analyte at the same concentration until the response time of the sensor to the analyte decreased drastically (usually more than 15% of the initial sensor response) (Kuswandi, 2008). The stability test results, which lasted for one month, showed a % decrease in the range of 0.005-0.061, indicating that the sensor is stable because it shows the % decrease, which is still far from 15%.

Comparison of mercury testing using a UV-vis spectrophotometer and sensor

A comparison of mercury testing using the UV-Vis spectrophotometer and the sensor methods was carried out to know if there were significant differences between the two methods. The results of testing the two methods were analyzed using a T-test Two-Sample Assuming Unequal Variances in Microsoft Excel. If the value of < 0.05, then H0 is rejected, meaning there is a significant effect between one independent variable and the dependent variable. Meanwhile, if the value is > 0.05, then H0 is accepted, meaning there is no significant effect between one independent variable and the dependent variable (Miller & Miller, 2010). The results obtained from the five samples can be seen in Table 3. The results of the p-value between the two methods are more than = 0.05, indicating no significant difference between the UV-Vis spectrophotometer method and the sensor method, so this sensor can be used to detect the presence of Mercury.

Sensor application

The sensor was applied to the sample directly to determine the sensor's direct response in detecting the presence or absence of mercury in the sample. The results of the application of the sensor on the sample can be seen in Figure 9, where from these results, it can be seen that the sensor has been optimum in detecting the presence of Mercury due to a change in colour according to the mercury standard.

Table 3. Comparative test results of uv-vis spectrophotometer with sensor

Sample	UV-Vis Spectrophotometer (ppm)	Sensor (ppm)	P (T<=t) two tail
1	15,476	15,066	0,692
	15,830	15,596	
	15,013	14,689	
2	13,419	13,092	0,787
	13,275	13,002	
	13,166	13,677	
3	12,507	12,618	0,940
	12,450	12,560	
	14,052	13,772	
4	13,664	12,882	0,112
	13,886	13,243	
	13,865	12,972	
5	15,598	15,453	0,463
	15,821	15,101	
	15,895	15,812	

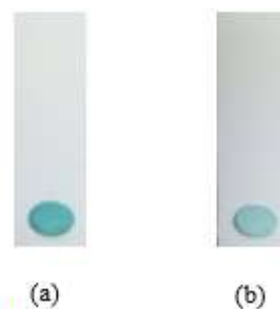


Figure 9. (a) Sensor before reacting; (b) sensor after being reacted with the sample

CONCLUSION

The optimal condition of the sensor is formula 6 with a ratio of methylene blue: AgNO3 : gallic acid: ascorbic acid = 0.5 : 7 : 1.5 : 1. The addition of buffer in this sensor is not required, and blue is the most optimum colour in generating sensor responses based on test concentrations. The sensor has a response time characterization in the 3rd minute, linear in the range of 0.5-250 ppm, LOD of 0.206 ppm and LOQ of 0.265 ppm. This sensor provides selective, precise, and accurate results. The sensor is stable for more than one month on storage at room temperature (25°C). The sensor includes measurement results that are not statistically significant when compared to the UV-Vis spectrophotometer method.

ACKNOWLEDGMENT

The author would like to thank the Pharmacy Laboratory of Ma Chung University which has supported this research by providing good facilities.

AUTHOR CONTRIBUTIONS

Conceptualization, M. H. A.; Methodology, M. H. A.; Software, M. H. A., S. Y.; Validation, M. H. A., E. M.; Formal Analysis, S. Y.; Investigation, S. Y.; Resources, M. H. A., E. M.; Data Curation, M. H. A.; Writing - Original Draft, S. Y.; Writing - Review & Editing, E. M.; Visualization, S. Y.; Supervision, M. H. A.; Project Administration, E. M.; Funding Acquisition, M. H. A.

FUNDING STATEMENT

This research did not receive any specific grant from funding agencies in the public, commercial, or not-for-profit sectors.

CONFLICT OF INTEREST

The authors declared no conflict of interest.

REFERENCES

- Clayden, J., & Greeves, N. S. (2012). *Organic Chemistry* (Second). New York: Organic Chemistry Frontiers.
- Hermanto, D., Kuswandi, B., Siswanta, D. & Mudasir. (2019). Inhibitive Determination of Hg(II) in Aqueous Solution Using Urease Amperometric Biosensor. *Indonesian Journal of Chemistry*; 19; 786–795. doi: 10.22146/ijc.40617.
- Hidayat, M. A., Puspitaningtyas, N., Gani, A. A. & Kuswandi, B. (2017). Rapid Test for the Determination of Total Phenolic Content in Brewed-filtered Coffee Using Colorimetric Paper. *Journal of Food Science and Technology*; 54; 3384–3390. doi: 10.1007/s13197-017-2757-7.
- Huber, L. (2007). *Validation and Qualification in Analytical Laboratories* (Second Ed.). New York: Informa Healthcare USA, Inc.
- Jamaluddin, A. M. & Reazul, H. M. (2003). A Rapid Spectrophotometric Method for the Determination of Mercury in Environmental Samples using Bis (salicylaldehyde) orthophenylenediamine'. *Research Journal of Chemical Sciences*; 1; 46–59.
- Kristianingrum, S. (2009). Kajian Teknik Analisis Merkuri yang Sederhana, Selektif, Prekonsentrasi, dan Penentuannya Secara Spektrofotometri. *Prosiding Seminar Nasional Penelitian, Pendidikan Dan Penerapan MIPA*, 345–350.
- Kumar, V., Singh, D. K., Mohan, S., Bano, D., Gundampati, R. K. & Hasan, S. H. (2017). Photochemistry and Photobiology. *Journal of Photochemistry & Photobiology, B: Biology*; 168; 67-77. doi: 10.1016/j.jphotobiol.2017.01.022.
- Kuswandi, B. (2008). *Sensor Kimia*. Jember: Program Studi Farmasi Universitas Jember.
- Miller, J. N., & Miller, J. C. (2010). *Statistics and Chemometrics for Analytical Chemistry*. In *Pearson Education Limited* (Sixth). Gosport: Ashford Colour Press Ltd.
- Mona, R. K., Pontoh, J., & Yamlean, P. V. Y. (2018). Analisis Kandungan Merkuri (Hg) pada Beberapa Krim Pemutih Wajah Tanpa Ijin BPOM yang Beredar di Pasar 45 Manado. *Jurnal Ilmiah Farmasi*, 7; 240-248.
- Nethercote, P. & Ermer J. (2012). *Method Validation in Pharmaceutical Analysis. A Guide To Best Practice*. Weinheim: Wiley VCH.



Characterization of microencapsulated Saga Leaves Extract (*Abrus precatorius* L.) and Analgetic Activity Tests in Male Mice (*Mus musculus*)

Nabilah Nauli Jehan^{1,2*}, Titik Sunarni², Dian Marlina²

¹Departement of Pharmacy, Sekolah Tinggi Ilmu Kesehatan An Nasher, Cirebon, Indonesia

²Master Program of Pharmaceutical Science, Faculty of Pharmacy, Universitas Setia Budi, Surakarta, Indonesia

*Corresponding author: naulijehann@gmail.com

Submitted: 7 March 2023

Revised: 9 December 2023

Accepted: 13 December 2023

Abstract

Background: Saga leaves are one of the plants that have analgesic activity. Saga leaves contain phenol compounds, flavonoids, tannins, alkaloids, and saponins. Phenol has instability with oxygen, light, and high temperatures. Therefore, the microencapsulation process is necessary. Microcapsule characterization in this study included encapsulation efficiency, particle size, distribution value and morphology. **Objective:** This research was to determine the characterization of microcapsules and the analgesic activity of saga leaf extract microcapsules in male mice. **Methods:** The microencapsulation process conducted in this study was carried out using the spray drying method. Saga leaf extract was coated with the coating material in the ratio of 1:20. Several ratios of maltodextrin (MD) and soy protein isolate (SPI) (100%:0%); (75%:25); (50%:50%); (25%:75%) were applied as the coating material. The encapsulation efficiency was determined by comparing the total phenol content of the extract and microcapsule. Particle size and distribution values were tested using a particle size analyzer. Microcapsule morphology was seen using scanning electron microscopy. Analgesic activity test using the tail-flick method with mice as test animals. Data analysis in this study used one-way ANOVA. **Results:** The encapsulation efficiency obtained was 31.40-80.29%. The particle size obtained in the microcosm was 17.70-30.90 μm . The distribution value obtained was 1.42-2.45. The morphology of the microcapsule obtained was round and had wrinkles. The analgesic activity obtained in this study resulted in significantly different pain inhibition values before and after microencapsulation. **Conclusion:** The characteristics of microcapsule preparations are well-known, and the analgesic activity of various microcapsules was 42.43-57.15%.

Keywords: analgesic activity, microencapsulation, phenol, saga leaf extract

How to cite this article:

Jehan, N. N., Sunarni, T. & Marlina, D. (2023). Characterization of microencapsulated Saga Leaves Extract (*Abrus precatorius* L.) and Analgetic Activity Tests in Male Mice (*Mus musculus*). *Jurnal Farmasi dan Ilmu Kefarmasian Indonesia*, 10(3), 280-289. <http://doi.org/10.20473/jfiki.v10i32023.280-289>

INTRODUCTION

The saga plant grows wild in the forest or the yard of the house. Saga leaves have a sweet and bitter taste at the end when consumed. The bitter taste elicited from saga leaves is due to the presence of abrine (Agustina *et al.*, 2020). The content found in saga leaves, according to Nisak *et al.* (2021) are flavonoids, tannins, saponins, alkaloids and phenols. These phenolic compounds are unstable to oxygen, light or high temperatures, so their use will be a problem (Yang *et al.*, 2016). Analgesic activity in research conducted by Indawati *et al.* (2020) with a dose of 110 mg/20 g BW of mice had a strength of 60.81% but was weaker than acetosal.

In recent years, drug development has been carried out in pharmaceutical preparations and technology for the manufacture of herbal-based drugs, one of which is microencapsulation. Saga leaves are herbal medicines that will be developed in microcapsule preparations because they have a bitter taste and retain the phenolic compounds contained therein (Agustina *et al.*, 2020) (Yang *et al.*, 2016). Siregar and Kristanti (2019) stated that microcapsules with a core and coating material ratio of 1:20 managed to coat the core material well compared to a 1:10 ratio. The content of total phenolic compounds from microcapsules resulted from a ratio of 1:20, which is greater than that of 1:10.

Maltodextrin is the most commonly used coating material in the microencapsulation process. Maltodextrin is obtained from hydrolysis of corn starch acid has a degree of dextrose equivalence between 10 to 20. Maltodextrin is also biodegradable and biocompatible, increases oxidation and stability, and prevents degradation (Wati *et al.*, 2020). In the world of food, soybeans are often used in intermediate products, namely protein isolates. Soy protein isolate coatings were used because the protein was a coating material that was capable of carrying active compounds and drugs so that it can optimize delivery on target (Dewandari *et al.*, 2013).

Preparation characterization is essential for microencapsulation to determine the quality of the preparation. Characterization of the microencapsulation includes particle size, distribution value (span), encapsulation efficiency of phenolic compounds and morphology. The particle size in microcapsules has a size range of 1-1000 μm . Encapsulation efficiency is a comparison between the total contents and the surface of the microcapsule. The distribution value (Span) is a measure of the width of the particle distribution to the microcapsules and aims to determine whether the particle distribution is uniform or not.

Nevertheless, scientific evidence regarding the microencapsulation of saga leaf extract has never been carried out. The results of this study will be able to provide information about the microencapsulation of saga leaf extract in relation to the analgesic activity of the ethanol extract of saga leaves. The aims of the study were to determine the characterization of microcapsules of ethanol extract of saga leaves from a combination of maltodextrin and soy protein isolate coatings using the spray drying method based on the test parameters of particle size, distribution value, encapsulation efficiency of phenolic compounds, morphology and to determine the analgesic activity in male mice.

MATERIALS AND METHODS

Materials

The materials to be used in this study were saga leaf *Simplicia* obtained at B2P2TOOT Tawangmangu, maltodextrin DE 10-12 (Chemipan Co., LTD), soy protein isolate (SPI), 70% ethanol (Merck), folin-ciocalteu, ibu profen, Na CMC, sodium acetate (Merck), distilled water, concentrated HCl, methanol (Merck), magnesium, mayer, wagner, dragendorf, FeCl_3 (Merck), Na_2CO_3 (Merck), AlCl_3 , NaOH.

Tools

The tools used in this study were glassware (Pyrex), analytical balance (OHAUS Paj 1003), test tubes, rotary evaporator (BUCHI Rotavapor R-205, Germany), spray dryer (BUCHI B-290, BUCHI Labortechnik AG, Switzerland), PSA (Mastersizer 3000), SEM (FEI Quanta FEG 200 HR-SEM), UV-Vis Spectrophotometry (Shimadzu UV-1800), vortex, stopwatch, oral3 syringe and tail flick analgesic meter.

Method

Extraction of Saga Leaf

Saga leaves that had been dried in the sun for three days (dry) were then crushed using a blender. Then, it was filtered using a 40 mesh sieve until powder was obtained. Saga leaf powder was macerated using 70% ethanol with a ratio of sample and solvent of 1:10 g/v for 6 hours with occasional stirring. The sample was allowed to stand for 18 hours, and then the filtrate was filtered. The remaining saga leaf pulp was remacerated using half the amount of the first solvent. The sample was again filtered using filter paper and evaporated at a temperature of 40-50°C (Indonesian Herbal Pharmacopeia, 2017).

Determination of water content

Weigh the sample as much as 10 grams and then put it into a dry flask. 100 mL of water-saturated Toluene was put into the flask, and the tool. Boil using low heat until

no water drips; drain the water during the process. ed. The results of the water content obtained were recorded by looking at the volume on the scale of the tool. Moisture content is calculated in %b/v (Indonesian Herbal Pharmacopeia, 2017).

Determination of drying shrinkage

The determination of drying shrinkage was used using a moisture balance tool. We weighed a sample of saga leaf simplisia as much as 2 grams above the tool, then closed and waited until the % drying shrinkage appeared, which was marked by an alarm sound.

Phytochemical screening

Flavonoids

Take 0.1 g of concentrated extract of saga leaves into 2-3 mL of ethanol solution, heated, and enough magnesium powder and 2 mL of concentrated HCl were added. Colour changes to red, yellow, or orange indicate the presence of flavonoids (Hanani, 2021).

Alkaloid

Identification of alkaloids was carried out by adding mayer, dragendorff and wagner reagents. About 0.5 g of concentrated extract was added into 2 mL of concentrated HCl, then filtered. The filtrate obtained was divided into three parts then added mayer, dragendorff and wagner reagents (Hanani, 2021).

Tannins

A concentrated extract of 0.1 g was dissolved in 5 mL of hot water plus 2-3 drops of 5% FeCl solution. The presence of tannin content was indicated by a change in colour to blue or blackish green (Hanani, 2021).

Saponin

A total of 0.5 g of extract dissolved with 70% ethanol was added to 10 mL of warm water, and then shaken for 1 minute. Added HCl 2N as much as 2-3 drops. Observed the foam formed for 30 seconds (Hanani, 2021).

Phenol

Take 0.5 mL of the test solution with a concentration of 11 mg/mL and 0.5 mL of a gallic acid reference solution with a concentration of 150 µg/mL in a test tube, then add 2.5 mL of folin ciocalteu reagent. Dilute with distilled water at a ratio of 1/10 v/v in a test tube. Let stand for 10 minutes, add 7.5 mL of 1M sodium carbonate solution, and observe the colour of the solution with the naked eye (Rollando & Monica, 2018).

Encapsulation of saga leaf extract

Preparation of microcapsules using the ratio of core material: coating material, which is 1:20. Weighed 1 gram of extract and put it into a glass beaker.

Maltodextrin, and soy protein isolate were added according to the formula weighing, and 79 mL of aquabidest was added, stirred until homogeneous with a magnetic stirrer at 700 rpm for 15 minutes. Put the preparation into a bottle and label it according to the formula. After that, the suspension was sprayed using a spray dryer with the temperature according to the formula for 1 hour. The microcapsule preparation was stored at room temperature for seven days.

Total phenolic analysis

The total phenolic content was analyzed with some modifications of the method listed in the Indonesian Herbal Pharmacopoeia (IHP) (Indonesian Herbal Pharmacopoeia, 2017). Make a 400 ppm gallic acid standard curve solution and then dilute it with a concentration series of 60, 50, 40, 30 and 20 ppm. Samples of 0.01 g extract and 0.21 g microcapsules were dissolved in 10 mL methanol p.a, homogenized with a vortex for 30 minutes and then filtered. Then 1 mL of sample was added with 5 mL of 7.5% folin ciocalteu and 4 mL of 1% sodium hydroxide. The solution was homogenized and incubated for 40-51 minutes in a dark room. Measurement of total phenolic absorption using a wavelength of 764 nm in UV-Vis spectrophotometry.

Total flavonoid analysis

The total flavonoid content was analyzed with some modifications of the methods listed in the IHP (Indonesian Herbal Pharmacopoeia, 2017). A 400 ppm quercetin standard curve solution was prepared and then diluted with a concentration series of 60, 50, 40, and 30 ppm. Samples of 0.02 g extract and 0.42 g microcapsules were dissolved in 10 mL ethanol p.a, homogenized with a vortex for 30 minutes, and then filtered. A sample of 0.5 mL was added to 1.5 mL ethanol p.a, 0.1 mL 10% aluminium chloride, 0.1 mL 1 M sodium acetate and 2.8 mL distilled water. The solution was homogenized and incubated for 16-32 minutes. Total flavonoid absorbance was measured using a wavelength of 441 nm in UV-Vis spectrophotometry.

Microencapsulation characterization

Encapsulation efficiency

Determination of encapsulation efficiency (%) was done according to Isailovic (2012). The encapsulation efficiency was calculated by comparing the total phenol content in the microcapsules with the extract.

$$\text{Encapsulation efficiency} = \frac{\text{total phenolic microcapsule}}{\text{total phenolic extract}} \times 100 \%$$

Table 1. Saga leaf extract microcapsule preparation formula

Formula	Extract (g)	Maltodextrin (g)	Soy Protein Isolate (g)	Aquabidest (mL)	Inlet Temperature (°C)
F1	1	20	0	79	115
F2	1	5	15	79	115
F3	1	10	10	79	120
F4	1	15	5	79	125
F5	1	0	20	79	125

Particle size and distribution values

The particle size of the microcapsules was analyzed using a particle size analyzer (PSA) master-sizer 3000 laser diffraction (Malvern Instrument) carried out by dispersing the microcapsules with distilled water as much as 10 mL homogenized using a vortex mixer after homogeneous the sample was inserted into the cuvette in the tool until the appropriate intensity is reached and observed the analysis results (Siregar & Kristanti, 2019). Determination of the distribution value is obtained using the following formula:

$$\text{Span value} = \frac{D(90) - D(10)}{D(50)}$$

Description:

D(90) = Particle diameter at 90%

D(10) = Particle diameter at 10%

D(50) = Particle diameter at 50%

Morphology

Morphological analysis of microcapsules was determined according to Dewandri et al. (2013). The microcapsules obtained were analyzed for morphology using Scanning Electron Microscopy (SEM) Samples were placed in a sample holder and then coated with gold particles using a fine coater. Samples were analyzed and viewed morphologically at 1000x intensity and magnification.

Analgesic activity test

The test animals used were male mice aged 6-8 weeks, weighing 18-25 g. A total of 40 mice were randomly divided into eight treatment groups (each group of 5 mice). Group I mice (negative control) were treated with 1% CMC Na suspension orally. Group II mice (positive control) were given a suspension of 0.54 mg/20 g BW of ibu profen. Group III was treated with saga leaf extract 8 mg/20 g BW. Group IV, V, VI, VII, and VIII mice were each treated with saga leaf extract microcapsules 160 mg/20 g BW.

The analgesic test method used in this study was tail flick. The tail flicks analgesic meter will induce pain by irradiating the mice's tails with infrared at a wavelength of 70 foci. The nociceptive pain response was measured at 30, 60, 90 and 120 minutes.

Data analysis

The data obtained were analyzed in two ways: ANOVA analysis test and LSD analysis. ANOVA analysis is expressed as mean ± SD, where the test results are significant if $p \leq 0.05$. LSD further analysis was conducted with a 95% confidence level.

RESULTS AND DISCUSSION

Characteristics of saga leaf extract

In this study, saga leaf simplisia had a moisture content of 7.33% and a drying shrinkage of 11.67%. The water content of the simplisia is said to meet the requirements, but the drying shrinkage does not meet the criteria because it is more than 10%. This is likely to cause enzymatic processes and damage caused by microbes. The drying shrinkage of simplisia is more significant than the water content because the residual substances that evaporate during the shrinkage process are not only water but several compounds that can disappear at a temperature of 105°C. The research results of saga leaf extract are presented in Table 2.

Table 2. Characteristics of saga leaf extract

Characteristics	Value
Yield (%)	35.79
Water content (%)	3.33 ± 0.47
Total phenol (%)	6.70 ± 0.01
Total flavonoids (%)	3.66 ± 0.00

Note: average value based on three replications

The yield of ethanol extract of saga leaf obtained was 35.79%. The yield in this study is greater than the research by Nisak *et al.* (2021), which obtained a value of 31.4%. This is because this study used 70% ethanol solvent, which is more polar than 96% ethanol. So that, the yield ethanol extract of saga leaf obtained will be and more significant because the polar secondary metabolic will be more extracted. According to Situmeang (2019), the yield of saga leaf extract obtained was 10%. This happens because it uses a solvent with a low level of polarity so that it cannot attract polar compounds. The water content obtained in this study was 3.33% ± 0.470. This is in accordance with the requirements in FHI (Indonesian Herbal Pharmacopoeia) that the moisture

content of a good extract should not be more than 10%. The moisture content of saga leaf extract in research by Nisak *et al.* (2021) obtained a % moisture content of 2.83%.

Phytochemical screening

Phytochemical screening was carried out to determine the secondary metabolite compounds contained in the sample. Several kinds of secondary metabolites were tested, namely flavonoids, alkaloids, tannins, phenols, and saponins. These results have similarities with the results obtained in a study by Nisak *et al.* (2021). The results of the phytochemical screening of saga leaf extract are presented in Table 3. The table shows that all tests carried out are positive.

Total phenol and flavonoid content in extracts

Determination of phenolic content was carried out with folin-ciocalteu reagent, which will oxidize the hydroxyl group of phenol group compounds to produce complex compounds marked by the colour of the yellow solution turning blue-green. The process runs slowly in an acidic atmosphere, so in the test, sodium hydroxide is added, which is alkaline, so as to make the reaction faster. The standard solution used was gallic acid, which was one of the stable phenolics and was classified as a simple phenol group capable of high reactivity to folin-ciocalteu. The maximum wavelength was obtained at 764 nm, and the operating time was 40-51 minutes. The correlation coefficient value obtained was 0.9977, and the linear regression equation for gallic acid absorbance obtained $y = 0.010x + 0.1143$, which was used to determine the total phenolic content in extracts and microcapsules of saga leaf extract.

Flavonoids are natural phenol class compounds that are distributed in various plants. The determination of total flavonoids in extracts and microcapsules of saga leaf extract used UV-Vis spectrophotometry with a maximum wavelength of 441 nm and an operating time of 16-32 minutes. The reagent used in the determination of total flavonoids was aluminium chloride, which was often referred to as the colourimetric method. This

method is a very simple method for testing flavonoids of essential flavone and flavonol groups so that they react with Al (III) to turn the sample into a yellow color. The linear regression equation obtained is $y = 0.0098$ and R^2 value = 0.9954. Table 2 states that the phenol and flavonoid content in saga leaf extract is 6.70% and 3.66%, respectively.

The high phenol content can be caused by several factors, one of which is the use of solvents during the extraction process. The solvent used in the extraction is ethanol, which has polar properties that can attract polar compounds such as phenols, flavonoids, tannins, steroids, and alkaloids (Dia *et al.*, 2015). Aside from the use of proper solvents, the mature saga leaf sample is what causes the high amounts of a sample. As a result, the content of secondary metabolites is larger in the older ones. Anwar *et al.* (2017) discovered that older leaves had greater phenolic levels when comparing phenolic levels based on leaf age in *Aquilaria beccariana* plants.

Characterization of saga leaf extract microcapsules

Total phenol and flavonoid content in microcapsules

From Table 4, the results of the total phenolic content in the extract and microcapsule preparations produced higher levels. This could occur due to the influence of the temperature used during the microencapsulation process using spray drying. In line with research by Kistriyani *et al.* (2020), the total phenolic content in microcapsules decreased after encapsulation, where the phenolic content in the extract was 0.34 g/mL, while in microcapsules, the complete phenolic content was 0.09 g/mL. In microcapsules, F1 is lower than F2; this is because soy protein isolate has a high viscosity, so it allows the homogenization process between the extract and the dressing to be uneven. So, the sample content taken has a trim level. The combination of maltodextrin is essential to homogenize the preparation because it has a lower viscosity so the highest level is obtained in F2.

Table 3. Phytochemical screening results of saga leaf extract

Phytochemical Test	Reagent	Results
Flavonoid	Magnesium dan HCl Concentrated	Yellow (+)
Alkaloid	a. Mayer b. Wagner c. Dragendroff	a. Beige precipitate (+) b. Brown precipitate (+) c. Orange precipitate (+)
Tanin	FeCl ₃	Blackish Green (+)
Phenol	Folin-ciocalteu dan Na ₂ CO ₃	Purple-black (+)
Saponin	HCl 2N	Foam stabil (+)

Table 4. Characterization of saga leaf extract microcapsules

Sample	Total phenol (%)	Total flavonoids (%)	Encapsulation efficiency of total phenol (%)	Particle size (μm)	Distribution value
F1	5.15 \pm 0.01	3.20 \pm 0.03	76.89 \pm 0.26	30.17 \pm 0.57	2.36 \pm 0.08
F2	5.38 \pm 0.00	3.20 \pm 0.01	80.29 \pm 0.27	25.23 \pm 0.57	1.63 \pm 0.02
F3	4.83 \pm 0.02	2.22 \pm 0.00	72.16 \pm 0.33	23.60 \pm 0.37	1.77 \pm 0.03
F4	2.80 \pm 0.01	1.70 \pm 0.00	41.75 \pm 0.14	17.87 \pm 0.04	1.42 \pm 0.01
F5	2.10 \pm 0.01	1.53 \pm 0.00	31.40 \pm 0.12	-	-

The microcapsule F3 formula obtained a viscosity that was not too high, but in this preparation, a temperature of 120°C was used to produce a preparation that was dry enough. As for microcapsules F4 and F5 using a temperature of 125°C, this is because the nature of maltodextrin has high hygroscopicity, causing the ability to bind saga leaf extract to decrease and requires a high temperature during the spray drying process to produce a preparation that is dry enough. The influence of higher temperatures will affect the degradation of polyphenols and the release of phenolic components such as hydroxyl groups, resulting in a decrease in phenolic levels. Phenolic compounds are thermolabile and oxidative compounds, so they can influence the in the reduction of phenolic levels at high temperatures. The temperature in the encapsulation process can hydrolyze polyphenolic compounds into simpler phenolic compounds (Mahardani and Yuanita, 2021).

The flavonoid content produced in microcapsules of saga leaf extract is 3.20% \pm 0.01 - 1.53% \pm 0.00. The levels obtained are lower than the flavonoid levels in the extract. This is in line with the results obtained in the measurement of phenolic compounds. Flavonoids degrade when the temperature is above 90°C. Flavonoids are heat sensitive due to their hydroxyl and ketone groups, as well as unsaturated double bonds (Qiao *et al.*, 2014). The concentration of phenol and flavonoid totals in the F2 formula has the highest level; this is in line with research by Sadiyah *et al.* (2022) that treatment with a high concentration of soy protein isolate produced higher flavonoid levels than the treatment with a high concentration of maltodextrin. Soy protein isolate has good protection against oxidation. However, the use of maltodextrin combined with soy protein isolate aims to produce an amorphous glass matrix that acts as a barrier to the oxidation process during the encapsulation process (Sadiyah *et al.*, 2022). Total flavonoids of 3.20% and total phenols of 5.38% in the F2 formula were the highest values in this study.

Encapsulation efficiency of total phenol

The encapsulation efficiency of total phenol was a determination that aims to determine how many active compounds are trapped in the encapsulation process and

determine the success rate of the encapsulation process. The results of the encapsulation efficiency are in Table 4. From the analysis, it was found that each group of microcapsules had significant differences in encapsulation efficiency. The most excellent encapsulation efficiency in this study was obtained in the F2 microcapsule formula and the most negligible efficiency in the F5 formula. Several factors influence encapsulation efficiency. Specifically, the coating material utilized, as well as the ratio of active ingredient and coating material temperature during encapsulation, as well as the viscosity drying rate and surface cracks. The combination of maltodextrin coating material and soy protein isolate was effectively used in research conducted by Sadiyah *et al.* (2022) with the encapsulation method using a spray dryer. The ratio of the active compound and the coating material in this study used a ratio of 1:20, which is in line with research conducted by Siregar and Kristanti (2019), which states that with this ratio, the results obtained are better microcapsule characteristics, including encapsulation efficiency and total phenol than used comparison with the ratio of the active compound and the dressing material 1:10.

Particle size and distribution value

The results of the data analysis obtained said that there were significant differences in particle size and distribution value of each group of microcapsule formula. It can be concluded that each combination concentration can affect the results of particle size and distribution value. The results of the particle size and distribution value are in Table 4. The results of the particle size obtained: the greater the concentration of soy protein isolate the greater the particle size produced. This is because the viscosity of the suspension is higher than the concentration of soy protein isolate. This is due to the higher viscosity of the suspension compared to the maltodextrin treatment with more concentration. The higher the viscosity, the larger the droplets formed during the encapsulation process and the larger the particle size. In line with research by Metaviani *et al.* (2013), the particle size obtained gets more extensive if the concentration of maltodextrin gets smaller. The particle size values obtained in this study ranged from

17-30 μm . This is in line with what was stated by Hidayah (2016) that the particle size produced using a spray dryer is in the range of 10-400 μm .

The distribution value is set to determine the distribution of particle sizes produced during the encapsulation process. The distribution value is obtained from the particle size value at 90% minus the particle size value at 10% divided by the particle size value at 50%. This happens because there are differences in the concentration of the coating material or perhaps when the formula loading process is not evenly distributed, resulting in a very high distribution value. The distribution value of microcapsules with concentration F4 was found to be the best value. This value indicates that the presence of maltodextrin plays a role in the uniformity of particle distribution. This is because, theoretically, the smaller the distribution value. The better the uniform particle size distribution (Krishnaiah *et al.*, 2012). Because the preparation was water soluble, the distribution value for microcapsule F5 could not be read.

Morphology test

From the results obtained, it can be seen that the shape of the microcapsules is round. There are clumps that are not uniform and irregular. This is in line with research conducted by Krishnaiah *et al.* (2012), most particles have a round shape and show little agglomeration. There are differences in the morphology of F1 and F2 microcapsules with other formulas. The results of F1 microcapsules have a larger size and are more heterogeneous. In the morphology of microcapsules with F1 concentration, it can be seen that smaller particles are attracted to and attached to larger

particles around them. This happens because of the heterogeneity, which makes the force of attraction and clumping between the particles stronger (Sari, 2021).

From Figure 1, the results obtained show that the shape of the microcapsules is round, and some clumps are not uniform and irregular. This is in line with research conducted by Krishnaiah *et al.* (2012), most particles have a round shape and show little agglomeration. There are differences in the morphology of F1 and F2 microcapsules with other formulas. The results of F1 microcapsules have a larger size and are more heterogeneous. In the morphology of microcapsules with F1 concentration, it can be seen that smaller particles are attracted to and attached to larger particles around them. This happens because of the heterogeneity of the particles, which makes the force of attraction and clumping between the particles stronger (Sari, 2021).

The suspension between the active compound and the coating in this study used aquabidest so that the interaction between maltodextrin and aquabidest causes the hydroxyl groups contained therein to dissolve (Yuliaty & Susanto, 2015). DE describes Maltodextrin (dextrose Equivalent), where the higher the DE value, the higher the water solubility, so this is related to the microcapsule morphology. The maltodextrin used in this study has a DE value of 10-11, which is high, so preparations with high maltodextrin concentrations will cause the preparation to be hygroscopic. From this, it is important to combine with soy protein isolate to produce preparations with good morphology.

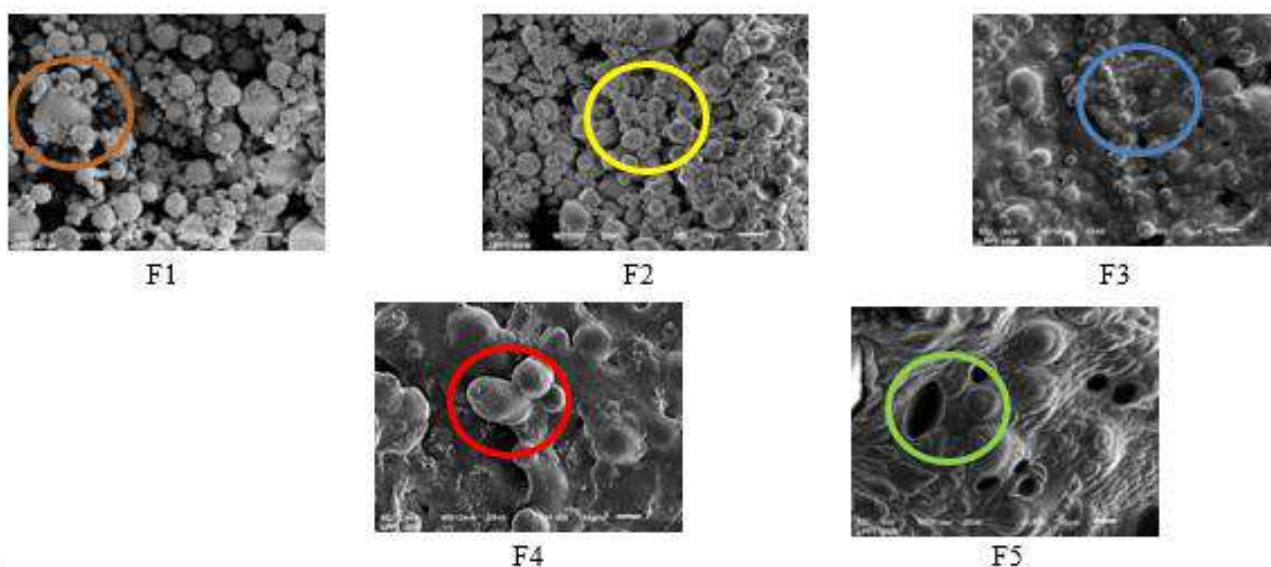


Figure 1. Surface morphology of saga leaf extract microcapsules of all groups with SEM

Analgesic activity test

The tail flick method was used to investigate analgesic activity in eight different test groups. This study was approved by the ethics commission of health research at Dr. Moewardi Hospital with letter number 1.369/X/HREC/2022. In Figure 2 $\Delta T1$, the results of the analysis of the extract group and microcapsule preparations showed significant differences with the positive control. In the F2 microcapsules group, there were significant differences in the negative, positive and extract groups. The F4 microcapsule group only had a significant difference in the positive and extract groups in $\Delta T2$, and in $\Delta T3$ there was only a significant difference in the negative and extract groups. In $\Delta T4$ groups F1, F2, F3, and F4, there were significant differences between the negative, positive, and extract control groups. Meanwhile, in the F5 microcapsule group, there were no significant differences from the negative, positive, and extract control groups. In Figure 2, it was obtained that the positive control group has an inhibitory response that is significantly different from the negative control group. This happens because ibuprofen has not given a maximum response because the absorption of ibuprofen in blood plasma takes 30-60 minutes and will reach onset after one hour, so that the response that appears is not significantly different compared to saga leaf extract preparations tested. Saga leaf extract gives a response that is not significantly different from ibuprofen, this is because the ethanol extract of saga leaves contains flavonoids, terpenoids and other secondary metabolites that function as analgetics. However, the microcapsule preparation is significantly different from ibuprofen at $\Delta T2$, this is because the microcapsule preparation has a coating which results in the release time of the active substance requiring a longer time. The microcapsule preparation reaches the highest pain inhibition time at 90 minutes.

The microcapsule preparation will pass through the human digestive tract so that the outer layer of the microcapsule will dissolve in the stomach due to the lower pH atmosphere, so that only the core material is absorbed in the small intestine. The length of the active substance release process is due to the content of the coating more than the active substance. The greater the active substance content. The process of releasing the active substance from microparticles increases more (Sinha *et al.* 2004).

The data Increase in pain inhibition was continued with the one-way ANOVA test and the results of the analysis in the positive control group were significantly different compared to the other groups because the sig value <0.05 . The extract and microcapsule groups all have significant differences because they get a sig value <0.05 . In the F1 microcapsule group, there is no significant difference from the F2 and F3 groups because it gets a sig value >0.05 . In microcapsules F4 and F5, there is no significant difference in the value of increasing pain inhibition. Based on Table 5. the results of the acquisition of pain inhibition produced by the extract group. F1. F2 and F3 microcapsules are more than 50%. according to Puspitasari *et al.* (2003). it was stated that they had analgesic activity. The content of secondary metabolite compounds such as flavonoids present in the sample can influence this, which are thought to have analgesic activity with a mechanism of action capable of inhibiting the cyclooxygenase pathway that produces pain mediators such as prostaglandins, histamine, bradykinin and leukotrien. The presence of flavonoids can also affect the metabolic activity of arachidonic acid enzymes. The higher the flavonoid content, the higher the arachidonic acid content that can inhibit cyclooxygenase. resulting in high analgesic power.

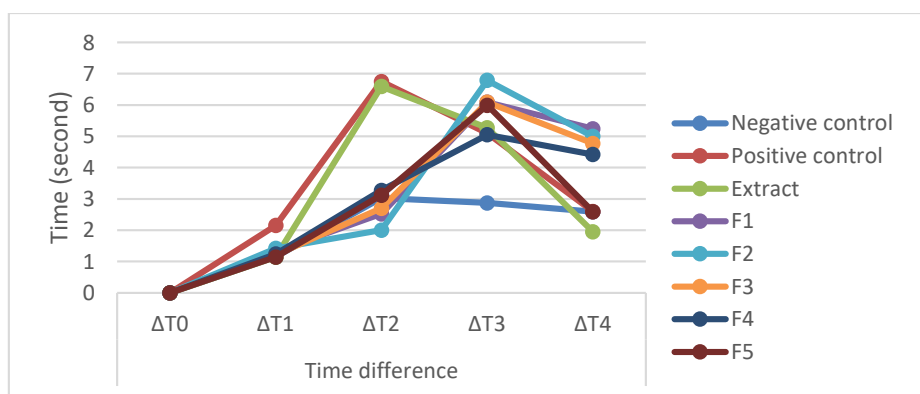


Figure 2. Data graph of the average difference in pain inhibition response time

Table 5. AUC data and percentage of pain inhibition

Sample	AUC data (Total ± SD)	Increase in pain inhibition (%) (Mean ± SD)
Negative Control	242.67 ± 6.05	-
Positive Control	458.67 ± 11.66	89.01 ± 1.62
Extract 8mg/20gr	418.92 ± 8.47	72.67 ± 2.82
F1 160 mg/20gr	376.44 ± 8.51	55.25 ± 5.96
F2 160 mg/20gr	381.33 ± 10.11	57.15 ± 2.15
F3 160 mg/20gr	371.52 ± 9.16	53.15 ± 4.12
F4 160 mg/20gr	352.98 ± 13.04	45.48 ± 4.95
F5 160 mg/20gr	345.66 ± 15.72	42.43 ± 5.06

CONCLUSION

The results of microencapsulation characterization of saga leaf extract from a combination of maltodextrin and soy protein isolate based on particle size parameters, distribution values, phenolic compound encapsulation efficiency and morphology by spray drying method each obtained an average value of 17.70-30.90 µm; 1.42-2.45; 31.40-80.29% and round shape and has wrinkles, respectively. The analgesic activity obtained in this study resulted in significantly different pain inhibition values before and after microencapsulation. The analgesic activity of various microcapsules was 42.43-57.15%.

SUGGESTION

The results of the high distribution value in microencapsulation of saga leaf extract are too high so it needs to be improved in terms of manufacturing and the ratio of coating materials for further research.

ACKNOWLEDGMENT

The author would like to thank STIKES An Nasher Cirebon for funding the Masters program.

AUTHOR CONTRIBUTIONS

Conceptualization, N. N. J., T. S., D. M.; Methodology, N. N. J., T. S., D. M.; Software, N. N. J.; Validation, N. N. J.; Formal Analysis, N. N. J., T. S., D. M.; Investigation, N. N. J.; Data Curation, N. N. J., T. S., D. M.; Writing - Original Draft, N. N. J.; Writing - Review & Editing, T. S.; Visualization, D. M.; Supervision, T. S., D. M.; Project Administration, N. N. J.

FUNDING STATEMENT

This research did not receive any specific grant from funding agencies in the public, commercial, or not for profit sectors.

CONFLICT OF INTEREST

The authors declared no conflict of interest.

REFERENCES

- Agustina, R., Cahyana. A. H. & Tjandrawinata. R. R. (2020). Abrine (N-methyltryptophan) an Alkaloid from *Abrus precatorius* Linn. Leaves Extract. *AIP Conference Proceedings*; 22-42. doi: 10.1063/5.0007888.
- Anwar. K., Rahmanto, B., Triyasmono, L. & Rizki, M. I. (2017). The Influence of Leaf Age on Total Phenolic, Flavonoids, and Free Radical Scavenging Capacity of *Aquilaria beccariana*. *Research Journal of Pharmaceutical Biological and Chemical Sciences*; 18; 129-133.
- Dewardari, K. T., Yuliani. S. & Yasni. S. (2013). Ekstraksi dan Karakterisasi Nanopartikel Ekstrak Sirih Merah (*Piper crocatum*). *Jurnal Penelitian Pascapanen Pertanian*; 10; 65-71. doi: 10.21082/jpasca.v10n2.2013.58-65.
- Dia, P. S. S., Nurjanah. N. & Mardiono, J. A. (2015). Chemical Composition, Bioactive Components, and Antioxidant Activities from Root, Bark and Leaf Lindur. *Jurnal Pengolahan Hasil Perikanan Indonesia*; 18; 205-219. doi: 10.17844/jphpi.2015.18.2.205.
- Hanani, E. (2021). Analisis fitokimia. Jakarta: EGC.
- Indawati. I., Didin. A. & Muhimatul. U. (2020). Uji Efek Analgetik Ekstrak Etanol Daun Saga (*Abrus precatorius* L.) terhadap Mencit Putih (*Mus musculus*) Jantan yang Diinduksi Asam Asetat. *Medimuh*; 1; 1-6.
- Indonesian Herbal Pharmacopeia. (2017). Farmakope Herbal Indonesia Edisi II Tahun 2017. *Pocket Handbook of Nonhuman Primate Clinical Medicine*; 213-218.
- Kistriyani, L., Fauziyyah, F. & Rezeki, S. (2020). Profil Release Enkapsulasi Antosianin. Flavonoid dan Fenolik pada Kulit Semangka Menggunakan

- Metode Spray Drying. *Eksergi*; 17; 33-38. doi: 10.31315/e.v17i2.3098.
- Krishnaiah, D., Sarbatly, R. & Nithyanandam, R. (2012). Microencapsulation of *Morinda citrifolia* L. Extract by Spray Drying. *Chemical Engineering Research and Design*; 90; 622–632. doi: 10.1016/j.cherd.2011.09.003.
- Metaviani, J. & Darmadji, P. (2013). Mikroenkapsulasi Ekstrak Bunga Rosella (*Hisbiscus Sabdariffa* L.) dengan Enkapsulan Maltodekstrin Menggunakan Metode Pengeringan Semprot (Spray Drying). *Skripsi*; Universitas Gadjah Mada, Yogyakarta.
- Nisak, S. K., Pambudi, D. S. & Waznah, U. (2021). Uji Antibakteri Ekstrak Etanol Daun Saga (*Abrus precatorius* L.) Terhadap Bakteri *Streptococcus mutan* ATCC 31987 dan *Staphylococcus aureus* ATCC 25923PK /5. *Seminar Nasional Kesehatan*; 1; 385–392.
- Puspitasari, H., Listyawati, S. & Widiyani, T. (2003). Aktivitas Analgetik Ekstrak Umbi Teki (*Cyperus rotundus* L.) pada Mencit Putih (*Mus musculus* L.) Jantan. *Biofarmasi*; 1; 50-57.
- Qiao, L., Sun, Y., Chen, R., Yu, F., Zhang, W., Xi, L. & Ye, X. (2014). Sonochemical Effects on 14 Flavonoids Common in Citrus: Relation to Stability. *PLoS ONE*; 9; 1–10. doi: 10.1371/journal.pone.0087766.
- Rollando & Monica. E. (2018). Penetapan Kandungan Fenolik Total dan Uji Aktivitas Antioksidan Fraksi Air Ekstrak Metanol Kulit Batang Faloak (*Sterculia quadrifida* R.BR). *Scientia Jurnal Farmasi dan Kesehatan*; 8; 29-36. doi: 10.36434/scientia.v8i1.119
- Sadiyah, I., Rossi, I. & Cahyana, Y. (2022). Karakteristik dan Senyawa Fenolik Mikrokapsul Ekstrak Daun Kelor (*Moringa Oleifera*) dengan Kombinasi Maltodekstrin dan Whey Protein Isolat. *Jurnal Teknologi Industri Pertanian*; 32; 273–282.
- Sari. N. (2021). Mikroenkapsulasi Ekstrak Daun Ubi Jalar (*Ipomoea Batatas* L.) dengan Variasi Glukomanan dan Maltodekstrin sebagai Enkapsulan menggunakan Metode Spray Drying. *Tesis*; Universitas Gadjah Mada, Yogyakarta.
- Siregar. T. M. & Kristanti. C. (2019). Mikroenkapsulasi Senyawa Fenolik Ekstrak Daun Kenikir (*Cosmos caudatus* K.). *Jurnal Aplikasi Teknologi Pangan*; 8; 31–37. doi: 10.17728/jatp.3304.
- Situmeang, J. H. M. (2019). Uji Antimikroba Ekstrak Daun Saga (*Adenantha pavonina*) pada Penekanan Pertumbuhan Bakteri *Escherichia coli*. *Skripsi*; Universitas Sumatera Utara, Medan.
- Wati, R. R., Sriwidodo & Chaerunisaa, A. Y. (2020). Review Teknik Mikroenkapsulasi pada Ekstrak Mangosteen (A Review of Microencapsulation Techniques in Mangosteen Extract). *Journal of Current Pharmaceutical Sciences*; 3; 241–248. doi: 10.14692/jfi.12.1.19.
- Yang, R., Gao, Y., Zhou, Z., Strappe, P. & Blanchard, C. (2016). Fabrication and Characterization of Ferritin Chitosan Lutein Shell Core Nanocomposites and Lutein Stability and Release Evaluation in Vitro. *RSC Advances*; 6; 35267–35279. doi: 10.1039/c6ra04058f.
- Yuliawaty, S. T. & Susanto, W. H. (2015). Effect of Drying Time and Concentration of Maltodextrin on the Physical Chemical and Organoleptic Characteristic of Instant Drink Noni Leaf (*Morinda citrifolia*). *Jurnal Pangan dan Agroindustri*; 3; 41–51. doi: 10.1016/j.aaspro.2015.01.045



Fibrinolytic Protease Production: Impact of Initial pH and Temperature in Solid-State Fermentation by *Rhizopus microsporus* var. *oligosporus* FNCC 6010

Rebhika Lusiana¹, Achmad Toto Poernomo^{2*}, Achmad Syahrani²

¹Master Program of Pharmaceutical Sciences, Faculty of Pharmacy, Universitas Airlangga, Surabaya, Indonesia

²Department of Pharmaceutical Sciences, Faculty of Pharmacy, Universitas Airlangga, Surabaya, Indonesia

*Corresponding author: achmad-t-p@ff.unair.ac.id

Submitted: 30 May 2023

Revised: 23 October 2023

Accepted: 31 October 2023

Abstract

Background: Fibrinolytic enzyme is one of the cardiovascular disease therapies. *Rhizopus microsporus* var. *oligosporus* is microorganism that has been evaluated to produce fibrinolytic protease by fermentation. This study conducted fermentation of *helianthi annui* semen (sunflower seed) by *Rhizopus microsporus* var. *oligosporus* to produce fibrinolytic enzyme. **Objective:** This study aims to determine the effect of Initial pH and incubation temperature and its optimization in the production of fibrinolytic protease by *Rhizopus microsporus* var. *oligosporus* FNCC 6010 in solid-state fermentation on *helianthi annui* semen (sunflower seed) substrate. Optimum condition was determined by maximum protease and fibrinolytic activity. **Method:** A crude enzyme of protease fibrinolytic was obtained from the supernatant extract of fermented sunflower seed. Protease activity was measured by the skimmed milk agar (SMA) plate method, and fibrinolytic activity was determined by the fibrin agar plate method. **Result:** It was found that the starting pH affects both the proteolytic and fibrinolytic activity of enzymes that are produced in fermentation. The starting pH of 5.0 showed higher fibrinolytic and proteolytic activity values compared to the starting pH of 7.0. The incubation temperature 33 ± 1 °C had the higher activity compared to 28 ± 1 °C or 37 ± 1 °C. **Conclusion:** Initial pH and incubation temperature affect the proteolytic and fibrinolytic activity of crude enzyme extracted from fermented sunflower seed by *Rhizopus microsporus* var. *oligosporus*. The optimum condition for producing fibrinolytic protease in the state fermentation method was an initial pH of 5.0 and an incubation temperature of 33 ± 1 °C.

Keywords: fibrinolytic enzyme, protease, *Rhizopus microsporus* var. *oligosporus*, solid state fermentation

How to cite this article:

Lusiana, R., Poernomo, A. T. & Syahrani, A. (2023). Fibrinolytic Protease Production: Impact of Initial pH and Temperature in Solid-State Fermentation by *Rhizopus microsporus* var. *oligosporus* FNCC 6010. *Jurnal Farmasi dan Ilmu Kefarmasian Indonesia*, 10(3), 290-299. <http://doi.org/10.20473/jfiki.v10i32023.290-299>

INTRODUCTION

Cardiovascular diseases (CVDs) such as stroke, high blood pressure, arrhythmia, peripheral vascular disease, and valvular heart disease are the leading causes of death (Altaf *et al.*, 2021). Thrombosis, or accumulation of fibrin clots in blood vessels, is one of the risk factors for cardiovascular disease. Cardiovascular disease is usually followed by the rupture of atherosclerotic plaques and erosion, which activates coagulated proteins, leading to thrombus formation (Kotb, 2014).

The fibrinolytic enzyme is one of the thrombosis treatments that belong to the group of proteases. It catalyses the breakdown of fibrin clots by converting the inactive plasminogen to active plasmin or directly lysing the fibrin into fibrin degradation products (Krishnamurthy *et al.*, 2018). Microorganisms like bacteria and fungi are sources of fibrinolytic protease. These microorganisms have benefits over plants and animals in that they may be grown in huge quantities and in a short amount of time using fermentation techniques (Miglani *et al.*, 2017).

Rhizopus microsporus var. oligosporus is a fungus commonly used in the manufacture of tempeh (Nout & Kiers, 2005). Fermentation by *R. oligosporus* produces a wide variety of enzymes, including proteases (Lim *et al.*, 2022). A previous study reported that *R. microsporus var. oligosporus* made fibrinolytic enzymes by fermentation (Sarao *et al.*, 2010). Other studies have revealed that *Rhizopus species* can produce fibrinolytic proteases, including *R. oryzae* (Sada *et al.*, 2021); *Rhizopus chinensis* 12 (Xiao-Lan *et al.*, 2005); *R. microsporus var. tuberosus* (Zhang *et al.*, 2015); and *Rhizopus oligosporus* (Poernomo *et al.*, 2017).

The method commonly used to produce fibrinolytic enzymes from fungi is solid-state fermentation (SSF). Technically, solid-state fermentation (SSF) is used to produce microbial metabolites (Sambo *et al.*, 2021). This method is preferred rather than submerged fermentation (SmF) because the yield of enzymes in such cultivation systems increases significantly by 1.5 times greater (Muhammed *et al.*, 2020; Sharma *et al.*, 2021).

The SSF process is carried out on a solid substrate with certain environmental conditions. The substrate functions as a growth medium, which is a source of nutrients, including nitrogen, carbon, and minerals as activators and vitamins (Srivastava *et al.*, 2019; Ahamed *et al.*, 2022).

Sunflower seeds are rich in valuable compounds that are important as a fermentation media, such as

protein, carbon, and nitrogen with the percentage of 21%, 44.23%, and 0.41%, respectively (Grasso *et al.*, 2020; Hermansyah *et al.*, 2019; Karefyllakis *et al.*, 2019). In the previous study, sunflower oil cake was used as a growth medium of *Candida guilliermondii* by solid state fermentation to produce fibrinolytic enzymes (Rashad *et al.*, 2012). Furthermore, another study reported that sunflower meal had been reported as a substrate for producing protease enzyme from *R. oligosporus* (Rauf *et al.*, 2010).

Initial pH and incubation temperature are the critical factors that affect enzyme production in solid state fermentation method (Srivastava *et al.*, 2019). Initial pH has an important influence on the production of proteolytic enzymes because each microorganism grows best at its specific pH that exhibits its maximum metabolic activity (Kotb, 2015). The optimal pH of the medium helps in maintaining the homeostasis of electrical charge in the membrane and proteins in the medium by regulating proton pumps and transporting nutrients across the membrane (Muhammed *et al.*, 2020). pH also affects the enzymatic processes and transport of various components that support cell growth and enzyme formation (Rauf *et al.*, 2010). Buffers are commonly employed to maintain pH during microbial growth and are added to the media along with the nutrients required for growth (Madigan *et al.*, 2015).

During the fermentation process, the incubation temperature has an impact on the metabolic activity of microorganisms and the growth of fungi (Rauf *et al.*, 2010). Temperature also affects the stability of the enzymes produced (Kotb, 2013; Sada *et al.*, 2021). Furthermore, an increase of incubation temperature causes a rise of enzyme activity up to a certain point, and after that, there can be an effect on the growth of microorganisms and allow enzyme denaturation to occur (Vinuthna & Raju, 2022). It was reported that *R. oligosporus* shows faster growth of mycelium at a temperature of 25 – 37 °C (Nout & Kiers, 2005).

This research aims to develop fermented helianthi annui semen by *R. microsporus var. oligosporus* FNCC 6010 to produce fibrinolytic enzymes in solid-state fermentation. The impact of starting pH and incubation temperature on enzyme synthesis will be examined. The proteolytic activity of the crude enzyme was assayed using the skimmed milk agar (SMA) plate method, and the fibrinolytic activity of the crude enzyme was determined using the fibrin plate method. The optimum Initial pH and incubation temperature of enzyme production will be defined by the higher proteolytic and fibrinolytic activity that the crude extract had.

MATERIALS AND METHODS

Materials

R. microsporus var. oligosporus obtained from Food and Nutrition Culture Collection (FNCC) 6010, Universitas Gadjah Mada, Helianthi annui semen from House of Organix, Kec. Cilincing, Kota Jakarta Utara, Daerah Khusus Ibukota Jakarta, Potatoes Dextrose Broth (PDB) Himedia®, skimmed milk powder Nutrifood Indonesia, Nattokinase Swanson®, fibrin bovine Sigma®, agarose AA®, methylene blue Sigma-Aldrich, distilled water.

Equipment

Autoclave electric HL – 340 Series, Vertical Type Steam Sterilizer, Memmert Incubator, Genesys-20 Spectrophotometer, Sartorius Type BP 221S Digital Scales, Laminar Air Flow Cabinet, magnetic stirrer, Samsung refrigerator, ultracentrifuge HERMLE Z36HK, Hettich Zentrifugen EBA 20 centrifuge, Vortex Thermolyne Maxi Mix, Fisher Versamix pH-meter, micro pipette, Eppendorf, Eppendorf tube rack, Philips juicer.

Methods

Enrichment of *Rhizopus microsporus var. oligosporus* FNCC 6010

Enrichment of *R. microsporus var. oligosporus* was done in Potato dextrose agar (PDA) slant media by taken 1 $\hat{\text{O}}$ se from *R. microsporus var. oligosporus* FNCC 6010 culture stock, then the $\hat{\text{O}}$ se was scrapped into PDA slant and incubated in 33 ± 2 °C for 72 hours.

Rhizopus microsporus var. oligosporus spore suspension preparation

Ten mL of phosphate buffer 0,1M pH 5.00 or pH 7.00 is added into the culture of *R. microsporus var. oligosporus* on its tube. The tube is vortexed for \pm 10 minutes until the spore of *R. microsporus var. oligosporus* released from the media. The optical density of spore suspension was measured to get transmittance \pm 25% (λ 580) by spectrophotometer.

Fermentation and optimization process

Helianthi annui semen was washed three times and bubbled in distilled water for 25 minutes. The hull of the seeds was removed and doused in distilled water 1:3 (w/v) for 12 hours. At that point, the seed was re-boiled for 15 minutes. After that, the seed that had been boiled was cleared out, and dried at room temperature for 2 hours, and the moisture content test was done. The fermentation process was done by weighing 30 g of sunflower seed and putting it in a sterile container of 140 cm². Added 500 μ L of *R. microsporus var. oligosporus* spore suspension in pH 5.0 or pH 7.0, spread on the seed, and incubated at various incubation temperatures for 24

hours. Both parameters such as initial pH, incubation temperature in the state fermentation method, were optimized in one variable-at-a-time strategy.

The extraction process obtained protease fibrinolytic crude enzyme

Fermented sunflower seed was weighed at 20 g, and 50 mL phosphate buffer 0.1M pH 7.00 was added. It was blended for 2 minutes and centrifuged for 30 minutes at 6000 rpm. The supernatant was used as the crude enzyme.

Proteolytic activity assay

The proteolytic activity assay was done using the skimmed milk agar (SMA) method. Skimmed milk agar media was prepared by dissolving 3 g skim milk in 30 mL distilled water and 3 g agar in 100 mL distilled water. Pour skim milk solution into agar solution and heat it. Put 20 mL media into each tube, then sterilize at 121 °C for 15 minutes. Pour skim milk agar media into a sterile petri dish. Proteolytic activity assay was done by pipetting a 40 μ l sample or control to each hole of skim milk agar plate and incubating the plate at 33 ± 2 °C for 20 hours. Nattokinase (100g/10mL) was used as the positive control, and phosphate buffer 0.1M pH 7.00 was used as the negative control (Poernomo *et al.*, 2017). The proteolytic index was calculated by the equation below.

$$\text{Proteolytic index} = \frac{\text{average clear zone diameter (mm)}}{\text{media hole diameter (mm)}}$$

Fibrinolytic activity assay

A fibrinolytic activity assay was done by the fibrin plate method. The fibrin plate media was prepared by dissolving 1.5 g agar in 60 mL heated distilled water, and 0.5 g fibrin was added to the agar solution. Put one droplet pipette of methylene blue into fibrin media. The fibrin media was pasteurized for 3 minutes at 80 ± 2 °C. About 20 mL of fibrin media was poured into a sterile petri dish method modified (Poernomo *et al.*, 2021). Fibrinolytic activity assay was done by pipetting a 40 μ l sample or control to each hole of fibrin media on a petri dish. Incubated at 37 ± 2 °C for 24 hours. Nattokinase (100 g/10 mL) was used as the positive control, and phosphate buffer 0.1M pH 7.00 was used as negative control. The fibrinolytic index was calculated using the equation below.

$$\text{Fibrinolytic index} = \frac{\text{average clear zone diameter (mm)}}{\text{media hole diameter (mm)}}$$

Statistical analysis

Microsoft Excel (Office 2013, Microsoft) was used to calculate the average and standard deviation of both

the proteolytic index and fibrinolytic index. The proteolytic index and fibrinolytic index from the data were analyzed using SPSS statistical software (SPSS version 25.0, SPSS Inc., Chicago, IL, USA). Each data was performed by one-way ANOVA (analysis of variance) at a 5% confidence level to know if there was a significant difference from the index value. If there was significance, Tukey test was performed at 5% probability.

RESULTS AND DISCUSSION

The result of *R. microsporus var. oligosporus* enrichment on PDA media for 72 hours at a temperature of $33 \pm 1 \text{ }^\circ\text{C}$ is shown in Figure 1. PDA media is used because it was better compared to saborouds dextrose agar (SDA) based on the number of colonies grown in agar media (Poernomo *et al.*, 2017). The culture enrichment result on the PDA slant showed the forming of white hyphae with a black surface. Culture storage of *R. microsporus var. oligosporus* was at $4 \text{ }^\circ\text{C}$, and it was rejuvenated every four weeks on a new PDA during research use, referring to previous studies (Vinuthna & Raju, 2022).

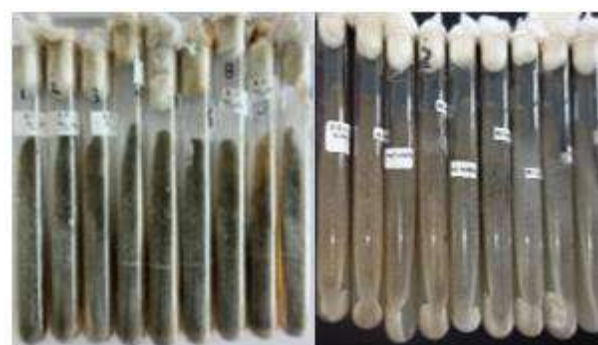


Figure 1. *Rhizopus microsporus var. oligosporus* FNCC 6010 culture on PDA slant with incubation time 72 hours and incubation temperature $33 \pm 2 \text{ }^\circ\text{C}$

R. microsporus var. oligosporus spore suspension was prepared by adding a phosphate buffer with a pH of 5.0 or pH 7.0 to the tube of culture until transmittance of T 25% at $\lambda 580 \text{ nm}$ was obtained. Percent transmittance was measured at $\lambda 580$ because in the λ range, 400 – 600 nm is the appropriate wavelength for observing microbial cell turbidity, which is a method for measuring spore suspension (Madigan *et al.*, 2015). The cell suspension looks cloudy because the cells scatter light that passes through the suspension. Since cell mass is proportional to the number of cells, turbidity can be used to estimate cell count and the technique is widely used in microbiology (Madigan *et al.*, 2015). In this

study, the transmittance value of each suspension of *R. microsporus var. oligosporus* was set to T 25% for each fermentation process to be reproducible. The number of cells used in the fermentation process was set to 10^7 CFU/mL (Poernomo *et al.*, 2017) because a lower number of cells can lead to longer incubation times and potential bacterial contamination. Furthermore, a higher number of cells may result in an excessive increase in temperature in the process and premature death of the fungus (Nout & Kiers, 2005).



Figure 2. Fermentation product of sunflower seed by *Rhizopus microsporus var. oligosporus* FNCC 6010 with (a) initial pH 5.0 and (b) pH 7.0; incubation time of 24 hours and incubation temperature $33 \pm 2 \text{ }^\circ\text{C}$

Visually, Figure 2 and Figure 3 showed that the fermentation products after 24 hours were white and had a specific odour. The white colour of the fermentation product is caused by the growth of mycelia in the growth medium (Hariyono *et al.*, 2021). At variable pH of 5.0 and 7.0 and incubation temperature $33 \pm 1 \text{ }^\circ\text{C}$ and 24 h incubation time, the fermented product physically looked similar. In temperature variations, the differences could be observed at temperatures $28 \pm 1 \text{ }^\circ\text{C}$ where the mycelia grew less frequently than at temperatures of $33 \pm 1 \text{ }^\circ\text{C}$ and $37 \pm 1 \text{ }^\circ\text{C}$. Previous research explained that at a temperature of $25 \text{ }^\circ\text{C}$ or below, the rate of the fermentation process decreases so that it takes a longer time to achieve results equivalent to fermentation at a temperature of $30 \text{ }^\circ\text{C}$ or higher (Nout & Kiers, 2005). In addition, at low temperatures, there is a possibility that bacterial contamination grows faster than the growth rate of *Rhizopus sp.* (Dwiatmaka *et al.*, 2022).

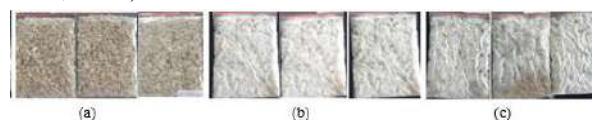


Figure 3. Fermentation product of sunflower seed by *Rhizopus microsporus var. oligosporus* FNCC 6010 with variations incubation temperature (a) $28 \pm 1 \text{ }^\circ\text{C}$; (b) $33 \pm 1 \text{ }^\circ\text{C}$; (c) $37 \pm 1 \text{ }^\circ\text{C}$; incubation time of 24 hours; initial pH fermentation of 5.0

The fermentation results were then extracted to obtain crude enzymes. In the solid-state fermentation method for enzyme production, fermentation results can

be used directly as a source of crude enzyme and easily harvested from the media (Sambo *et al.*, 2021). In this study, the crude enzyme was defined as an enzyme obtained from the fermentation of sunflower seed by *Rhizopus microsporus var. oligosporus* FNCC 6010, which was extracted with a phosphate buffer solvent at pH 7.0 and took the supernatant. Extraction was carried out with a pH of 7.0 because previous studies have revealed that the activity and stability of fibrinolytic enzymes produced by *Rhizopus microsporus var. tuberosus* are optimal at pH 7.0 (Zhang *et al.*, 2015). An essential step in enzyme downstream processing is the removal of the cells, solids, and colloids from the fermentation media which commonly using the ultracentrifugation process (Raju & Divakar, 2014). Enzymes were stored at < 5°C to prevent microbial contamination and maintain enzyme activity and stability.



Figure 4. Proteolytic activity of crude enzyme from fermented sunflower seed with fermentation condition variation in initial pH 5.0 (S5 R1, S5 R2, S5 R3) and initial pH 7.0 (S7 R1, S7 R2, S7 R3).

It was found that crude enzymes from fermented sunflower seeds showed a clear zone around the hole media in skim milk agar (SMA) plates. Nattokinase as positive control also demonstrated a clear zone, while phosphate buffer 0.1M pH 7 as negative control did not appear in a clear zone, according to Figure 4. The clear zone showed the proteolytic activity by hydrolysis of the

peptide bonds in casein that link amino acids together in the polypeptide chain in skimmed milk agar (Susanti *et al.*, 2019). The rising of protease activity is demonstrated by the higher clear zone in SMA media (Ahamed *et al.*, 2022)

In this study, the influence of the starting pH during the fermentation process was investigated at pH 5.0 and pH 7.0, incubation temperature of 33 1 °C, and an incubation period of 24 hours. The results showed that the value of the proteolytic index at pH 5.0 was higher than at pH 7.0, according to Table 1. Statistical analysis showed that there was a significant difference in proteolytic activity at initial pH 5.0 and pH 7.0 with Sig. 0.005 (< 0.05). Similar research showed that the protease production method in submerged fermentation by *Rhizopus microsporus var. oligosporus* is optimal at pH 5.5 (Sarao *et al.*, 2010). Previous research has revealed that the optimum pH of the media for protease synthesis from *Rhizopus oligosporus* IHS13 in sunflower meal, wheat bran, and rice bran is at pH 5.0. At pH above and below 5.0, there is a decrease in enzyme production and so below that pH (Haq & Mukhtar, 2004). Another study used pH 5.5 to produce proteases from *Rhizopus oryzae* in bread media (Benabda *et al.*, 2019).

The results of fibrinolytic activity are described in Figure 5. showed that at the initial pH condition of fermentation, 5.0 obtained a fibrinolytic index greater than at pH 7.0, according to Table 2. That was a statistical difference from value Sig. 0.030 (< 0.05). It was indicated by a clear zone around the hole in fibrin agar media. Other studies have shown that the fibrinolytic activity of enzymes produced by *Serratia rubidaea* KUAS001 at the initial pH of enzyme production 5.0 is better than at pH 7.0, and decreases with increasing pH (Anusree *et al.*, 2020). Each microorganism grows best at its specific pH, where it exhibits maximum metabolic activity, the fungus showed optimal metabolic activity in the pH range of 4 to 5 (Srivastava *et al.*, 2019).

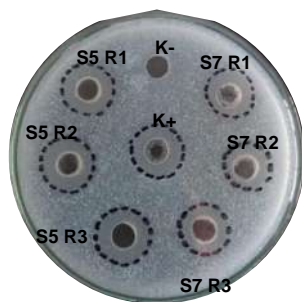


Figure 5. Fibrinolytic activity of crude enzyme from fermented sunflower seed with fermentation condition variation initial pH 5.0 (S5 R1, S5 R2, S5 R3) and initial pH 7.0 (S7 R1, S7 R2, S7 R3)

Table 1. Proteolytic index of crude enzyme from fermented sunflower seed incubation time 24 hours at 33 ± 1 °C initial pH variation

Sample/Control	Clear zone diameter (mm)	Mean clear zone diameter (mm) ± SD	Proteolytic index	Mean Proteolytic index ± SD
K+	14.03	14.03	2.00	2.00
K-	0.00	0.00	0.00	0.00
S5 R1	18.45		2.64	
S5 R2	18.60	18.40 ± 0.19	2.66	2.63 ± 0.03
S5 R3	18.15		2.59	
S7 R1	17.10		2.44	
S7 R2	16.10	16.63 ± 0.41	2.30	2.38 ± 0.06
S7 R3	16.10		2.39	

Note: K+ = positive control; K- = negative control; S5 R1, S5 R2, S5 R3 = crude enzyme from fermented sunflower seed in each pH 5 replication 1, 2 and 3; S7 R1, S7 R2, S7 R3 = crude enzyme from fermented sunflower seed in initial pH 7 replication 1, 2 and 3

Table 2. Fibrinolytic index of crude enzyme from fermented sunflower seed in initial pH variation

Sample/Control	Clear zone diameter (mm)	Mean clear zone diameter(mm)± SD	Fibrinolytic index	Mean Fibrinolytic index ± SD
K+	15.13	15.13	2.16	2.16
K-	0.00	0.00	0.00	0.00
S5 R1	15.13		2.16	
S5 R2	15.30	15.29 ± 0.12	2.19	2.18 ± 0.02
S5 R3	15.43		2.20	
S7 R1	14.70		2.10	
S7 R2	13.43	13.82 ± 0.28	1.92	2.01 ± 0.07
S7 R3	14.00		2.00	

Note: K+ = positive control; K- = negative control; S5 R1, S5 R2, S5 R3 = crude enzyme from fermented sunflower seed in initial pH of 5.0 replication 1, 2 and 3; S7 R1, S7 R2, S7 R3 = crude enzyme from fermented sunflower seed in initial pH 7.0 replication 1, 2 and 3

Further research was carried out on the variability of incubation temperature parameters of 28±1, 33±1, and 37±1 °C, initial pH 5.0, and incubation time of 24 hours. Based on the results of the proteolytic activity assay, shown in (Figure 6). it was found that the proteolytic index of the crude enzyme at an incubation temperature of 33±1 °C produced a larger value compared to temperatures of 28±1 °C and 37±1 °C according to Table 3. It was statistically different with the value Sig. 0.000 (<0.05). In enzyme production by microorganisms, an increase in the temperature of fermentation causes a rise in enzyme activity up to a certain point, and after that, there can be a decrease (Ahamed *et al.*, 2022; Boratyński *et al.*, 2018) in line with previous studies that revealed that there was an increase in protease activity produced by *Rhizopus oligosporus* IHS13 with substrates of wheat bran and rice bran at an incubation temperature of 25 °C to 30 °C then after that decreased at a temperature of 35 °C which showed that the organism was mesophyll (Haq & Mukhtar, 2004). Similar research on protease production by *Rhizopus oligosporus* shows that the

optimal fermentation temperature is 30 °C, which then decreases to 35 °C (Rauf *et al.*, 2010).



Figure 6. Proteolytic activity assay result of crude enzyme fermented sunflower seed with fermentation condition incubation temperature 28 ± 1 °C (S28 R1, S28 R2, S28 R3); 33 ± 1 °C (S33 R1, S33 R2, S33 R3); 37 ± 1 °C (S37 R1, S37 R2, S37 R3)

Table 3. Proteolytic index of crude enzyme from fermented sunflower seed in various incubation temperature

Sample/Control	Clear zone diameter (mm)	Mean clear zone diameter (mm) ± SD	Proteolytic index	Mean Proteolytic index ± SD
K+	18.37	18.37	2.62 ± 0.02	2.62
K-	0.00	0.00	0.00 ± 0.00	0.00
S28 R1	14.00		2.00	
S28 R2	14.63	14.53 ± 0.40	2.09	2.08 ± 0.06
S28 R3	14.97		2.14	
S33 R1	16.93		2.42	
S33 R2	16.93	17.01 ± 0.11	2.42	2.43 ± 0.02
S33 R3	17.17		2.45	
S37 R1	15.77		2.25	
S37 R2	15.60	15.74 ± 0.11	2.23	2.25 ± 0.02
S37 R3	15.87		2.27	

Note: K+ = positive control; K- = negative control; S28 R1, S28 R2, S28 R3 = crude enzyme fermented sunflower seed with fermentation condition incubation temperature 28 ± 1 °C; S33 R1, S33 R2, S33 R3 = crude enzyme fermented sunflower seed with fermentation condition incubation temperature 33 ± 1 °C; S37 R1, S37 R2, S37 R3 = crude enzyme fermented sunflower seed with fermentation condition incubation temperature 37 ± 1 °C

Table 4. Fibrinolytic index of the crude enzyme from fermented sunflower seed in various incubation temperature

Sample/Control	Clear zone diameter (mm)	Mean clear zone diameter (mm) ± SD	Fibrinolytic index	Mean Fibrinolytic index ± SD
K+	14.70	14.70	2.10	2.10 ± 0.05
K-	0.00	0.00	0.00	0.00 ± 0.00
S28 R1	13.23		1.89	
S28 R2	12.77	12.78 ± 0.37	1.82	1.83 ± 0.05
S28 R3	12.33		1.76	
S33 R1	15.90		2.27	
S33 R2	15.73	15.67 ± 0.22	2.25	2.24 ± 0.03
S33 R3	15.37		2.20	
S37 R1	14.13		2.02	
S37 R2	14.40	14.33 ± 0.14	2.06	2.05 ± 0.02
S37 R3	14.47		2.07	

Note: K+ = positive control; K- = negative control; S28 R1, S28 R2, S28 R3 = crude enzyme fermented sunflower seed with fermentation condition incubation temperature 28 ± 1 °C; S33 R1, S33 R2, S33 R3 = crude enzyme fermented sunflower seed with fermentation condition incubation temperature 33 ± 1 °C; S37 R1, S37 R2, S37 R3 = crude enzyme fermented *Helianthus annuus L. semen* with fermentation condition incubation temperature 37 ± 1 °C

Fibrinolytic activity assay results shown in (Figure 7) demonstrate that there was an increase in fibrinolytic activity in enzyme production with an incubation temperature from 28 ± 1 °C up to 33 ± 1 °C. Then, at the incubation temperature of 37 ± 1 °C, the fibrinolytic activity of the crude enzyme was decreased, according to (Table 4) The results statistically showed a significant difference between temperature variations at the value Sig. 0.000 (< 0.05). Similar research results revealed that *Rhizopus oryzae* FNCC 6078 for fibrinolytic enzyme production increased with increasing incubation temperature, and the optimum temperature was reached at 35 °C (Sada *et al.*, 2021). Environmental temperature

is one of the factors that greatly affect the growth and metabolism of organisms (Srivastava *et al.*, 2019). At low temperatures, rising temperatures increase the growth rate of organisms because the speed of reactions catalyzed by enzymes increases, so metabolism increases, resulting in more significant growth and production of enzymes by microorganisms. But the increase will reach a certain point until after that, too high temperatures can damage microorganisms by denaturation, transporters, other proteins, and plasma membranes. Temperatures too high for microorganisms promote stretching and eventual breakdown of weak hydrogen bonds in the enzyme, particularly in the

protease enzyme generated during the fermentation process. (Haq & Mukhtar, 2004).



Figure 7. Fibrinolytic activity assay result of crude enzyme fermented sunflower seed with fermentation condition incubation temperature 28 ± 1 °C (S28 R1, S28 R2, S28 R3); 33 ± 1 °C (S33 R1, S33 R2, S33 R3); 37 ± 1 °C (S37 R1, S37 R2, S37 R3)

CONCLUSION

The initial pH and incubation temperature for producing fibrinolytic protease from *Rhizopus microsporus var. oligosporus* FNCC 6010 on helianthi annui semen (sunflower seed) substrate in solid state fermentation affects both the proteolytic and fibrinolytic activity. The initial pH of 5.0 had higher activity than the initial pH of 7.0. The incubation temperature 33 ± 1 °C had the higher activity compared to 28 ± 1 °C or 37 ± 1 °C so the optimum condition was an initial pH of 5.0 and incubation temperature of 33 ± 1 °C.

AUTHOR CONTRIBUTIONS

Conceptualization, R. L., A. T. P., A. S.; Methodology, R. L., A. T. P., A. S.; Software, R. L.; Validation, R. L.; Formal Analysis, R. L.; Investigation, R. L.; Resources, R. L., A. T. P., A. S.; Data Curation, R. L., A. T. P., A. S.; Writing - Original Draft, R. L., A. T. P., A. S.; Writing - Review & Editing, R. L., A. T. P., A. S.; Visualization, R. L., A. T. P., A. S.; Supervision, R. L., A. T. P., A. S.; Project Administration, R. L., A. T. P., A. S.; Funding Acquisition, R. L., A. T. P., A. S.

FUNDING STATEMENT

This research did not receive any specific grant from funding agencies in the public, commercial, or not for profit sectors.

CONFLICT OF INTEREST

The authors declared no conflict of interest.

REFERENCES

- Ahamed, N. A., Arif, I. A., Al-rashed, S., Panneerselvam, A., & Ambikapathy, V. (2022). In Vitro Thrombolytic Potential of Fibrinolytic Enzyme from *Brevibacterium* sp. Isolated from the Root of the Plant, *Aloe castellorum*. *Journal of King Saud University - Science*; 34; 1-6. doi: 10.1016/j.jksus.2022.101868.
- Altaf, F., Wu, S. & Kasim, V. (2021). Role of Fibrinolytic Enzymes in Anti-Thrombosis Therapy. *Frontiers in Molecular Biosciences*; 8; 1–17. doi: 10.3389/fmolb.2021.680397.
- Anusree, M., Swapna, K., Aguilar, C. N. & Sabu, A. (2020). Optimization of Process Parameters for the Enhanced Production Of Fibrinolytic Enzyme by a Newly Isolated Marine Bacterium. *Bioresource Technology Reports*; 11; 1-7. doi: 10.1016/j.biteb.2020.100436.
- Benabda, O., Sana, M., Kasmi, M., Mnif, W. & Hamdi, M. (2019). Optimization of Protease and Amylase Production by *Rhizopus oryzae* Cultivated on Bread Waste Using Solid-State Fermentation. *Journal of Chemistry*; 2019; 1-10. doi: 10.1155/2019/3738181.
- Boratyński, F., Szczepańska, E., Grudniewska, A., Gniłka, R. & Olejniczak, T. (2018). Improving of Hydrolases Biosynthesis by Solid-State Fermentation of *Penicillium camemberti* on Rapeseed Cake. *Scientific Reports*; 8; 1–9. doi: 10.1038/s41598-018-28412-y.
- Dwiatmaka, Y., Yuniarti, N., Lukitaningsih, E. & Wahyuono, S. (2022). Fermentation of Soybean Seeds Using *Rhizopus Oligosporus* for Tempeh Production and Standardization Based on Isoflavones Content. *International Journal of Applied Pharmaceutics*; 14; 131–136. doi: 10.22159/ijap.2022v14i6.43785.
- Grasso, S., Pintado, T., Pérez-Jiménez, J., Ruiz-Capillas, C. & Herrero, A. M. (2020). Potential of a Sunflower Seed by-Product as Animal Fat Replacer in Healthier Frankfurters. *Foods*; 9; 1–14. doi: 10.3390/foods9040445.
- Haq, I. U. & Mukhtar, H. (2004). Biosynthesis of Proteases by *Rhizopus oligosporus* IHS13 in Low-Cost Medium by Solid-State Fermentation. *Journal of Basic Microbiology*; 44; 280–287. doi: 10.1002/jobm.200410393.
- Hariyono, C. M., Yuniarta, Harijono, Sriherwanto, C., Suja'i, I., Nadaviana, A., Junaedi, H., Ma'hadah, R. & Komarudin. (2021). Physico-chemical Characteristics of *Rhizopus* sp.-Fermented Fish

- Feed Pellets Containing Black Soldier Fly Larvae (*Hermetia illucens*) Meal. *IOP Conference Series: Earth and Environmental Science*; 744; 1-10. doi: 10.1088/1755-1315/744/1/012024.
- Hermansyah, B., Lokapirnasari, W. P. & Fikri, F. (2019). Pengaruh Substitusi Tepung Biji Bunga Matahari (*Helianthus annuus* L.) dalam Pakan Komersial dengan Konsentrasi Tertentu Terhadap Performa Ayam Pedaging. *Jurnal Medik Veteriner*; 2; 7-12. doi: 10.20473/jmv.vol2.iss1.2019.7-12.
- Karefyllakis, D., van der Goot, A. J. & Nikiforidis, C. V. (2019). Multicomponent Emulsifiers from Sunflower Seeds. *Current Opinion in Food Science*; 29; 35-41. doi: 10.1016/j.cofs.2019.07.005.
- Kotb, E. (2015). Purification and Partial Characterization of Serine Fibrinolytic Enzyme from *Bacillus megaterium* KSK-07 Isolated from Kishk, a Traditional Egyptian Fermented Food. *Applied Biochemistry and Microbiology*; 51; 34-43. doi: 10.1134/S000368381501007X.
- Kotb, E. (2013). Activity Assessment of Microbial Fibrinolytic Enzymes. *Applied Microbiology and Biotechnology*; 97; 6647-6665. doi: 10.1007/s00253-013-5052-1.
- Kotb, E. (2014). Purification and Partial Characterization of a Chymotrypsin-Like Serine Fibrinolytic Enzyme from *Bacillus amyloliquefaciens* FCF-11 Using Corn Husk as a Novel Substrate. *World Journal of Microbiology and Biotechnology*; 30; 2071-2080. doi: 10.1007/s11274-014-1632-1.
- Krishnamurthy, A., Belur, P. D. & Subramanya, S. B. (2018). Methods Available to Assess Therapeutic Potential of Fibrinolytic Enzymes of Microbial Origin: a Review. *Journal of Analytical Science and Technology*; 9; 1-11. doi: 10.1186/s40543-018-0143-3.
- Madigan, M. T., Martinko, J. M., Bender, K. S., Buckley, D. H. & Stahl, D. A. (2015). Microbial Growth and Control. In *Brock Biology of Microorganisms*. Boston: Pearson.
- Miglani, K., Kumar, R., Panwar, S. & Kumar, A. (2017). Microbial Alkaline Proteases: Optimization of Production Parameters and Their Properties. *Journal of Genetic Engineering and Biotechnology*; 15; 115-126. doi: 10.1016/j.jgeb.2017.02.001.
- Muhammed, A., Ali, M., Charan, S. & Bavisetty, B. (2020). Purification, Physicochemical Properties, and Statistical Optimization of Fibrinolytic Enzymes Especially from Fermented Foods: A Comprehensive Review. *International Journal of Biological Macromolecules*; 163; 1498-1517. doi: 10.1016/j.ijbiomac.2020.07.303.
- Nout, M. J. R. & Kiers, J. L. (2005). Tempe Fermentation, Innovation and Functionality: Update Into the Third Millenium. *Journal of Applied Microbiology*; 98; 789-805. doi: 10.1111/j.1365-2672.2004.02471.x.
- Poernomo, A. T., Isnaeni, & Purwanto. (2017). Thrombolytic Activity of Fibrinolytic Enzyme from Black Soybean Tempeh (Glycine Soja Sieb. Et Zucc) Fermented by *Rhizopus Oligosporus* FNCC 6010. *Research Journal of Pharmaceutical, Biological and Chemical Sciences*; 8; 1885-1896.
- Raju, E. V. N. & Divakar, G. (2014). An Overview on Microbial Fibrinolytic Proteases. *International Journal of Pharmaceutical Sciences and Research*; 5; 643-656. doi: 10.13040/IJPSR.0975-8232.5(3).643-56.
- Rashad, M. M., Mahmoud, A. E., Al-Kashef, A. S. & Nooman, M. U. (2012). Purification and Characterization of a Novel Fibrinolytic Enzyme by *Candida guilliermondii* Grown on Sunflower Oil Cake. *Journal of Applied Sciences Research*; 8; 635-645.
- Rauf, A., Irfan, M., Nadeem, M. & Ahmed, I. (2010). Optimization of Growth Conditions for Acidic Protease Production from *Rhizopus oligosporus* through Solid State Fermentation of Sunflower Meal. *International Scholarly and Scientific Research & Innovation*; 4; 898-901.
- Sada, A., Sugianto, N. E., & Poernomo, A. T. (2021). Produksi Enzim Fibrinolitik Tempe oleh *Rhizopus oryzae* FNCC 6078. *Berkala Ilmiah Kimia Farmasi*; 8; 1-6. doi: 10.20473/bikfar.v8i1.31202.
- Sambo, S., Magashi, A. M., Farouq, A. A. & Hassan, S. W. (2021). An Overview of the Solid State Fermentation in the Production of Fungal Protease Enzymes. *World Journal of Advanced Research and Reviews*; 9; 85-89. doi: 10.30574/wjarr.2021.9.3.0061.
- Sarao, L. K., Arora, M., Sehgal, V. K., & Bhatia, S. (2010). Production of Protease by Submerged Fermentation Using *Rhizopus microsporus* var *oligosporus*. *Internet Journal of Microbiology*; 9; 1-11.

- Sharma, C., Osmolovskiy, A., & Singh, R. (2021). Microbial Fibrinolytic Enzymes as Anti-Thrombotics: Production, Characterisation and Prodigious Biopharmaceutical Applications. *Pharmaceutics*; 13; 1-32. doi: 10.3390/pharmaceutics13111880.
- Srivastava, N., Srivastava, M., Ramteke, P. W. & Mishra, P. K. (2019). Solid-State Fermentation Strategy for Microbial Metabolites Production: An Overview. *New and Future Developments in Microbial Biotechnology and Bioengineering: Microbial Secondary Metabolites Biochemistry and Applications*; 2019; 345–354. doi: 10.1016/B978-0-444-63504-4.00023-2.
- Susanti, E., Lutfiana, N. Suharti & Retnosari, R. (2019). Screening of Proteolytic Bacteria from Tauco Surabaya based on Pathogenicity and Selectivity of its Protease on Milky Fish (*Chanos chanos*) Scales for Healthy and Halal Collagen Production. *IOP Conference Series: Materials Science and Engineering*; 509; 1-7. doi: 10.1088/1757-899X/509/1/012044.
- Xiao-Lan, L., Lian-Xiang, D., Fu-Ping, L., Xi-Qun, Z. & Jing, X. (2005). Purification and Characterization of a Novel Fibrinolytic Enzyme from *Rhizopus chinensis* 12. *Applied Microbiology and Biotechnology*; 67; 209–214. doi: 10.1007/s00253-004-1846-5.
- Zhang, S., Wang, Y., Zhang, N., Sun, Z., Shi, Y., Cao, X. & Wang, H. (2015). Purification and Characterisation of a Fibrinolytic Enzyme from *Rhizopus microsporus* var. *tuberosus*. *Food Technology and Biotechnology*; 53; 243–248. doi: 10.17113/ftb.53.02.15.3874.



Optimizing Gel Formulations Using Carbopol 940 and Sodium Alginate Containing *Andrographis paniculata* Extract for Burn-Wound Healing

Elsa Fitria Apriani, Naisa Kornelia, Annisa Amriani*

Department of Pharmacy, Faculty of Mathematics and Natural Sciences, Universitas Sriwijaya, Indralaya, Indonesia

*Corresponding author: annisaamriani@mipa.unsri.ac.id

Submitted: 17 July 2023

Revised: 2 September 2023

Accepted: 21 December 2023

Abstract

Background: *Sambiloto* leaves (*Andrographis paniculata* (Burm.f.) Nees) contain andrographolide (diterpene lactone), flavonoids, quinic acid, steroids, saponins, alkaloids, and tannins, which act as anti-inflammatory, antioxidant, antibacterial, and wound healing. **Objective:** This study optimizes the gelling ingredient in *Sambiloto* extract gel preparations (*Andrographis paniculata* (Burm.f.) Nees) as a wound healer in male Wistar rats. The gelling agent is an important component that can affect active substance release. **Methods:** Formula optimization was developed using the Regular Two-Level 2² Factorial Design method in Design-Expert 12 software. This study used 0.5%-1% carbopol 940 and 1%-5% sodium alginate. Carbopol 940 and Sodium Alginate have different characteristics, so they need to be optimized to produce a gel with good characteristics. **Results:** Physical property evaluation using factorial design revealed the optimal formula at 0.5% carbopol and 5% sodium alginate, with average pH, viscosity, and adhesion values of 5.17 ± 0.04 ; 2934.452 ± 286.871 cPs; and 194.236 ± 3.684 s. Centrifugation and cycling tests indicated no organoleptic changes, phase separation, or significant changes in pH. ANOVA analysis showed that the gel with 10% *Sambiloto* leaf extract had similar burn healing activity to the positive control, with a recovery rate of $99.72 \pm 0.47\%$ in 20 days. Scabs formed on the 8th day and peeled off on the 12th day. **Conclusion:** *Sambiloto* extract gel in the optimum formula has the potential to be developed as a burn wound-healing drug.

Keywords: *Andrographis paniculata* (Burm.f.) Nees, burn wound-healing, gel, optimization

How to cite this article:

Apriani, E. F., Kornelia, N. & Amriani, A. (2023). Optimizing Gel Formulations Using Carbopol 940 and Sodium Alginate Containing *Andrographis paniculata* Extract for Burn-Wound Healing. *Jurnal Farmasi dan Ilmu Kefarmasian Indonesia*, 10(3), 300-311. <http://doi.org/10.20473/jfiki.v10i32023.300-311>

INTRODUCTION

Skin is the human body's main protector from foreign objects considered dangerous. One of the triggers for diseases that can appear on the skin is the presence of open wounds. An open wound is damage to a unit or tissue component where specifically there is a damaged or missing tissue substance (Wijaya & Putri, 2013). Open wounds can be caused by burns by exposure to heat sources such as air, fire, chemicals, electricity, and radiation. Burns damage the skin and affect all body systems (Jeschke *et al.*, 2020; Tiwari, 2012).

The depth of tissue damage due to burns depends on the degree of heat from the source of the burn, the cause of the burn and the duration of contact with the body (Noer, 2006). According to the American Burn Association, second-degree burns (partial thickness burns) are burns whose depth of tissue can reach the dermis, usually found to be painful, pale when pressed, and marked by bullae filled with exudate fluid that come out of the blood vessels due to increased permeability of the walls (Shetty *et al.*, 2021).

Sambiloto (*Andrographis paniculata* (Burm.f.) Nees) is one of the Indonesian plants that have the potential to heal burns due to the content of secondary metabolites such as andrographolide (diterpene lactone), flavonoids, quinic acid, steroids, saponins, alkaloids and tannins (Mussard *et al.*, 2020). Sambiloto has many pharmacological activities, such as antibacterial, antioxidant, antiviral, antifungal, and anti-inflammatory properties, and it enhances the immune system (Rajanna *et al.*, 2021). Antibacterial, anti-inflammatory and antioxidant activities are closely related to the healing process of burns because they can accelerate epithelization and repair and strengthen skin cells. Based on research by Al-Bayaty *et al.* (2011), histologically, burn wounds treated with 10% bitter extract showed good healing. Research from Selvaraj *et al.* (2022) proves that bitter extract has an anti-inflammatory valuable mechanism in wound healing. The recent research from Ariawan *et al.* (2023) demonstrated that *Andrographis paniculata* extract affected wound healing, such as the rate of re-epithelialization, collagen density, angiogenesis, and wound length.

Burns can be treated with topical, oral, and other treatments. However, topical treatment is more comfortable for burn sufferers. A gel preparation is one of the preparations that are suitable for treating burns. Gel preparations have a cooling effect because they contain a lot of water, so substances penetrate tissues

better and accelerate wound healing (Rinaldi *et al.*, 2019). An essential component in the manufacture of gel is the gelling agent.

Carbopol is a gel base that has a clear appearance, good spreading power on the skin, and a cooling effect; it does not clog skin pores and is easily washed off with water (Niyaz *et al.*, 2011). The concentration of carbopol 940 as a gelling agent ranges from 0.5 – 2.0% (Rowe *et al.*, 2009). Sodium alginate is produced from brown algae with a mucilage content of up to 40%. Gel containing sodium alginate shows excellent distribution; besides that, sodium alginate has slippery properties, is not sticky, does not feel when used and shows emollient properties (moisturizes the skin) (Agoes, 2012). The concentration of sodium alginate as a gelling agent ranges from 1 – 5% (Rowe *et al.*, 2009). Singh *et al.* (2013) made diclofenac gel using gelling agents such as Carbopol 940, HPMC, gelatin, sodium alginate and Na CMC. The results of this study prove that the use of sodium alginate can increase the spreadability of the gel compared to other gelling agents, while the use of carbopol 940 can increase the release of the active substance compared to other gelling agents. Liu *et al.* (2008) also proved that the use of carbopol 940 was able to increase drug penetration and preparation stability. The combination of Carbopol 940 and sodium alginate in this study is expected to improve the characteristics of the gel.

Based on the description above, it is necessary to conduct research in the form of "Optimization of Gelling Agent in Sambiloto Extract Gel (*Andrographis paniculata* (Burm.f.) Ness) as Wound Healer in Wistar Strain Male Rats". The ethanol extract of Sambiloto leaves (*Andrographis paniculata* (Burm.f.) Ness) was prepared using the maceration method with a 96% ethanol solvent. Formula optimization was developed using the Regular Two-Level Factorial Design method in Design-Expert 12 software. This study used two factors, namely factor A as carbopol-940 and factor B as sodium alginate. Sambiloto extract gel (*Andrographis paniculata* (Burm.f.) Ness) was evaluated to obtain the optimum formula and then tested for burn healing activity for 20 days.

MATERIALS AND METHODS

Materials

The materials used in this study were Sambiloto leaves (*Andrographis paniculate* (Burm.f.) Ness from Lampung, Indonesia), Filter Paper (Whatman®, Indonesia), Distilled Water (Bratachem®, Indonesia), 96% ethanol (Bratachem®, Indonesia), Sodium Alginate

(Techno Phramchem[®], Indonesia), Carbopol 940 (Bratachem[®], Indonesia), Propylene glycol (Bratachem[®], Indonesia), Methyl Paraben (Bratachem[®], Indonesia), Propyl Paraben (Bratachem[®], Indonesia), Triethanolamine (Bratachem[®], Indonesia), Alcohol 70% (Bratachem[®], Indonesia), Lidocaine 2%[®], Veet[®], Binagel[®].

Tools

The tools used in this study included analytical balances 0.001 g and 0.0001 g (Ohaus[®]), oven (IMU55L[®]), pH meter (Lutron[®] pH Electrode PE-03), rotary evaporator (Biobase[®]), blender (Philips[®]), UV-Vis (Biobase[®]), magnetic stirrer (IKA C-MAG HS4[®]), spin bar, viscometer (Grace Instrument M3400[®]), micropipette (Dragon Lab[®]), glassware (Pyrex[®]), iron plate, stopwatch, mouse cage, drinking bottle, refrigerator (LG[®]).

Method

Preparation of sambiloto extract

The sambiloto plant used was identified at the Laboratorium Karakterisasi Kebun Raya Eka Karya Bali, BRIN with ID Number 53688. The simplicia powder of Sambiloto leaves was macerated using 96% ethanol with a ratio of 1:10 for 72 hours while stirring once every 6 hours in a dark place. The resulting filtrate was concentrated in a rotary evaporator at 50°C until an ethanol extract of Sambiloto leaves was obtained. The resulting extract was stored in a refrigerator at 4°C (Fardiyah *et al.*, 2020). The percent yield of the extract is calculated using the equation:

$$\% \text{ Extract yield} = \frac{\text{Extract weight}}{\text{Simplicia weight}} \times 100$$

Phytochemical screening

The phytochemical screening method is qualitative by looking at the occurring colour reactions. The test parameters that were carried out included the identification of flavonoids, saponins, tannins, alkaloids, steroids, and triterpenoids. Alkaloid testing was carried out using Dragendorff and Wagner reagents. If the reaction is positive for alkaloids, a red precipitate is formed using the Dragendorff reagent, and a brown precipitate is formed using Wagner's reagent. Flavonoid testing was done by adding magnesium and hydrochloric acid to the extract. Yellow, red, or orange solutions indicate the presence of flavonoids. Saponin testing is done by observing the foam formed from an extract and water mixture. The formation of persistent foam for 10 minutes indicates the presence of saponin. Tannin testing is carried out with FeCl3 reagent. The blackish-green colour indicates the presence of tannin. Testing for steroids and triterpenoids was performed

using glacial acetic acid and concentrated sulfuric acid reagents. A solution that is blue or green indicates the presence of steroids, while red or purple suggests the presence of triterpenoids (Depkes RI, 2017).

Formulation of gel containing sambiloto extract

The gel formula design was determined using Design-Expert series 12 software. Formula optimization was developed using the Regular Two-Level Factorial Design method in Design-Expert 12 software. The formulas used in this study were four formulas using two factors, namely carbopol-940 and sodium alginate, at two successive levels of 0.5-1% and 1-5% (Table 1).

Table 1. Formula of gel containing sambiloto extract

Material	Concentration (%)			
	F1	F2	F3	F4
Extract	10	10	10	10
Carbopol-940	1	0.5	1	0.5
Sodium Alginate	1	1	5	5
Triethanolamine	1	1	1	1
Propylene glycol	15	15	15	15
Methyl Paraben	0.18	0.18	0.18	0.18
Propyl Paraben	0.02	0.02	0.02	0.02
Distilled Water	Ad 100 mL	Ad 100 mL	Ad 100 mL	Ad 100 mL

The process begins with weighing the ingredients and continues with the preparation of the gel base. Sodium alginate developed with aquadest. Carbopol-940 was dispersed in distilled water and added with triethanolamine until a gel base was formed. The dispersed sodium alginate and carbopol mass are put into a mortar and ground until homogeneous. Methyl paraben and propyl paraben were dissolved in propylene glycol, added to the gel mass, and stirred until homogeneous. The ethanol extract of Sambiloto was added little by little to the gel mass, and 100 mL of distilled water was added and then stored in a tightly closed container (Mardiyanto *et al.*, 2022).

Evaluation of gel containing sambiloto extract

Organoleptic

Organoleptic tests were carried out by directly observing the shape of the gel prepared, its color, and its smell (Titaley, 2014).

Homogeneity

Preparations were taken at three different sampling points and smeared on transparent glass. The test preparation is declared homogeneous if there are no coarse grains (Nikam, 2017).

pH

The pH test is carried out by turning on the pH meter and then dipping the pH meter electrode into the

gel formula, which has been dissolved with distilled water. Topical preparations must match the skin's pH, namely 4.5-6.5 (Tranggono, 2007).

Viscosity

Viscosity was done using a viscometer. The speed is set at 60 rpm, and then the pointer on the tool is observed for the number on the viscosity scale. The gel has viscosity values ranging from 2000-4000 cps (Garg *et al.*, 2002).

Spreadability

The gel preparation was placed between two glass plates with weights on glass plates with a mass of 125 g. The diameter formed after 1 minute was measured. The specification for the diameter of the spread is 5-7 cm (Garg *et al.*, 2002).

Adhesion

The gel was placed between two glass objects and then pressed with a 1 Kg load for 5 minutes. The load is lifted from the object glass, and then the object glass is mounted on the test equipment with a load of 80 g. Good adhesion requires more than 4 seconds (Mukhlisah *et al.*, 2016).

Determine the optimum formula

Optimum formula selection was made using Design Expert 12 software based on desirability values close to 1 with response parameters pH, viscosity, spreadability, and adhesion. The closer the desirability value is to 1, the more perfect the desired formula is in the program (Raissi & Farsani, 2009).

Stability test

The physical stability test of the preparations was carried out using the centrifugation method and the cycling test. The centrifugation test was carried out at 3800 rpm for 5 hours, while the cycling test was carried out at 4°C and 40°C for 24 hours for six cycles. Parameters observed were organoleptic changes in the preparation, pH, and phase separation in gel preparations (Apriani *et al.*, 2018; Mardiyanto *et al.*, 2022).

Burn wound-healing activity test

Testing on animals has received ethical approval from Ahmad Dahlan University, number 02210066. The test animals were male white rats of the Wistar strain, aged 2-3 months, weighing 180-250g, and acclimatized for one week. The test animals were anesthetized first using lidocaine at a dose of 0.4 mL/KgBW subcutaneously. The rat's back was shaved about 3 cm below the ear using Veet® and a razor, marked with a rectangular shape with a size of 3 x 2 cm. An iron plate with a diameter of 1 cm was previously heated in boiling

water for 5 minutes to achieve sterile conditions and then induced on the rats' backs for 10 seconds (Akhoondinasab *et al.*, 2014).

The gel was administered by applying it to the wound on the rat twice a day, i.e., in the morning and evening, for 20 days after the burn induction. Wound healing parameters were determined from the area of wound healing, wound healing time, and the time the scab fell off.

Table 2. Treatment group of burn wound-healing activity test

Group	Note
Negative Control	Gel base
Positive Control	Binagel
Sample	Optimum formula for sambiloto extract gel

Observations on the healing of burns were carried out from days 0, 4, 8, 12, 16, and 20. Measurements of the wound area were carried out at intervals of 4 days. Binagel® was chosen as the positive control because it is a marketed burn preparation containing plant extracts.

Data analysis

Data analysis on the evaluation of gel preparations was carried out by calculating the factorial design using the Design Expert 12 Program. Data analysis was carried out by calculating the coefficient values of each factor, namely carbopol-940 and sodium alginate, to obtain an equation for the relationship between factors and responses. Data analysis on burn wound healing used the SPSS® application with a data normality test performed with Shapiro-Wilk to see the normality of data distribution. It continued with One-Way ANOVA, and then a Post Hoc Duncan Test was conducted if the p-value <0.05.

RESULTS AND DISCUSSION

The sambiloto extract produced in this study is dark green, has a distinctive smell, and is thick, with a yield percentage of 20.20%. The results of the phytochemical screening showed that Sambiloto extract contains flavonoids, saponins, tannins, steroids, triterpenoids, and alkaloids (Table 3). The results of this study are in line with the research by Hita *et al.* (2022), where the 96% ethanol extract of Sambiloto leaves was proven positive for containing flavonoids, alkaloids, tannins, triterpenoids, and saponins.

Table 4. Results of evaluation of gel containing sambiloto extract

Parameter	Formula			
	F1	F2	F3	F4
Organoleptic	Dark green, distinctive smell and thick	Dark green, distinctive smell and thick	Dark green, distinctive smell and thick	Dark green, distinctive smell and thick
Homogeneity	Homogeneous	Homogeneous	Homogeneous	Homogeneous
pH	5.25±0.03	5.56±0.01	5.38±0.03	5.17±0.04
Viscosity (cPs)	2391.66±135.94	2079.66±93.11	3732.33±173.07	2822.66±370.93
Spreadability (cm)	5.93±0.12	6.53±0.50	5.63±0.40	5.73±0.47
Adhesion (s)	90.67±2.08	39±1.00	195±5.00	162.67±2.52

Table 5. Results of model analysis

Parameter	Parameter				
	R ²	Adjusted R ²	Predicted R ²	Adequateprecision	p-value
pH	0.9651	0.9521	0.9216	19.6780	<0.0001
Viscosity	0.9226	0.8936	0.8259	12.9745	<0.0001
Spreadability	0.7287	0.6270	0.3896	6.4286	0.0018
Adhesion	0.9984	0.9977	0.9963	89.2441	<0.0001

Table 3. Result of phytochemical screening

Secondary Metabolites	Result
Flavonoid	+
Saponin	+
Tanin	+
Alkaloid	+
Steroid & Triterpenoid	+

Note : + indicates metabolites are present

Sambiloto extract is used as an active ingredient in making gel. In the manufacture of gels, the gelling agent is an essential factor in determining the results of the characterization of the resulting preparations. In this study, variations in the concentration of the gelling agent, namely carbopol-940 and sodium alginate, were carried out to produce four formulas. The gel preparations made in this study can be seen in Figure 1. The results of the evaluation of the preparations from the four formulas can be seen in Table 4.



Figure 1. Gel containing sambiloto extract

Based on Table 4, it is known that the four formulas have met the evaluation requirements for gel preparations, namely pH ranging between 4.5-6.5, viscosity with a value range of 2000-4000 cPs, spreadability ranging from 5-7 cm and adhesion is in the

range of 2-3000 seconds (Garg *et al.*, 2002). Measured parameters such as pH, viscosity, spreadability, and adhesion were continued for the optimization process by factorial design analysis using the Design-Expert 12@ program. Data analysis was carried out broadly divided into two, namely model analysis and response analysis.

The model analysis determines which parameters can be used to determine the optimum formula. A model can be good if the p-value is less than 0.05 with an R² value greater than 0.7, the difference between adjusted R² and predicted R² is not more than 0.2, and the adequate precision value is more than 4 (Apriani *et al.*, 2023). The model analysis results of measured parameters such as pH, viscosity, spreadability, and adhesion can be seen in Table 5.

The R² value is used to see how much the data population influences the factors used. For example, the value of R² at a pH of 0.9651 means that 96.51% of the data population is influenced by carbopol-940, sodium alginate, and the interaction between the two. The difference value of adjusted R² and predicted R² describes the difference between the system's predicted value and the (actual) measured value. The smaller than 0.2, the closer the similarity of the resulting values is. The adequate precision value indicates the robustness of the model, while the p-value indicates the significance of the effect. Based on Table 5, the pH, viscosity, and adhesion parameters show good model results. In contrast, the spreadability parameter shows poor model analysis results where the difference between adjusted

R2 and predicted R2 is more than 0.2. Based on these results, the parameters that can be continued to determine the optimum formula are pH, viscosity, and adhesion.

The following analysis performed was response analysis. Response analysis was carried out to see the

effect of the carbopol-940, sodium alginate, and the interaction of the two factors on the parameters of pH, viscosity, and adhesion. The response analysis results can be seen in Table 6 and Figure 2.

Table 6. Results of response analysis

Parameter		Intercept	A	B	AB
			(Carbopol 940)	(Sodium Alginate)	(Interaction)
pH	Coefficient	5.346	-0.024	-0.064	0.129
	<i>p-value</i>		0.0393*	0.0002*	<0.0001*
	% contribution		2.635	18.582	73.297
	Response Equation	$y = 5.346 - 0.024 A - 0.064 B + 0.129 AB$			
Viscosity	Coefficient	2756.580	305.417	520.917	149.417
	<i>p-value</i>		0.0014*	<0.0001*	0.0470*
	% contribution		22.241	64.699	5.323
	Response Equation	$y = 2756.58 + 305.417 A + 520.917 B + 149.417 AB$			
Adhesion	Coefficient	121.833	4.833	57.000	-27.000
	<i>p-value</i>		0.0006*	<0.0001*	<0.0001*
	% contribution		0.628	87.351	11.857
	Response Equation	$y = 121.833 + 4.833 A + 57.000 B - 27.000 AB$			

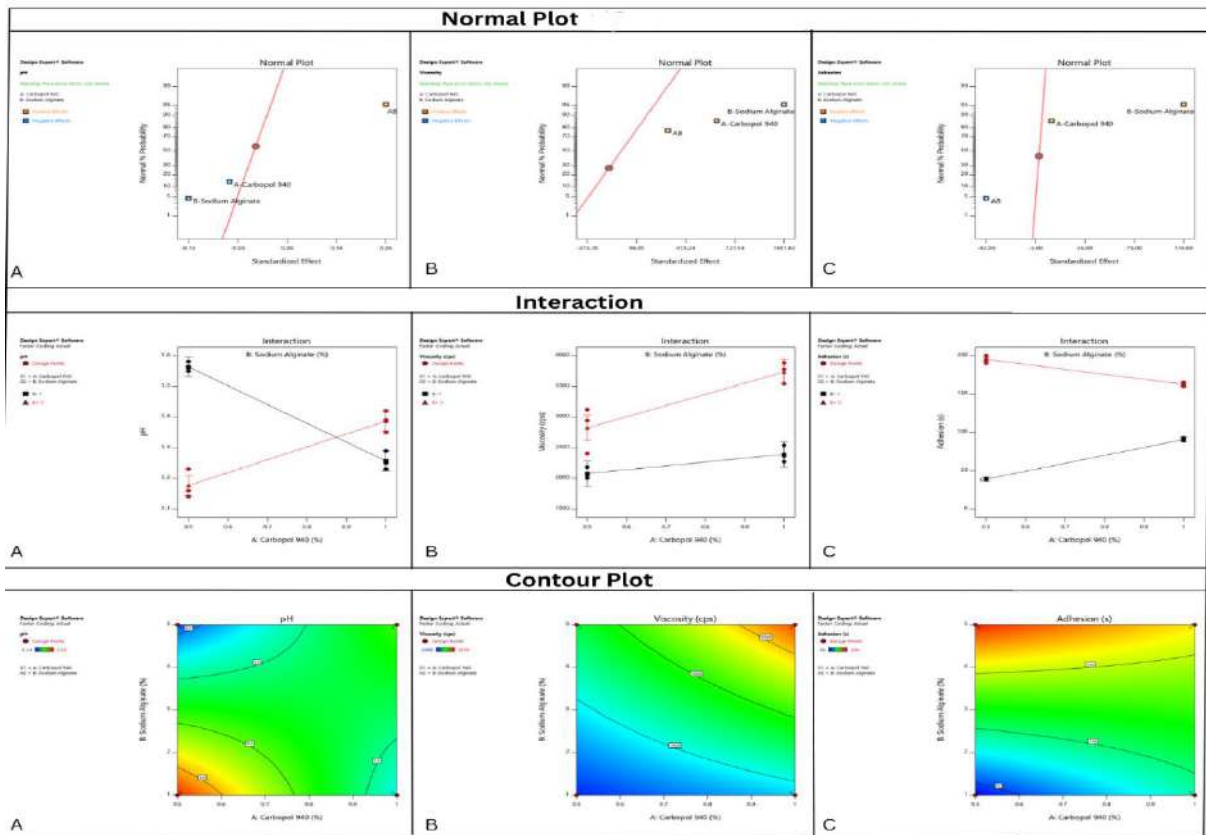


Figure 3. Graph of normal plot, interaction and contour plot of the parameters pH (A), Viscosity (B) and adhesion (C)

Based on Table 6, the concentrations of carbopol-940 and sodium alginate and their interactions significantly affect pH, viscosity, and adhesion parameters with a p-value <0.05. These results can also be supported by Figure 3, which is related to the normal plot graph where the factor points are outside the straight line, which indicates that the factor has an influence, both positive and negative. This positive and negative influence can be observed from where the point is in the negative or positive area. Besides that, it can also be seen from the notation of the coefficients whether there is a negative sign or not. The concentration of each carbopol-940 and sodium alginate has a negative effect on the pH value, where the higher the concentration used, the lower the pH value of the resulting gel preparation, while the interaction of the two factors has a negative effect on adhesion. The relationship between the interactions of carbopol-940 and sodium alginate can also be illustrated by the interaction graph in Figure 3. The pH parameter has a line crossing on the interaction graph, indicating a strong interaction between carbopol-940 and sodium alginate. These results can also be supported by the percent contribution from AB to a large pH of 73.297%. There is no line crossing when observed from the interaction graph on the parameters of viscosity and adhesion. However, the angle of inclination between the two lines is different, so interaction can occur even though it is small and is also supported by the percentage contribution of AB to the viscosity and adhesion of 5.323% and 11.857%.

The interaction between carbopol-940 and sodium alginate strongly influences the pH. The higher the interaction of the two factors, the higher the pH of the preparation. The increased concentration of carbopol-940 will lead to the concentration use of triethanolamine as a base agent to help develop carbopol 940. In addition, sodium alginate has a pH range of 6-8. This statement is the reason why the pH value of the gel preparation will increase when carbopol-940 and sodium alginate are used in high concentrations. The viscosity factor strongly influences the viscosity factor, where the percent contribution reaches 64,699%. Sodium alginate has more effect on viscosity than carbopol-940 because the concentration of sodium alginate used is more remarkable than carbopol-940.

In addition, carbopol-940 has a significant ability to absorb water so that the amount of free water contained in the gel also increases, causing the texture of the gel to get softer (Nurman *et al.*, 2019). The viscosity of sodium alginate is affected by temperature, solution level, and degree of polymerization. The main

property of sodium alginate is its ability to form gels in the presence of divalent cations (Cardenas *et al.*, 2003). If a lot of Ca²⁺ ions are released into the gel-making process, more cross-links that can be formed between alginate molecules are obtained from the increasing concentration of CaCO₃ (Remaggi *et al.*, 2022). Sodium alginate also influences the adhesion parameter, namely 87.351%. This result is related to the high viscosity of sodium alginate. The higher the viscosity, the higher the adhesive power of the preparation will be. Gel adhesion can affect the therapeutic effect. The longer the gel is attached to the skin, the more active substances will be absorbed by the skin so that the gel can provide a more prolonged therapeutic effect, and its use becomes more effective (Loyald *et al.*, 2014).

After analyzing the response, then proceed with determining the optimum formula. The optimum formula was determined using the Design Expert tool version 12. The optimum formula suggested by the system was a formula with a carbopol-940 concentration of 0.5% and a sodium alginate concentration of 5% with a desirability value of 0.997%. The results of confirmation of the characteristics of the optimum formula can be seen in Table 7. The optimum formula shows values between 95% PI low and 95% PI high. The optimum formula was further tested: stability test and burn healing activity test. The results of the stability test can be seen in Table 8.

Table 7. The result of the optimum formula confirmation analysis

Parameter	95% PI	95% PI	Result
	Low	High	
pH	4.990	5.363	5.17±0.04
Viscosity (cPs)	1613.445	4031.895	2934.452±286.871
Adhesion (sec)	178.406	211.594	194.236±3.684

Table 8. The result of optimum formula stability

Parameter	Observation result	
	Before	After
Organoleptic	Dark green, extract smell and thick	Dark green, extract smell and thick
pH	5.17±0.04	4.94±0.02
Syneresis	None	None

Based on Table 8, the optimum gel preparation formula did not experience organoleptic changes or syneresis, but there was a decrease in pH. The optimum formula in this study did not experience syneresis due to

the ability of the gelling agent combination between carbopol-940 and sodium alginate to maintain the bond strength of the gel matrix so that the solvent contained therein was not separated and came out onto the surface of the gel. The optimum formula experienced a decrease in pH of 0.23. The results of the paired-sample test analysis show that there is a significant difference where the significance value obtained is 0.02. A reduction in pH can occur due to the influence of speed and temperature, which causes the preparation to experience cation hydrolysis from TEA as a weak base to produce H⁺ ions (Lewis & Zhao, 2006).

Testing the burn healing activity of Sambiloto extract gel preparation in this study was carried out experimentally on Wistar male white rats with 3 test groups: the positive, negative, and optimum formula groups. The positive group was given Binagel[®] gel, the negative group was given a gel base, and the optimum formula group was given the optimum sambiloto extract gel preparation. Binagel[®] was chosen as a positive control because the preparation contains binahong extract derived from natural ingredients.

The primary goal of wound healing involves timely wound closure, prompt pain relief, and an aesthetically

acceptable scar. The results of % Recovery can be seen in Table 9 and Figure 4.

Based on the % recovery data, which can be seen in Table 9 and Figure 4, it can be seen that there was a significant increase in the positive group and the optimum formula from day 0 to 20. This result is inversely proportional to the negative group, which has a slower % recovery. The positive group had a healing percentage of up to 100% on day 20 and was not significantly different from the optimum formula based on post-hoc Duncan analysis. The percentage of wound healing on the fourth day in the positive, negative, and optimum formula groups was low. This result happened because, on day four, the wound healing process was still at the inflammatory stage. The inflammatory stage can be seen from the observation that there are signs of redness, inflammation occurs, it feels hot and painful, and it can even cause swelling in the wound. The inflammatory process allows white blood cells and platelets to limit more severe damage and accelerate wound healing (Gonzalez *et al.*, 2016). Furthermore, a scab will form after the inflammatory process occurs. Observations on the formation and release of scabs can be seen in Table 10.

Table 9. Result of % recovery

Group	Average %Recovery of Each Group ± SD					
	Day					
	0	4	8	12	16	20
Negative	0.00±0.00 ^a	-13.32±6.97 ^b	11.53±5.42 ^a	14.21±6.82 ^b	33.33±9.35 ^b	52.49±3.86 ^b
Positive	0.00±0.00 ^a	10.10±5.86 ^a	6.91±2.55 ^a	50.92±14.52 ^a	97.37±1.21 ^a	100.00±0 ^a
Optimum Formula	0.00±0.00 ^a	7.53±3.12 ^a	7.71±2.69 ^a	35.38±11.34 ^{ab}	92.08±5.99 ^a	99.72±0.48 ^a

Note: Values followed by lowercase letters (a/b) in the row indicate significant differences between groups in Duncan's post hoc test

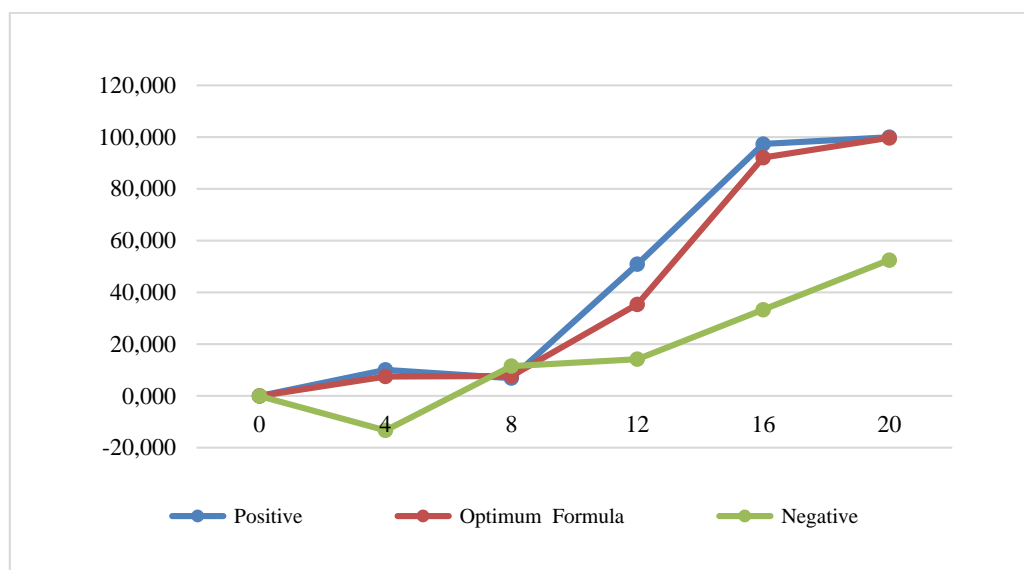


Figure 4. Graph of the percentage of burn healing for each group

Table 10. Scab observation results

Group	Average Day	
	Scab Formation	Scab Removal
Negative	12	16
Positive	8	12
Optimum Formula	8	12

Based on the above observations, it can be seen that the positive group and the optimum formula showed faster scab formation on the 8th day and faster scab removal on the 12th day and were significantly different when compared to the negative group. The formation of a scab indicates the initial proliferation process in wound healing. The proliferative stage is marked by the formation of granulations in the wound, namely fibroblasts and inflammatory cells. This phase occurs from day 4 to day 14. The scab that forms on the wound's surface can help hemostasis and prevent wound contamination due to microorganisms. Scabs are formed due to the denaturation of the skin layer proteins in the coagulation zone (Markiewicz-Gospodarek *et al.*, 2022).

On the 20th day, the percentage of wound healing in the positive group and the optimum formula reached $100 \pm 0.00\%$ and $99.72 \pm 0.48\%$. This result can happen because the wound has entered the remodelling phase. The remodelling phase occurs after the wound has been filled with granulation tissue and the re-epithelialization process is over. This phase aims to maximize the strength and structural integrity of new tissue, filling the wound, epithelial growth, and scar tissue formation (Velnar *et al.*, 2009). The negative group on the 20th day had not entered the remodelling stage because the percentage of wound healing was still minor, namely $52.49 \pm 3.86\%$.

The optimum formula of Sambilotto extract gel is proven to have wound-healing activity because it contains flavonoids, saponins, tannins, alkaloids, steroids, and triterpenoids, which help accelerate wound healing. Phytochemical compounds such as flavonoids have various biological activities such as antibacterial, anti-inflammatory, and antioxidant effects and are believed to benefit wound healing (Acar *et al.*, 2002). Tannin compounds support wound healing with their astringent and antimicrobial properties. Saponins function as cleansers and antiseptics to prevent the growth of microorganisms in wounds so that the wound does not experience severe infection and stimulates the formation of collagen I, a protein that plays a role in wound healing (Dong, 2020). Triterpenoids can

strengthen skin cells and improve repair, stimulate blood cells and the immune system, and can be natural antibiotics (Sutardi, 2016).

Sambilotto extract has been widely studied to contain the main component, andrographolide, a triterpenoid group (Valdiani *et al.*, 2012). In addition, Sambilotto extract also includes the most dominant flavonoid, quercetin (Fardiyah *et al.*, 2020). Antioxidants from quercetin compounds can trigger collagen production and increase Vascular Endothelial Growth Factor (VEGF), which is anti-inflammatory and antibacterial. Based on research by Yang *et al.* (2020), quercetin compounds have an anti-inflammatory effect by inhibiting the cyclooxygenase (COX) enzyme, which induces the formation of prostaglandins as inflammatory mediators, while antibacterial activity inhibits bacterial growth through inhibition of bacterial hydrolytic enzymes. Andrographolide compounds have activity as anti-inflammatory and antioxidant (Lin *et al.*, 2009). Andrographolide works as an anti-inflammatory agent by suppressing the production of the protein inducible nitric oxide synthase in RAW 264.7 cells (iNOS) (Chiou *et al.*, 2000). The unsaturated α,β -lactone structure (α,β -unsaturated lactone) part of the andrographolide molecular structure can neutralize the superoxide anion so that andrographolide acts as an antioxidant (Yan *et al.*, 2018).

CONCLUSION

Carbopol-940 and sodium alginate concentrations influence the evaluation of gel preparations, namely pH, viscosity, and adhesion. The higher the carbopol-940 and sodium alginate concentration will increase the viscosity and adhesiveness values, but lower the pH value. The optimum formula based on the optimization of the factorial design analysis on the evaluation response of the preparation was obtained at a concentration of 0.5% carbopol-940 and 5% sodium alginate with the average characteristics of pH, viscosity, and adhesion, respectively 5.17 ± 0.04 ; 2934.452 ± 286.871 cPs; and 194.236 ± 3.684 s. The optimum formula shows values between 95% PI low and 95% PI high. The optimum gel preparation of Sambilotto extract has fairly good physical stability. The optimum gel preparation of Sambilotto extract was also shown to have a good effect on healing burns with a %recovery of 99.72%, on the 20th day, and based on the results of ANOVA, there was no significant difference to the positive control.

AUTHOR CONTRIBUTIONS

Conceptualization, E. F. A., A. A.; Methodology, E. F. A., A. A.; Software, E. F. A., A. A.; Validation, E. F. A., A. A., N. K.; Formal Analysis, E. F. A., A. A., N. K.; Investigation, E. F. A., A. A., N. K.; Resources, E. F. A., A. A., N. K.; Data Curation, E. F. A., A. A., N. K.; Writing - Original Draft, E. F. A., A. A.; Writing - Review & Editing, E. F. A., A. A.; Visualization, E. F. A., A. A.; Supervision, E. F. A., A. A.; Project Administration, E. F. A., A. A.; Funding Acquisition, E. F. A., A. A.

FUNDING STATEMENT

This research did not receive any specific grant from funding agencies in the public, commercial, or not for profit sectors.

CONFLICT OF INTEREST

The authors declared no conflict of interest.

REFERENCES

- Acar, T., Teylidiz, R., Vahapogxlu, H., Karakayali, S. & Aydin, R. (2002). Efficacy of Micronized Flavonoid Fraction on Healing in Thermally Injured Rat. *Annals of Burns and Fire Disasters*; 15; 41-44.
- Agoes, G. (2012). Sediaan Farmasi Likuida-Semisolid (1 ed.). Bandung: Penerbit ITB.
- Akhoondinasab, M. R., Akhoondinasab, M. & Saberi, M. (2014). Comparison of Healing Effect of *Aloe Vera* Extract and Silver Sulfadiazine in Burn Injuries in Experiment Rat Mode. *World journal of Plastic Surgery*; 3; 29-34.
- Al-Bayaty, F., Abu-Hasan, M. H. & Abdulla, M. A. (2011). Effect of *Andrographis paniculata* Leaf Extract on Wound Healing in Rats. *Natural Product Research*; 26; 423-429. doi: 10.1080/14786419.2010.496114.
- Apriani, E. F., Nurleni, N., Nugrahani, H. N. & Iskandarsyah, I. (2018). Stability Testing of Azelaic Acid Cream Based Ethosome. *Asian Journal of Pharmaceutical and Clinical Research*; 11; 270-273. doi: 10.22159/ajpcr.2018.v11i5.23218.
- Apriani, E. F., Shiyani, S., Hardestyari, D., Starlista, V. & Febriani, M. (2023). Factorial Design for The Optimization of Clindamycin HCl-Loaded Ethosome with Various Concentration of Phospholipon 90G and ethanol. *Research Journal of Pharmacy and Technology*; 16; 1561-1568. doi: 10.52711/0974-360X.2023.00255.
- Ariawan, D., Perwirayudha, M. G., Juniantito, V., Julia, V & Sulistyani, L. D. (2023). Effects of *Andrographis paniculata* Extract as a Wound Dressing in the Proliferation Phase of Rats Palatal Mucosa Wound Healing. *Journal of International Dental and Medical Research*; 16; 510-516.
- Cardenas, A, Monal, W. A., Goycoolea, F. M., Ciapara, I. H. & Peniche, C. (2003). Diffusion through Membranes of the Polyelectrolyte Complex of Chitosan and Alginate. *Macromolecular Bioscience*; 3; 535-539. doi: 10.1002/mabi.200300031.
- Chiou, W. F, Chen, C. F. & Lin, J. J. (2000). Mechanisms of Suppression of Inducible Nitric Oxide Synthase (iNOS) Expression in RAW 264.7 Cells by Andrographolide. *British Journal of Pharmacology*; 129; 1553-1560. doi: 10.1038/sj.bjp.0703191.
- Depkes RI. (2017). Farmakope Herbal Indonesia Edisi II. Jakarta: Kemenkes RI.
- Dong, S. (2020). Antibacterial Activity and Mechanism of Action Saponins from *Chenopodium quinoa* Willd, Husks Against Foodborne Pathogenic Bacteria. *Industrial Crops and Products*; 149; 1-14. doi: 10.1016/j.indcrop.2020.112350.
- Fardiyah, Q., Ersam, T., Suyanta, Slamet, A., Suprpto & Kurniawan, F. (2020). New Potential and Characterization of *Andrographis paniculata* L. Ness Plant Extracts as Photoprotective Agent. *Arabian Journal of Chemistry*; 13; 8888-8897. doi: 10.1016/j.arabjc.2020.10.015.
- Garg, A., Aggarwal, D., Garg, S. & Singla, A. (2002). Spreading of Semisolid Formulation: An Update Pharmaceutical Technology. *Pharmaceutical Technology*; 26; 84-105.
- Gonzalez, A. C., Costa, T. F., Andrade, Z. A. & Medrado, A. R. (2016). Wound Healing - A Literature Review. *Anais Brasileiros De Dermatologia*; 91; 614-620. doi: 10.1590/abd1806-4841.20164741.
- Hita, I. P. G. A. P., Arimbawa, P. E. & Suryaningsih, N. P. A. (2021). Characterization and Screening Active Phytochemical Compounds of 70% Ethanol Extract of Mahogany Seed (*Swietenia mahagoni* Jacq.). *Ad-Dawaa' Journal of Pharmaceutical Sciences*; 4; 1-8. doi: 10.24252/djps.v4i1.21225.
- Jeschke, M. G., van Baar, M. E., Choudhry, M. A., Chung, K. K., Gibran, N. S. & Logsetty, S. (2020).

- Burn Injury. *Nature Reviews Disease Primers*; 6; 1-25. doi: 10.1038/s41572-020-0145-5.
- Lewis, D. & Zhao, X. (2006). Synthesis of Triethanolamine Trisulphate and Its Application to Cellulosic Fibres. *Coloration Technology*; 120; 172-179. doi: 10.1111/j.1478-4408.2004.tb00225.x.
- Lin, F. L., Wu, S. J. & Lee, S. C. (2009). Antioedema and Analgesic Activities of *Andrographis paniculata* Extracts and their Active Constituent Andrographolide. *Phytotherapy Research*; 23; 958-964. doi: 10.1002/ptr.2701.
- Liu, W., Hu, M., Liu, W., Xue, C., Xu, H. & Yang, X.L. (2008). Investigation of the Carbopol Gel of Solid Lipid Nanoparticles for the Transdermal Iontophoretic Delivery of Triamcinolone Acetonide Acetate. *International Journal of Pharmaceutics*; 364; 135-141. doi: j.ijpharm.2008.08.013.
- Loyald, V., Ansel, C. & Howard. (2014). Ansel's Pharmaceutical Dosage Forms and Drug Delivery Systems, 9 ed. Wolter Kluwer: Lippincott Williams & Wilkins.
- Mardiyanto, M., Apriani, E. F. & Alfarizi, M. H. (2022). Formulation and In-vitro Antibacterial Activity of Gel Containing Ethanolic Extract of Purple Sweet Potato Leaves (*Ipomoea batatas* (L.) Loaded Poly Lactic Co-Glycolic Acid Submicroparticles against *Staphylococcus aureus*. *Research Journal of Pharmacy and Technology*; 15; 3599-3605. doi: 10.52711/0974-360X.2022.00603.
- Markiewicz-Gospodarek, A., Koziół, M., Tobiasz, M., Baj, J., Radzikowska-Büchner, E. & Przekora, A. (2022). Burn Wound Healing: Clinical Complications, Medical Care, Treatment, and Dressing Types: The Current State of Knowledge for Clinical Practice. *International Journal of Environmental Research and Public Health*; 19; 1-25. doi: 10.3390/ijerph19031338.
- Mukhlisah, N. R. I., Sugihartini, N. & Yuwono, T. (2016). Daya Iritasi Dan Sifat Fisik Sediaan Salep Minyak Atsiri Bunga Cengkeh (*Syzygium Aromaticum*) Pada Basis Hidrokarbon Unguentum Volatile Oil of *Syzygium Aromaticum*. *Majalah Farmaseutik*; 12; 372-376.
- Mussard, E., Jousselin, S., Cesaro, A., Legrain, B., Lespessailles, E., Esteve, E., Berteina-Raboin, S. & Toumi, H. (2020). *Andrographis paniculata* and Its Bioactive Diterpenoids Against Inflammation and Oxidative Stress in Keratinocytes. *Antioxidants*; 9; 530. doi: 10.3390/antiox9060530.
- Nikam, S. (2017). Anti-acne Gel of Isotretinoin: Formulation and Evaluation. *Asian Journal of Pharmaceutical and Clinical Research*; 10 (11): 257-266. doi:10.22159/ajpcr.2017.v10i11.19614
- Niyaz, B., Kalyani, P. & Divakar, G. (2011). Formulation and Evaluation of Gel Containing Fluconazole-Antifungal Agent. *International Journal of Drug Development & Research*; 3; 109-128.
- Noer, M. S. (2006). Penanganan Luka Bakar Akut. Surabaya: Airlangga University Press.
- Nurman, S., Yulia, R., Irmayanti, Noor, E. & Candra Sunarti, T. (2019). The Optimization of Gel Preparations Using the Active Compounds of Arabica Coffee Ground Nanoparticles. *Scientia Pharmaceutica*; 87; 1-16. doi: 10.3390/scipharm87040032
- Raissi, S. & Farsani, R. E. (2009). Statistical Process Optimization through Multi Response Surface Methodology. *World Academy of Sciences, Engineering and Technology*; 51; 267-271. doi: 10.5281/zenodo.1083451.
- Rajanna, M., Bharathi, B., Shivakumar, B. R., Deepak, M., Prashanth, D., Prabakaran, D., Vijayabhaskar, T. & Arun, B. (2021). Immunomodulatory Effects of *Andrographis paniculata* Extract in Healthy Adults E An Open-Label Study. *Journal of Ayurveda and Integrative Medicine*; 12; 529-534. doi: 10.1016/j.jaim.2021.06.004.
- Remaggi, G., Catanzano, O., Quaglia, F. & Elviri, L. (2022). Alginate Self-Crosslinking Ink for 3D Extrusion-Based Cryoprinting and Application for Epirubicin-HCl Delivery on MCF-7 Cells. *Molecules*; 27; 882. doi: 10.3390/molecules27030882.
- Rinaldi, R., Fauziah, F. & Musfira, Y. (2019). Studi Formulasi dan Efektivitas Gel Ekstrak Etanol Daun Sirih (*Piper betle* L.) terhadap Penyembuhan Luka Bakar pada Kelinci (*Oryctolagus cuniculus*). *Jurnal Dunia Farmasi*; 4; 23-33. doi: 10.33085/jdf.v4i1.4564.
- Rowe, R. C., Sheskey, P. J. & Quin, M. (2009). Handbook of Pharmaceutical Excipients, 6th edition. United Kingdom: Pharmaceutical Press.
- Selvaraj K, Gayatri Devi R, Selvaraj J, Jothi Priya A. (2022). In Vitro Anti-Inflammatory and Wound Healing Properties of *Andrographis echioides* and *Andrographis paniculata*. *Bioinformation*; 18; 331-336. doi: 10.6026/97320630018331.

- Shetty, A. J., Sweta, K. M. & Ramesh, P. B. (2021). A Case Series of Second-Degree Burn Patients Managed with Patoladi Vikeshika, an Ayurvedic contact Layer Dressing. *Journal of Ayurveda and Integrative Medicine*; 12; 544-548. doi: 10.1016/j.jaim.2021.03.011.
- Singh, M. P., Nagori, B. P., Shaw, N. R., Tiwari, M. & Jhanwar, B. (2013). Formulation Development & Evaluation of Topical Gel Formulations Using Different Gelling Agents and Its Comparison with Marketed Gel Formulation. *International Journal of Pharmaceutical Erudition*; 3; 1-10.
- Sutardi. (2016). Bioactive Compounds in Pegagan Plant and Its Use for Increasing Immune System. *Jurnal Litbang Pertama*; 35; 1-5.
- Titaley, S. (2014). Formulasi dan Uji Efektifitas Sediaan Gel Ekstra Etanol Daun Mangrove Api-Api (*Avicennia marina*) Sebagai Antiseptik Tangan. *Pharmacon*; 3; 99-106. doi: 10.35799/pha.3.2014.4781.
- Tiwari, V. K. (2012). Burn wound: How it differs from Other Wounds?. *Indian Journal of Plastic Surgery: Official Publication of the Association of Plastic Surgeons of India*; 45; 364-373. doi: 10.4103/0970-0358.101319.
- Tranggono, R. I. (2007). Buku Pengantar ilmu Kosmetik. Jakarta: Pustaka Utama.
- Valdiani, A., Kadir, M. A., Tan, S. G., Talei, D., Abdullah, M. P. & Nikzad, S. (2012). Nain-e Havandi *Andrographis paniculata* Present Yesterday, Absent Today: a Plenary Review on Underutilized Herb of Iran's Pharmaceutical Plants. *Molecular Biology Reports*; 39; 5409-5424. doi: 10.1007/s11033-011-1341-x.
- Velnar, T., Bailey, T. & Smrkolj, T. (2009). The Wound Healing Process: an Overview of Cellular and Molecular Mechanism. *The Journal of international Medical Research*; 37; 1528-2542. doi: 10.1177/147323000903700531.
- Wijaya, A. S. & Putri, Y. M. (2013). Keperawatan Medikal Bedah 2, Keperawatan Dewasa Teori dan Contoh Askep. Yogyakarta: Nuha Medika.
- Yan, Y., Fang, L. H. & Du, G. H. (2018). *Andrographolide*. Singapore: Springer Nature Singapore.
- Yang, D., Wang, T., Long, M. & Li, P. (2020). Quercetin: Its Main Pharmacological Activity and Potential Application in Clinical Medicine. *Oxidative Medicine and Cellular Longevity*; 2020; 1-13. doi: 10.1155/2020/8825387.



Effect of CaCl₂ Crosslinker Concentration On The Characteristics, Release and Stability of Ciprofloxacin HCl-Alginate-Carrageenan Microspheres

Amiruddin¹, Muh. Agus Syamsur Rijal^{2,3}, Dewi Melani Hariyadi^{2,3*}

¹Master Program in Pharmaceutical Sciences, Faculty of Pharmacy, Universitas Airlangga, Surabaya, Indonesia

²Departement of Pharmaceutical Sciences, Faculty of Pharmacy, Universitas Airlangga, Surabaya, Indonesia

³Nanotechnology and Drug Delivery System Research Group, Faculty of Pharmacy, Universitas Airlangga, Surabaya, Indonesia

*Corresponding author: dewi-m-h@ff.unair.ac.id

Submitted: 3 August 2023

Revised: 16 October 2023

Accepted: 25 October 2023

Abstract

Background: Ciprofloxacin HCl is a broad-spectrum fluoroquinolone antibiotic that has the lowest MIC against *Mycobacterium tuberculosis* but has limitations in oral use, so inhalation microspheres are made. **Objective:** This study aimed to investigate the effect of CaCl₂ crosslinker concentration on the characteristics, release and stability of ciprofloxacin-alginate-carrageenan microspheres. **Methods:** Microspheres were prepared by ionotropic gelation using aerosolization with calcium chloride 0.5M (F1), 1.0M (F2), 1.5M (F3), 2.0M (F4) as crosslinker and then dried using freeze dryer. **Results:** Ciprofloxacin-alginate-carrageenan microspheres formed of yellowish-white powder, smooth morphology and excellent flow properties with the particle size of less than 5µm, drug loading and entrapment efficiency were between 2.05% - 2.42% and 75.34% - 98.09%, yield was between 84.69% - 97.57%, moisture content of less than 10%. Ciprofloxacin-alginate-carrageenan microspheres with 1.5M crosslinker (F3) was the optimal formula. For 12 hours, ciprofloxacin released was 49.89% - 63.78% at pH 7.4, and the kinetics of drug release showed that of Korsmeyer-peppas with a mechanism based on fickian diffusion. The microspheres were discovered to be stable for up to 28 days of storage. **Conclusion:** The increased concentration of the CaCl₂ crosslinker from 0.5M to 2.0M decreased the particle size and drug release but increased the yield, drug loading and entrapment efficiency.

Keywords: calcium chloride, characteristics, ciprofloxacin microspheres, release, stability

How to cite this article:

Amiruddin, Rijal, M. A. S. & Hariyadi, D. M. (2023). Effect of CaCl₂ Crosslinker Concentration On The Characteristics, Release and Stability of Ciprofloxacin HCl-Alginate-Carrageenan Microspheres. *Jurnal Farmasi dan Ilmu Kefarmasian Indonesia*, 10(3), 312-323. <http://doi.org/10.20473/jfiki.v10i32023.312-323>

INTRODUCTION

Ciprofloxacin HCl is a broad-spectrum fluoroquinolone antibiotic that inhibits the bacterial DNA replication enzymes DNA-gyrase and topoisomerase IV (Thai *et al.*, 2022). Ciprofloxacin has the lowest minimum inhibitory concentration (MIC) against *Mycobacterium tuberculosis*, which ranges from 0.125 to 2.0 µg/mL (Heifetz & Lindholm-levy, 1987). Ciprofloxacin for oral use has a short half-life of 3-5 hours (Katzung *et al.*, 2012). Around 70% of the Ciprofloxacin HCl is absorbed after oral administration. Ciprofloxacin is then metabolized in the liver by 15% and then excreted by 40-50% of the oral dose (Bayer Health Care Pharmaceuticals Inc, 2021). Thus, the delivery system needs to change the route or modify the release to increase the efficacy of ciprofloxacin. Inhalation delivery systems to target the lungs have advantages such as the ability to target alveolar macrophages containing TB bacilli, high drug concentrations in lung tissue maintained, avoidance first-pass metabolism, faster onset of action and smaller doses compared to intravenous and oral administration and ensure limited systemic side effects (Misra *et al.*, 2011). Inhalation delivery systems to target the lungs can be achieved by microencapsulation methods that can achieve targets and control drug release (Santa-maria *et al.*, 2012). The dosage form with microspheres is needed for delivery of the lungs so that the drug design is encapsulated with microparticle technology (Lengyel *et al.*, 2019).

Microspheres have a small diameter of 1 µm to 1000 µm with spherical particles consisting of drugs, proteins or synthetic polymers (Kadam & Suvarna, 2015). For the inhalation route, the particle size ranges from 1 µm to 5 µm for lung deposition (Gaber *et al.*, 2021). One of the things that affect the effectiveness of microspheres as a drug delivery system is the selection of polymers and crosslinkers used as matrices and crosslinking of microspheres (Lee *et al.*, 2012). The type of polymer used can be derived from nature or synthetic, but natural polymers have the advantages of being cheap, readily to use, biocompatible, biodegradable and able to do a multitude of chemical modifications (Rajeswari *et al.*, 2017). A combination of alginate and carrageenan polymer was selected in this research because it is a natural polymer that is biodegradable, economical, widely used for encapsulation (Hariyadi *et al.*, 2019) not accumulating in organs and not toxic in its administration (Hariyadi *et al.*, 2019). Alginate is a naturally occurring polysaccharide polymer that is generally found in the cell walls of brown algae

(Phaeophyceae) species (Lee & Mooney, 2012). Alginate provides the highest mucoadhesive ability compared to other polymers (Adrian *et al.*, 2019). However, alginate has poor mechanical properties and a porous structure, which causes the microspheres to burst release, so it needs to be combined with carrageenan, which is capable of providing sustained release (Abdelghany *et al.*, 2017). Carrageenans is a natural polysaccharide polymer found in the family Rhodophyceae of marine red algae, and kappa carrageenan is one of the carrageenan types which has many advantages (Tecante & Núñez, 2012).

Crosslinkers in biodegradable polymers are very important in controlling the swelling and degradation rate of the microspheres. Ca²⁺ ions are most preferred for developing microparticles compared to Rb⁺, Cs⁺, K⁺, Na⁺, Li⁺, Ba²⁺, Sr²⁺, and Mg²⁺, because Ca²⁺ is the safest for the body (Tecante & Núñez, 2012). The use of CaCl₂ crosslinker in alginate and carrageenan polymers is used because sodium alginate has a high carboxyl group content and a high affinity for bivalent cations such as Ca²⁺ ions, whereas kappa carrageenan and Ca²⁺ form crosslinks due to electrostatic attraction forces. Concurrently, neighbouring Ca²⁺ and OSO₃ generate a network of crosslinks between macromolecular networks (Yu *et al.*, 2019). The combination of alginate and carrageenan polymer with a ratio of 1:1 with CaCl₂ crosslinkers has an increased swelling degree at neutral pH. It shows the most optimal encapsulation efficiency with a release degree of 92% so this ratio was chosen to provide a maximum therapeutic effect (Kolesnyk & Burban, 2015). The combination of alginate and carrageenan polymer as a microsphere matrix with a ratio (1:1) at a concentration of 0.9% and a 0.5M CaCl₂ crosslinker obtained optimum microsphere characteristics but still had low drug loading and encapsulation efficiency and an increase in polymer concentration above a concentration of 0.9% was thought to be cannot be stirred and forms a matrix of microspheres, so it is suggested to increase drug loading and encapsulation efficiency of these microspheres (Wijaksana, 2022). Microspheres produced with increased crosslinking concentrations resulted in small particle size, high entrapment efficiency, and drug loading (Hariyadi *et al.*, 2014).

Several methods can prepare microspheres utilising a combination of alginate and carrageenan polymer with calcium chloride crosslinker. This study used the ionotropic gelation method with aerosolization technique because this method produces microspheres chemically based on the ability of polyelectrolytes to

cross over the ion counter to form a gel (Hariyadi *et al.*, 2019). The advantages of this method that it is easy, fast, relatively inexpensive, does not use organic solvents, and uses low temperature, thereby reducing drug damage (Pasquale *et al.*, 2021), and aerosolization techniques can produce small and uniform particle sizes (Hariyadi *et al.*, 2018). In the process of making microspheres, drying is required, paying attention to the stability of the active pharmaceutical ingredients. Drying is carried out using the freeze-drying technique and needs to be added with lyoprotectant (Laura *et al.*, 2010). The lyoprotectant used in this study was maltodextrin (Hariyadi *et al.*, 2016). This study will produce ciprofloxacin HCl-alginate-carrageenan microspheres with various concentrations of CaCl₂ crosslinker, which are made using ionotropic gelation technique by aerosolization method to investigate the effect of CaCl₂ crosslinker concentration on the characteristics, release and stability of ciprofloxacin-alginate-carrageenan microspheres. Physical characteristics include organoleptic, morphology, particle sizes, drug loading, entrapment efficiency, yield, moisture content and flow properties.

MATERIALS AND METHODS

Materials

Ciprofloxacin HCl (Zhejiang Ltd., China), Sodium Alginate (Sigma Aldrich, USA), Kappa-Carrageenan (KCN, Pasuruan, Indonesia), CaCl₂.2H₂O (PT.Sumber Utama Kimia Murni, Indonesia), Maltodextrin (Bratachem Chemistry, Indonesia), Aquadestillata (PT.Sumber Utama Kimia Murni, Indonesia), Phosphate Buffered Saline Tablet (Oxoid, England). NaH₂PO₄ (CV. CIMS, Indonesia), KH₂PO₄ (CV. CIMS, Indonesia), NaCl (CV. CIMS, Indonesia), KCl (CV. CIMS, Indonesia). All composition and reagent use pharmaceutical grade.

Tools

UV-Vis spectrophotometer (Shimadzu UV 1800 spectrophotometer, Japan), FT-IR spectrophotometer (Perkin Elmer Instrument, USA), Differential Scanning Calorimeter/DSC (Mettler Toledo FT 900 Thermal System, USA), Analytical balance (Chyo Balance corporation Kyoto, Japan), Spray aerosol, Freeze dryer (Eyela FD-81, Japan), optical microscope (PS AIR FI

31-032, China), stirring plate (Dragon Lab MSPro, China), centrifuge (Rotofix 32, Germany), Scanning Electronic Microscope (JEOL, Japan), Climatic chamber, Moisture analyzer (Mettler Toledo HB43-S, USA) and Thermoshakers (Gerhardt, Germany).

Method

Preparation of ciprofloxacin-alginate-carrageenan microspheres

Microspheres were made by applying the ionotropic gelation method with aerosolization techniques, with a 0.2% drug concentration. The drug was dissolved into a combination of alginate carrageenan polymer solution with a ratio of 1:1 (w/w) at a concentration of 0.9% of each polymer. The ciprofloxacin-alginate-carrageenan solution was sprayed into various CaCl₂ cross-agent solutions with different concentrations, namely 0.5M, 1.0M, 1.5M, 2.0M at 40 psi and stirred continuously for 2 hours at a speed of 1000 rpm. The microsphere was collected by centrifugation at 2500 rpm for 6 minutes, followed by two washes with distilled water. The microspheres was resuspended in 5% maltodextrin solution and then dried with a freeze dryer at -80°C until the humidity met the requirements (Hariyadi *et al.*, 2022). Furthermore, ciprofloxacin-alginate-carrageenan microspheres that form were evaluated. The formula of microspheres can be seen in Table 1.

FTIR spectroscopic analysis

FTIR spectroscopy is a crucial analytical method that identifies several distinctive functional groups in molecules of any substance. FTIR spectra of all raw materials and microsphere formulations were obtained using an FT-IR (Perkin Elmer Instrument) spectrophotometer. The FTIR band spectra were examined to investigate the structural integrity in the different formulations after scanning at wavenumbers 4000 - 500 cm⁻¹.

DSC analysis

The thermal properties of all raw materials were determined using a DSC TGA (Mettler Toledo FP 900). Samples of about 5mg of all formulas were scanned (from 30°C to 250°C) at a heating rate of 10°C/min. The characteristic of the prominent DSC peak, which represents the endothermic peak shown by temperature, was determined.

Table 1. Formula of ciprofloxacin-alginate-carrageenan microspheres

Materials	Functions	F1	F2	F3	F4
Ciprofloxacin HCl	API	0.2%	0.2%	0.2%	0.2%
Sodium alginate	Polymer	0.9%	0.9%	0.9%	0.9%
Kappa carrageenn	Polymer	0.9%	0.9%	0.9%	0.9%
Calcium chloride	Crosslinker	0.5M	1.0M	1.5M	2.0M

*drying with freeze dry added with 5% maltodextrin

Physical characterization of microspheres

Organoleptics

All formulas of ciprofloxacin-alginate-carrageenan microsphere were observed for their organoleptic appearance, including shape and colour.

Morphology

Morphology was evaluated using Scanning Electron Microscopy (SEM). The gold-coated samples were mounted for 120 seconds and were then examined with an SEM microscope (JEOL) at a working distance of 10 mm and 15mm, with 15 kV beam energy.

Particle size

Microspheres of 300 particles were determined using an optical microscope (PS AIR FI 31-032) and Image Raster Software. The average diameter was calculated using the equation:

$$Diameter\ average = \frac{\sum nd}{\sum n}$$

n = a number of microspheres observed

d = size of the microspheres (Dhakar *et al.*, 2010).

Drug loading and entrapment efficiency

50 mg of microsphere was added to Citrate Buffer, which has a pH of 4.4 and was stirred for 7 hours at 1000rpm. The solution was filtered, and then a UV-Vis spectrophotometer was used to measure the absorbance of the solution at a wavelength of 275 nm (taken from in-house validation). The amount of the drug was determined using a validated in-house standard calibrated plot. The drug loading and entrapment efficiency was calculated using the equation (Balagani *et al.*, 2011):

$$Drug\ loading = \frac{Weight\ of\ drug}{Weight\ of\ microspheres} \times 100\%$$

$$EE = \frac{Drug\ content\ in\ microspheres}{Theoretical\ drug\ content\ in\ formula} \times 100\%$$

Yield

The yield was calculated according to the total recoverable final weight of microparticles to evaluate efficiency in producing microspheres. The yield was calculated using the equation (Balagani *et al.*, 2011):

$$Yield = \frac{Weight\ of\ dry\ microspheres}{Total\ weight\ materials} \times 100\%$$

Moisture content

Moisture content was measured using the Moisture Analyzer (Mettler Toledo HB43-S). The microspheres are weighed with a minimum weight of 500 mg then distributed evenly in the pan and the sample is burned and the moisture content is measured in the range of 100-140°C (Hariyadi *et al.*, 2019).

Flow properties

A graduated cylinder of 10 mL was used to measure bulk and tapped densities. The sample was mechanically

tapped 500 times after being put into a cylinder. The tapped volume was recorded, and the bulk density and tapped density were calculated (Lane 2016).

Bulk density

The ratio of powder weight bulk density compared to the initial volume of the untapped powder, as below equation (Lane 2016):

$$\rho\ bulk = \frac{Powder\ weight\ (g)}{Initial\ volume\ of\ powder\ (ml)}$$

Tapped density

Tapped density was determined by the ratio of powder weight compared to final volume of the tapped powder as below equation (Lane 2016):

$$\rho\ tapp = \frac{Powder\ weight\ (g)}{Volume\ of\ powder\ after\ tapping\ (ml)}$$

$$Carr's\ index = \frac{\rho\ tapped - \rho\ bulk}{\rho\ bulk} \times 100\%$$

$$Hausner\ ratio = \frac{Tapped\ density}{Bulk\ density}$$

Parameters of Carr's index and Hausner's ratio are shown in Table 2.

Table 2. Carr's index and Hausner ratio of powder flow

Flow character	Carr's index (%)	Hausner ratio
Excellent	<10	1.00-1.11
Good	11-15	1.12-1.18
Fair	16-20	1.19-1.25
Passable	21-25	1.26-1.34
Poor	26-31	1.35-1.45
Very poor	32-37	1.46-1.59
Very, very poor	>38	>1.60

In vitro release study

Ciprofloxacin release from the microspheres was tested in phosphate-buffered saline (PBS) at a pH level of 7.4 (Karimi *et al.*, 2016). The released test was carried out using a Thermoshaker (Gerhardt) at 37°C with 100 rpm. 500 mg of microspheres were added to 100 mL PBS solution (pH 7.4) on a Thermoshaker at 37 ± 0.5°C and stirred at 100 rpm. A snippet of samples (5.0 mL) was taken at the minutes of 0, 15, 30, 60, 90, 120, 180, 240, 360, 480, 600 and 720 minutes. In each snippet of samples, the same volume of release media was replaced, and the snippet of samples was filtered using millipore filter paper 0.45 µm. The sample absorbance was observed with a UV-Vis spectrophotometer (Shimadzu UV-1800) at the wavelength of 268 nm (Hariyadi *et al.*, 2019).

Drug release kinetics

The drug release kinetics were investigated to describe the drug release pattern. The mechanism of

drug release from microspheres was examined using various kinetic equations, such as zero-order kinetic, first-order kinetic, Korsmeyer-peppas and Higuchi (Bruschi, 2015). The release kinetics of a drug can be determined from the price of R^2 from the linear regression equation obtained from each formula. If R^2 approached one, it could be assumed that the kinetic followed the release of the regression equation from the corresponding kinetics model.

Stability test

Ciprofloxacin-alginate-carrageenan microspheres were tested for accelerated stability. The microspheres were placed into a vial and stored for 28 days at room $25 \pm 2^\circ\text{C}$ and $40 \pm 2^\circ\text{C}$, RH $75 \pm 5\%$. The stability of the prepared formulations was tested by organoleptic property, moisture content and drug loading (Hariyadi & Hendradi, 2020).

Data analysis

All data are presented in mean \pm SD. For physical characteristics and drug release, the statistical data was analyzed using one-way analysis of variance with a confidence degree of 95% ($\alpha = 0.05$). For stability test, the statistical data was analyzed using two-way analysis of variance with a confidence degree of 95% ($\alpha = 0.05$).

RESULTS AND DISCUSSION

Characterization of microspheres

This study investigated the effect of CaCl_2 crosslinker concentration on the formation and physical characterization of ciprofloxacin microspheres using a combination of alginate and carrageenan polymers produced by ionotropic gelation methods using aerosolization techniques. Result of characterization by FTIR spectra and analysis of F1 to F4 were presented in Table 3. The functional groups of ciprofloxacin HCl, sodium alginate, kappa carrageenan, all microsphere formulas, and the possibility of wavenumber presence or shifting were investigated.. Referring to the

ciprofloxacin, the wavenumber of the characteristic peak of quinolone N-H bending, OH stretching, C=O stretching, C-H stretching and C-F stretching was present in all formulas of microspheres indicated the stability of ciprofloxacin in the microspheres. For formulations F1 to F4, the shift of the wavenumber of quinolone N-H band of ciprofloxacin HCl was from 1612.62 cm^{-1} to between 1602.23 cm^{-1} and 1661.17 cm^{-1} ; the OH group from 3516.74 cm^{-1} to between 3529.87 cm^{-1} and 3558.08 cm^{-1} ; the CH group from 2914.76 cm^{-1} to between 2915.03 cm^{-1} and 2937.59 cm^{-1} ; the C=O group from 1699.31 cm^{-1} to between 1724.68 cm^{-1} to 1731.16 cm^{-1} ; the C-F group from 1043.55 cm^{-1} to between 1005.25 cm^{-1} and 1013.94 cm^{-1} . The wave shift in sodium alginate occurred in the C-C group from 1080.87 cm^{-1} to between 1075.11 cm^{-1} and 1113.43 cm^{-1} ; the guluronic group from 884.91 cm^{-1} to between 925.44 cm^{-1} and 930.61 cm^{-1} ; the mannuronic group from 810.48 cm^{-1} to between 844.94 cm^{-1} and 849.63 cm^{-1} . The wave shift in kappa-carrageenan occurred in the S=O from 1223.52 cm^{-1} to between 1224.16 cm^{-1} and 1247.41 cm^{-1} ; the galactose sulfat from 841.94 cm^{-1} to between 844.96 cm^{-1} and 849.63 cm^{-1} and the loss of the C-O-C group. These indicated that there were chemical interactions between the combination of alginate-carrageenan polymer and CaCl_2 crosslinker to form microspheres. Chemical interactions between groups that occurs predict that the alginate polymer has carboxyl groups on two opposite G blockchains. In contrast, the kappa carrageenan polymer has a sulphate group in its structure (Yu *et al.* 2019). The combination of alginate-carrageenan polymer with the CaCl_2 crosslinker causes the interaction of the carboxyl guluronic group from the alginate polymer and the sulphate group from carrageenan polymer to bind to Ca^{2+} ions to form a network or matrix to entrapped the drug (Wathoniyyah 2016).

Table 3. FTIR of all microspheres formula

Functional group	Wave Number (cm^{-1})						
	Ciprofloxacin HCL	Sodium Alginate	Kappa carrageenan	F1	F2	F3	F4
OH stretch	3516.74	3310.90	3352.32	3532.21	3556.43	3558.08	3529.87
CH stretch	2914.76	2895.76	2892.99	2923.13	2918.83	2915.03	2937.59
C=O stretch	1699.31	1592.77		1729.30	1724.68	1731.16	1728.55
Quinolone N-H bending	1612.62			1604.16	1661.17	1602.23	1602.90
OH bending	1263.03			1245.69	1247.41	1224.16	1239.42
C-F stretch	1043.55			1013.94	1011.97	1005.25	1011.50
C-C stretch		1080.87		1076.84	1075.92	1113.43	1075.11
Guluronic finger		884.91		926.71	925.44	926.29	930.61
Mannuronic finger		810.48		847.20	849.63	848.99	844.96
S=O			1223.52	1245.69	1247.41	1224.16	1239.42
Galactose sulphate			841.94	847.20	849.63	848.99	844.96

DSC result of all materials showed that the endothermic peak of ciprofloxacin HCL at 153.3°C, sodium alginate endothermic peak at 127.8°C, kappa-carrageenan showed a prominent characteristic endothermic peak at 124.8°C, calcium chloride dihydrate endothermic peak at 175.6 °C and maltodextrin endothermic peak at 139.4°C. All of these DSC peaks indicate the raw material is up to standard.

Organoleptics of microspheres

The organoleptic results of ciprofloxacin-alginate-carrageenan microspheres made by ionic gelation method with aerosolization technique and then dried by freeze drying showed that all microspheres formulas F1 to F4 were in the form of yellowish-white powder and did not agglomerate.

Morphology of microspheres

The morphology of the ciprofloxacin-alginate-carrageenan microspheres using SEM can be seen in Figure 1 and Figure 2. All the microsphere formulas F1 to F4 are spherical with smooth surfaces. The microspheres have a smooth texture because the viscosity of the polymer is sufficient to form cross-links with the crosslinker (Hariyadi *et al.*, 2019).

Physical characteristics of microspheres

Physical characteristics of ciprofloxacin-alginate-carrageenan microspheres can be seen in Table 4.

Particle size

The result showed that ciprofloxacin-alginate-carrageenan microspheres resulted in particle size between $2.17 \pm 0.03 \mu\text{m}$ and $2.50 \pm 0.03 \mu\text{m}$ (Table 4). The results of the particle size of all formulas are less than $5 \mu\text{m}$ suitable for the inhalation route so that microspheres can be deposited in the alveoli (Gaber *et al.*, 2021). If the particle size of the microsphere is and more significant than $5 \mu\text{m}$, the particles will only reach the oropharynx, whereas if it is less than $1 \mu\text{m}$, the particles will be expelled with the expired air (Ashish *et al.*, 2012). Based on statistical analysis ($p < 0.05$), the increase of CaCl_2 crosslinker concentration from 0.5M to 2.0M reduced the particle size of the microspheres (Hariyadi *et al.*, 2018). According to some reports, gelation occurs immediately when a drop of polymer solution comes into contact with calcium ions. When Ca^{2+} ions penetrate to the inside of the polymer solution droplets, water is forced out of the droplets, which causes the microspheres to contract and resulting in smaller particle sizes being formed until saturation occurs so that the particle size does not shrink again (Manjanna *et al.*, 2010; Ra *et al.*, 2014). and a PDI of 0.0033, which was < 0.30 . This indicates a narrow size distribution, and the particle size of the microspheres is homogeneously dispersed (Li *et al.*, 2014).

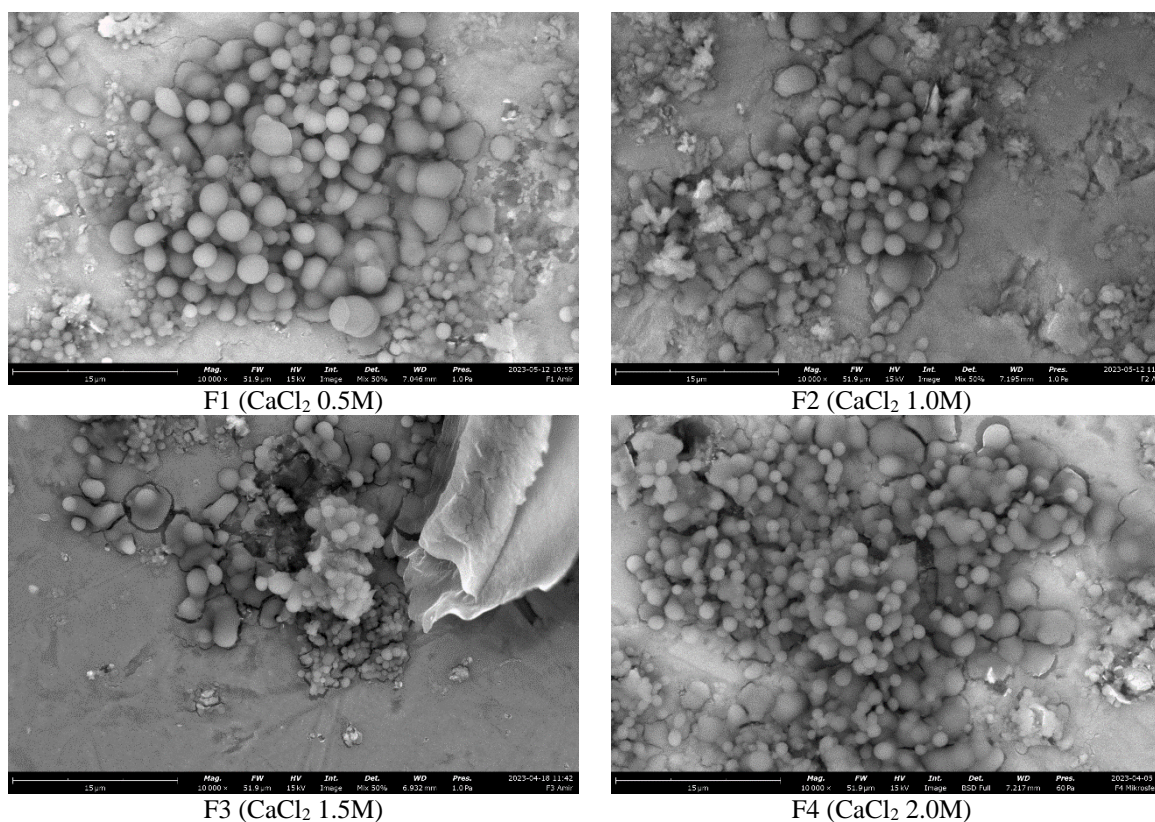


Figure 1. Morphological examination of ciprofloxacin-alginate-carrageenan microspheres formula using SEM at 10000x magnification

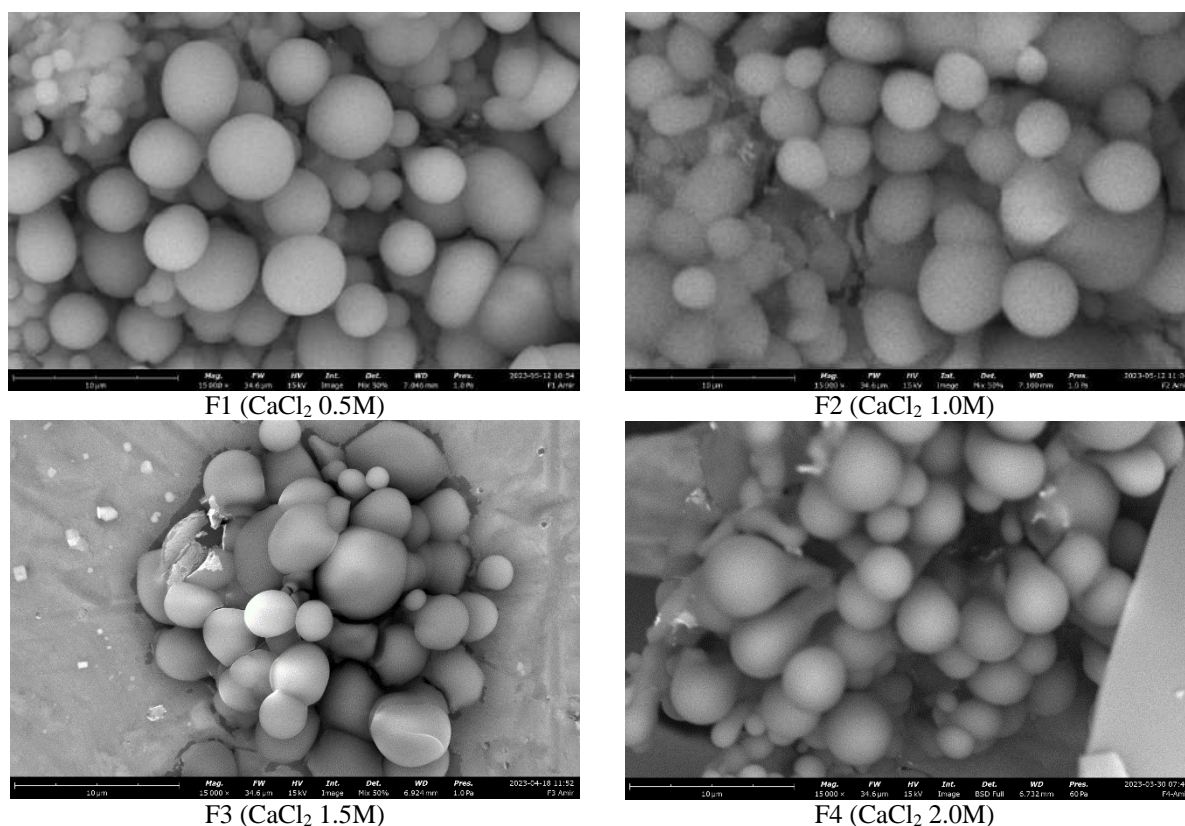


Figure 2. Morphological examination of ciprofloxacin-alginate-carrageenan microspheres formula using SEM at 15000x magnification

Table 4. Physical characteristics of ciprofloxacin-alginate-carrageenan microspheres

Formula	Particle size (µm)	Drug loading (%)	Efficiency entrapment (%)	Yield (%)	Moisture content (%)	Carr's index (%)	Hausner ratio
F1	2.50 ± 0.03	2.05 ± 0.02	75.34 ± 1.46	84.69 ± 0.88	2.59 ± 0.36	5.27 ± 1.11	1.05 ± 0.01
F2	2.29 ± 0.03	2.32 ± 0.01	86.61 ± 2.52	87.07 ± 1.85	2.75 ± 0.75	6.76 ± 0.66	1.07 ± 0.01
F3	2.21 ± 0.02	2.42 ± 0.02	98.09 ± 0.67	93.71 ± 1.09	2.84 ± 0.69	10.32 ± 1.87	1.10 ± 0.02
F4	2.17 ± 0.03	2.37 ± 0.07	96.81 ± 2.19	97.57 ± 0.50	3.16 ± 0.65	14.52 ± 1.53	1.15 ± 0.02

Drug loading and entrapment efficiency

For drug loading and entrapment efficiency, the results are consistent by showing the same pattern of increasing the crosslinker concentration of CaCl₂ from 0.5M to 1.5M increased ciprofloxacin-alginate-carrageenan microsphere drug loading and entrapment efficiency (Table 4). Based on statistical analysis, a significant difference was found between the effect of crosslinker concentration on increasing drug loading and entrapment efficiency (p<0.05). Drug loading increased from 2.05% ± 0.02 to 2.42% ± 0.02 and a similar result of entrapment efficiency was also found to increase from 75.34% ± 1.46 to 98.09% ± 0.67. The highest drug loading and entrapment efficiency was found in the microsphere formulation with a CaCl₂ crosslinker concentration of 1.5M and decreased at a concentration of 2.0M, but the decrease was not significant (p>0.05). The increase in drug loading and

encapsulation efficiency of ciprofloxacin-alginate-carrageenan microspheres occurs because the higher crosslinker concentration causes more availability of Ca²⁺ ions, which crosslinked with carboxyl guluronic groups from alginate and sulphate groups from carrageenan and forms a network or matrix so that drug loading and entrapment efficiency becomes higher until there is a saturation of the crosslinker and polymer bonds so that drug loading and encapsulation efficiency do not increase anymore (Hariyadi *et al.*, 2014).

Yield

The yield of ciprofloxacin-alginate-carrageenan microspheres is seen in Table 4. Yield value showed the smallest value that was for F1 (CaCl₂ 0.5M) at 84.69% ± 0.88, and the highest was F4 (CaCl₂ 2.0M) at 97.57% ± 0.50. These results indicated that the ionotropic gelation method with aerosolization techniques was a potential method for producing ciprofloxacin-alginate-

carrageenan microspheres (Hariyadi *et al.*, 2022). Based on statistical analysis ($p < 0.05$), this means that there is a significant difference. The increase of CaCl_2 crosslinker concentration from 0.5M to 2.0M increased the yield of the microspheres. The high yield value at greater crosslinker concentrations may be due to all the available polymer gelating with the crosslinker (Gedam *et al.*, 2018).

Moisture content

The examination of moisture content was done to determine moisture content in the microspheres after the drying process. The moisture content of ciprofloxacin-alginate-carrageenan microspheres showed at about $2.59\% \pm 0.36$ to $3.16\% \pm 0.65$ (Table 4). The moisture content is less than 5%, so it is preferred for better aerosol performance (Saha *et al.*, 2022). Microsphere particles with high moisture content can cause degradation of the microspheres and reduce their stability (Varela *et al.*, 2022; Shan *et al.*, 2016). The statistical analysis found no significant difference between the increase in CaCl_2 crosslinker concentration and the resultant moisture content ($p > 0.05$).

Flow properties

Carr's index and Hausner ratio measurements were used to determine the flow properties of ciprofloxacin-alginate-carrageenan microspheres. Carr's index ranged from $5.27\% \pm 1.11$ to $14.52\% \pm 1.53$, and the hausner ratio from 1.05 ± 0.01 to 1.15 ± 0.02 (Table 4). According to the values of Carr's index and the Hausner ratio, F1, F2, and F3 have excellent flow properties, while F4 has good flow properties so that it is microspheres are suitable for inhalation routes targeting the lungs. Based on statistical analysis ($p < 0.05$), this means that there is a significant difference. The increase of CaCl_2 crosslinker concentration from 0.5M to 2.0M increased Carr's index and Hausner's ratio of ciprofloxacin-alginate-carrageenan microspheres. The increase in the Carr's index and Hausner ratio occurs because the higher concentration of CaCl_2 crosslinker in the microspheres will affect the compaction of the microspheres, which results in cohesive-adhesive forces of the particles so that agglomeration tends to occur and causes a significant decrease in volume which is observed with an increase in the density of microsphere particles (Lane, 2016).

In vitro release study

Ciprofloxacin HCl was released from microspheres in all formulas for 12 hours in phosphate buffer media

at $\text{pH } 7.4 \pm 0.05$ can be seen in Figure 3. For 12 hours, the cumulative percentage of ciprofloxacin HCl released from microspheres F1 ($63.78\% \pm 1.67$), F2 ($56.86\% \pm 2.39$), F3 ($50.29\% \pm 1.74$) and F4 ($49.89\% \pm 0.85$). Increasing the concentration of the CaCl_2 crosslinker from 0.5M to 2.0M causes a decrease in the release of ciprofloxacin-alginate-carrageenan microspheres. A significant reduction in release ($p < 0.05$) occurred; however, at an increase in the concentration of CaCl_2 from 1.5M to 2.0M, there was a decrease in the release rate, although there was no significant difference including ($p > 0.05$). The observed reduction in drug release with increased calcium chloride is related to the formation of tight junctions between uronic acid residues from alginate and sulphate from carrageenan with calcium ions (Wathoniyyah 2016). The greater the concentration of the CaCl_2 crosslinker in the microspheres, the greater the strength of the ionic bonds and cross-links so that the network or bonds that are formed are more stable, stiff and compact and cause the degree of swelling and sensitivity of the matrix to decrease. It causes a decrease in drug release (Berger *et al.*, 2004; Ra *et al.*, 2014). According to some reports, drug release is also correlated with microsphere characteristics such as particle size and entrapment efficiency (Freiberg & Zhu, 2004; Lin *et al.*, 2018). The smaller particle size of the microspheres indicates that the microspheres are rigid and have low matrix porosity so that drug release is slower compared to larger microsphere particle size (Lin *et al.*, 2018), and drugs encapsulated in a matrix provide the opportunity for a slower release effect so that low of entrapment efficiency caused a faster of drug release (Freiberg & Zhu, 2004; Jerome *et al.*, 2020).

Drug release kinetics

Release kinetics model showed that kinetics follows the korsmeyer-peppas kinetic model with the highest R^2 value and close to 1 for each formula F1 = 0.9942, F2 = 0.9962, F3 = 0.9902, F4 = 0.9915 (Table 5). The release exponent (n) of all formulations showed that it was $n < 0.43$, and then the drug release was based on fickian diffusion, which describes the drug controlled by diffusion mechanism (Bruschi, 2015). In diffusion-controlled systems, the polymeric chains, either by inherent semipermeability or by swelling form pores into which the drug can diffuse and be released into the media (Jerome *et al.*, 2020).

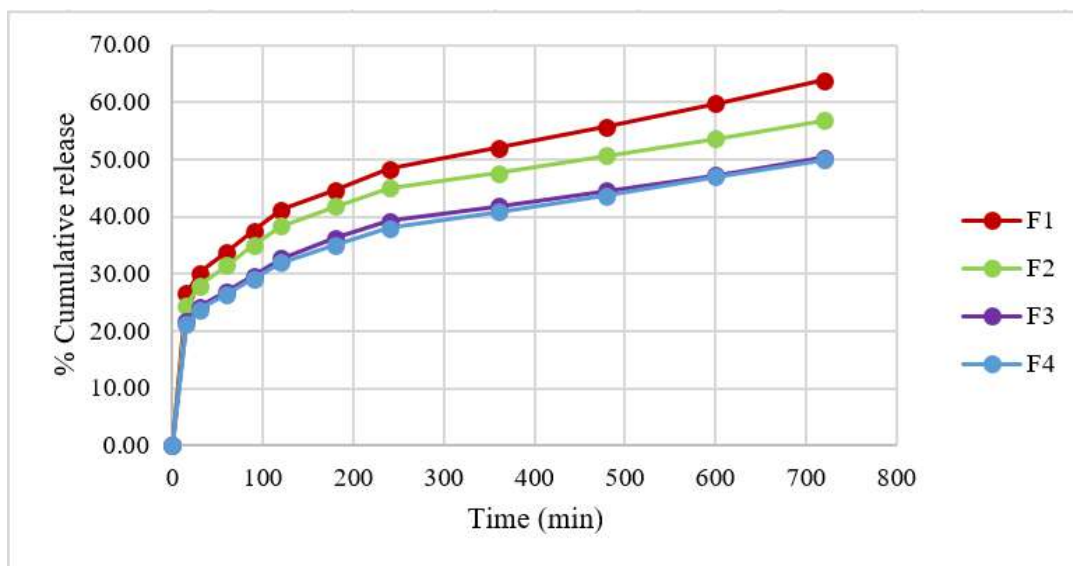


Figure 3. Release profile of ciprofloxacin HCl-alginate-carrageenan microspheres from all formulas

Table 5. Release kinetics with release exponent (n) of ciprofloxacin-alginate-carrageenan microspheres

Formula	Zero order	First order	Higuchi	Korsmeyer-Peppas
F1	R ² = 0.7084	R ² = 0.8469	R ² = 0.8923	n = 0.2272
F2	R ² = 0.6714	R ² = 0.7930	R ² = 0.8699	n = 0.2184
F3	R ² = 0.6941	R ² = 0.7950	R ² = 0.8835	n = 0.2215
F4	R ² = 0.7103	R ² = 0.8096	R ² = 0.8928	n = 0.2254

Table 6. Moisture content and drug loading in stability test at 0 days and 28 days

Sample	Day	Moisture content (%)		Drug loading (%)	
		25°C	40°C	25°C	40°C
F1	0	2.59 ± 0.36	2.59 ± 0.36	2.05±0.02	2.05±0.02
	28	2.95 ± 0.36	3.00 ± 0.21	2.03±0.07	2.02±0.04
F2	0	2.75 ± 0.75	2.75 ± 0.75	2.32±0.01	2.32±0.01
	28	2.83 ± 0.65	2.84 ± 0.58	2.29±0.15	2.28±0.06
F3	0	2.84 ± 0.69	2.84 ± 0.69	2.42±0.02	2.42±0.02
	28	3.05 ± 0.70	2.99 ± 0.63	2.39±0.14	2.38±0.05
F4	0	3.16 ± 0.65	3.16 ± 0.65	2.38±0.07	2.38±0.07
	28	3.42 ± 0.59	3.44 ± 0.66	2.34±0.08	2.33±0.16

Stability test

Results of stability testing after 28 days of storage at 25°C and 40°C can be seen in Table 6. Organoleptic observation of all formulas of ciprofloxacin-alginate-carrageenan microspheres did not show any changes; the colour was still yellowish-white and did not agglomerate. In terms of moisture content and drug loading at 25°C and 40°C compared from 0-day to 28 days of storage, it was found that there was no significant difference between the effects of temperature and time on increasing moisture content and decreasing drug loading (p>0.05), which indicated that the ciprofloxacin-alginate-carrageenan microspheres remained stable (Kalalo *et al.*, 2022). To determine the possibility of microsphere instability, more time and high temperature are required to see a substantial

difference in the physical stability of ciprofloxacin-alginate-carrageenan microspheres.

CONCLUSION

Ciprofloxacin-alginate-carrageenan microspheres were successfully formed using the ionotropic gelation with aerosolization technique. Yellowish-white microspheres with small particle size and smooth morphology were obtained from the system. Increasing the concentration of the CaCl₂ crosslinker from 0.5M to 2.0M decreased the particle size, drug release and increased the drug loading, entrapment efficiency and yield. The microspheres containing 1.5M CaCl₂ crosslinker had the maximum drug loading and entrapment efficiency with excellent flow properties and were stable for 28 days.

ACKNOWLEDGMENT

Authors thanks to Faculty of Pharmacy Universitas Airlangga for the facilities and research support.

AUTHOR CONTRIBUTIONS

Conceptualization, D. M. H.; Methodology, D. M. H., M. A. S. R.; Software, A.; Validation, D. M. H., M. A. S. R.; Formal Analysis, A.; Investigation, A.; Resources, A., D. M. H.; Data Curation, A.; Writing - Original Draft, A.; Writing - Review & Editing, D. M. H., M. A. S. R.; Visualization, A.; Supervision, D. M. H., M. A. S. R.; Project Administration, A., D. M. H., M. A. S. R.; Funding Acquisition, D. M. H.

FUNDING STATEMENT

This research did not receive any specific grant from funding agencies in the public, commercial, or not for profit sectors.

CONFLICT OF INTEREST

The authors declared no conflict of interest.

REFERENCES

- Abdelghany, S., Alkhalwaldeh, M. & Alkhatib, H. S. (2017). Carrageenan-Stabilized Chitosan Alginate Nanoparticles Loaded with Ethionamide for the Treatment of Tuberculosis. *Journal of Drug Delivery Science and Technology*; 39; 442–449. doi: 10.1016/j.jddst.2017.04.034.
- Adrian, G., Mihai, M. & Vodnar, D. C. (2019). The Use of Chitosan, Alginate, and Pectin in the Biomedical and Food Sector-Biocompatibility, Bioadhesiveness, and Biodegradability. *Polymers*; 11; 7–11.
- Ashish, K., Hiralal, A. C. & Prajka, U. (2012). Pulmonary Drug Delivery System. *International Journal of PharmTech Research*; 4; 293–305.
- Balagani, P. K., Chandiran, I., Bhavya, B. & Manubolu, S. (2011). Microparticulate Drug Delivery System: A Review. *Indian Journal of Pharmaceutical Science & Research*; 1; 19-37.
- Bayer Health Care Pharmaceuticals Inc. (2021). Ciprofloxacin Hydrochloride (Tablets and Oral Suspension) Draft; 26-30. Whippany: Bayer Health Care Pharmaceuticals Inc.
- Berger, J. R., Mayer, M., Felt, J. M., Peppas, O. N. A. & Gurny, R. (2004). Structure and Interactions in Covalently and Ionically Crosslinked Chitosan Hydrogels for Biomedical Applications. *European Journal of Pharmaceutics and Biopharmaceutics*; 57; 19–34. doi: 10.1016/S0939-6411(03)00161-9.
- Bruschi, M. L. B. T. (2015). Mathematical Models of Drug Release. In *Strategies to Modify the Drug Release from Pharmaceutical Systems*; 63-86. Sawston: Woodhead Publishing.
- Dhakar, R. C., Maurya, S. D., Sagar, B., Bhagat, S., Kumar, S. & Jain, C. (2010). Variables Influencing the Drug Entrapment Efficiency of Microspheres: A Pharmaceutical Review. *Der Pharmacia Lettre*; 2; 102-116.
- Freiberg, S., & Zhu, X. X. (2004). Review Polymer Microspheres for Controlled Drug Release. *International Journal of Pharmaceutics*; 282; 1–18. doi: 10.1016/j.ijpharm.2004.04.013.
- Gaber, D. M. & Nafee, N. & Abdallah, O. Y. (2021). Inhalable Nano-Embedded Microspheres as an Emerging Way for Local Treatment of Lung Carcinoma: Benefits, Methods of Preparation & Characterization. *Advances in Medical, Pharmaceutical and Dental Research Journal*; 1; 7–16. doi: 10.21622/AMPDR.2021.01.1.007.
- Gedam, S., Jadhav, P., Talele, S. & Jadhav, A. (2018). Effect of Crosslinking Agent on Development of Gastroretentive Mucoadhesive Microspheres of Risedronate Sodium. *International Journal of Applied Pharmaceutics*; 10; 133–40. doi: 10.22159/ijap.2018v10i4.26071.
- Hariyadi, D. M., Hendradi, E., Rahmadi, M., Bontong, E. S. & Islam, N. (2022). In-Vitro Physicochemical Properties And Antibacterial Activity Of Ciprofloxacin Carrageenan Inhalable Microspheres. *Rasayan Journal of Chemistry*; 15; 132–142. doi: 10.31788/RJC.2022.1516652.
- Hariyadi, D. M., Hendradi, E. & Sharon, N. (2019). Development of Carrageenan Polymer for Encapsulation of Ciprofloxacin HCL: In Vitro Characterization. *International Journal of Drug Delivery Technology*; 9; 89–93. doi: 10.25258/ijddt.9.1.14.
- Hariyadi, D. M., Purwanti, T. & Adilla, S. (2018). Influence of Crosslinker Concentration on the Characteristics of Erythropoietin-Alginate Microspheres. *Journal of Pharmacy & Pharmacognosy Research*; 6; 250–259.
- Hariyadi, D. M., Hendradi, E., Purwanti, T., Permana, F. F. D. G. & Ramadani, C. N. (2014). Effect of Cross Linking Agent and Polymer on the Characteristics of Ovalbumin Loaded Alginate Microspheres. *International Journal of Pharmacy and Pharmaceutical Sciences*; 6; 469–474.

- Hariyadi, D. M., Hendradi, E. & Kurniawan, T. D. (2019). Alginate Microspheres Encapsulating Ciprofloxacin HCl: Characteristics, Release and Antibacterial Activity. *International Journal of Pharma Research and Health Sciences*; 7; 3020–3027. doi: 10.21276/ijprhs.2019.04.02.
- Hariyadi, D. M., Purwanti, T. & Wardani, D. (2016). Stability of Freeze-Dried Ovalbumin-Alginate Microspheres with Different Lyoprotectants. *Research Journal of Pharmacy and Technology*; 9; 20–26. doi: 10.5958/0974-360X.2016.00005.6.
- Hariyadi, D. M. & Hendradi, E. (2020). Optimization Performance and Physical Stability of Ciprofloxacin HCL- Ca Alginate Microspheres : Effect of Different Concentration of Alginate. *International Journal of Drug Delivery Technology*; 89–94. doi: 10.25258/ijddt.10.1.15.
- Heifetst, L. B. & Lindholm-levy, P. J. (1987). Bacteriostatic and Bactericidal Activity of Ciprofloxacin and Ofloxacin Against Mycobacterium Tuberculosis and Mycobacterium Avium Complex. *National Jewish Center for Immunology and Respiratory Medicine*; 68; 267–276.
- Jerome, A., Onda, M. & Aquino, J. A. (2020). Evaluation of Factors Affecting the Microencapsulation of Mefenamic Acid with Cellulose Acetate Phthalate. *Pharmaceutical Sciences Asia*; 47; 130–141. doi: 10.29090/psa.2020.02.018.0055.
- Kadam, N. R. & Suvarna. (2015). Microsphere: A Brief Review. *Asian Journal of Biomedical and Pharmaceutical Sciences*; 5; 13–19. doi: 10.15272/ajbps.v5i47.713.
- Kalalo, T., Miatmoko, A., Tanojo, H., Erawati, T., Hariyadi, D. M. & Rosita, N. (2022). Effect of Sodium Alginate Concentration on Characteristics, Stability and Drug Release of Inhalation Quercetin Microspheres. *Jurnal Farmasi Dan Ilmu Kefarmasian Indonesia*; 9; 107–114. doi: 10.20473/jfiki.v9i22022.107-114.
- Karimi, K., Pallagi, E., Szabó-révész, P., Csóka, I. & Ambrus, R. (2016). Development of a Microparticle-Based Dry Powder Inhalation Formulation of Ciprofloxacin Hydrochloride Applying the Quality by Design Approach. *Drug Design, Development and Therapy*; 10; 3331–3343. doi: 10.2147/DDDT.S116443.
- Katzung, B. G., Masters, S. B. & Trevor, A. J. (2012). Basic & Clinical Pharmacology Twelfth Edition; 834-838. New York: McGraw-Hill Education.
- Kolesnyk, I. S. & Burban, A. (2015). Alginate / κ - Carrageenan Microspheres and Their Application for Protein Drugs Controlled Release. *Chemistry and Chemical Technology*; 9; 485–492. doi: 10.23939/chcht09.04.485.
- Lane, J. (2016). Powder Flow. North Bethesda: United States Pharmacopeia.
- Laura, T Furlan Rodríguez, Antonio Pérez Padilla, and Mercedes E Campderrós. (2010). Inulin like Lyoprotectant of Bovine Plasma Proteins Concentrated by Ultrafiltration. *Food Research International*; 43; 788–796. doi: 10.1016/j.foodres.2009.11.015.
- Lee, Kuen Yong, and David J. Mooney. (2012). Alginate: Properties and Biomedical Applications. *Progress in Polymer Science (Oxford)*; 37; 106–126. doi: 10.1016/j.progpolymsci.2011.06.003.
- Lengyel, Miléna, Nikolett Kállai-Szabó, Vince Antal, András József Laki and István Antal. (2019). Microparticles, Microspheres, and Microcapsules for Advanced Drug Delivery. *Scientia Pharmaceutica*; 87; 1-31. doi: 10.3390/scipharm87030020.
- Li, L., Wang, Q., Li, H., Yuan, M. & Yuan, M. (2014). Preparation, Characterization, In Vitro Release and Degradation of Cathelicidin-BF-30-PLGA Microspheres. *PLoS ONE*; 9; 1–7. doi: 10.1371/journal.pone.0100809.
- Lin, X., Yang, H., Su, L., Yang, Z. & Tang, X. (2018). Effect of Size on the in Vitro/in Vivo Drug Release and Degradation of Exenatide-Loaded PLGA Microspheres. *Journal of Drug Delivery Science and Technology*; 45; 346-356 doi: 10.1016/j.jddst.2018.03.024.
- Manjanna, K. M., Pramod, T. M. & Shivakumar, B. (2010). Calcium Alginate Cross-Linked Polymeric Microbeads for Oral Sustained Drug Delivery in Arthritis. *Drug Discoveries & Therapeutics*; 4; 109–122.
- Misra, A., Hickey, A. J., Rossi, C., Borchard, G., Terada, H., Makino, K., Fourie, P. B. & Colombo, P. (2011). Inhaled Drug Therapy for Treatment of Tuberculosis. *Tuberculosis*; 91; 71–81. doi: 10.1016/j.tube.2010.08.009.
- Pasquale, S. S., Pedroso-Santana, Y., Nicolas, K., Patrick, J. & Bocchetta, M. P. (2021). Ionotropic Gelation of Chitosan Flat Structures and Potential Applications. *Molecules*; 26; 1–28.
- Ra, A. C., Chun, Y. G., Kim, B. K. & Park, D. J. (2014). Preparation of Alginate – CaCl₂ Microspheres as

- Resveratrol Carriers. *Journal of Materials Science*; 49; 4612–4619. doi: 10.1007/s10853-014-8163-x.
- Saha, T., Sinha, S., Harfoot, R. & Quiñones-mateu, M. E. (2022). Manipulation of Spray-Drying Conditions to Develop an Inhalable Ivermectin Dry Powder. *Pharmaceutics*; 14; 1–20.
- Santa-maria, M., Scher, H. & Jeoh, T. (2012). Microencapsulation of Bioactives in Cross-Linked Alginate Matrices by Spray Drying. *Journal of Microencapsulation*; 29; 286–195. doi: 10.3109/02652048.2011.651494.
- Rajeswari, S., Prasanthi, T., Sudha, N., Swain, R. P., Satyajit Panda and Vinusha Goka. (2017). Natural Polymers : A Recent Review. *World Journal of Pharmacy and Pharmaceutical Sciences*; 6; 472–494. doi: 10.20959/wjpps20178-9762.
- Shan, L., Tao, E. X., Meng, Q. H., Hou, W. X., Liu, K., Shang, H. C., Tang, J. B. & Zhang, W. F. (2016). Formulation, Optimization, and Pharmacodynamic Evaluation of Chitosan/Phospholipid/ β -Cyclodextrin Microspheres. *Drug Design, Development and Therapy*; 10; 417–429. doi: 10.2147/DDDT.S97982.
- Tecante, A. & Núñez, C. (2012). Solution Properties of κ -Carrageenan and Its Interaction with Other Polysaccharides in Aqueous Media. *Rheology In Tech*; 241–264.
- Thai, T., Salisbury, B. H. & Zito, P. M. (2022). Ciprofloxacin. London: Treasure Island (FL).
- Varela-Fernández, R. (2022). Design, Optimization, and in Vitro Characterization of Idebenone-Loaded PLGA Microspheres for LHON Treatment. *International Journal of Pharmaceutics*; 616; 1–19. doi: /10.1016/j.ijpharm.2022.121504.
- Wathoniyah, M. (2016). Pembuatan Dan Karakterisasi Komposit Sodium Alginat-Karagenan Dengan Crosslinker CaCl₂ Dan Plasticizer Gliserol Sebagai Material Drug Release. *Skripsi*; Fakultas Sains dan Teknologi Universitas Airlangga, Surabaya.
- Wijaksana, A. (2022). Pengaruh Konsentrasi Kombinasi Polimer Alginat-Karagenan Terhadap Pelepasan Dan Aktivitas Antibakteri Dari Pulmosfer Ciprofloxacin HCl. *Skripsi*; Fakultas Farmasi Universitas Airlangga, Surabaya.
- Yu, F., Cui, T., Yang, C., Dai, X. & Ma, J. (2019). κ -Carrageenan / Sodium Alginate Double-Network Hydrogel with Enhanced Mechanical Properties, Anti-Swelling, and Adsorption Capacity. *Chemosphere*; 237; 1–7. doi: 10.1016/j.chemosphere.2019.124417.



Patient Satisfaction with Pharmaceutical Services at a Hospital Outpatient Pharmacy in West Sumatra, Indonesia

Dian Ayu Juwita, Nurul Qalbi Desri, Dita Permatasari*

Department of Pharmacology and Clinical Pharmacy, Faculty of Pharmacy, Universitas Andalas, Padang, Indonesia

*Corresponding author: ditapermatasari@phar.unand.ac.id

Submitted: 3 August 2023

Revised: 16 October 2023

Accepted: 25 October 2023

Abstract

Background: Patient satisfaction stands as a metric for evaluating the quality of pharmaceutical services. The presence of community requests for high-quality pharmaceutical services has driven pharmacy personnel to enhance these services, aiming to establish patient satisfaction. **Objective:** The objective of this research is to assess the degree of patient satisfaction with pharmaceutical services in the outpatient pharmacy and to explore how this satisfaction is linked to the patients' sociodemographics. **Methods:** Conducted at Padang Panjang Hospital's Outpatient Pharmacy in West Sumatra, Indonesia, this descriptive research employed a questionnaire administered directly to patients. The method used involves a questionnaire consisting of 20 questions divided into two dimensions: Friendly Explanation (containing 11 questions) and Managing Therapy (containing nine questions). The questionnaire's validity ($r > 0.632$) and reliability (0.97). Data analysis was performed utilizing the Likert scale. **Results:** There were a total of respondents in this study (365 patients). Most of them (64.4%) were female, in the pre-elderly age group (45.2%), had completed high school (41.1%), and were housewives (31.8%). In general, the level of patient satisfaction is categorized as satisfied, with an average score of 3.49. Specifically, the "Friendly Explanation" got a score of 3.69, and the "Management of Therapy" got a score of 3.25. The study indicated notable statistical disparities in patient satisfaction levels based on age, education, and occupation ($p < 0.05$), but gender did not have a significant impact ($p > 0.05$). **Conclusion:** In summation, the study found that patients were satisfied with the pharmaceutical services at Padang Panjang Hospital's Outpatient Pharmacy.

Keywords: friendly explanation, managing therapy, outpatient pharmacy, patient satisfaction, pharmaceutical services

How to cite this article:

Juwita, D. A., Desri, N. Q. & Permatasari, D. (2023). Patient Satisfaction with Pharmaceutical Services at a Hospital Outpatient Pharmacy in West Sumatra, Indonesia. *Jurnal Farmasi dan Ilmu Kefarmasian Indonesia*, 10(3), 324-330. <http://doi.org/10.20473/jfiki.v10i32023.324-330>

INTRODUCTION

Health efforts are integrated and sustainable activities to enhance community health through prevention, health promotion, curative and disease rehabilitation (Ministry of Health Republic of Indonesia, 2018). Pharmaceutical services not only include trading and preparation of drugs but also providing information about them. In addition, it ensures medication safety, rational medication, and improved quality of life (Bratkowska *et al.*, 2020). Patient satisfaction reflects pharmaceutical services in the interaction of medical services with patients and the health care system. Promptness in pharmaceutical service delivery coupled with effective communication between pharmacy personnel and patients increases patient satisfaction with pharmaceutical services (Ostrowska *et al.*, 2022). Evaluating patient satisfaction is a complex and multi-dimensional challenge. Various aspects can affect its value. However, some key points were highlighted, such as the availability of prescribed drugs, service delays, and drug counselling services (Nigussie & Edessa, 2018).

The Indonesian government still has many weaknesses in public services. This is proven by the existence of public complaints through online media or by reading letters about service procedures, service facilities, and infrastructure (Fadila *et al.*, 2022). Most hospitals in Indonesia have not carried out the expected pharmaceutical service activities (Larasanty *et al.*, 2019). This is caused by several constraints, such as the capacity of pharmacists, the limited capacity of hospital management to the hospital pharmacy function, hospital management policies, and little knowledge of pharmacists in hospitals (Fadila *et al.*, 2022). Because of circumstances like this, hospital pharmacy services are limited to a single commodity, namely the provision and distribution of pharmaceuticals.

The Padang Panjang Hospital is a referral hospital that provides public services. Based on data on patient visits to the outpatient Pharmacy at Padang Panjang Hospital, there has been an increase in visits from 2020, as many as 43,083 to 2021, which is 48,568. The quality of pharmaceutical services at the hospital may be affected as the number of patients looking for medical treatment rises. A surge in daily prescription numbers will result in a greater need for prompt and precise services. Patients are impatient and decide to take medicine the next day. This becomes a problem because the prescriptions on the following day will accumulate and affect the quality of service at that time. Hospitals that collaborate with BPJS sometimes have issues with

the BPJS service network. The high number of prescriptions served by pharmacies results in decreased prescription service speed and will lead to demands or criticism from patients who redeem drugs. This is one of the indicators of pharmaceutical services that can be measured by satisfaction.

Numerous studies have been conducted to assess the extent of patient satisfaction concerning pharmaceutical services within hospital settings. Certain patients express dissatisfaction with the pharmaceutical services rendered in hospitals, attributing this to a deficiency in the knowledge of pharmacy personnel. As per the viewpoints expressed by respondents, inadequate availability of prescribed medications in pharmacies is also a contributing factor (Nigussie & Edessa, 2018). However, some patients are satisfied because the pharmacist explains the information on drug use in an easy-to-understand manner (Bratkowska *et al.*, 2020). There are differences in the level of satisfaction. This research has never been done at the Padang Panjang Hospital. The primary goal of this study is to evaluate the levels of patient satisfaction regarding pharmaceutical services provided at the Outpatient Pharmacy within Padang Panjang Hospital. This assessment aims to provide insights into the calibre of healthcare services experienced by patients.

MATERIALS AND METHODS

Study design

This study employs an observational descriptive design utilizing a cross-sectional methodology through a prospective questionnaire-based survey. The criteria for inclusion encompassed individuals aged 18 years or older who acquired medications from an outpatient pharmacy, those who had undergone multiple treatments at the polyclinic and subsequently obtained medications from the outpatient pharmacy, and individuals who demonstrated their willingness to participate by completing an informed consent form. This study was not conducted on patients who did not redeem the drug on the same day as the treatment schedule.

Instrument

The instrument development was based on the instrument previously developed by Larson *et al.* (2002). Subsequently, Dedy Almasdy conducted the instrument development process, starting with the translation of the instrument into the Indonesian language. This was followed by the assessment of agreement levels among experts ($\kappa = 0.53$), validity testing ($r > 0,632$), and reliability testing (Cronbach

alpha = 0.97) (Almasdy & Deria, 2015). This questionnaire consists of 20 questions divided into two dimensions: Friendly Explanation (containing 11 questions) and Managing Therapy (containing nine questions). The Friendly Explanation dimension includes questions about service friendliness, the professionalism of pharmacy staff, timeliness of service, and how well pharmacists respond to patient questions. Meanwhile, the Managing Therapy dimension includes questions about the pharmacist's efforts to ensure proper medication functioning, improve patient health, and address medication-related issues.

Data analysis

Because of circumstances like this, hospital pharmacy services are limited to a single commodity, namely the provision and distribution of pharmaceuticals. (Table 1).

Table 1. Interpretation of satisfaction level values (Larson *et al.*, 2002)

No	Range	Value
1	1 - 1,8	Dissatisfied
2	>1,8 - 2,6	Less satisfied
3	>2,6 - 3,4	Quite satisfied
4	>3,4 - 4,2	Satisfied
5	>4,2 - 5	Very satisfied

The Spearman test approach was employed to establish the correlation between patient characteristics and patient satisfaction, age and education factors. Meanwhile, in the case of the gender variable, the Mann-Whitney test was employed to ascertain the connection

between patient characteristics and patient satisfaction. Furthermore, the Kruskal Wallis test, facilitated through the SPSS tool, was utilized to discern the relationship between patient characteristics and patient satisfaction, particularly concerning the work variable.

Ethical approval

Ethical clearance for this research was granted by the Research Ethics Committee of the Faculty of Medicine, Universitas Andalas, Indonesia (Approval No. 692/UN.16.2/KEP-FK/2022). The participants were requested to complete informed consent forms to demonstrate their voluntary participation.

RESULTS AND DISCUSSION

A collective of 365 patients was included in the study, and the predominant characteristics of respondents, as delineated in Table 2, encompassed being female (64.4%), belonging to the pre-elderly age group (45.2%), having attained a high school education (41.1%), and being housewives (31.8%).

Our research marks the inaugural attempt to assess the degree of patient satisfaction with pharmaceutical services within Padang Panjang Hospital's outpatient pharmacy. This evaluation is seen from 2 dimensions: the Friendly Explanation and the Managing Therapy dimension. The study used a questionnaire consisting of 2 dimensions: questions 1 to 11 (the friendly explanation dimension) and questions 12 to 20 (the managing therapy dimension) (Table 3).

Table 2. Sociodemographic characteristics of patients (n = 365)

Demographic characteristics	Frequency	Percentage
Gender		
Male	130	35.9
Female	235	64.4
Age (years)		
Adult (18-44)	94	25.8
Pre-elderly (45-59)	165	45.2
Elderly (≥ 60)	106	29.0
Last education		
Primary school	57	15.6
Junior high school	82	22.5
Senior high school	150	41.1
Diploma	22	6.0
Bachelor	54	14.8
Profession		
Student	18	4.9
Public/Private Servants	55	15.1
Self-employed	73	20.0
Retired	38	10.4
Housewives	116	31.8
Other	65	17.8

In the Friendly Explanation dimension, the highest percentage of dissatisfied patients was on the question item on the speed of the pharmacy serving prescriptions. This is due to the high level of pharmacy service, which causes the long waiting time. In addition, to redeem BPJS patients' drugs, they must first enter their data into the BPJS service application. However, pharmacies have problems with the complex BPJS service network, so pharmacists need to do it manually by looking at the history of previous patients, especially if there are many patient visits on that day so that the speed of prescription service decreases. A similar incident can be seen in the study of Mohamed (2022); he stated that the reported average dispensing time (ADT) is longer than in other studies. This may be because pharmacists spend a long time explaining to patients insured and uninsured drugs in prescription according to the applicable BPJS (Osman *et al.*, 2022). This is identical to the results of the Lee *et al.* study (Lee *et al.*, 2015).

Conversely, the dimension of "friendly explanation" witnessed the most substantial percentage of respondents expressing a state of very satisfaction, specifically in relation to the query about the clarity of information provided by the pharmacist concerning the medication received and its usage. Patients are satisfied because when the drug is received, the pharmacist always tells them the name of the drug and its use.

Patients conveyed satisfaction with the practice of pharmacists promptly informing them about the medication's identity and purpose upon dispensing. Coinciding with these findings, a study conducted in Ethiopia demonstrated comparable patient satisfaction levels concerning critical medication guidelines, including administration instructions (83.2%), recommended timing (76.4%), and label comprehensibility (67.6%). At the same time, in line a study in Ethiopia showed the highest patient satisfaction level towards some of the vital medication instructions such as the administration instructions (83.2%), the advising time (76.4%) and the label clarity (67.6%) (Semegn & Alemkere, 2019).

Within the context of the therapy management aspect, the highest percentage of dissatisfied patients is the question item on the consultation time questionnaire provided by the pharmacist for the patient. The Padang Panjang Hospital pharmacy has a counselling room. However, in recent years, counselling activities have not been carried out. This is due to the COVID-19 pandemic, so counselling activities are limited and rarely carried out. Most patients said they were dissatisfied because they had never done counselling at

the pharmacy. This unsatisfactory occurrence finds support in a study undertaken by Larasanty *et al.* (2019), where it was unveiled that patients expressed a desire for pharmacists to allocate more time to addressing their medical inquiries and furnishing supplementary details about their prescribed medications (Larasanty *et al.*, 2019).

Meanwhile, the very satisfying level in the Managing therapy dimension is the question of the pharmacist's information about how many times and how long the drug should be taken. Patients expressed satisfaction with the information delivered by the pharmacist during the medication dispensing process. When discharged, successful patient counselling and proper drug education will improve patient adherence and treatment satisfaction, improving their clinical outcomes (Sanii *et al.*, 2016).

Table 4 shows the patient satisfaction levels in pharmaceutical services. In general, patient satisfaction with pharmaceutical services in the "friendly explanation" aspect was rated as content, attaining an average score of 3.69. On the other hand, the "managing therapy" dimension exhibited a reasonably satisfactory level, achieving an average score of 3.25. Furthermore, our results showed a statistically significant difference in age, education, and profession toward patient satisfaction level, but not gender (Table 5).

In this research, the overall patient satisfaction score averaged 3.49, falling within the satisfied range (between 3.4 and 4.2). This finding mirrors outcomes from a study in Sudan (with a mean satisfaction score of approximately 3.11) and surpasses the results from a 2018 study in Pakistan (about 2.78) (Aziz *et al.*, 2018; Osman *et al.*, 2022). Analyzing the responses provided by patients in the questionnaire, it is evident that a connection exists between the highest satisfaction levels within two dimensions. Specifically, patients expressed satisfaction with the pharmaceutical services concerning information about prescribed medications and their usage. Furthermore, patients also indicated satisfaction with detailed guidance regarding the timing, duration, and method of medication administration.

Table 3. Patient satisfaction level

	Average	Interpretation
Overall	3.49	Satisfied
Friendly explanation dimension	3.69	Satisfied
Managing therapy dimension	3.25	Quite satisfied

Table 4. Patient satisfaction level in pharmaceutical services

No	Questionnaire Items	Patient satisfaction level (%)				
		1	2	3	4	5
1	The appearance of the pharmacy is attractive and follows its function	0.00	3.29	17.53	57.26	21.92
2	Pharmacists' answers to your questions	1.92	4.93	27.95	50.41	14.79
3	Smooth communication between you and the pharmacist	0.27	8.49	31.78	49.59	9.86
4	The pharmacist's ability to explain problems related to your medicine	0.00	5.75	28.22	52.88	13.42
5	Speed Pharmacies serve your recipe	5.21	33.70	25.75	28.49	6.85
6	The ability of pharmacists to provide services	0.00	4.66	33.15	48.22	13.97
7	Clarity of information the pharmacist provides regarding the drugs you receive and their uses.	0.00	3.01	29.59	45.21	22.19
8	The directions are given by the pharmacist on how to use your medicine	0.00	4.11	45.21	36.99	13.70
9	Services provided by the pharmacy as a whole	0.00	3.56	21.10	53.42	21.92
10	Pharmacists answer your questions well	0.82	4.38	38.36	49.59	6.85
11	Hospitality and courtesy of Pharmacy officers in carrying out their duties	0.82	3.84	23.01	52.88	19.45
12	Pharmacists show concern for your health condition	1.10	6.58	37.26	50.41	4.66
13	Pharmacists explain how to store drugs properly	6.85	18.63	37.26	31.78	5.48
14	Pharmacist involvement in solving problems related to your medication	1.37	8.49	36.71	47.67	5.75
15	The pharmacist gives information about how many times and how long the drug should be taken	0.27	3.84	27.67	45.48	23.01
16	Pharmacists advise you to maintain or improve your health.	1.92	15.07	27.40	48.49	7.12
17	Confidentiality of the personal information you share with the pharmacist	0.27	6.03	35.34	49.86	8.22
18	Pharmacists' explanation of things to avoid while taking your medicine	10.41	21.64	32.05	31.23	4.66
19	The explanation is given by the pharmacist about the possible adverse drug side effects	12.60	22.19	33.15	29.59	2.47
20	Consultation time provided by the pharmacist for you	31.78	22.19	25.75	18.63	1.64
Average		3.78	10.23	30.71	43.90	11.40

In addition to explaining the patient satisfaction level based on these dimensions, this study also examines the association between sociodemographic characteristics and patient satisfaction level. Our results described a statistically significant difference for age, education, and profession toward patient satisfaction level, but not gender. Similar to the study done in northwestern Ethiopia, these areas of sociodemographic characteristics significantly differ in patient satisfaction levels (Surur *et al.*, 2015). Similar to that is the analysis performed by Alrasheedi *et al.* in 2019, which is done in the Kingdom of Saudi Arabia (Alrasheedi *et al.*, 2019). These aspects influence their understanding and reaction to the health services they receive. In contrast, in two studies in Pakistan (Aziz *et al.*, 2018) and Ethiopia (Molla *et al.*, 2022), no significant difference was observed in patient satisfaction concerning their demographic characteristics.

Table 5. The correlation between sociodemographic characteristics and the degree of patient satisfaction among the patient population (n = 365)

Demographic characteristics	Toward Patient Satisfaction (p-value)
Gender	0.065
Age (years)	0.039 ^(*)
Last education	0.000 ^(*)
Profession	0.000 ^(*)

* = a significant relationship

Note: Gender using the Mann-Whitney test; age and last education using the Spearman Rank test; and profession using the Kruskal Wallis test

We acknowledge the constraints within our study. Initially, this research was undertaken solely within a single hospital in West Sumatra, Indonesia, implying that conclusions may not comprehensively mirror patients' experiences across Indonesia. Furthermore, the study comprised a relatively modest participant pool, and the duration of the study itself was limited, which

might restrict its ability to represent the broader spectrum of hospital patients accurately. All these limitations will affect the final result, including the need and quality of pharmaceutical services. However, this is the first study of this type in West Sumatra. Further studies involving a more general and more diverse patient population are needed.

CONCLUSION

Patients' satisfaction levels regarding pharmaceutical services within the Outpatient Pharmacy at Padang Panjang Hospital are generally deemed satisfactory, registering an average score of 3.49. The "Friendly Explanation" dimension scored 3.69, while the "Managing Therapy" dimension scored 3.25. Moreover, our findings indicated a notable and statistically significant variation concerning patient satisfaction based on age, education, and profession. Conversely, gender appears to have no discernible impact on patient satisfaction.

ACKNOWLEDGMENT

The authors extend their gratitude to individuals who contributed substantially to this study.

AUTHOR CONTRIBUTIONS

Conceptualization, D. P., D. A. J., N. Q. D.; Methodology, D. P., D. A. J.; Software, D. P., N. Q. D.; Validation, D. P., D. A. J.; Formal Analysis, D. P., D. A. J., N. Q. D.; Investigation, D. P., N. Q. D.; Resources, D. P., N. Q. D.; Data Curation, D. P., D. A. J., N. Q. D.; Writing - Original Draft, D. P., D. A. J., N. Q. D.; Writing - Review & Editing, D. P., D. A. J.; Visualization, D. P., D. A. J., N. Q. D.; Supervision, D. P., D. A. J.; Project Administration, D. P., D. A. J.; Funding Acquisition, D. P., D. A. J.

FUNDING STATEMENT

This research did not receive any specific grant from funding agencies in the public, commercial, or not for profit sectors.

CONFLICT OF INTEREST

The authors declared no conflict of interest.

REFERENCES

Almasdy, D. & Deria, P. D. (2015). Pengembangan Instrumen Penilaian Kepuasan Pasien Terhadap Pelayanan Kefarmasian di Rumah Sakit (Development of the Instrument Patient Satisfaction for Pharmaceutical Services in

Hospital). *Jurnal Sains Farmasi & Klinis*; 1; 170–175. doi: 10.29208/jsfk.2015.1.2.32.

Alrasheedi, K. F., AL-Mohaithef, M., Edrees, H. H., & Chandramohan, S. (2019). The Association Between Wait Times and Patient Satisfaction: Findings from Primary Health Centers in the Kingdom of Saudi Arabia. *Health Services Research and Managerial Epidemiology*; 6; 233339281986124. doi: 10.1177/2333392819861246.

Aziz, M. M., Ji, W., Masood, I., Farooq, M., Malik, M. Z., Chang, J., Jiang, M., Atif, N., & Fang, Y. (2018). Patient Satisfaction with Community Pharmacies Services: A Cross-sectional Survey from Punjab; Pakistan. *International Journal of Environmental Research and Public Health*; 15; 1-14. doi: 10.3390/ijerph15122914.

Bratkowska, K., Religioni, U., Krysiński, J., & Merks, P. (2020). Quality of Pharmaceutical Services in Independent Pharmacies and Pharmacy Chains in Poland from the Patient Perspective. *Patient Preference and Adherence*; 14; 2459–2467. doi: 10.2147/PPA.S284014.

Fadila, A. N., Hidayati, I. R., Yunita, S. L., Titani, M., & Atmadani, R. N. (2022). Patient Satisfaction of Pharmaceutical Services During the Covid-19 Pandemic in the Public Healthcare Center of Singosari, Malang. *KnE Medicine*; 2; 1–14. doi: 10.18502/kme.v2i3.11846.

Larasanty, L. P. F., Cahyadi, M. F., Sudarni, N. M. R., & Wirasuta, I. M. A. G. (2019). Patient Satisfaction with Pharmaceutical Care Services Provided at Primary-level and Secondary-level Health Facilities in Indonesia's Health Coverage System. *Journal of Health Research*; 33(1); 80–88. doi: 10.1108/JHR-06-2018-0033.

Lee, S., Godwin, O. P., Kim, K. & Lee, E. (2015). Predictive Factors of Patient Satisfaction with Pharmacy Services in South Korea: A Cross-sectional Study of National Level Data. *PLoS One*; 10; 1-9. doi: 10.1371/journal.pone.0142269.

Larson, L. N., Rovers, J. P. & MacKeigan, L. D. (2002). Patient Satisfaction with Pharmaceutical Care: Update of a Validated Instrument. *Journal of the American Pharmacists Association*; 42; 44–50.

Ministry of Health Republic of Indonesia. (2018). Peraturan Menteri Kesehatan Republik Indonesia Nomor 10 Tahun 2018 (Regulation of the Minister of Health of the Republic of Indonesia Nomor 10 of 2018 concerning Supervision in the Health

- Sector). Jakarta: Ministry of Health Republic of Indonesia.
- Molla, M., Sisay, W., Andargie, Y., Kefale, B. & Singh, P. (2022). Patients' Satisfaction with Outpatient Pharmacy Services and Associated Factors in Debre Tabor Comprehensive Specialized Hospital, Northwest Ethiopia: A Cross-sectional Study. *PLoS One*; 17; 1-13. doi: 10.1371/journal.pone.0262300.
- Nigussie, S. & Edessa, D. (2018). The Extent and Reasons for Dissatisfaction from Outpatients Provided with Pharmacy Services at Two Public Hospitals in Eastern Ethiopia. *Frontiers in Pharmacology*; 9; 1-8. doi: 10.3389/fphar.2018.01132.
- Osman, M. A., Hussain, S. A., & Omar, A. M. (2022). Assessment of Patient Satisfaction Toward Pharmaceutical Benefit Package Provided by a Health Insurance Corporation of Khartoum State. *F1000Research*; 11; 204. doi: 10.12688/f1000research.108760.1.
- Ostrowska, M., Drozd, M., Patryn, R. & Zagaja, A. (2022). Prescriptions as Quality Indicators of Pharmaceutical Services in Polish Community Pharmacies. *BMC Health Services Research*; 22; 1-8. doi: 10.1186/s12913-022-07772-2.
- Sanii, Y., Torkamandi, H., Gholami, K., Hadavand, N., & Javadi, M. (2016). Role of Pharmacist Counseling in Pharmacotherapy Quality Improvement. *Journal of Research in Pharmacy Practice*; 5; 132. doi: 10.4103/2279-042x.179580.
- Semegn, S. & Alemkere, G. (2019). Assessment of Client Satisfaction with Pharmacist Services at Outpatient Pharmacy of Tikur Anbessa Specialized Hospital. *PLoS One*; 14; 1-10. doi: 10.1371/journal.pone.0224400.
- Surur, A. S., Teni, F. S., Girmay, G., Moges, E., Tesfa, M. & Abraha, M. (2015). Satisfaction of Clients with the Services of an Outpatient Pharmacy at a University Hospital in Northwestern Ethiopia: A Cross-sectional Study Health Systems and Services in Low and Middle Income Settings. *BMC Health Services Research*; 15; 1-8. doi: 10.1186/s12913-015-0900-6.



Formulation and Characterization of Instant Powder Combination of Ginger, Bangle, and Lemon Extract as an Antioxidant

Nur Aji^{1,2*}, Shandra Isasi Sutiswa^{1,2}

¹Department of Pharmacy, Poltekkes Kemenkes Tasikmalaya, Tasikmalaya, Indonesia

²Center of Excellent Health and Disaster Emergency (CoE HADE) Center Poltekkes Kemenkes Tasikmalaya, Tasikmalaya, Indonesia

*Corresponding author: nuraji090689@gmail.com

Submitted: 8 August 2023

Revised: 24 October 2023

Accepted: 31 October 2023

Abstract

Background: Degenerative disease is a decreasing organ function; clinical manifestations can affect the whole body, which is caused by oxidative stress. Ginger, bangle, and lemon have antioxidant properties. The combination of the three is expected to increase antioxidant activity. **Objective:** This study aimed to determine the potential antioxidant activity of the mixture of the three samples formulated as instant powder. **Methods:** This research is an experimental laboratory. This study will examine the effect of variations in extract concentration and PEG-40 HCO concentration on instant powder's characteristics and antioxidant activity. **Results:** Individually, ginger extract has extreme antioxidant activity ($IC_{50} = 23.57 \pm 0.13 \mu\text{g/mL}$) and bangle strong ($IC_{50} = 64.89 \pm 0.15 \mu\text{g/mL}$), while lemon has weak antioxidant activity ($IC_{50} > 500 \mu\text{g/mL}$). Combining ginger, bangle, and lemon with a simplex axial method obtained the combination of ginger: bangle: lemon with the ratio of 4/6: 1/6: 1/6. Adding a mixture of extracts affects the solubility and antioxidant activity of the extracts. The greater the amount of extract, the lower the solubility, and the antioxidant activity did not increase with addition. The addition of PEG-40 HCO increases the solubility of the extract in the instant powder. Antioxidant activity increased to the "medium" category ($121.90 \mu\text{g/mL}$) after adding PEG-40 HCO at a concentration of 2.70%. The unfavourable impact of PEG-40 HCO addition on instant powders is the angle of repose, flow time, and compressibility. **Conclusion:** The ginger, bangle, and lemon can be combined and made into instant powder with potential antioxidant activity in the moderate category.

Keywords: antioxidant, bangle, ginger, instant powder, lemon

How to cite this article:

Aji, N. & Sutiswa, S. I. (2023). Formulation and Characterization of Instant Powder Combination of Ginger, Bangle, and Lemon Extract as an Antioxidant. *Jurnal Farmasi dan Ilmu Kefarmasian Indonesia*, 10(3), 331-346. <http://doi.org/10.20473/jfiki.v10i32023.331-346>

INTRODUCTION

Degenerative disease decreases organ function, which generally affects the elderly. Clinical manifestations of degenerative can affect all organs of the body. Degenerative conditions in Indonesia, such as hypertension, diabetes mellitus, stroke, and chronic kidney failure, increased in 2018 from 2013. The 2018 Basic Health Research results found that stroke prevalence was 7% in 2013 and 10.9% in 2018. The prevalence of chronic kidney disease was 2% in 2013 to 4% in 2018. The prevalence of diabetes mellitus was 1.8% in 2013 to 1.9% in 2018. The prevalence of diabetes mellitus is high in people with higher education and state civil servants (Fridalni *et al.*, 2019). During the Covid 19 pandemic, people with degenerative diseases have a higher risk of being exposed and tend to experience worse complications from this disease (Sari & Widiharti, 2021).

Degenerative diseases are caused by oxidative stress in the presence of free radicals in biochemical mechanisms that occur in the body. Free radicals are considered dangerous because they become very reactive in trying to get their electron pair (Odinga *et al.*, 2020). Antioxidants can slow down the oxidation process of free radicals, thereby protecting cells from damage caused by unstable molecules known as free radicals (Sadiq, 2023). The mechanism of the body's resistance to oxidative stress is through endogenous antioxidants. If the number of free radicals and reactive species in the body exceeds the ability of endogenous antioxidants, then the body requires the intake of exogenous antioxidants (Martemucci *et al.*, 2022).

Ginger rhizome has antioxidant activity. Ginger oleoresin, as an active substance, can ward off free radicals, such as 6-gingerol and 6-shogaol, which are known to have relatively high antioxidant activity, with a mechanism to stabilize free radicals by complementing the lack of electrons possessed by free radicals and inhibiting the occurrence of chain reactions from the formation of free radicals (Ahmed *et al.*, 2022). Apart from the ginger plant, other plants such as Bangle and Lemon also have antioxidant activity due to the content of flavonoid compounds. In addition, the content of flavonoids in bangle plants also functions as an immunostimulant. In addition, the bangle is rich in curcuminoid compounds, which also have antioxidant potential (Nurkhasanah *et al.*, 2019).

The potential bangle, ginger, and lemon plants, which contain antioxidants, can be used to prevent degenerative diseases (Veurink *et al.*, 2020). In addition, antioxidants are essential to maintain body immunity,

especially during a pandemic. A combination of bangle, ginger, and lemon is formulated into an instant powder. The advantages of instant powder formulas are product quality that is more practical and hygienic (Çopur *et al.*, 2019). Based on this, researchers are interested in making an instant powder combination of ginger, bangle, and lemon extracts as an antioxidant. This study aims to see the effect of adding a mixture of extracts and PEG-40 HCO on the characteristics of instant powder: solubility, pH, antioxidant activity, angle of repose, flow rate, and powder density. PEG-40 HCO is a solubilizer agent of hydrogenated castor oil derivatives. The hydrogenated castor oil is obtained by hydrogenation of virgin castor oil (Rowe *et al.*, 2009). PEG-40 HCO is known to have the advantages of having good solubility in a reasonably wide polarity range, is non-toxic, and can be used for oral dosage forms (Rachmawati *et al.*, 2017).

MATERIALS AND METHODS

The research was conducted in an experimental laboratory divided into four work stages. The first is the manufacture of extracts and testing of extract parameters. The second stage was optimizing the combination of extracts and instant powder fillers. The third stage is the formulation of ginger and lemon bangle instant powder. The fourth step is to test the characteristics of the extract and the antioxidant activity of the instant powder dosage form.

Instruments and materials

Making the extract involves a macerator and rotary evaporator (InScienPro). In the process of testing the antioxidant activity, total curcuminoids, total flavonoids, and total polyphenols using tools: microanalytical balance (Sartorius), UV-Vis spectrophotometer (Agilent Cary 60), and micropipette (Joanlab). Instant powder production involves a dehydrator (Athome), grinder, and other standard glassware (Pyrex). The powder characteristics test involved a pH meter (Dixon Tech), a slide micrometre (Srate), and a centrifuge (Health HC8).

Phytochemical screening using reagents: Mayer (DPH), Dragendorff (DPH), sulfuric acid P (Emsure), acetic acid anhydrous (Isolab), FeCl₃ (Sigma), gelatin (Fisher Saintific), NaCl (Merck), zinc dust (Emplura), HCl P (Emsure), chloroform (Merck) and ammonia (Emsure). Several standard reagents used in determining extract parameters were gallic acid (Merck), curcumin (Merck), DPPH/1,1-diphenyl-2-picrylhydrazil (Sigma), and Quercetin (Merck). In the manufacturing process, they have used excipients: maltodextrin DE 18-20

(Ambrosia), Sucralose (Anhui Jinhe), and PEG-40 HCO (Evonik).

The research sample was ginger (*Zingiber officinale* L.) simplicia obtained from B2P2TOOT. Bangle extract, which was extracted using 96% ethanol (DPH) from the *Zingiber montanum* (J.Koenig) Link ex A simplicia, plant which had been determined at Herbarium Bandungense ITB with the Voucher code FIPIA-DEP29. Lemon is a local fruit obtained from the CLemon, which is a local fruit obtained from the city of Tasikmalaya.

Extraction

The extract was prepared based on the 2nd Indonesian Herbal Pharmacopoeia, using 96% ethanol. Weighed 1 Kg of simplicia was crushed and sieved using mesh number 40. The simplicia powder was then considered, and 995 grams were obtained. The simplicia work was divided into five macerators; ginger simplicia powder was put into the macerator and added with 96% ethanol at a ratio of 1:10. Soak it for the first 6 hours while occasionally stirring and let stand for 18 hours. The solvent replacement was carried out once with the same type and amount, and the treatment was carried out the same way as the first day. All macerate was collected, filtered, and then concentrated in a vacuum rotary evaporator with a speed of 60 RPM, pressure -0.6 mmHg, and a temperature of 60°C. The condensed extract is then calculated in yield using equation 1 (Kemenkes RI, 2017).

$$Yield (\%) = \frac{Extract\ weight\ (gram)}{Simplicia\ weight\ (gram)} \times 100\% \dots \dots \dots [1]$$

Test the water content of the extract

The distillation of toluene determines the water content. First, the toluene is saturated with water; the samples are weighed in 2 grams. The pieces are put into a round bottom flask and added toluene. The toluene distillation device is assembled, making sure the district and burette are clean and dry. The flask was heated for 15 minutes; after the toluene started to boil, the distillation was set at two drops/second. After all the water is distilled, heating is continued for 5 minutes. Allow the receiving tube to cool to room temperature and the water to separate at the bottom of the burette. Moisture content is calculated based on volume percent per sample weight (DepKes RI, 2000).

Phytochemical screening

Phytochemical screening was performed according to Farnsworth (1966) and Hanani (2015) procedures. Phytochemical screening includes compounds: alkaloids, tannins, polyphenols, flavonoids, saponins,

triterpenoids, and steroids. The procedure in the following description:

- a. For the alkaloids test, the extract is put into a test tube with 28% ammonia, and then 10 mL of chloroform is added. The chloroform phase was separated and acidified with 2 N hydrochloric acid. The acid layer was separated and used for alkaloid testing: with Mayer reagent (Potassium mercuri-iodide solution), the addition of a few drops of Mayer reagent raises a white precipitate, indicating the presence of alkaloids. Dragendorff (Iodobismutat solution): The addition of this reagent raises a brownish-red precipitate, indicating the presence of alkaloids.
- b. In the tannin test, the extract is put into a test tube, diluted with 2 mL of water and then divided into two tubes. In the 1st tube, add 2-3 drops of FeCl₃ 1%. The presence of a blue precipitate or blue-black colour indicates the presence of galanin and ellagitannin, while the green or turquoise colour indicates the presence of condensed tannins. In the 2nd tube, added 1% gelatin (in 10% NaCl) formed a precipitate indicating the presence of tannins.
- c. In the polyphenol test, the extract is put into a test tube, diluted with water, and then a few drops of FeCl₃ 1% are added. The presence of a blue precipitate, and blue-black, green and turquoise colours indicate the presence of polyphenolic compounds.
- d. In the flavonoid test, the extract was put into a test tube, added 2 mL of 80% ethanol, and then stirred and filtered. Filtrate added 3-4 spatulas of magnesium powder and 0.5 mL of HCl P. The presence of flavonoids is indicated by the production of an orange-to-red hue that can be drawn with amyl alcohol or octyl alcohol.
- e. For the saponin test, the extract is put into a test tube with 10 mL of water, then stirred and shaken vigorously vertically for 30 seconds. If the foam is formed with a height of more than 3 cm, which is persistent for 30 minutes, then the sample contains saponin.
- f. Testing for steroids and triterpenoids, the extract is put into a test tube, chloroform is added, and then the chloroform phase is separated and evaporated. Three drops of anhydrous acetic acid and one drop of concentrated sulfuric acid were added to the residue (Liebermann-Burchard). The magenta or violet colour formation indicates that the simplicia contains triterpenoid group compounds. The presence of a greenish-blue colour indicates the presence of steroids.

Determination of total curcuminoid levels of bangle extract

Test for total curcuminoids using UV-Vis spectrophotometry (Kemenkes RI, 2017). Preparation of the test solution begins by carefully weighing approximately 100 mg of the extract, placing it in an Erlenmeyer flask, and adding 10 mL of ethanol P, sonicating until the extract is dissolved. Filter into a 10 mL volumetric flask, rinse the filter paper with ethanol P, and add ethanol P up to volume. The sample solution was diluted ten times by taking 0.1 mL of input into a 10 mL volumetric flask and adding ethanol P up to the mark. A reference solution was prepared by carefully weighing approximately 10 mg of curcumin, putting it into a 10 mL volumetric flask, and adding ethanol P up to the mark. Make a series of dilutions for the reference solution with levels 1, 2, 3, 4, 5, and 6 µg/mL, respectively. Blank solution using Ethanol P. Measurements were made by pipetting 3 mL of the test solution separately, each series of the Reference solution and the Blank solution into the appropriate containers, measuring the absorbance at the maximum absorption wavelength of approximately 420 nm. Create a calibration curve to determine the regression equation. The sample concentration is calculated in weight percent (% w/w) with equation 2 where *k* is the curcuminoid concentration in µg/mL, *f* is the dilution factor, *v* is the sample volume before dilution (mL), and *w* is the sample weight.

$$\text{Curcuminoid (\%)} = \frac{k \times v \times f}{w} \times 100\% \dots \dots \dots [2]$$

Determination of total polyphenol levels

The reference solution was diluted ten times for a 100 µg/mL concentration. The reference solutions were

made in serial dilutions with successive concentrations of 1, 2, 3, 4, and 5 µg/mL, as seen in Table 1.

A total of 1 mL of the test solution was taken, and each series of reference solutions was put into the appropriate container; at each concentration, 0.5 mL of F-C solution was added. The mixture was allowed to stand for 8 minutes, then 0.5 mL of saturated Na₂CO₃ was added and incubated for 1 hour at room temperature, after which 10 mL of water was added. The wavelength absorption of each solution was measured at a wavelength of 740 nm. Blank measurements were carried out the same way, without adding the test solution. A calibration curve was created, and the gallic acid equivalent (GAE) sample concentration was calculated (Aji *et al.*, 2023; Kemenkes RI, 2017).

Determination of total flavonoid levels

Weighed 0.1 gram of sample and put it into an Erlenmeyer, then 10 mL of ethanol P sonicated was added until the extract dissolved. Filter into a 10 mL volumetric flask, rinse the filter paper with ethanol P, and add up to the mark. The reference solution was prepared by carefully weighing 10 mg of quercetin, putting it into a 10 mL volumetric flask, dissolving it, and adding ethanol P up to the mark. Make serial dilutions of 20, 30, 40, 50, and 60 µg/mL solutions. The assay started by pipetting 0.5 mL of the test solution separately and each series of reference solutions into the appropriate container, adding 1.5 mL of ethanol P, 0.1 mL of 10% aluminum chloride, 0.1 mL of 1 M sodium acetate, and 2.8 water (Table 2). Shake the solution for 30 minutes at room temperature. Measure the absorbance at λ_{max}. Create a calibration curve and calculate the levels in the presence of quercetin equivalent (QE) flavonoids (Islam *et al.*, 2022; Kemenkes RI, 2017).

Table 1. Series of dilution tests for total polyphenol content by gallic acid equivalence method

No.	Gallic Ac. (mL)	F-C (mL)	Na ₂ CO ₃ (mL)	Water (mL)	Final Volumes (mL)	Gallic Acid Concentration (µg/mL)
1	0.00	0.50	0.50	9.00	10.00	0.00
2	0.10	0.50	0.50	8.90	10.00	1.00
3	0.20	0.50	0.50	8.80	10.00	2.00
4	0.30	0.50	0.50	8.70	10.00	3.00
5	0.40	0.50	0.50	8.60	10.00	4.00
6	0.50	0.50	0.50	8.50	10.00	5.00

Table 2. Determination of total flavonoids by quercetin equivalence method

Quercetin (µg/mL)	Vol. Quercetin (mL)	AlCl ₃ (mL)	Na-Acetate (mL)	Ethanol (mL)	Water (mL)	Quercetin Final Concentration (µg/mL)
20.00	0.50	0.10	0.10	1.50	2.80	2.00
30.00	0.50	0.10	0.10	1.50	2.80	3.00
40.00	0.50	0.10	0.10	1.50	2.80	4.00
50.00	0.50	0.10	0.10	1.50	2.80	5.00
60.00	0.50	0.10	0.10	1.50	2.80	6.00

Table 3. Dilution series and addition of DPPH test reagents

Sample Code	Methanol (mL)	Sample (mL)	DPPH (mL)	Sample Concentration (µg/mL)
Control	4.00	0.00	1.00	0.00
A1	3.75	0.25	1.00	5.00
A2	3.50	0.50	1.00	10.00
A3	3.00	1.00	1.00	20.00
A4	2.00	2.00	1.00	40.00
A5	0.00	4.00	1.00	80.00

Antioxidant activity assay of ginger extract, bangle, and lemon juice

Sample stock solutions and 1,1-difenil-2-pikrilhidrazil (DPPH) were prepared at a concentration of 100 µg/mL, then the samples and DPPH were reacted as shown in Table 3, with a total volume of 5 mL to obtain sample concentrations of 5, 10, 20, 40, and 80 µg/mL. The solution concentration series were incubated at 37°C for 30 minutes and protected from light. After that, the absorbance at a wavelength of 517 nm was calculated using a UV-Vis spectrophotometer (Agilent Carry 60) and the percent inhibition (*Pi*) using equation 3. The value of *Ab* is the absorbance of the control, while *As* is the absorbance of the sample. The results of the calculation are entered in a linear regression equation with the extract concentration µg/mL as the abscissa (x-axis) and the % inhibition activity value as the coordinate (y-axis). The IC₅₀ value is calculated by the equation $y = ax+b$ (Aji *et al.*, 2023; Sirivibulkovit *et al.*, 2018). The IC₅₀ category can be seen in Table 4.

$$Pi = \frac{Ab-As}{Ab} \times 100\% \dots\dots\dots [3]$$

Table 4. Category IC₅₀ of antioxidant activity (Zamzani & Triadisti, 2021)

Antioxidant Intensity	Score IC ₅₀ (µg/mL)
Very Strong	<50
Strong	50-100
Currently	100-250
Weak	250-500

Antioxidant assay combination of ginger extract, bangle, and lemon juice

The simple axial approach is used to determine combinations involving three samples simultaneously. This approach estimates the optimal mix of extracts, minimizing the amount used. (Cavalcanti *et al.*, 2021). The combinations follow Figure 1 and Table 5. Combination 1, ginger, bangle and lemon extracts were 1/3: 1/3: 1/3, combination 2 is 4/6: 1/6: 1/6, combination

3 is 1/6: 1/6: 4/6, and combination 4 is 1/6: 4/6: 1/6 (Cornell, 2011).

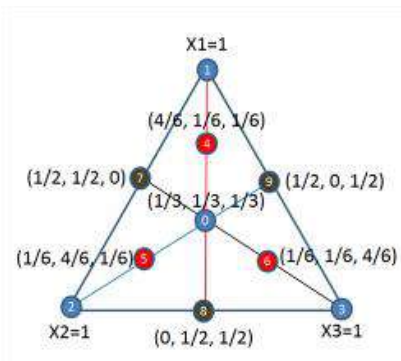


Figure 1. A simple axial diagram of the ginger-bangle-lemon combination (Cornell, 2011)

Table 5. Combinations of ginger extract: bangle: lemon

Combination	X1 (Ginger)	X2 (Bangle)	X3 (Lemon)
1	1/3	1/3	1/3
2	4/6	1/6	1/6
3	1/6	1/6	4/6
4	1/6	4/6	1/6

All formula combinations were made into 100 µg/mL stock concentrations and then made into five concentration variations and one blank. Each concentration was added with 100 µg/mL DPPH (Table.3); then, the absorbance was measured. The next step was calculating the percent inhibition and making a linear regression curve, which sought the IC₅₀ value. The sample stock solution was diluted into five graded concentration variations. Add 1.0 mL of 150 mg/L DPPH solution until the total volume of the solution is 5.0 mL (Julizan, 2019).

Measure the absorbance of the solution using a spectrophotometer at a wavelength of 517 nm, calculate the inhibition ability of each sample concentration as a percent inhibition (equation 3), and Plot the sample's concentration value and % inhibition on the standard curve. The concentration of 50% inhibition (IC₅₀) is determined using the linear regression.

Instant powder formulation with the added combination of extracts

The formulation was based on a combination of extracts with the highest antioxidant activity. The selected extract combinations were then made into instant powder with increased concentrations of 100, 200, 300, 400, and 500 times their IC₅₀ values. The instant powder is formulated with the addition of fillers maltodextrin dextrose equivalent (DE) 18-20 and sucralose as a sweetener. Sucrose was used at a concentration of 0.24%. Maltodextrin is chosen with DE 18-20, which is very soluble in water. The formula uses maltodextrin as a filler with an amount of 1-99% (Rowe *et al.*, 2009). The instant powder formula can be seen in Table 8. After being formulated, the instant powder was tested for antioxidant activity, organoleptic observation, solubility, sedimentation, and clarity tests. Antioxidant activity test using a sample weight of 100 mg.

Instant powder formulation with the addition of PEG-40 HCO

PEG-40 Hydrogenated Castor Oil or PEG-40 HCO is a surfactant that can help dissolve instant powder in water (Kadian & Nanda, 2022). The addition of PEG-40 HCO is expected to increase antioxidant activity by increasing the solubility of instant powder when dissolved in water. The instant powder formula with the successive addition of PEG-40 HCO from 0, 1, 3, 9, and 27% can be seen in Table 9. After the formulation, the antioxidant activity was tested with a sample size of 100 mg. Powder characteristic test includes parameters: organoleptic, dissolving time, clarity, sedimentation, angle of repose, flow time, bulk density, incompressible density, and Hausner factor. In addition to the characteristics of the formula with the best antioxidant activity, a proximate test was also carried out.

Instant powder characteristics test

Instant powder organoleptic was carried out macroscopically and microscopically. Macroscopic observations include the form of aroma, colour, and taste. The microscopic observation of powder particle shape. Microscopic observation using a binocular microscope with a slide micrometre. The instant powder is put on the micrometre slide, dripped with liquid paraffin, and covered using a cover glass.

The solubility test was performed by dissolving instant powder in water with a ratio of 1:10 up to 1:100 at 10 mL volume intervals. They stirred the solution using a magnetic stirrer at a speed of 2400 rpm for 5 minutes. Percent transmittance (%T) is used to measure the clarity of a solution or dispersion system quantitatively. A high %T value means that the particle

size is getting smaller, and the level of transparency is increased (Abdassah, 2017). The turbidity of the solution was measured using UV-Vis photometer spectroscopy at a wavelength of 800 nm, and the %T value was calculated. The sedimentation test carried out the solubility test results by placing the sample in a centrifugation tube and rotating it at 4000 rpm for 5 minutes. The centrifugation results were then seen for the presence or absence of sediment.

The dissolution time test was carried out by weighing 1 gram of instant powder in a 100 mL glass, and then the dissolving time of the powder in water was recorded. The time needed to dissolve is less than 5 minutes (Schorsch *et al.*, 2001).

The angle of repose is a fixed angle between the heap of conical particles and the horizontal plane when a certain amount of powder is poured into the measuring device. A good angle of repose between 25- 40°. The angle of repose is determined by the equation $\tan \alpha = h/r$, where α is the angle of repose, h is the height of the cone, and r is the radius of the cone (Husni *et al.*, 2020).

The flow time is determined by weighing 25 grams of powder poured into the measuring funnel. The funnel lid is opened slowly; the granules are allowed to flow out. Time was recorded with a stopwatch until all the granules flowed out. A good flow time is ≤ 10 grams/second or 100 grams ≤ 10 seconds (Hudha & Widyaningsih, 2015).

The pH value is determined by weighing 1 gram of instant powder dissolved in 100 mL of distilled water. Take measurements using a calibrated pH meter in the test range using a standard buffer.

The bulk density (ρ) test was carried out by weighing 30 grams of powder (W_o), then putting it into a 100 mL measuring cup and observing its volume (V_o). The formula calculates the bulk ρ value: W_o/V_o . The compress ρ test is carried out by weighing 30 grams of powder (W_o) input into a 100 mL measuring degree and measuring the volume (V_t). Then, place it on the tap density tester by tapping 1,250 times and recording the volume (V_{t1}). If the difference between V_t and V_{t1} is not more than 2 mL, then V_t is used. The W_o/V_t formula calculates the compress ρ value. The incompressible ρ value is affected by the particle size (Abdullah & Imtihani, 2022). The Hausner factor is a method of determining the flow properties of powders by measuring ρ bulk and ρ compressed. A ratio of <1.25 indicates good characteristics, and >1.50 means poor characteristics (Kusumo & Mita, 2018). In addition to the Hausner ratio, the percent (%) compressibility value

is also specified. The Hausner factor is calculated using equation 4, and % compressibility using equation 5.

$$\text{Hausner Factor} = \frac{\rho_{\text{Compress}}}{\rho_{\text{Bulk}}} \dots\dots\dots[4]$$

$$\% \text{ Compressibility} = \frac{\rho_{\text{Compress}} - \rho_{\text{Bulk}}}{\rho_{\text{Compress}}} \dots\dots\dots[5]$$

Data analysis

Descriptive analysis was done for the parameter data of extract and powder characteristics. In comparison, regression analysis determines total curcuminoid levels, total polyphenols, total flavonoids, and antioxidant activity.

RESULTS AND DISCUSSION

Extraction results and extract parameters test

Bangle is an extract obtained by the maceration method using 96% methanol. Bangle extract was brought based on previous research by Aji *et al.* (2023). Ginger extract is made using the maceration method with 96% ethanol solvent. The result of ginger extraction yielded 8.74%. In contrast, in lemon fruit juice, from 500 grams of fresh fruit, 120 mL of liquid is obtained. Water level testing was done on ginger and bangle extracts. The water content obtained was as much as 5.64±1.63% for ginger extract and 9.09±0.61% for bangle extract. The water content of both extracts meets the Indonesian Herbal Pharmacopoeia requirements (Kemenkes RI, 2017).

Phytochemical screening aims to identify the content of secondary metabolite compounds of a natural material. The results of phytochemical screening can be seen in Table 6. Plants are an essential source of bioactive compounds for developing new therapeutic agents. Some of them have antioxidant activity. Based on Table 6, concentrated extracts of ginger and bangle were identified as having the same group of compounds: alkaloids, polyphenols, flavonoids, and triterpenoids. While lemon identified only polyphenols. Several secondary metabolite compounds, such as polyphenols and flavonoids, are known to have antioxidant activity (Nhu-Trang *et al.*, 2023).

Total curcuminoid level testing was done on the bangle, associated with the yellow pigment content caused by complex curcuminoid content such as cassumunin A, B, and C (Kabkrathok *et al.*, 2022). The total curcuminoid level testing result from the bangle is 1.82±0.01%. This value is much lower than the previous research conducted by Aji *et al.* (2023), which amounted to 3.84%. The low level of total curcuminoid can be

caused by several factors in the extract storage process, such as temperature, water content, and pH. Curcuminoids will be stable at acidic pH (<7) in aqueous solution and very unstable at neutral and alkali pH (>7). In contrast, high temperature is a catalyst for accelerating curcuminoid degradation (Kharat *et al.*, 2017).

Table 6. Results of phytochemical screening

No.	Group of Compounds	Ext. EtOH 96% Ginger	Ext. EtOH 96% Bangle	Lemon Juice
1	Alkaloids	+	+	-
2	Polyphenol	+	+	+
3	Tannin	-	-	-
4	Flavonoids	+	+	-
5	Saponins	-	-	-
6	Steroids	-	-	-
7	Triterpenoids	+	+	-

(+) present, (-) absent

Total polyphenol (Figure 2a) and total flavonoid (Figure 2b) levels were tested on all three samples. The test results can be seen in Figures 2a and 2b. The highest level of phenols is found in the ginger extract, followed by bangle and lemon, with the lowest concentration. In this study, the total polyphenol content of ginger was 1.22 mgGAE/g compared to previous research by Ghafoor *et al.* (2020), where the total polyphenol content was much higher at 9.32 mgGAE/g. The low polyphenol content may occur due to the simplified heating-drying process. In previous studies, the drying method of simplicia used freeze-dried so that the oxidation of polyphenolic compounds could be minimized with low temperatures. Similarly, the total polyphenol content in this study obtained 0.64 mgGAE/g in previous research by (2022), which amounted to 3.81 mgGAE/g. Both used the same extraction method and solvent. The main content of ginger rhizome is oleoresin in the form of gingerol and shogaol derivatives (Van *et al.*, 2023). The gingerol and shogaol compounds (Figures 3a and 3b) are polyphenolic compounds that can react with the F-C reagent and be read in the test (Nikolaeva *et al.*, 2022). In the bangle, the main compound is curcuminoid (Figure 3c), which has a polyphenol functional group and can react with the F-C reagent. The lowest content is lemon juice; unlike ginger and bangle extract, lemon is not concentrated, so it has the lowest range.

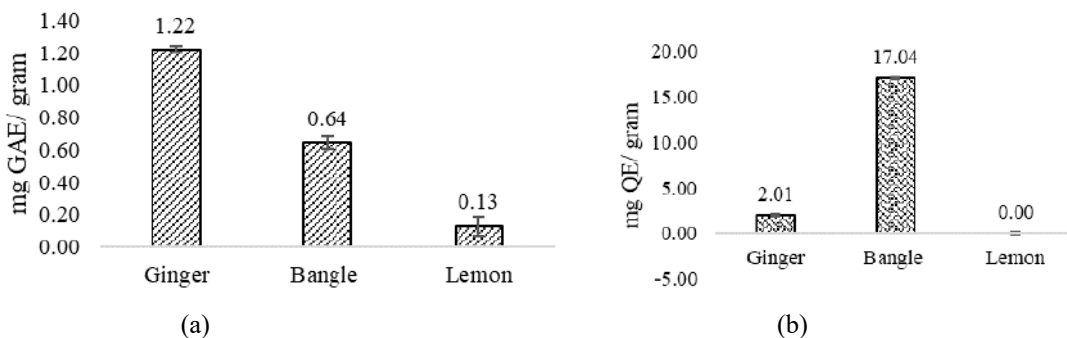


Figure 2. (a) Total polyphenol level as gallic acid equivalent (GAE), and (b) total flavonoid level as quercetin equivalent (QE)

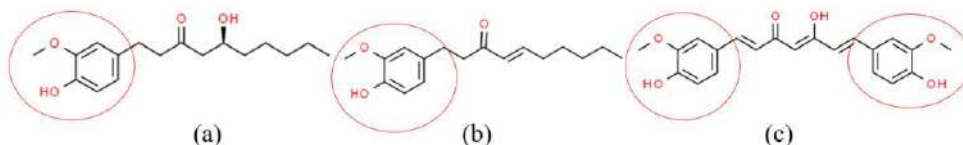


Figure 3. Phenol functional group in compounds (a) 6-gingerol, (b) 6-shogaol, and (c) curcumin

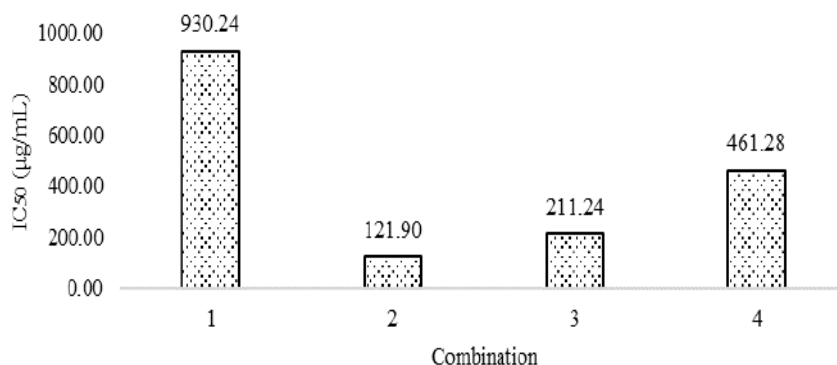


Figure 4. Antioxidant activity of the combination of ginger extract, bangle, and lemon juice

Different from the total polyphenol content test in the total flavonoid test, the bangle has the highest flavonoid content compared to the other two samples. For total flavonoid levels in this study, it was 2.01 mgQE/g, based on previous research by (2022), with levels of 1.69 mgQE/g. In this study, flavonoid levels were slightly higher than in the previous study. This study and the previous one were ginger rhizomes sourced from the same harvest site. One of the reasons for the difference is the different harvest times. As for bangle in, this study has a level of 17.04 mgQE/g, while in the previous research it was 21.93 mgQE/g. This and previous studies used the same extraction method and solvent but different sources. Based on this, the drying method, harvest time and harvest location significantly affect the levels of total polyphenol content and total flavonoids. Based on the research of Hassan *et al.* (2019) besides curcuminoid bangle is known to contain five flavonoid derivatives, namely kaempferol 3-O-

rhamnopyranoside, kaempferol 3-O-(3''-O-acetyl) rhamnopyranoside, kaempferol 3-O-methyl ether, kaempferol 3-O-(4''-O-acetyl) rhamnopyranoside, and kaempferol 3-O-(3,4''-di-O-acetyl) rhamnopyranoside.

Antioxidant test results of ginger extract, bangle, and lemon juice individually and in combination

The results of the antioxidant activity test of the three samples can be seen in Table 7. The antioxidant activity is correlated with the total polyphenol level; the higher the total polyphenol level in the extract, the higher the antioxidant activity (Muflihah *et al.*, 2021). The IC₅₀ value is the concentration of the sample solution needed to inhibit 50% of DPPH free radicals. The lower the IC₅₀ value, the higher the activity (Ramadhan *et al.*, 2022). Ginger extract has very strong antioxidant activity (<50 µg/mL), the bangle has strong activity (50-100 µg/mL), and lemon has weak activity (> 500 µg/mL) (Zamzani & Triadisti, 2021).

Table 7. Antioxidant activity of ginger, bangle, and lemon

Sample	IC ₅₀ (µg/mL)	SD
Ext. EtOH 96% Ginger	23.57	0.13
Ext. EtOH 96% Bangle	64.89	0.15
Lemon Juice	4,268.02	0.11

SD : Standard deviation

Based on the results (Figure 4), the antioxidant activity of combination number two with the composition of ginger (4/6), bangle (1/6): and lemon (1/6) is the composition that has the highest activity with the category of "medium" potential. The combination is done using a simple axial. Although lemon juice has weak antioxidant activity, it contains organic acids that can stabilize curcuminoids (Asencio *et al.*, 2018; Zheng *et al.*, 2017). Curcuminoid compounds are stable in aqueous solutions at acidic pH (<7) (Manju & Sreenivasan, 2011). The content of organic acids such as citric acid and malic acid in the lemon will create acidity in the extract combination (Sánchez-Bravo *et al.*, 2022). The combination of extracts has lower antioxidant activity than single extracts (ginger and bangle). The decrease may occur due to dilution from the effect of mixing extracts that have intense antioxidant activity with weak ones (Harun & Rahmawati, 2022). In addition to antioxidant activity, the working mechanism of the characteristic components in the extract can be used as a target in combination design. For example, 6-gingerol regulates lipogenesis, fatty acid oxidation, mitochondrial dysfunction, and oxidative stress (Cerdá *et al.*, 2022). Curcumin affects the treatment of diabetes by improving

β-cell function, preventing β-cell death, and reducing insulin resistance (Quispe *et al.*, 2022).

Instant powder formulation results with the addition of extract combinations

Based on the optimization results, combination number two was selected to proceed to the formulation stage. The IC₅₀ value of combination extract number two is 121.90 µg/mL or 0.0122%. At this stage, the effect of adding extracts on instant powder's characteristics and antioxidant activity will be seen. The extracts were increased to 100, 200, 300, 400, and 500 times from the IC₅₀ value. The formula can be seen in Table 8.

The result of organoleptic observation (Figure 5) macroscopically shows that the dosage form is pale yellow to yellow. The yellow colour's intensity increases as the added extract's concentration increases. Similarly, the aroma will increase with the addition of extracts. All instant powders have a powder form with a smooth texture. The instant powder has a sweet, sour, and spicy taste. The sour and spicy flavour will increase with the addition of extract. The results of microscopic (Figure 6) observation of all formulas (F1 to F5) have a crystal shape with a heterogeneous structure and size.

Table 8. Formulation of instant powder with the addition of combination extract number 2

No.	Materials	Concentration % (w/w)				
		F1	F2	F3	F4	F5
1	Combination of Extracts 2	1.22	2.44	3.66	4.88	6.10
2	Sucralose	0.24	0.24	0.24	0.24	0.24
3	Maltodextrin DE 18-20	98.54	97.32	96.1	94.8	93.6
				0	8	6



Figure 5. The appearance of instant powder

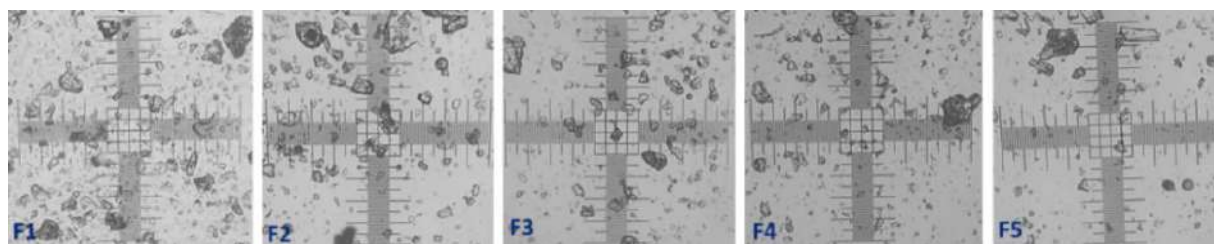


Figure 6. Microscopic appearance of instant powder on a micrometre slide (1 Division = 0.01 mm)

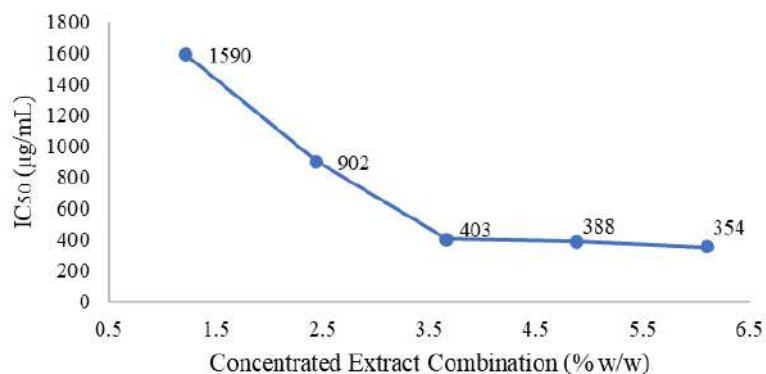


Figure 7. Effect of adding Extract Combination No. 2 on Antioxidant Activity

The effect of adding extract combination on the antioxidant activity can be seen in Figure 7. The instant powder antioxidant activity from formula F1 to formula F3 shows an increase in antioxidant activity marked by a decrease in the IC₅₀ value. However, in formulas F3, F4, and F5, the increase in concentration is not directly proportional to the increase in antioxidant activity, which is shown by a graph that slopes toward the average. The saturation of the solution causes the phenomenon; the higher the concentration of the extract, the more precipitates are formed. In line with the theory, it is supported by the results of testing the clarity of the instant powder solution shown in Figure 8. The results of the clarity test show that the higher the extract concentration, the lower the percentage of transmittance (%T) will be. The decreasing value of %T shows the increasing value of turbidity. In addition, the result of qualitative sedimentation testing in Figure 9 shows that

the higher the extract is added, the more sediment is formed. One of the efforts to increase the solubility of the extract in the instant powder is by adding surfactants such as PEG-40 HCO, a polyoxyethylene derivative of castor oil with an HLB value of 15.

Instant powder formulation with PEG-40 HCO addition

Based on optimization, adding extracts affects antioxidant activity and powder instant characteristics. Instant powder formula F5 produces the highest activity but low solubility. The decrease in solubility is caused by the high concentration of the extract so that saturation occurs. The solubility of formula F5 can be improved by adding surfactants, one of which is PEG-40 HCO. The addition of surfactant is expected to increase instant powder's solubility and antioxidant activity. The instant powder formula with the addition of PEG-40 HCO can be seen in Table 9.

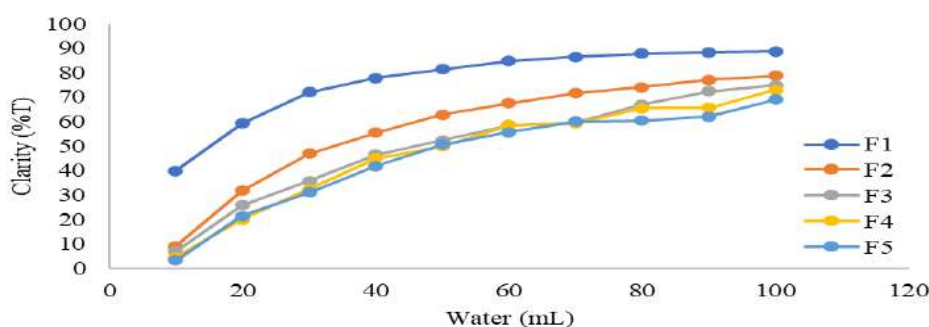


Figure 8. The effect of adding combination extract No. 2 on the clarity of the instant powder solution

Table 9. Instant powder formula with the addition of PEG-40 HCO

No.	Materials	Concentration % (w/w)				
		F5a	F5b	F5c	F5d	F5e
1	Extract Combination 2	6.10	6.10	6.10	6.10	6.10
2	PEG 40 HCO	0.00	0.10	0.30	0.90	2.70
3	Sucralose	0.24	0.24	0.24	0.24	0.24
4	Maltodextrin DE 18-20	93.66	93.56	93.36	92.76	90.96

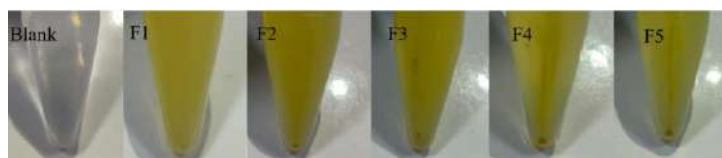


Figure 9. Instant powder solution sedimentation test results



Figure 10. The appearance of instant powder with the addition of PEG-40 HCO

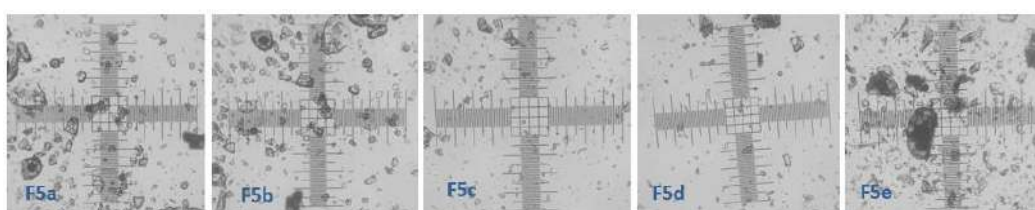


Figure 11. Microscopic appearance of instant powder with the addition of PEG-40 HCO

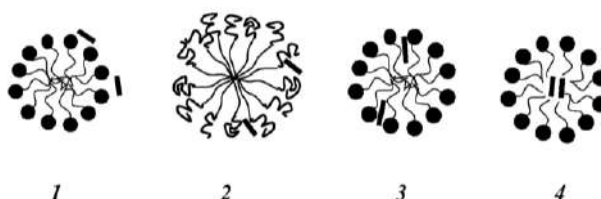


Figure 12. The loci of active compound (-) on surfactant micelle structure (Rangel-Yagui *et al.*, 2005)

The results of organoleptic observation (Figure 10) of the five formulas do not have any characteristic differences. The five formulas have a yellow colour, a typical bangle aroma, a sour, spicy, sweet taste, a powder form, and a smooth texture. Likewise, from the microscopic observation (Figure 11), the powder from formula F5a to formula F5e did not experience any change in morphology. Microscopically, instant powder has a crystal shape.

The bias of the effect of adding excipients on antioxidant activity, all excipients were tested for antioxidant activity. The results were that PEG-40 HCO, maltodextrin DE 18-20, and sucralose did not have antioxidant activity. Clarity test results (Figure 13b) show that the higher the addition of PEG-40 HCO, the higher the %T, which means the more transparent the solution. The results of the sedimentation test can be seen in Figure 14. The higher the addition of PEG-40 HCO, the less sediment formed, and the intensity of the yellow colour increases. The solubility test results show that all formulas (F5a to F5e) dissolve in less than 5

minutes. The test results prove that adding PEG-40 HCO increases the solubility of the extract from the instant powder, which impacts the increase in antioxidant activity (Figure 13a).

One of the reasons for using PEG-40 HCO is the ability to solubilize well ginger and bangle extracts containing water-insoluble oleoresin and curcumin, which PEG-40 HCO can enhance with a relatively small concentration of 2.70%. The phenomenon of increased solubility by surfactants is due to micellar solubilization. An important property of micelles that has a special meaning in pharmaceuticals is their ability to increase solubility, the spontaneous dissolution of a substance through a reversible interaction with surfactant micelles in water to form a thermodynamically stable isotropic solution (Sari & Nurhardiyanti, 2023). The extract is a multi-component that has hydrophilic to hydrophobic compounds. There are several possible solubility loci for active substances in micelles, as shown in Figure 12.

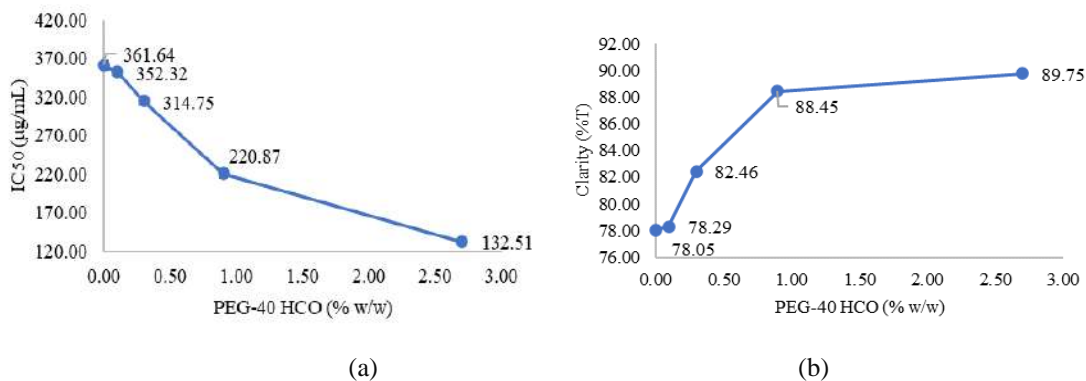


Figure 13. Effect of adding PEG-40 HCO to (a) antioxidant activity, and (b) clarity of solution instant powder



Figure 14. Effect of PEG-40 HCO addition on sediment formation

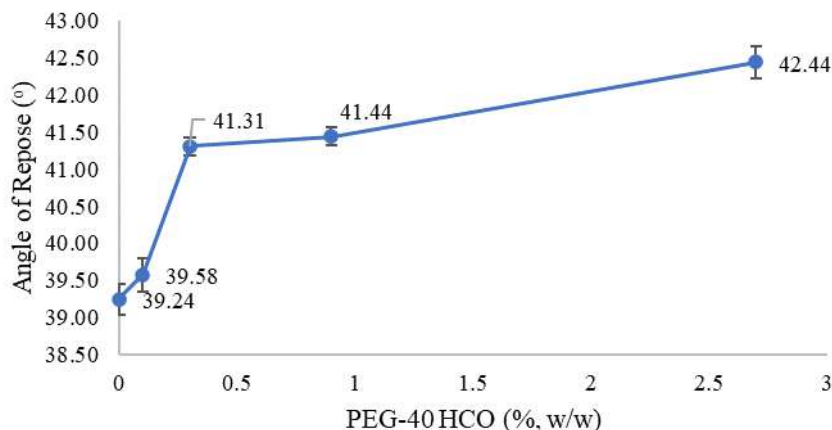


Figure 15. Effect of adding PEG-40 HCO against the repose angle of the powder

Hydrophilic compounds can be adsorbed on the surface of micelles (1); drugs with intermediate solubility should be placed in the middle position in micelles, such as between the hydrophilic head groups of micelles (2) and in the palisade layer between the hydrophilic group and the first few carbon atoms of the hydrophobic group, which is the outer core (3), and hydrophobic drugs that are not soluble at all can be placed in the micelle core (4) (Rangel-Yagui *et al.*, 2005).

The angle of rest is one of the parameters of powder flow properties. Based on Figure 15, the higher the addition of PEG-40 HCO, the higher the angle of repose. An excellent quiet angle is 25-40°. So, in the formula F5c-F5e, the powder has a wrong angle of repose. The

shape and size of the particles influence the angle of repose. The finer the particle size of a mass or material, the more difficult it is to flow and form an angle with a high slope. The larger the angle produced, the worse the powder flow quality is (Mehrabani *et al.*, 2023). According to the theory, the addition of PEG-40 HCO (Figure 16) affects the flow rate; the higher the PEG-40 HCO is added, the more the powder flow rate decreases. The five formulas do not meet the requirements where the good powder has a flow speed of more than 10 grams/second (Sarabandi *et al.*, 2019). In addition, PEG-40 HCO is a liquid substance that cannot be dried at the temperature of drying powder it can increase the cohesion and adhesion of particles. This is likely to be

one of the factors in the deterioration of the powder flow.

The formulas of F5a-F5e have a pH in the range of 4.16-4.20 (Figure 17); in this value degree, the formulas have an acidic nature due to the addition of lemon juice. The acidic pH value of the instant powder aims to increase the stability of the curcuminoids in the powder instant. Curcuminoids will decompose at neutral to alkaline pH (Zheng & McClements, 2020). Curcumin is more stable in oily or acidic pH environments (Martínez-Guerra *et al.*, 2019; Zheng *et al.*, 2017).

The results of the powder density test can be seen in Figure 18. The Hausner ratio (Figure 18a) of all formulas (F5a to F5e) shows good characteristics (<1.25). The compressibility values (Figure 18b) of F5a, F5b, and F5c are in a poor category (26 to 31%), while the formulas F5d and F5e are in a reasonably good category (20 to 25%) (Kusumo & Mita, 2018).

The proximate test was carried out on the formula with the highest antioxidant activity, the F5e formula. They were testing carried out in the Laboratory UNPAD Central. The test results can be seen in Table 10.

Table 10. Proximate value of instant powder with the addition of PEG-40 HCO

No.	Parameters	Concentration (%)	Method
1	Water content	5.58	Gravimetry
2	Ash Content	0.10	Gravimetry
3	Fat level	5.90	Soxhlet
4	Protein Content	0.21	Kjeldahl
5	Carbohydrate Content	88.21	By Difference
6	Total Sugar Content	18.09	Anthrone

CONCLUSION

Ginger and bangle have robust ($IC_{50} = 23.57 \pm 0.13$ $\mu\text{g/mL}$) and strong ($IC_{50} = 64.89 \pm 0.15$ $\mu\text{g/mL}$) antioxidant activities, while lemon has weak activity ($IC_{50} > 500$ $\mu\text{g/mL}$). The combination of bangle ginger and lemon using the simple Axial method obtained combination No.2 with the composition ginger (4/6): bangle (1/6): lemon (1/6). This combination has moderate activity (121.90 $\mu\text{g/mL}$). Combination No. 2 extracts can be formulated in instant powder. The formula with the highest antioxidant activity is the F5 formula, with a concentration increase of 500 times the IC_{50} value. Adding PEG-40 HCO to the F5 formula aims to improve the solubility of the extract in instant powder. Results The addition of PEG-40 HCO affected the

solubility of the extract and antioxidant activity. After adding PEG-40 HCO, the solubility and antioxidant activity increased. However, with the addition of PEG-40 HCO, some of the characteristics of the instant powder experienced a decrease in quality, such as angle of repose, flow time, and compressibility.

ACKNOWLEDGEMENT

We thank the Poltekkes Kemenkes Tasikmalaya for their assistance and contributions in funding our research grants. Also, remember the students: Arum Puspitasari, Ibnu Dn Jiyauhaq, and Astrid Adinda Wulandari, who have assisted in the research.

AUTHOR CONTRIBUTIONS

Conceptualization, D. P., D. A. J., N. Q. D.; Methodology, D. P., D. A. J.; Software, D. P., N. Q. D.; Validation, D. P., D. A. J.; Formal Analysis, D. P., D. A. J., N. Q. D.; Investigation, D. P., N. Q. D.; Resources, D. P., N. Q. D.; Data Curation, D. P., D. A. J., N. Q. D.; Writing - Original Draft, D. P., D. A. J., N. Q. D.; Writing - Review & Editing, D. P., D. A. J.; Visualization, D. P., D. A. J., N. Q. D.; Supervision, D. P., D. A. J.; Project Administration, D. P., D. A. J.; Funding Acquisition, D. P., D. A. J.

FUNDING STATEMENT

This research did not receive any specific grant from funding agencies in the public, commercial, or not for profit sectors.

CONFLICT OF INTEREST

The authors declared no conflict of interest.

REFERENCES

- Abdassah, M. (2017). Nanoparticles with Ionic Gelation. *Farmaka*; 15; 45–52. doi: 10.24198/jf.v15i1.12138.
- Abdullah, H. S. & Imtihani, H. N. (2022). Formulation and Evaluation of Solid Dispersion Granules of Mangrove Crab (*Scylla serrata*) Shell Chitosan Extracts With Chitosan: PVPK-30 1:2. *Jurnal Kefarmasian Akfarindo*; 7; 45–51. doi: 10.37089/jofar.vi0.119.
- Ahmed, N., Karobari, M. I., Yousaf, A., Mohamed, R. N., Arshad, S., Basheer, S. N., Peeran, S. W., Noorani, T. Y., Assiry, A. A. & Alharbi, A. S. (2022). The Antimicrobial Efficacy Against Selective Oral Microbes, Antioxidant Activity and Preliminary Phytochemical Screening of Zingiber

- officinale. *Infection and Drug Resistance*; 15; 2773–2785. doi: 10.2147/IDR.S364175.
- Aji, N., Kumala, S., Mumpuni, E. & Rahmat, D. (2022). Antibacterial Activity and Active Fraction of Zingiber Officinale Roscoe, *Zingiber montanum* (J. Koenig) Link ex A., and *Zingiber zerumbet* (L.) Roscoe ex Sm. Against *Propionibacterium acnes*. *Pharmacognosy Journal*; 14; 103-111. doi: 10.5530/pj.2022.14.15.
- Aji, N., Kumala, S., Mumpuni, E. & Rahmat, D. (2023). Comparison of Sunscreen and Antioxidant Activities: 70% And 96% Ethanol Extract From Bangle (*Zingiber montanum* (J. Koenig) Link ex A.) Rhizome. *Medical Sains: Jurnal Ilmiah Kefarmasian*; 8; 605–614. doi: 10.37874/ms.v8i2.557.
- Aji, N., Puspitasari, A., Nafisah, H. & Armilda, L. H. V. (2023). Antioxidant and Anti-Propionibacterium acnes Activities of Citronella Oil and Clove Oil, and Their Formulation Into Emulgel. *Pharmaceutical Journal of Indonesia*; 20; 64–70. doi: 10.30595/pharmacy.v0i0.12629.
- Asencio, A. D., Serrano, M., García-Martínez, S. & Pretel, M. T. (2018). Organic Acids, Sugars, Antioxidant Activity, Sensorial and Other Fruit Characteristics of Nine Traditional Spanish Citrus Fruits. *European Food Research and Technology*; 244; 1497–1508. doi: 10.1007/s00217-018-3064-x.
- Cavalcanti, V. P., Aazza, S., Bertolucci, S. K. V., Rocha, J. P. M., Coelho, A. D., Oliveira, A. J. M., Mendes, L. C., Pereira, M. M. A., Morais, L. C. & Forim, M. R. (2021). Solvent Mixture Optimization in The Extraction of Bioactive Compounds and Antioxidant Activities From Garlic (*Allium sativum* L.). *Molecules*; 26; 60-26. doi: 10.3390/molecules26196026.
- Cerdá, B., Marhuenda, J., Arcusa, R., Villaño, D., Ballester, P. & Zafrilla, P. (2022). Ginger in the Prevention of Cardiovascular Diseases. *Functional Food*; 14; 943-959. doi: 10.5772/intechopen.98161.
- Çopur, Ö. U., İncedayı, B. & Karabacak, A. Ö. (2019). Technology and Nutritional Value of Powdered Drinks: Production and Management of Beverages. Cambridge: Elsevier. doi: 10.1016/B978-0-12-815260-7.00002-X.
- Cornell, J. A. (2011). Axial Design: A Primer on Experiments with Mixtures. Florida: John Wiley & Sons.
- DepKes RI. (2000). Metode Ekstraksi: Parameter Standar Umum Ekstrak Tanaman Obat. Jakarta: Departemen Kesehatan Republik Indonesia.
- Farnsworth, N. R. (1966). Biological and Phytochemical Screening of Plants. *Journal of Pharmaceutical Sciences*; 55; 225–276. doi: 10.1002/jps.2600550302.
- Fridalni, N., Minropa, A., & Sapardi, V. S. (2019). Early Recognition of Degenerative Diseases. *Jurnal Abdimas Saintika*; 1; 129–135. doi: 10.4161/cc.23067.
- Ghafoor, K., Al Juhaimi, F., Özcan, M. M., Uslu, N., Babiker, E. E. & Mohamed Ahmed, I. A. (2020). Total Phenolics, Total Carotenoids, Individual Phenolics and Antioxidant Activity of Ginger (*Zingiber officinale*) Rhizome as Affected by Drying Methods. *LWT - Food Science and Technology*; 126; 109-354. doi: 10.1016/j.lwt.2020.109354.
- Hanani, E. (2015). Identifikasi Fenol, Tanin, Flavonoid, Alkaloid, Saponin, Steroid dan Triterpenoid: Analisis Fitokimia. Jakarta: Penerbit Buku Kedokteran EGC.
- Harun, N. & Rahmawati, K. A. (2022). The Antioxidant Activity of Extract Combination Juice Ginger Rhizome, Turmeric, Galangal And Kaempferia Galanga. *Jurnal Kesehatan Bakti Tunas Husada: Jurnal Ilmu Ilmu Keperawatan, Analisis Kesehatan Dan Farmasi*; 22; 8–14. doi: 10.36465/jkbth.v22i1.893.
- Hassan, M., Adhikari-Devkota, A., Imai, T. & Devkota, H. P. (2019). Zerumbone and Kaempferol Derivatives from the Rhizomes of *Zingiber montanum* (J. Koenig) Link ex A. Dietr. from Bangladesh. *Separations*; 6; 10-31. doi: 10.3390/separations6020031.
- Hudha, M. & Widyaningsih, T. D. (2015). Effervescent Powder Based on Beluntas Leaf Extract (*Pluchea indica* Less) as a Natural Antioxidant Source. *Jurnal Pangan Dan Agroindustri*; 3; 1412–1422. doi: 10.21776/jpa.v3i4.264.
- Husni, P., Fadhiilah, M. L. & Hasanah, U. (2020). Formulation and Physical Stability Test of Instant Granules of Genjer (*Limnocharis flava* (L.) Buchenau.) Dry Powder as a Fiber Adding Supplement. *Jurnal Ilmiah Farmasi Farmasyifa*; 3; 1–8. doi: 10.29313/jiff.v3i1.5163.
- Islam, A., Acikalın, R., Ozturk, B. & Aglar, E., (2022). Effects of Aloe vera Gel and Modified Atmosphere Packaging Treatments on Quality Properties and Bioactive Compounds of Plum

- (*Prunus salicina* L.) Fruit Throughout Cold Storage and Shelf Life. *Erwerbs-Obstbau*; 65; 71-82. doi: 10.1016/j.postharvbio.2022.111855.
- Julizan, N. (2019). Validation of Antioxidant Activity Determination by DPPH Methode. *Kandaga-Media Publikasi Ilmiah Jabatan Fungsional Tenaga Kependidikan*; 1; 1-8. doi: 10.24198/kandaga.v1i1.21473.
- Kabkrathok, P., Jarussophon, S., Unger, O., Lomarat, P., Reutrakul, V., Pittayanurak, P., Bongcheewin, B., & Anantachoke, N. (2022). Mass Spectral Analysis of Secondary Metabolites From *Zingiber montanum* Rhizome Extract Using UHPLC-HR-ESI-QTOF-MS/MS. *Phytochemical Analysis*; 33; 57-71. doi: 10.1002/pca.3068.
- Kadian, R. & Nanda, A. (2022). A Comprehensive Insight on Self Emulsifying Drug Delivery Systems. *Recent Advances in Drug Delivery and Formulation: Formerly Recent Patents on Drug Delivery & Formulation*; 16; 16-44. doi: 10.2174/2667387815666211207112803.
- Kemenkes RI. (2017). Uji Fenol Total, Kurkuminoid Total dan Flavonoid Total: Farmakope Herbal Indonesia Edisi 2 (2nd ed.). Jakarta: Kementerian Kesehatan Republik Indonesia.
- Kharat, M., Du, Z., Zhang, G. & McClements, D. J. (2017). Physical and Chemical Stability of Curcumin in Aqueous Solutions and Emulsions: Impact of pH, Temperature, and Molecular Environment. *Journal of Agricultural and Food Chemistry*; 65; 1525-1532. doi: 10.1021/acs.jafc.6b04815.
- Kusumo, N. N., & Mita, S. R. (2018). Review: Effect of Natural Binder on Paracetamol Granulation Results. *Farmaka*; 14; 228-235. doi: 10.24198/jf.v14i1.10777.
- Manju, S. & Sreenivasan, K. (2011). Conjugation of Curcumin onto Hyaluronic Acid Enhances its Aqueous Solubility and Stability. *Journal of Colloid and Interface Science*; 359; 318-325. doi: 10.1016/j.jcis.2011.03.071.
- Martemucci, G., Costagliola, C., Mariano, M., D'andrea, L., Napolitano, P. & D'Alessandro, A. G. (2022). Free Radical Properties, Source and Targets, Antioxidant Consumption and Health. *Oxygen*; 2; 48-78. doi: 10.3390/oxygen2020006.
- Martínez-Guerra, J., Palomar-Pardavé, M., Romero-Romo, M., Corona-Avendaño, S., Rojas-Hernández, A., & Ramírez-Silva, M. T. (2019). New Insights on The Chemical Stability of Curcumin in Aqueous Media at Different pH: Influence of The Experimental Conditions. *International Journal of Electrochemical Science*; 14; 5373-5385. doi: 10.20964/2019.06.24.
- Mehrabi, M., Gardy, J., Talebi, F. A., Farshchi, A., Hassanpour, A. & Bayly, A. E. (2023). An Investigation of The Effect of Powder Flowability on The Powder Spreading in Additive Manufacturing. *Powder Technology*; 413; 117-997. doi: 10.1016/j.powtec.2022.117997.
- Muflihah, Y. M., Gollavelli, G. & Ling, Y.-C. (2021). Correlation Study of Antioxidant Activity With Phenolic and Flavonoid Compounds in 12 Indonesian Indigenous Herbs. *Antioxidants*; 10; 1530. doi: 10.3390/antiox10101530.
- Nhu-Trang, T.-T., Nguyen, Q.-D., Cong-Hau, N., Anh-Dao, L.-T. & Behra, P. (2023). Characteristics and Relationships Between Total Polyphenol and Flavonoid Contents, Antioxidant Capacities, and The Content of Caffeine, Gallic Acid, and Major Catechins in Wild/Ancient and Cultivated Teas in Vietnam. *Molecules*; 28; 34-70. doi: 10.3390/molecules28083470.
- Nikolaeva, T. N., Lapshin, P. V., & Zagorskina, N. V. (2022). Method for Determining the Total Content of Phenolic Compounds in Plant Extracts with Folin-Denis Reagent and Folin-Ciocalteu Reagent: Modification and Comparison. *Russian Journal of Bioorganic Chemistry*; 48; 1519-1525. doi: 10.1134/S1068162022070214.
- Nurkhasanah, N., Sulistyani, N. & Ghifarizi, M. A. (2019). The Effect of Bengle (*Zingiber cassumunar* Roxb.) Rhizome Chloroform Extract on Nitric Oxide and Reactive Oxygen Intermediate Secretions in Vitro. *Ahmad Dahlan International Conference Series on Pharmacy and Health Science (ADICS-PHS 2019)*; 1; 100-104. doi: 10.2991/adics-phs-19.2019.9.
- Odinga, E. S., Waigi, M. G., Gudda, F. O., Wang, J., Yang, B., Hu, X., Li, S. & Gao, Y. (2020). Occurrence, Formation, Environmental Fate and Risks of Environmentally Persistent Free Radicals in Biochars. *Environment International*; 134; 105-172. doi: 10.1016/j.envint.2019.105172.
- Quispe, C., Herrera-Bravo, J., Javed, Z., Khan, K., Raza, S., Gulsunoglu-Konuskan, Z., Daştan, S. D., Sytar, O., Martorell, M., Sharifi-Rad, J. & Calina, D. (2022). Therapeutic Applications of Curcumin in Diabetes: A Review and Perspective. *BioMed Research International*; 2022; 1-14. doi: 10.1155/2022/1375892.

- Rachmawati, H., Novel, M. A., Ayu, S., Berlian, G., Tandrasasmita, O. M., Tjandrawinata, R. R. & Anggadiredja, K. (2017). The In Vitro–In Vivo Safety Confirmation of PEG-40 Hydrogenated Castor Oil as a Surfactant For Oral Nanoemulsion Formulation. *Scientia Pharmaceutica*; 85; 1-18. doi: 10.3390/scipharm85020018.
- Ramadhan, R., Tosepu, R., Phuwapraisirisan, P., Amirta, R., Phontree, K., Firdaus, Y. F. H., Abdulgani, N., Muttaqin, M. Z. & Saparwadi, S. (2022). Evaluation of Non-Timber Forest Products Used as Medicinal Plants From East Kalimantan (Indonesia) to Inhibit A-Glucosidase and Free Radicals. *Biodiversitas Journal of Biological Diversity*; 23; 1-8. doi: 10.13057/biodiv/d231102.
- Rangel-Yagui, C. de O., Pessoa Jr, A. & Tavares, L. C. (2005). Micellar Solubilization of Drugs. *Journal of Pharmaceutical Sciences*; 8; 147–163. doi: 10.1208/s12249-008-9057-5.
- Rowe, R. C., Sheskey, P. & Quinn, M. (2009). Castor Oil, Hydrogenated: *Handbook of Pharmaceutical Excipients Fifth Edition*. London: Libros Digitales-Pharmaceutical Press.
- Sadiq, I. Z. (2023). Free Radicals and Oxidative Stress: Signaling Mechanisms, Redox Basis For Human Diseases, and Cell Cycle Regulation. *Current Molecular Medicine*; 23; 13–35. doi: 10.2174/1566524022666211222161637.
- Sánchez-Bravo, P., Noguera-Artiaga, L., Martínez-Tomé, J., Hernández, F., & Sendra, E. (2022). Effect of Organic and Conventional Production on The Quality of Lemon “Fino 49.” *Agronomy*; 12; 9-80. doi: 10.3390/agronomy12050980.
- Sarabandi, K., Mahoonak, A. S., & Akbari, M. (2019). Physicochemical Properties and Antioxidant Stability Of Microencapsulated Marjoram Extract Prepared By Co - Crystallization Method. *Journal of Food Process Engineering*; 42; 1-12. doi: 10.1111/jfpe.12949.
- Sari, A. K. & Nurihardiyanti, N. (2023). Increasing the Solubility of Active Pharmaceutical Ingredients With the Micellar Solubilization Method. *Pharmaceutical Science Journal*; 3; 94–101. doi: 10.52031/pharse.v3i1.508.
- Sari, D. J. E. & Widiharti, W. (2021). Implementation of a Healthy Lifestyle as an Effort to Control Concomitant Diseases (COMORBID). *Indonesian Journal of Community Dedication in Health (IJCDH)*; 2; 30–33. doi: 10.30587/ijcdh.v2i01.3128.
- Schorsch, C., Wilkins, D. K., Jones, M. G. & Norton, I. (2001). Gelation of Casein-Whey Mixtures: Effects of Heating Whey Proteins Alone or in The Presence of Casein Micelles. *Journal of Dairy Research*; 68; 471–481. doi: 10.3168/jds.S0022-0302(04)73265-8.
- Sirivibulkovit, K., Nouanthavong, S., & Sameenoi, Y. (2018). Based DPPH Assay for Antioxidant Activity Analysis. *Analytical Sciences*; 34; 795–800. doi: 10.2116/analsci.18P014.
- Van, B., Abdalla, A. N., Algarni, A. S., Khalid, A., Zengin, G., Aumeeruddy, M. Z. & Mahomoodally, M. F. (2023). Zingiber officinale Roscoe (Ginger) and its Bioactive Compounds in Diabetes: A Systematic Review of Clinical Studies and Insight of Mechanism of Action. *Current Medicinal Chemistry*; 31; 887–903. doi: 10.2174/0929867330666230524122318.
- Veurink, G., Perry, G., & Singh, S. K. (2020). Role of Antioxidants and a Nutrient Rich Diet in Alzheimer’s Disease. *Open Biology*; 10; 78-84. doi: 10.1098/rsob.200084.
- Zamzani, I. & Triadisti, N. (2021). Limpasu Pericarpium: An Alternative Source of Antioxidant From Borneo With Sequential Maceration Method. *Jurnal Profesi Medika: Jurnal Kedokteran dan Kesehatan*; 15; 60-68. doi: 10.33533/jpm.v15i1.2820.
- Zheng, B. & McClements, D. J. (2020). Formulation of More Efficacious Curcumin Delivery Systems Using Colloid Science: Enhanced Solubility, Stability, and Bioavailability. *Molecules*; 25; 1-25. doi: 10.3390/molecules25122791.
- Zheng, B., Zhang, Z., Chen, F., Luo, X. & McClements, D. J. (2017). Impact of Delivery System Type on Curcumin Stability: Comparison of Curcumin Degradation in Aqueous Solutions, Emulsions, and Hydrogel Beads. *Food Hydrocolloids*; 71; 187–197. doi:10.1016/j.foodhyd.2017.05.022.



Analysis of Molecular Docking and Dynamics Simulation of Mahogany (*Swietenia macrophylla* King) Compounds Against the PLpro Enzyme SARS-COV-2

Lalu Sanik Wahyu Fadil Amrulloh^{1*}, Nuraini Harmastuti¹, Andri Prasetyo², Rina Herowati¹

¹Master Program of Pharmaceutical Science, Faculty of Pharmacy, Universitas Setia Budi, Surakarta, Indonesia

²Faculty of Pharmacy, Universitas Pancasila, Jakarta, Indonesia

*Corresponding author: sanik.lalu@gmail.com

Submitted: 10 August 2023

Revised: 10 December 2023

Accepted: 19 December 2023

Abstract

Background: Using natural ingredients as antivirals can be considered a treatment for SARS-CoV-2. One of the potential plants, mahogany (*Swietenia macrophylla* King), is widely used in various countries as an antiviral treatment. Paparin-like protease (PLpro) is an essential cysteine protease that regulates viral replication and interferes with the regulation of immune sensing. **Objective:** This study aims to predict which compounds in the mahogany plant have good affinity, patterns, and stability interaction against the target protein of SARS-CoV-2. **Methods:** The drug-likeness parameter using SwissADME was used to screen compounds that will be docked against PLpro using the Autodock program. The parameters observed in molecular docking analysis are the value of bond energy and interaction model to amino acid residues. The compounds in mahogany plants that have the best interactions were then analyzed using molecular dynamics simulation methods to determine the stability of their bonds based on the values of Root Mean Square Deviation (RMSD) and Root Mean Square Fluctuation (RMSF). **Results:** Twenty-two compounds met the drug-likeness requirements. Molecular docking analysis showed that the compounds predicted to have the best binding affinity and have an interaction pattern similar to natural ligands towards the molecular target of PLpro are 7-deacetoxy-7-oxogedunin and 3 β -hydroxy-stigmast-5-en-7-one. The molecular dynamics simulation results revealed that based on the RMSD and RMSF values, the compound 3 β -hydroxy-stigmast-5-en-7-one showed higher stability than 7-deacetoxy-7-oxogedunin. **Conclusion:** 3 β -hydroxy-stigmast-5-en-7-one and 7-deacetoxy-7-oxogedunin were predicted to have good interaction with PLpro; however, 3 β -hydroxy-stigmast-5-en-7-one showed the higher interaction stability.

Keywords: antiviral, mahogany, molecular docking, molecular dynamics simulation, SARS-CoV-2

How to cite this article:

Amrulloh, L. S. W. F., Harmastuti, N., Prasetyo, A. & Herowati, R. (2023). Analysis of Molecular Docking and Dynamics Simulation of Mahogany (*Swietenia macrophylla* King) Compounds Against the PLpro Enzyme SARS-COV-2. *Jurnal Farmasi dan Ilmu Kefarmasian Indonesia*, 10(3), 347-359. <http://doi.org/10.20473/jfiki.v10i32023.347-359>

INTRODUCTION

Coronavirus disease 2019 (Covid-19) is caused by Severe Acute Respiratory Syndrome Coronavirus 2 (SARS-CoV-2). This disease emerged in Hubei Province, China (Yu *et al.*, 2020). SARS-CoV-2 causes respiratory problems similar to those caused by the Severe Acute Respiratory Syndrome Coronavirus (SARS-CoV) in 2003 and the Middle East Respiratory Syndrome Coronavirus (MERS-CoV) in 2012. All three come from the Coronaviridae, a family of viruses that have an RNA genome with a single positive sense strand (Tu *et al.*, 2020). Globally, the weekly number of COVID-19 cases was from October 31 to November 6, 2022, with more than 2.1 million new cases reported. Weekly death toll, with around 9400 deaths reported. As of November 6, 2022, 629 million confirmed cases and 6.5 million deaths have been reported globally (WHO, 2022). According to data from the COVID-19 Handling Task Force, as of November 16, 2022, there were 6 million positive cases and 159 thousand deaths (Satgas Penanganan Covid-19, 2022).

Several treatment approaches have been made to inhibit SARS-CoV-2. Remdesivir can inhibit SARS-CoV-2 infection, as can nafamostat, which is a MERS-CoV inhibitor, which can prevent membrane fusion and inhibit SARS-CoV-2 infection (Wang *et al.*, 2020). The re-use of drugs, including antiviral agents (ivermectin, nitazoxanide, lopinavir, remdesivir, tocilizumab), supporting agents (azithromycin, corticosteroids, vitamin C, vitamin D), and vaccines, is being tried to meet the urgent demand against the COVID-19 pandemic (Chen *et al.*, 2022).

Apart from using synthetic antivirals, the use of natural ingredients as antivirals can also be considered as a treatment for SARS-CoV-2. A number of active compounds from natural products have shown potential antiviral activity (Septiana, 2020). One of them worthy of research is the mahogany plant (*Swietenia macrophylla* King). Mahogany belongs to the Meliaceae family. Mahogany is widely used in various countries as a treatment for antivirals. Toona sinensis leaves, which are also included in the Meliaceae family, have antiviral effects against SARS-CoV (Petrera, 2015). There are various compounds in mahogany, such as polyphenols, fatty acid esters, essential oils, steroids, lignans and limonoids (Moghadamtousi *et al.*, 2013). In general, polyphenols are believed to have various uses, such as antioxidants, anti-inflammatories, antivirals, and antibacterials (Mulu *et al.*, 2021). Limonoids, as triterpenoid derivatives, have activity as antiviral, antifungal, antibacterial, anticancer, and antimalarial

(Vardhan & Sahoo, 2020). As an antiviral, 3-hydroxy caruilignan C (3-HCL-C) isolated from *S. macrophylla* stems causes a decrease in protein and RNA levels, thereby interfering with hepatitis C virus replication (Musarra-Pizzo *et al.*, 2021). From various databases and references, 22 compounds contained in the mahogany plant have been collected. However, it is not yet known how the antiviral mechanism action of the mahogany plant. Studies are needed to determine which of these compounds play a role in antiviral activity and the target proteins of these compounds.

Drug development efforts can be carried out by molecular modelling or in silico tests, which play a role in designing, discovering, and optimizing bioactive compounds in the drug development process. The in silico test can be carried out by means of molecular docking, which functions to predict the activity of a compound in target cells. The docking will align the ligand into the target cell and produce a bond energy value indicating the amount of energy required to form the bond between the ligand and the receptor. The lower the bond energy, the stronger the bond. The stronger the link between the ligand and the receptor, the more active it is. (Kesuma *et al.*, 2018). It is now known that there are many potential targets for anti-SARS-CoV-2 work, one of which is PLpro (paparin-like protease), which functions to split polyprotein replication into non-structural proteins (Chen *et al.*, 2022). After carrying out molecular docking, proceed with Molecular Dynamics (MD) Simulations. The MD simulation aims to determine the stability of the ligand-receptor interaction; this is done because molecular docking has not been able to provide information regarding the stability of the ligand-receptor interaction in space and time (Dewi *et al.*, 2022).

This study will carry out an analysis of the molecular docking of compounds in mahogany plants that have been screened for drug-likeness as test ligands for the protein PLpro of the SARS-CoV-2 virus. Molecular docking was carried out using Autodock 4 software, the MGL tool, and Biovia Discovery Studio as visualization tools. Ligand-protein interactions and the best pattern of amino acid residues will be followed by MD simulation testing using Yasara software so that the stability value of the ligand-protein bond is obtained.

MATERIALS AND METHODS

Materials

The material used in this study was the SMILES code of the test ligand obtained from PubChem, which was made in a three-dimensional structure using the

VEGA ZZ application. The three-dimensional structure of the macromolecule, namely PLpro (PDB ID: 7QCG), was downloaded from the Protein Data Bank (RCSB PDB).

Tools

The tools used in this study were a set of TOSHIBA Dynabook B35/Y with Intel(R) Core(TM) i5-5200U Processor specifications, 8.0 Giga Byte RAM, 500 Giga Byte SSD hard disk, Intel(R) HD Graphics Graphics Card 5500, AutoDock 4.0, AutoDockTool, Biovia Discovery Studio, VEGA ZZ, Notepad++, SwissADME (<http://www.swissadme.ch/>), and YASARA Dynamics.

Method

Test ligand screening

The drug-likeness parameter of the mahogany plant compound was conducted using the SwissADME webserver (<http://www.swissadme.ch/>) to screen the compounds before the molecular docking analysis process. Canonical SMILES of mahogany plant compounds were obtained from PubChem. The Canonical SMILES code was copied and pasted into the "Enter a list of SMILES here" box, and the "Run!" button was clicked. The drug-likeness profile of the compound was carried out to determine whether a compound meets the requirements as an oral drug candidate or not (Daina *et al.*, 2017).

Preparation of the three-dimensional structure of the test ligand

The three-dimensional structure of the test ligands was created using the VEGA ZZ application. The first step was to copy the Canonical SMILES test ligand from PubChem and then paste it into Vega ZZ by selecting the Edit > Build > SMILES menu. The SMILES code obtained from PubChem was then pasted into the dialogue box that appears, then clicked Build. After that, select the Calculate > Charge & Potential menu, and a dialogue box will appear. In the Force Field section, select "AUTODOCK", and in the Charges section, select "Gasteiger", then click "Fix". Then, minimize it by choosing the Calculate > Ampp > Minimization menu. In the Minimization Steps box, enter 10,000 and then run. The three-dimensional structure obtained is then saved in the.pdb format for molecular anchoring; if it is still in the form of a two-dimensional structure, it must first be converted into a three-dimensional structure by clicking Edit > Coordinates > Convert to 3D.

Test ligand preparation

The preparation of the test ligand structures was carried out using AutoDockTools to add hydrogen atoms and charges to the ligands. First, open the three-

dimensional structure of the test ligand by selecting the File menu > Read molecule, then selecting Edit > Hydrogens > Add menu. After that, select "All Hydrogens", "noBondOrder", and "Yes" in the Add Hydrogens dialogue box that will appear. Then select the Edit menu again > Charges > Compute Gasteiger. The next step is to create a ligand file in the pdbqt format by selecting the Ligand > Input > Choose menu, selecting the prepared ligand file, and then selecting "Select Molecule for AutoDock4". Then select the Ligand menu > Torsion tree > Detect root to identify the ligand root. After that, select the Ligand > Torsion tree > Choose Root menu, then select the Ligand > Torsion tree > Choose Torsions > Done menu to identify the number of the torque. Then select Ligand > Torsion tree > Set Number of Torsions > Dismiss. Then select the Ligand menu > Output > Save as file with the pdbqt format.

Macromolecules download

The 3D structure of the receptor used, the PLpro protein (PDB ID: 7QCG) was downloaded from the RCSB PDB website (<https://www.rcsb.org/>). The 3D structure of the protein is downloaded in ".pdb" file format. The file is then saved in the work folder.

Macromolecular preparation

Macromolecule preparation was carried out using Biovia Discovery Studio. First of all, open the macromolecule file by selecting File > Open from the menu. Then pressed CTRL+H simultaneously so that the protein molecules appeared. Clicked Water > Delete to remove the water molecules. The next step is to separate the macromolecular complex into individual protein (receptor) and ligand files by clicking on Ligand Groups > selecting native ligand > Copy > Paste in the new Molecule Window, and then saving as (ligand name).pdb, the resulting ligand file is obtained. separated from the protein. After that, return to the initial molecule window and select Ligand Group > Delete, to remove natural ligands. Then select Hetatm > Delete to remove other residues (if any).

Then, the protein files that have been separated from their natural ligands are added hydrogen and cargo using AutoDockTools by selecting the menu File > Read Molecule > Edit > Hydrogens > Add. After that, select "Polar Only", "noBondOrder", and "Yes" in the Add Hydrogens dialogue box that will appear. Then select the Edit menu again > Charges > Add Kollman Charges. The next step is to create a protein file with the .pdbqt format, which will be used to determine the grid parameters, by selecting the Grid > Macromolecule > Choose menu, selecting the protein file that has been

prepared, then selecting "Ok" and save the file with the format name .pdbqt.

Furthermore, the preparation of the native ligand structure first opens the three-dimensional structure file of the native ligand, which has been separated from the protein by selecting the File > Read molecule menu, then selecting Edit > Hydrogens > Add menu. After that, select "All Hydrogens", "noBondOrder", and "Yes" in the Add Hydrogens dialogue box that will appear. Then select the Edit menu again > Charges > Compute Gasteiger. The next step is to create a ligand file in the .pdbqt format by selecting the Ligand > Input > Choose menu, selecting the prepared ligand file, and then selecting "Select Molecule for AutoDock4". Then select the Ligand menu > Torsion tree > Detect root to identify the ligand root. After that, select the Ligand > Torsion tree > Choose Root menu, then select the Ligand > Torsion tree > Choose Torsions > Done menu to identify the number of the torque. Then select Ligand > Torsion tree > Set Number of Torsions > Dismiss. Then select the Ligand menu > Output > Save as file with the .pdbqt format. The .pdbqt files of macromolecules and ligands, the autodock4.exe and autogrid4.exe application files, and the AD4.1_bound.dat files (obtained from <https://autodocksuite.scripps.edu/force-fields/>) are placed in the same folder.

Molecular tethering method validation

In this validation process, we will compare the conformation of the natural ligand to the receptor in the experimental crystallographic structure with the conformation of the natural ligand that is redocked to the receptor using AutoDockTools by setting the Grid box x, y, z, centre x, y, z, spacing by default. The results of this comparison are expressed by the root mean square deviation (RMSD) value. The docking method is said to be valid if the RMSD value is $\leq 2 \text{ \AA}$. If the RMSD value obtained is greater than 2 \AA , then the procedure used is invalid, so the Grid box x, y, z, and centre x, y, z spacing values are adjusted manually until $\text{RMSD} \leq 2 \text{ \AA}$ is obtained.

Molecular docking process

The molecular docking process was carried out using AutoDock4.0 (AD4.0) and AutoDockTools (ADT). Protein and ligand structures that have been optimized separately are stored in the same folder. Before carrying out the docking process, a grid parameter file is first prepared with the following steps: select Grid > Macromolecule > Open: protein file format .pdbqt. Then select the menu Grid > Set Map

Types > Open: ligand file (native ligand during the Validation process) format .pdbqt. Then select the Grid > Grid box menu, then select the Center > Center on ligand menu (for Default validation) and set the size x, y, z, centre x, y, z, and spacing in the Grid Options dialogue box that will appear (Following the Grid value Validation box for test ligands). Then select the File menu > Close saving current, then select the Grid > Output > Save GPF menu and save it in the .gpf format. You need to pay attention to naming the file because wrong naming will not make docking work. The next step is to run Autogrid by clicking the Run menu > Run AutoGrid, then on "Program Pathname" select the file "autogrid4.exe" while on "Parameter Filename" select the file with the ".gpf" format earlier, then click "Launch" and wait for the process walk to finish. After the autogrid process is complete, the next step is to prepare a docking parameter file with the following steps, selecting the Docking > Macromolecule > Set Rigid Filename menu and selecting a protein file with the .pdbqt format. Then select the Docking menu > Ligand > Choose > Select the ligand > Select Ligand > Accept. Next, determine the docking parameters by selecting the Docking menu > Search Parameters > Genetic Algorithm, setting the Number of GA Runs to 100, and setting the Population Size to 150 in the dialogue box that will appear, then clicking Accept. After that, select the Docking menu > Docking Parameters > Accept. Then select the Docking menu > Other Options > AutoDock4.2 Parameters > a Set Autodock4.2 Options box will appear > in the Include Parameter_file in dpf click "Yes" > in the Enter Parameter_File section, it is written "AD4.1_bound.dat". Then select the Docking > Output > Lamarckian GA menu and save it in the .dpf format. The next step is to run Autodock by clicking the Run menu > Run AutoDock, then on "Program Pathname" select the file "autodock4.exe" while on "Parameter Filename" select the file with the ".dpf" format earlier, then click Launch and wait for the process to run until finished. The docking results obtained were then analyzed and visualized using the Biovia Discovery Studio.

Molecular dynamics simulation process

The two best test ligands that have the smallest bond-free energy values and amino acid residues that are similar to the native ligands (If a compound has the best or smallest bond-free energy values but does not interact with amino acid residues that are similar to the native ligand, then the compound has the best interaction pattern and cannot be said to have the same activity as

natural ligands) are followed by MD simulation tests. The MD simulation process is carried out using YASARA Dynamics. The structures of the test-protein ligand complex and the native-protein ligand complex are placed in the same folder. Before running the program, set the script to "md_run.mcr" with 0.9% NaCl, pH 7.4, at a temperature of 298K, and the simulation duration is 20 ns and uses ForceField AMBER14 (Parihar *et al.*, 2022; Shree *et al.*, 2022). After that, proceed with running the YASARA program. Then select the menu Options > Macro & Movie > Set Target (select the target you want to analyze in .pdb format). Next, re-select the menu Options > Macro & Movie > Play Macro > md_run.mcr > OK (pre-set script) and wait for the process to run until it finishes automatically. After the process is complete, an analysis of the ligand-protein is carried out by selecting the Options menu > Macro & Movie > Set Target (selecting the target to be analyzed in .pdb format). Then select Option > Macro & Movie > Play Macro > md_analyze.mcr > OK, wait for the process to run until it's finished. The data obtained were analyzed for RMSD and RMSF values.

RESULTS AND DISCUSSION

Test ligand screening

Drug-likeness screening qualitatively assesses the possibility of a molecule becoming an oral drug in terms of bioavailability using the SwissADME website. At SwissADME, there are five Drug-likeness filters, namely Lipinski, Ghose, Veber, Egan, and Muegge. In this study, the Lipinski filter was chosen because Lipinski analyzed 2,245 drugs from the World Drugs Index database, and this filter is known as Lipinski's rule-of-five (Lipinski *et al.*, 1997).

Based on Table 1, it can be seen that there were 22 compounds tested for drug-likeness that were predicted to have the opportunity to become oral drugs, although of the 22 compounds, there were some that violated or did not meet the requirements. However, this is tolerable because each compound only violates one rule. According to Lipinski's rules, in general, a drug can be administered in oral if it does not violate more than one criterion (Lipinski *et al.*, 1997). Drug-likeness is based on oral drugs because oral administration of drugs is one of the most commonly used methods in clinical practice. Oral medications can be taken easily by patients, do not

require special medical assistance, and usually provide greater convenience compared to other routes of administration (Santos *et al.*, 2016).

Preparation of three-dimensional structures and preparation of test ligands and macromolecules

The canonical SMILES code of 22 compounds in mahogany obtained from Pubchem was then made into a three-dimensional structure using the VegaZZ application. The three-dimensional structure of the target protein was obtained from the Protein Data Bank with a PDB code and 7QCG 1.75 Å (PLpro) resolution. This macromolecule meets the criteria, namely having a three-dimensional structure obtained from crystallographic X-ray results with a resolution of < 3 Å (Mukherjee *et al.*, 2010; Sándor *et al.*, 2010). The macromolecule used is already complex with its natural ligands, so it is easy to determine the active side of the macromolecule.

Molecular docking method validation

Method validation was carried out to determine whether the molecular docking method used was reliable or valid by comparing the crystallographic conformation of the natural ligand and the natural ligand that was redocked against the target protein using AutodockTools. The validation process needs to determine the grid box or central coordinates, where the interaction of the ligand and protein is known as the active site of the protein. The centre of the grid box is generally determined based on the centre of mass of the naturally occurring ligand, while the dimensions of the grid box are based on the size of the ligand and the binding site on the protein that contains the essential amino acids for the protein's activity. The centre and gridbox dimensions of the macromolecules used in this study can be seen in Table 2. Parameters observed in the validation process were RMSD values and interactions that occurred between the crystallographic ligands and the redocked ligands with residues of target protein amino acids. The smaller the RMSD value, the closer the ligand position is to the natural ligand conformation. An RMSD value < 2 Å indicates that the error of the calculation results is smaller, so that the calculation can be said to be more accurate, whereas an RMSD value > 2 Å indicates that the deviation from the calculation results is more remarkable so that the docking results obtained cannot be used as a reference (Mukherjee *et al.*, 2010; Sándor *et al.*, 2010).

Table 1. Drug-likeness prediction results (Moghadamtousi *et al.*, 2013) & (<http://ijah.apps.cs.ipb.ac.id/>)

Compound	Lipinski Rules Parameter				Results
	Molecular weight ≤ 500	MLOGP ≤ 4,15	N or O ≤ 10	NH or OH ≤ 5	
Secomahoganin	x	✓	✓	✓	Yes
12α-Acetoxywietenphragmin D	x	✓	x	✓	No
12α-Acetoxywietenphragmin C	x	✓	x	✓	No
Swietenialide D	x	✓	x	✓	No
7-deacetoxy-7-oxogedunin	✓	✓	✓	✓	Yes
6-O-Acetylswietenphragmin E	x	✓	x	✓	No
Swietenitin A	x	✓	x	✓	No
Swietenitin B	x	✓	x	✓	No
Swietenitin C	x	✓	x	✓	No
Swietenitin D	x	✓	x	✓	No
Swietenitin E	x	✓	x	✓	No
Swietenitin F	x	✓	x	✓	No
Swietenitin G	x	✓	x	✓	No
Swietenitin H	x	✓	x	✓	No
Swietenitin I	x	✓	x	✓	No
Swietenitin J	x	✓	x	✓	No
Swietenitin K	x	✓	x	✓	No
Swietenitin L	x	✓	x	✓	No
Swietenitin M	x	✓	x	✓	No
Swietenolide	✓	✓	✓	✓	Yes
Swietenine	x	✓	✓	✓	Yes
Swietenolide diacetate	x	✓	✓	✓	Yes
3β,6-Dihydroxydihydrocarapin	✓	✓	✓	✓	Yes
Augustineolide	x	✓	x	✓	No
Andirobin	✓	✓	✓	✓	Yes
Proceranolide	✓	✓	✓	✓	Yes
3,6-O,O-diacetylswietenolide	x	✓	✓	✓	Yes
Swietenolide monohydrate	x	✓	✓	✓	Yes
Swietemacrophine	x	✓	x	✓	No
1-O-Acetylkhayanolide B	x	✓	x	✓	No
Epoxyfebrinin B	x	✓	x	✓	No
Roxburghiadiol A	✓	x	✓	✓	Yes
β-Sitostenone	✓	x	✓	✓	Yes
3β-hydroxy-stigmast-5-en-7-one	✓	x	✓	✓	Yes
β-Sitosterol	✓	x	✓	✓	Yes
Stigmasterol	✓	x	✓	✓	Yes
γ-Himachalene	✓	x	✓	✓	Yes
Cadina-1,4-diene	✓	x	✓	✓	Yes
Swietemacrophyllanin	✓	✓	✓	x	Yes
Catechin	✓	✓	✓	✓	Yes
Epicatechin	✓	✓	✓	✓	Yes
Scopoletin	✓	✓	✓	✓	Yes
3-Hydroxy Caruillignan C	✓	✓	✓	✓	Yes

Information: Yes = Meets the requirements (violated 1 rule), No = Does not meet the requirements (violated > 1 rule), ✓ = complies with Lipinski's rule, ✗ = does not comply with Lipinski's rule

Table 2. Gridbox parameters

Macromolecular Code	Gridbox					
	Center			Dimensions (Å)		
	X	Y	Z	X	Y	Z
7QCG	69,93	28,744	-29,08	40	40	40

Table 3. Redocking result from RMSD value

Target Protein Name	Natural ligands	PDB code	RMSD (Å)	Condition
PLpro	AKOS003853619	7QCG	1.391	< 2 Å

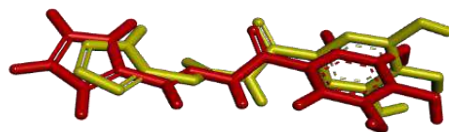


Figure 1. Crystallographic (red) and Redocked (yellow) ligand overlay results

Table 4. Redocking result from RMSD value

Compound	Bond Energy (kcal/mol)	Amino Acid Residues Hydrogen Bonds	Involved in Interactions Besides Hydrogen Bonds
AKOS003853619 (native ligand)	-4,32	Met206, Ser170, Arg166	Gln174, Met208, Tyr207, Arg183, Leu199, Glu203, Val202
7-Deacetoxy-7-oxogedunin	-7,55	Arg166 , Lys232	Val202, Gln174, Ser170, Met208, Phe216, Leu185, Tyr207, Leu199, Arg183, Met206, Glu203
3β-hydroxy-stigmast-5-en-7-one	-7,36	-	Tyr171, Gln174, Glu203 , Leu185, Lys232, Leu199, Tyr207, Met208, Met206, Val202, Arg166, Ser170, Glu167

Bold: similarity of amino acids interacting with natural ligands.

Based on the RMSD values and the overlay of the redocking results of the four natural ligands on their target proteins in Table 3 and Figure 1, it can be seen that the positions of the redocked ligands are close to those of the crystallographic ligands and occupy the same active sites because they interact with amino acids, which also interact with the crystallographic ligands. The redocking process is important because it helps validate the docking method and assess its accuracy. In molecular docking, the process of redocking occurs when the ligand (molecule under test) is placed back into the active site of the target protein after calculating its initial energy and placement. If the redocking ligand approaches the crystallographic ligand position, occupies the same active position, and interacts with amino acids that also interact with crystallographic ligands, this indicates consistency between the docking results and the crystallographic structure (de Oliveira *et al.*, 2022; Venkatesh, 2022). These results suggest that the docking method used is valid and that the protein and ligand docking processes can be carried out using AutodockTools.

Analysis of molecular docking results

Based on this study, 22 compounds in the mahogany plant were tethered to the target protein using the molecular docking method, namely AutodockTools.

Molecular docking aims to predict the binding mode and affinity of a small molecule for the active site of a particular target protein, and the result is a value that describes the bond-free energy, i.e., the amount of energy required by the ligand to form a bond with the receptor (Guedes *et al.*, 2013). Evaluation of the test ligand in molecular docking involves assessing a number of factors, including the free bond energy and the similarity of the amino acid residue to the natural ligand. These two factors play a role in the selection of ligands that have the potential to bind specifically and effectively to the target protein. Bond energy is one of the most critical factors in determining the stability of the ligand-receptor complex (de Oliveira *et al.*, 2022). Lower free bond energy values tend to be better at molecular docking. The lower the free bond energy value between the target molecule and the ligand, the more stable the bond complex is (Kurczab, 2017). The similarity of the amino acid residues of the test ligands with the natural ligands in the target protein can increase the chances of producing, suitable binding complexes. This is because the binding of natural ligands to the target protein is determined by specific interactions between the ligand and amino acid residues in the active site of the protein (Wu & Huang, 2023).

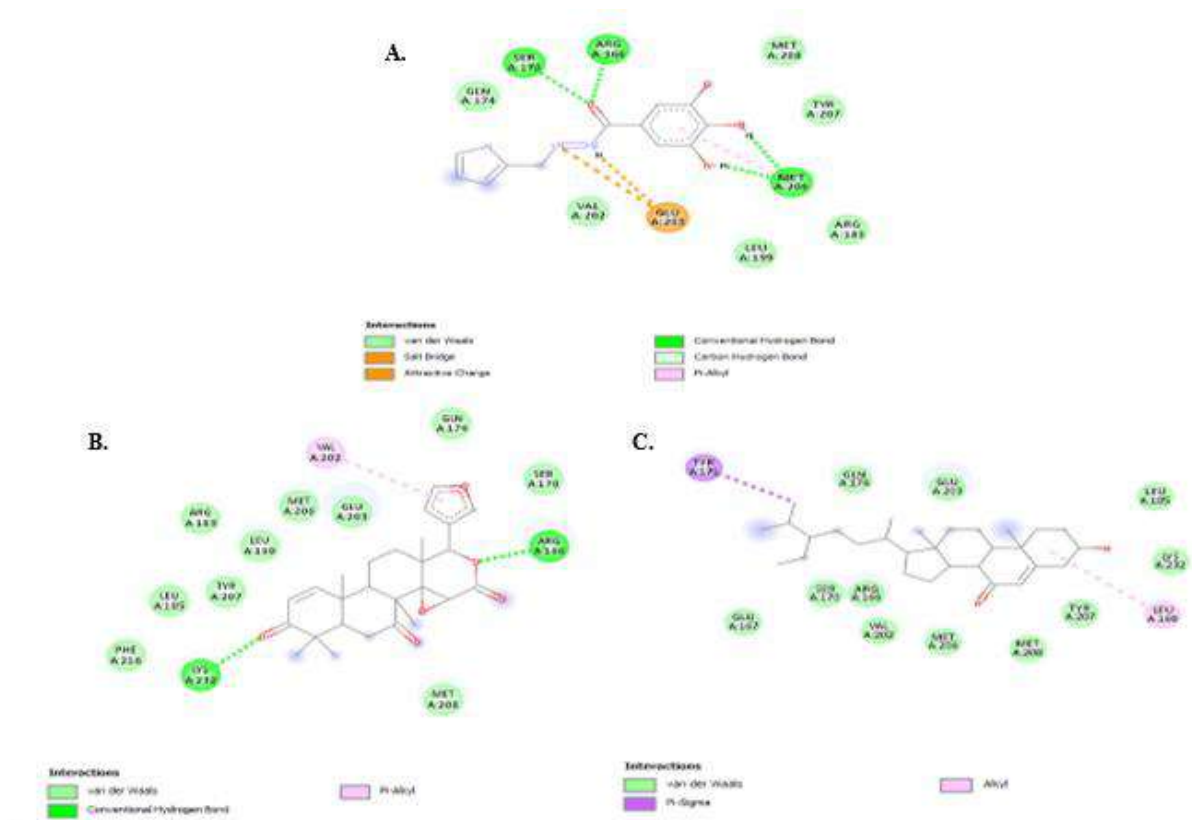


Figure 2. Interaction diagram of the test ligand compared to the natural ligand; (A) AKOS003853619 (natural ligand), (B) 7-Deacetoxy-7-oxogedunin, and (C) 3β-hydroxy-stigmast-5-en-7-one

Based on Table 4, two compounds have lower bond energies and interact with amino acid residues that are similar to natural ligands. AKOS003853619, which is a natural inhibitor and ligand of 7QCG, interacts with amino acid residues present on the active side through hydrogen bonds, van der Waals bonds, π -alkyl bonds, and salt bridges (Figure 2). According to Ewert *et al.* (2022), natural ligands in 7QCG form hydrogen bonds with Arg166, Ser170, and Met206 and form additional side chains with Gln174. The interaction of the Glu203 side chain achieves further stabilization. In the context of protein structure, the number associated with an amino acid, such as "Glu203", refers to the position of that amino acid in the protein sequence. This number is used to identify and refer to specific amino acids in protein structures, especially when discussing their functional properties or locations (Pulido *et al.*, 2014).

Compound 7-deacetoxy-7-oxogedunin has the lowest bond-free energy value in PLpro protein, followed by 3β-hydroxy-stigmast-5-en-7-one. The values of the two test ligands were smaller when compared to AKOS003853619 (Table 4) because there were more amino acid residues that interacted with the two test ligands than with the natural ligands. Compound 7-deacetoxy-7-oxogedunin has a smaller

free bond energy value compared to 3β-hydroxy-stigmast-5-en-7-one because 7-deacetoxy-7-oxogedunin has the same amino acid residue as the natural ligand, while 3β-hydroxy-stigmast-5-en-7-one lacks one residue similar to that of the natural ligand (Table 4).

Based on the results of molecular docking, the two best test ligands on the target protein have the potential as anti-SARS-CoV-2 candidates because these test ligands interact with the identical amino acid residues as the natural ligands of the target protein. The results of molecular docking indicated that several compounds from the mahogany plant had interactions with the tested molecular targets. Some of them have better free bond energy values than natural ligands. A compound can be known to have activity against a target protein by observing two parameters, namely bond energy and interaction pattern. If a compound has the best bond energy value but does not interact with amino acid residues that are similar to natural ligands, then the compound does not have the best interaction pattern and cannot be said to have the same activity as natural ligands (Salem *et al.*, 2023). Next, the two best test ligands will be subjected to MD simulation tests to find

out whether the tested ligands have good bond stability with macromolecules compared to natural ligands.

Analysis of molecular dynamics simulation results

Based on this study, two compounds in the mahogany plant were tethered to the target protein using the MD simulation method, namely YASARA Dynamics. MD simulation aims to study the movement and interaction of atoms in a molecular system. These simulations provide a deeper understanding of the physical and chemical properties of molecules, including their structure, stability, dynamics, and reactivity. The stability of the ligand-protein bond can be determined by calculating the RMSD and RMSF values (Patel *et al.*, 2021). Prior to the start of the analysis, the simulation conditions were set with 0.9% NaCl, pH 7.4, at a temperature of 298K, and the duration of the simulation was 20 ns. Setting 0.9% NaCl, pH 7.4, at 298K is often used in laboratory practice to try to replicate environmental conditions similar to those of

the human body. A simulation time of 20 ns can provide initial insight into the stability of the RMSD and RMSF (Parihar *et al.*, 2022; Shree *et al.*, 2022).

RMSD analysis involves a comparison of the conformational change of the simulated system with the initial or experimental structure. Monitoring RMSD over time makes it possible to assess system stability and identify periods of equilibrium and fluctuation. Higher RMSD values indicate more significant structural deviation from the reference structure, indicating increased flexibility or conformational changes. RMSF measures the flexibility or local mobility of individual atoms or residues in a biomolecular system during an MD simulation. It provides information about regions that undergo significant conformational changes or exhibit high flexibility. Atoms with a low RMSF show stability and a lack of fluctuation, while atoms with a high RMSF show greater flexibility or movement (Wu *et al.*, 2022).

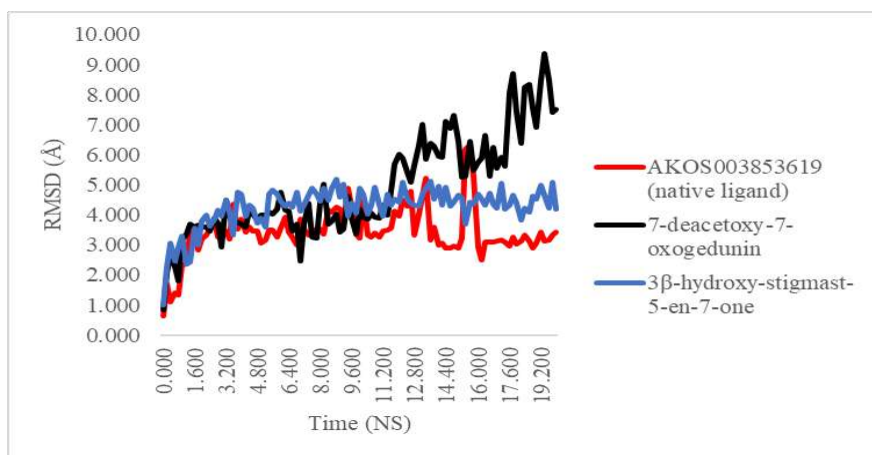


Figure 3. Comparison of RMSD values between native ligand (red), 7-deacetoxy-7-oxogedunin (black), and 3β-hydroxy-stigmast-5-en-7-one (blue)

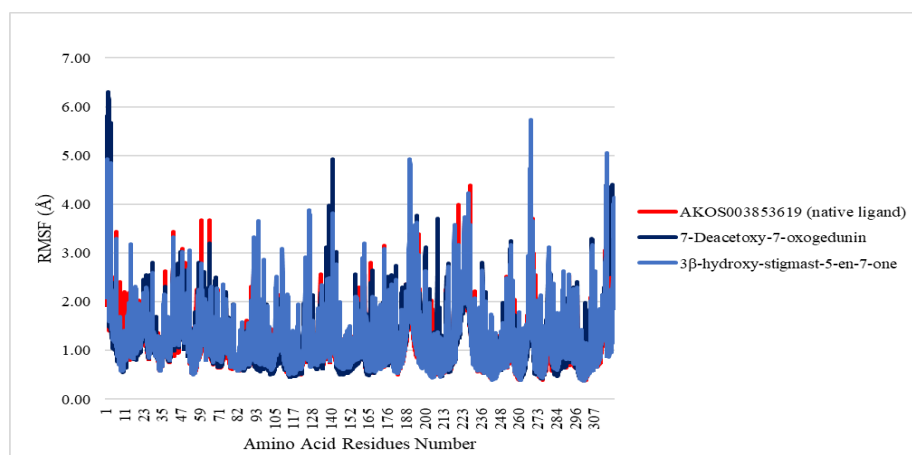


Figure 4. Comparison of RMSF values between AKOS003853619 (red), 7-Deacetoxy-7-oxogedunin (black), and 3β-hydroxy-stigmast-5-en-7-one (blue). (amino acid residue number = Met206, Ser170, Arg166, Gln174, Met208, Tyr207, Arg183, Leu199, Glu203, and Val202)

Table 5. Redocking result RMSD

	Average (Å)		
	Native Ligand	7-deacetoxy-7-oxogedunin	3β-hydroxy-stigmast-5-en-7-one
RMSD (Å)	3.423 ± 0.833	4.902 ± 1.697	4.250 ± 0.684
RMSF (Å)	1.182 ± 0.668	1.230 ± 0.727	1.247 ± 0.678

CONCLUSION

Based on Figure 3, the natural protein-ligand complex is more stable than 7-deacetoxy-7-oxogedunin and 3β-hydroxy-stigmast-5-en-7-one. This result can also be proven by the RMSD average value of the natural ligand, which is smaller than 7-deacetoxy-7-oxogedunin and 3β-hydroxy-stigmast-5-en-7-one (Table 5). Based on the results of the graphs and averages, it can be seen that the stability of the 3β-hydroxy-stigmast-5-en-7-one ligand with the PLpro protein is close to the stability of the bond of the natural protein-ligand complex. Meanwhile, the graph of 7-deacetoxy-7-oxogedunin began to increase at 11 ns, which means that the stability of the bond decreased. If the RMSD value is below 5 Å (Angstrom), it can be said to be a relatively stable value in molecular dynamics simulations. In contrast, if it is above 5 Å, it indicates significant conformational changes and large structural changes and means low stability (Rudnev *et al.*, 2022). The flexibility of the structure of each compound can influence conformational changes over time. Compounds with stable and well-defined structures throughout the simulation are likely to have better stability. The presence of intermolecular forces involved, such as hydrogen bonds, van der Waals interactions, and electrostatic interactions, can also influence the stability and bond energy values. High RMSD values can be affected by various conditions, such as temperature and pH, and also by interactions between the ligand-protein; this can change the structural conformation of the ligand-protein bond so that the stability becomes poor (Kordzadeh & Saadatabadi, 2022; Oliwa & Shen, 2015). The lower the RMSD value, the more stable the bond between the ligand and the protein, and it shows that the two structures (natural ligand and 3β-hydroxy-stigmast-5-en-7-one) are more similar to each other (Guterres & Im, 2020).

Based on Figure 4, the test ligands 7-deacetoxy-7-oxogedunin and 3β-hydroxy-stigmast-5-en-7-one have RMSF graphs that are almost similar to the test ligands. The natural protein-ligand complexes were more stable than the tested ligands, as indicated by the lower RMSF values of natural ligands than 7-deacetoxy-7-

oxogedunin and 3β-hydroxy-stigmast-5-en-7-one (Table 5). The RMSF value will outline the conformational shifts of each amino acid residue, which gives an idea of its flexibility. The lower the RMSF value, the more stable the positions of the ligands and amino acids are (Elfita *et al.*, 2022). Based on the RMSF results, the amino acid residues of natural ligands such as Met206, Ser170, Arg166, Gln174, Met208, Tyr207, Arg183, Leu199, Glu203, and Val202 did not change and remained stable. Likewise, the amino acid residues in the test ligands 7-deacetoxy-7-oxogedunin and 3β-hydroxy-stigmast-5-en-7-one were similar to the natural ligands, did not change and remained stable. Docking and MD results may differ because docking only evaluates binding energy or binding affinity. MD, on the other hand, stresses the ligand-protein complex's long-term stability (Chen, 2014).

ACKNOWLEDGEMENT

Based on the research that has been done, it can be concluded that 3β-hydroxy-stigmast-5-en-7-one and 7-deacetoxy-7-oxogedunin were predicted to have good interaction with PLPro. Compound 3β-hydroxy-stigmast-5-en-7-one showed higher interaction stability, so it is expected to maintain a better inhibitory effect of PLpro than 7-deacetoxy-7-oxogedunin.

AUTHOR CONTRIBUTIONS

Conceptualization, L. S. W. F. A., N. H., A. P., R. H.; Methodology, L. S. W. F. A., N. H., A. P., R. H.; Software, L. S. W. F. A., N. H., A. P., R. H.; Validation, L. S. W. F. A., N. H., A. P., R. H.; Formal Analysis, L. S. W. F. A., N. H., A. P., R. H.; Investigation, L. S. W. F. A., N. H., A. P., R. H.; Resources, L. S. W. F. A., N. H., A. P., R. H.; Data Curation, L. S. W. F. A., N. H., A. P., R. H.; Writing - Original Draft, L. S. W. F. A., N. H., A. P., R. H.; Writing - Review & Editing, L. S. W. F. A., N. H., A. P., R. H.; Visualization, L. S. W. F. A., N. H., A. P., R. H.; Supervision, L. S. W. F. A., N. H., A. P., R. H.; Project Administration, L. S. W. F. A., N. H., A. P., R. H.; Funding Acquisition, L. S. W. F. A., N. H., A. P., R. H.

FUNDING STATEMENT

This research did not receive any specific grant from funding agencies in the public, commercial, or not for profit sectors.

CONFLICT OF INTEREST

The authors declared no conflict of interest.

REFERENCES

- Chen, Y.-C. (2014). Beware of docking!. *Trends in Pharmacological Sciences*; 36; 1–18. doi: 10.1016/j.tips.2014.12.001.
- Chen, T.-H., Tsai, M.-J., Chang, C.-S., Xu, L., Fu, Y.-S. & Weng, C.-F. (2022). The Exploration of Phytocompounds Theoretically Combats SARS-CoV-2 Pandemic Against Virus Entry, Viral Replication and Immune Evasion. *Journal of Infection and Public Health*; 16; 1–39. doi: 10.1016/j.jiph.2022.11.022.
- Daina, A., Michielin, O. & Zoete, V. (2017). SwissADME: a Free Web Tool to Evaluate Pharmacokinetics, Drug-Likeness and Medicinal Chemistry Friendliness of Small Molecules. *Scientific Reports*; 7; 1–13. doi: 10.1038/srep42717.
- de Oliveira, T. A., Medaglia, L. R., Maia, E. H. B., Assis, L. C., de Carvalho, P. B., da Silva, A. M. & Taranto, A. G. (2022). Evaluation of Docking Machine Learning and Molecular Dynamics Methodologies for DNA-Ligand Systems. *Pharmaceuticals*; 15; 1–15. doi: 10.3390/ph15020132.
- Dewi, R. S., Anggraeni, A., Bahti, H. H., Yusuf, M., Hardianto, A. & Mutholib, A. (2022). Simulasi Dinamika Molekuler Ligan Disedokurbutil ditiofosfat (DSBDTP) untuk Ekstraksi Logam Tanah Jarang. *SainsMath: Jurnal MIPA Sains Terapan*; 1; 1–8.
- Elfita, L., Apriadi, A., Supandi, S. & Dianmurdedi, S. (2022). Studi Penambatan Molekuler dan Simulasi Dinamika Molekuler Senyawa Turunan Furanokumarin terhadap Reseptor Estrogen Alfa (ER- α) Sebagai Anti Kanker Payudara. *Jurnal Sains Farmasi & Klinis*; 9; 255–264. doi: 10.25077/jsfk.9.3.255-264.2022.
- Ewert, W., Günther, S., Miglioli, F., Falke, S., Reinke, P. Y. A., Niebling, S., Günther, C., Han, H., Srinivasan, V., Brognaro, H., Lieske, J., Lorenzen, K., Garcia-Alai, M. M., Betzel, C., Carcelli, M., Hinrichs, W., Rogolino, D. & Meents, A. (2022). Hydrazones and Thiosemicarbazones Targeting Protein-Protein-Interactions of SARS-CoV-2 Papain-like Protease. *Frontiers in Chemistry*; 10; 1–13. doi: 10.3389/fchem.2022.832431.
- Guedes, I. A., de Magalhães, C. S., & Dardenne, L. E. (2013). Receptor–ligand Molecular Docking. *Biophysical Reviews*; 6; 75–87. doi: 10.1007/s12551-013-0130-2.
- Guterres, H. & Im, W. (2020). Improving Protein-Ligand Docking Results with High-Throughput Molecular Dynamics Simulations. *Journal of Chemical Information and Modeling*; 60; 2189–2198. doi: 10.1021/acs.jcim.0c00057.
- Kesuma, D., Siswando, S., Purwanto, B. T. & Hardjono, S. (2018). Uji In Silico Aktivitas Sitotoksik dan Toksisitas Senyawa Turunan N-(Benzoil)-N'- Feniltiourea Sebagai Calon Obat Antikanker. *JPSCR: Journal of Pharmaceutical Science and Clinical Research*; 3; 1-11. doi: 10.20961/jpscr.v3i1.16266.
- Kordzadeh, A. & Saadatabadi, A. R. (2022). Effects of the Temperature and the pH on the Main Protease of Sars-Cov-2: A Molecular Dynamics Simulation Study. *Biointerface Research in Applied Chemistry*; 12; 7239–7248. doi: 10.33263/BRIAC126.72397248.
- Kurczab, R. (2017). The Evaluation of QM/MM-Driven Molecular Docking Combined with MM/GBSA Calculations as a Halogen-Bond Scoring Strategy. *Acta Crystallographica Section B: Structural Science, Crystal Engineering and Materials*; 73; 188–194. doi: 10.1107/S205252061700138X.
- Lipinski, C. A., Lombardo, F., Dominy, B. W. & Feeney, P. J. (1997). Experimental and Computational Approaches to Estimate Solubility and Permeability in Drug Discovery and Development Settings. *Advanced Drug Delivery Reviews*; 23; 3–25. doi: 10.1016/S0169-409X(96)00423-1.
- Moghadamtousi, S. Z., Goh, B. H., Chan, C. K., Shabab, T. & Kadir, H. A. (2013). Biological Activities and Phytochemicals of *Swietenia macrophylla* King. *Molecules*; 18; 10465–10483. doi: 10.3390/molecules180910465.
- Mukherjee, S., Balius, T. E., & Rizzo, R. C. (2010). Docking Validation Resources: Protein Family and Ligand Flexibility Experiments. *Journal of Chemical Information and Modeling*, 50(11), 1986–2000. <https://doi.org/10.1021/ci1001982>
- Mulu, A., Gajaa, M., Woldekidan, H. B. & Wmariam, J. F. (2021). The Impact of Curcumin Derived Polyphenols on the Structure and Flexibility

- COVID-19 Main Protease Binding Pocket: A Molecular Dynamics Simulation Study. *PeerJ*; 9; 1–16. doi: 10.7717/peerj.11590.
- Musarra-Pizzo, M., Pennisi, R., Ben-Amor, I., Mandalari, G. & Sciortino, M. T. (2021). Antiviral Activity Exerted by Natural Products against Human Viruses. *Viruses*; 13; 1-30. doi: 10.3390/v13050828.
- Oliwa, T. & Shen, Y. (2015). cNMA: A Framework of Encounter Complex-Based Normal Mode Analysis to Model Conformational Changes in Protein Interactions. *Bioinformatics*; 31; i151–i160. doi: 10.1093/bioinformatics/btv252.
- Parihar, A., Sonia, Z. F., Akter, F., Ali, M. A., Hakim, F. T. & Hossain, M. S. (2022). Phytochemicals-Based Targeting RdRp and Main Protease of SARS-CoV-2 using Docking and Steered Molecular Dynamic Simulation: A promising Therapeutic Approach for Tackling COVID-19. *Computers in Biology and Medicine*; 145; 1-13. doi: 10.1016/j.compbiomed.2022.105468.
- Patel, A. H., Patel, R. B., Memon, M. J., Patel, S. S., Desai, S. A. & Meshram, D. B. (2021). Docking, Binding Free Energy Estimation, and MD Simulation of Newly Designed CQ and HCQ Analogues Against the Spike-ACE2 Complex of SARS-CoV-2. *International Journal of Quantitative Structure-Property Relationships*; 6; 77–89. doi: 10.4018/IJQSPR.2021100105.
- Petrera, E. (2015). Antiviral and Immunomodulatory Properties of Meliaceae Family. *Journal of Biologically Active Products from Nature*; 5; 241–254. doi: 10.1080/22311866.2015.1081569.
- Pulido, R., Baker, S. J., Barata, J. T., Carracedo, A., Cid, V. J., Chin-Sang, I. D., Davé, V., den Hertog, J., Devreotes, P., Eickholt, B. J., Eng, C., Furnari, F. B., Georgescu, M.-M., Gericke, A., Hopkins, B., Jiang, X., Lee, S.-R., Lösche, M., Malaney, P., ... & Leslie, N. R. (2014). A Unified Nomenclature and Amino Acid Numbering for Human PTEN. *Science Signaling*; 7; 1-10. doi: 10.1126/scisignal.2005560.
- Rudnev, V. R., Nikolsky, K. S., Petrovsky, D. V., Kulikova, L. I., Kargatov, A. M., Malsagova, K. A., Stepanov, A. A., Kopylov, A. T., Kaysheva, A. L. & Efimov, A. V. (2022). β -Corner Stability by Comparative Molecular Dynamics Simulations. *International Journal of Molecular Sciences*; 23; 1-14. doi: 10.3390/ijms231911674.
- Salem, I. M., Mostafa, S. M., Salama, I., El-Sabbagh, O. I., Hegazy, W. A. H. & Ibrahim, T. S. (2023). Design, Synthesis and Antitumor Evaluation of Novel Pyrazolo[3,4- d]Pyrimidines Incorporating Different Amino Acid Conjugates as Potential DHFR Inhibitors. *Journal of Enzyme Inhibition and Medicinal Chemistry*; 38; 203–215. doi: 10.1080/14756366.2022.2142786.
- Sándor, M., Kiss, R. & Keserü, G. M. (2010). Virtual Fragment Docking by Glide: a Validation Study on 190 Protein–Fragment Complexes. *Journal of Chemical Information and Modeling*; 50; 1165–1172. doi: 10.1021/ci1000407.
- Santos, G. B., Ganesan, A. & Emery, F. S. (2016). Oral Administration of Peptide-Based Drugs: Beyond Lipinski's Rule. *ChemMedChem*; 11; 2245–2251. doi: 10.1002/cmdc.201600288.
- Satgas Penanganan Covid-19. (2022). Data Sebaran Situasi Virus COVID-19. <https://covid19.go.id/>
- Septiana, E. (2020). Prospek Senyawa Bahan Alam Sebagai Antivirus Dalam Menghambat SARS-CoV-2. *Bio Trends*; 11; 30–38.
- Shree, P., Mishra, P., Selvaraj, C., Singh, S. K., Chaube, R., Garg, N. & Tripathi, Y. B. (2022). Targeting COVID-19 (SARS-CoV-2) Main Protease through Active Phytochemicals of Ayurvedic Medicinal Plants–Withania Somnifera (Ashwagandha), *Tinospora cordifolia* (Giloy) and *Ocimum sanctum* (Tulsi)—a Molecular Docking Study. *Journal of Biomolecular Structure and Dynamics*; 40; 190–203. doi: 10.1080/07391102.2020.1810778.
- Tu, Y., Chien, C., Yarmishyn, A. A., Lin, Y., Luo, Y.-H., Lin, Y.-T., Lai, W.-Y., Yang, D.-M., Chou, S.-J., Yang, Y.-P., Wang, M.-L., & Chiou, S.-H. (2020). A Review of SARS-CoV-2 and the Ongoing Clinical Trials. *International Journal of Molecular Sciences*; 21; 1-19. doi: 10.3390/ijms21072657.
- Vardhan, S. & Sahoo, S. K. (2020). In Silico ADMET and Molecular Docking Study on Searching Potential Inhibitors from Limonoids and Triterpenoids for COVID-19. *Computers in Biology and Medicine*; 124; 1-12. doi: 10.1016/j.compbiomed.2020.103936.
- Venkatesh. (2022). Molecular Docking of Ganomestanol with Sars-Cov-2 Mpro. *Asian Journal of Pharmaceutical and Clinical Research*; 15; 46–47. doi: 10.22159/ajpcr.2022.v15i2.43679.
- Wang, M., Cao, R., Zhang, L., Yang, X., Liu, J., Xu, M., Shi, Z., Hu, Z., Zhong, W. & Xiao, G. (2020). Remdesivir and Chloroquine Effectively Inhibit

the Recently Emerged Novel Coronavirus (2019-nCoV) In Vitro. *Cell Research*; 30; 269–271. doi: 10.1038/s41422-020-0282-0.

World Health Organization (WHO). (2022). World Health Organization. Coronavirus disease 2019 (COVID-19) Weekly Epidemiological Update, Edition 117, published 9 November 2022. <https://www.who.int/publications/m/item/weekly-Epidemiological-Update-on-Covid-19---9-November-2022>.

Wu, J., Zhou, Y., Zhang, J., Zhang, H.-X., & Jia, R. (2022). Molecular Dynamics Simulation Investigation of the Binding and Interaction of the EphA6–Odin Protein Complex. *The Journal of*

Physical Chemistry B; 126; 4914–4924. <https://doi.org/10.1021/acs.jpcc.2c01492>

Wu, Q. & Huang, S.-Y. (2023). HCovDock: an Efficient Docking Method for Modeling Covalent Protein–Ligand Interactions. *Briefings in Bioinformatics*; 24; 1-10. doi: 10.1093/bib/bbac559.

Yu, R., Chen, L., Lan, R., Shen, R., & Li, P. (2020). Computational Screening of Antagonists Against the SARS-CoV-2 (COVID-19) Coronavirus by Molecular Docking. *International Journal of Antimicrobial Agents*; 56; 106012. doi: 10.1016/j.ijantimicag.2020.106012.



Five Years Outpatients Antibiotics Consumption at Public Tertiary Hospital in Bengkulu According to Access, Watch and Reserve Classification

Yusna F. Apriyanti¹, Saepudin^{2*}, Siti Maisharah S. Gadzi³

¹Master Program of Pharmacy, Department of Pharmacy, Faculty of Mathematics and Natural Sciences, Universitas Islam Indonesia, Indonesia

²Department of Pharmacy, Faculty of Mathematics and Natural Sciences, Universitas Islam Indonesia, Indonesia

³School of Pharmaceutical Sciences, Universiti Sains Malaysia, Malaysia

*Corresponding author: saepudin@uii.ac.id

Submitted: 5 October 2023

Revised: 6 December 2023

Accepted: 13 December 2023

Abstract

Background: Access, Watch, and Reserve (AWaRe) antibiotics classification was released in 2019 by the World Health Organization (WHO) to enhance antimicrobial stewardship programs in all healthcare facilities. As a result, WHO advises global action to increase the availability of antibiotics from the Access group by more than 60%. **Objective:** to determine antibiotics consumption for outpatients at a public tertiary hospital in Bengkulu, Sumatera-Indonesia, from 2018 to 2022, focusing on antibiotics from Access class according to the AWaRe classification from WHO and Ministry of Health Republic of Indonesia (MoHRI). **Methods:** This is a cross-sectional survey analyzing aggregate data on antibiotics use for outpatients at the hospital during the study period. Data on antibiotics were collected from the hospital pharmacy department, while data on patient visits were collected from the medical records department. The quantity of antibiotics used was calculated using the ATC/DDD method and expressed in DDD/1000 patient-day (PD), which was then converted into a percentage. **Results:** During the study period, 50-60% and 65-73% out of 14-19 antibiotic agents are from Access class according to WHO and MoHRI AWaRe classification, respectively. Quantitatively, according to the WHO and MoHRI AWaRe classification, the consumption of antibiotics from the Access class was 25-50% and 33-71% of total consumption, respectively. In addition, the segment of drug utilization 90% (DU90%) of antibiotics was dominated by antibiotics from Watch class. **Conclusion:** The hospital has not yet met the WHO target for antibiotic consumption from the Access class, highlighting the need for some effective efforts from Watch class to limit the usage of antibiotics.

Keywords: antibiotics consumption, antibiotics resistance, ATC/DDD, AWaRe classification 2

How to cite this article:

Amrulloh, L. S. W. F., Harmastuti, N., Prasetyo, A. & Herowati, R. (2023). Analysis of Molecular Docking and Dynamics Simulation of Mahogany (*Swietenia macrophylla* King) Compounds Against the PLpro Enzyme SARS-COV-2. *Jurnal Farmasi dan Ilmu Kefarmasian Indonesia*, 10(3), 360-368. <http://doi.org/10.20473/jfiki.v10i32023.360-368>

INTRODUCTION

The prevalence of antimicrobial resistance (AMR) has become a significant threat to global public health (Nwobodo *et al.*, 2022; Xiao, 2023), and it was estimated that the number of AMR-related fatalities in 2019 was 4.95 million globally (Daneman *et al.*, 2023; Wilson *et al.*, 2022). Ranjbar *et al.* (2022) listed *Escherichia coli*, *Staphylococcus aureus*, *Klebsiella pneumoniae*, *Streptococcus pneumoniae*, and *Acinetobacter baumannii* as the six most lethal pathogens associated with antibiotic resistance. The overuse of antibiotics and high prescription of broad-spectrum antibiotics have been known to be the development of AMR (Dadgostar, 2019). Nationally, in Indonesia, high empirical use of broad-spectrum antibiotics and inadequate adherence to recommendations have been reported from a survey investigating antibiotics in six hospitals (Limato *et al.*, 2021).

Responding to the threat of AMR requires regulations to control antibiotic use; in 2021 The Ministry of Health Republic of Indonesia (MoHRI) released a National Guideline on antibiotic use to strengthen and emphasize the implementation of antibiotics stewardship strategy. This guideline aims to improve patient outcomes through a coordinated program related to antibiotic use one important recommended strategy is to categorize antibiotics into AWaRe (Access, Watch, Reserve) classification (MoHRI, 2021). This categorization was determined following the same categorization previously released by the World Health Organization (WHO) as a tool for evaluating antibiotic consumption to optimize antibiotic use and further slow down the progress of AMR. As part of the worldwide plan to prevent AMR, WHO has set a target of at least 60% availability and usage of antibiotics in the Access class from total antibiotic consumption. (WHO, 2020).

Reports on the evaluation of antibiotics use in Indonesia that have been published until 2022 indicate that the consumption of antibiotics from the Watch group continues to dominate in health facilities, up to more than 60% (Azyenela *et al.*, 2022). Another study also reported that 30% of antibiotic use was irrational, and ceftriaxone was found to be the most used antibiotic (Diah, 2022). Similar findings have also been reported from an evaluation of antibiotic use conducted in Vietnam revealing a high proportion of antibiotic prescriptions for acute respiratory infections (ARI) in primary health care and high use of antibiotics from Watch class in children (Nguyen *et al.*, 2023). These

indicate that monitoring and evaluation of antibiotics use to achieve the prudent use of antibiotics should be continuously conducted.

To achieve the target of rational use of antibiotics, continuous studies to evaluate the profile and quality of antibiotics use are required both quantitatively and qualitatively (WHO, 2015). For quantitative evaluation, the Anatomical Therapeutic Chemical/Defined Daily Dose (ATC/DDD) method is recommended as one important key of the antibiotics stewardship program (WHO, 2022). The quantity of antibiotics used expressed in the DDD unit can provide a picture of the overall consumption of antibiotics and trends in their use for assessing the achievement of antibiotic control goals (Hollingworth & Kairuz, 2021). The purpose of this study was to capture the profile of antibiotic use for outpatients at a public tertiary teaching hospital in Bengkulu, Sumatera – Indonesia, specifically in accordance with the AWaRe classification by following the AWaRe categorization released by WHO and MoHRI.

MATERIALS AND METHODS

Study design

This study is a cross-sectional survey using aggregate data on antibiotics use for outpatients at a public tertiary teaching hospital in Bengkulu, Sumatera, Indonesia. Retrospective data of antibiotics use for five years during 2018-2022 were used for this study, including all systemic antibiotics coded as J01 in the ATC classification. The hospital has granted permission to conduct this study through the permission letter number 074/35/BID-DIK/II/2023.

Method of collecting data

Data were collected from the Hospital Pharmacy Department (HPD) using the Hospital Information System (SIMRS). Antibiotic use-related data were collected, including the name of antibiotic agents, dosage form and dosage strength, as well as the monthly quantity of antibiotics used during the study period (2018-2022). Data on the number of patient visits per year were collected from the medical record department.

Data analysis

The quantity of each antibiotic was calculated in DDD units by dividing the consumption of each antibiotic in grams by the DDD value as determined by WHO (WHO, 2022). The final unit used to express the quantity of antibiotic use in this study is DDD/1000 patient-days (DDD/1000PD), which is the unit widely used and globally accepted to quantify drug use for outpatients. The calculation of DDD/1000PD was

conducted by combining the data on antibiotics use and the data on the number of outpatient visits. This is accomplished by multiplying the quantity of antibiotic use per month expressed in DDD by 1000, and then the result is divided by the number of outpatient visits per month accordingly (Apriyanti & Saepudin, 2023). The antibiotics found in this study were then categorized as 'Access', 'Watch', and 'Reserve' by following the 2019 WHO AWaRe classification as well as the 2021 MoHRI AWaRe classification. Antibiotics not listed in those classifications were categorized as 'Unclassified'. The proportion of the consumption of antibiotics from each Access, Watch, and Reserve class was then determined by calculating the quantity of antibiotics in each class, expressed in DDD/1000PD, relative to the total antibiotic consumption. Finally, the proportion of antibiotic use from each class during the study period was calculated.

RESULTS AND DISCUSSION

Based on the generic names, this study identified 19 antibiotic agents that were used for the outpatient at the hospital during the study period. Table 1 displays all antibiotic agents used at the hospital categorized by following the AWaRe categorization released by WHO and MoHRI. Fourteen antibiotic agents were used consistently during the study period, and the highest number of antibiotic agents was found in 2018, in which 19 antibiotic agents were used. Meanwhile, the lowest number of antibiotic agents was found in 2022, with only 14 antibiotic agents used this year.

Ten and thirteen antibiotic agents used for outpatients at the hospital are from the Access class according to WHO and MoHRI AWaRe categorization, respectively. In the meantime, 9 and 5 antibiotic agents used for outpatients at the hospital are from Access class according to WHO and MoHRI AWaRe categorization, respectively. There are some differences in term of AWaRe categorization released by WHO and MoHRI, as the categorization released by MoHRI was determined by accommodating some circumstances related to antibiotics use nationally in Indonesia. For instance, erythromycin, spiramycin, and ciprofloxacin are categorized in the Access class by MoHRI, while WHO categorized those antibiotic agents in the Watch class. Meanwhile, pipemidic acid is listed in Watch class according to the WHO AWaRe categorization, and it is not listed in the MoHRI categorization. As the results of different categorizations, this study found that 50-60% and 65-73% of the 14-19 antibiotics used for outpatients

at the hospital are from the Access class following WHO and MoHRI AWaRe classification, respectively.

In terms of the quantity, the consumption of antibiotics for outpatients at the hospital tends to fluctuate during the study period. On average, antibiotics consumption for outpatients at the hospital per year during the study period is 140.9 DDD/1000PD, with the highest and the lowest quantities of antibiotics were found in 2021 and 2022, with 155.1 DDD/1000PD and 106.1 DDD/1000PD, respectively. In contrast with the quantity of antibiotics consumption, the highest and the lowest number of outpatient visits were found in 2018 and 2021, with 105,142 and 58,226 visits, respectively. The quantity of antibiotics used was expressed in DDD/1000PD to eliminate the influence of the number of outpatient visits so that the quantity can be compared adequately. In comparison with the previously reported findings, the quantity of antibiotics used in this study is significantly lower compared to antibiotics consumption in Sao Paulo, Brazil, with 889.11 DDD/1000PD (Assis *et al.*, 2022).

The selection of antibiotic agents used in hospitals could be influenced by the pattern of infectious diseases, as well as the policies on antibiotic use. Figure 1 shows that antibiotic agents from the quinolone subgroup, including ciprofloxacin, levofloxacin, ofloxacin, and other quinolones such as pipemidic acid, were the most commonly used antibiotics, especially from 2018 to 2020. Among the quinolone subgroup, ciprofloxacin was the most used antibiotic (19.35 DDD/1000PD). Other studies have reported that ciprofloxacin and other quinolone antibiotics are commonly prescribed in hospitals (Feroche & Alemu, 2021; Rehman *et al.*, 2019). However, the use of fluoroquinolone antibiotics needs to be evaluated continuously, as their use is frequently inappropriate, and there is a significant increase in bacterial resistance to ciprofloxacin and other fluoroquinolone groups (Dobbyn *et al.*, 2022). The ATC J01 M group and other quinolone groups, such as pipemidic acid, are also extensively used for outpatients at the hospital with an average quantity of 21.66 DDD/1000PD. Due to its effective antibacterial activity against gram-negative and some gram-positive (Alves *et al.*, 2020), pipemidic acid is extensively used as a therapeutic agent to treat urinary tract infections.

In addition to the use of the quinolone subgroup, Figure 1 also shows that the other beta-lactam antibiotics were commonly used with relatively consistent in terms of quantity during the study period. First and third-generation of cephalosporins were used for outpatients at the hospital, and interestingly, the

consumption of cefixime, which is categorized within Watch class, was higher (24.14 DDD/1000 PD) than cefadroxil (11.14 DDD/1000PD) which is categorized

within Access class in both categorizations released by WHO and MoHRI.

Table 1. Antibiotic Consumption for outpatients at the hospital following ATC Classification and AWaRe Categorization from WHO and MoHRI during 2018-2022

ATC Code		AWaRe Categorization		Quantity of Antibiotic Use (DDD/1000PD)				
		WHO	MoHRI	2018	2019	2020	2021	2022
J01A	TETRACYCLINES			1.08	0.87	0.81	0.51	0.85
J01AA02	Doxycycline	ACCESS	ACCESS	1.08	0.87	0.81	0.51	0.85
J01B	AMPHENICOLS			0.95	1.44	0.73	0.24	0.88
J01BA01	Chloramphenicol	ACCESS	ACCESS	0.06	0.08	0.18	0.15	0.06
J01BA02	Thiamphenicol	ACCESS	ACCESS	0.89	1.36	0.54	0.09	0.82
J01C	BETA-LACTAM ANTIBACTERIALS, PENICILLINS			45.16	44.89	25.91	22.02	20.76
J01CA01	Ampicillin	ACCESS	ACCESS	0.00				
J01CA04	Amoxicillin	ACCESS	ACCESS	41.35	43.49	25.07	21.40	20.76
J01CR02	Amoxicillin/clavulanic acid	ACCESS	ACCESS	3.81	1.40	0.84	0.62	
J01D	OTHER BETA-LACTAM ANTIBACTERIALS			31.38	34.04	38.16	40.30	32.51
J01DB05	Cefadroxil	ACCESS	ACCESS	13.57	15.37	11.38	6.64	8.73
J01DD08	Cefixime	WATCH	WATCH	17.81	18.67	26.78	33.67	23.78
J01E	SULFONAMIDES AND TRIMETHOPRIM			10.65	8.82	6.60	4.72	2.24
J01EE01	Sulfamethoxazole/trimethoprim	ACCESS	ACCESS	10.65	8.82	6.60	4.72	2.24
J01F	MACROLIDES, LINCOSAMIDES, AND STREPTOGRAMINS			6.09	7.04	20.75	49.06	8.17
J01FA01	Erythromycin	WATCH	ACCESS	2.08	1.82	3.33	1.74	0.15
J01FA02	Spiramycin	WATCH	ACCESS	0.02	0.01			
J01FA09	Clarithromycin	WATCH	WATCH	0.57	2.69	1.88		
J01FA10	Azithromycin	WATCH	WATCH	2.52	1.73	15.13	46.90	5.03
J01FF01	Clindamycin	ACCESS	ACCESS	0.90	0.79	0.41	0.43	2.98
J01M	QUINOLONE ANTIBACTERIALS			51.39	51.52	46.93	35.99	35.37
J01MA01	Ofloxacin	WATCH	WATCH	1.55	0.27	0.13		
J01MA02	Ciprofloxacin	WATCH	ACCESS	29.40	24.60	17.75	12.78	12.22
J01MA12	Levofloxacin	WATCH	WATCH	2.56	2.60	3.78	1.47	3.80
J01MB04	Pipemidic acid	WATCH	Uncategorized	17.88	24.05	25.28	21.74	19.36
J01X	OTHER ANTIBACTERIALS			2.40	2.62	3.13	2.24	5.29
J01XD00	Metronidazole	ACCESS	ACCESS	2.40	2.62	3.13	2.24	5.29
				149.10	151.24	143.02	155.09	8

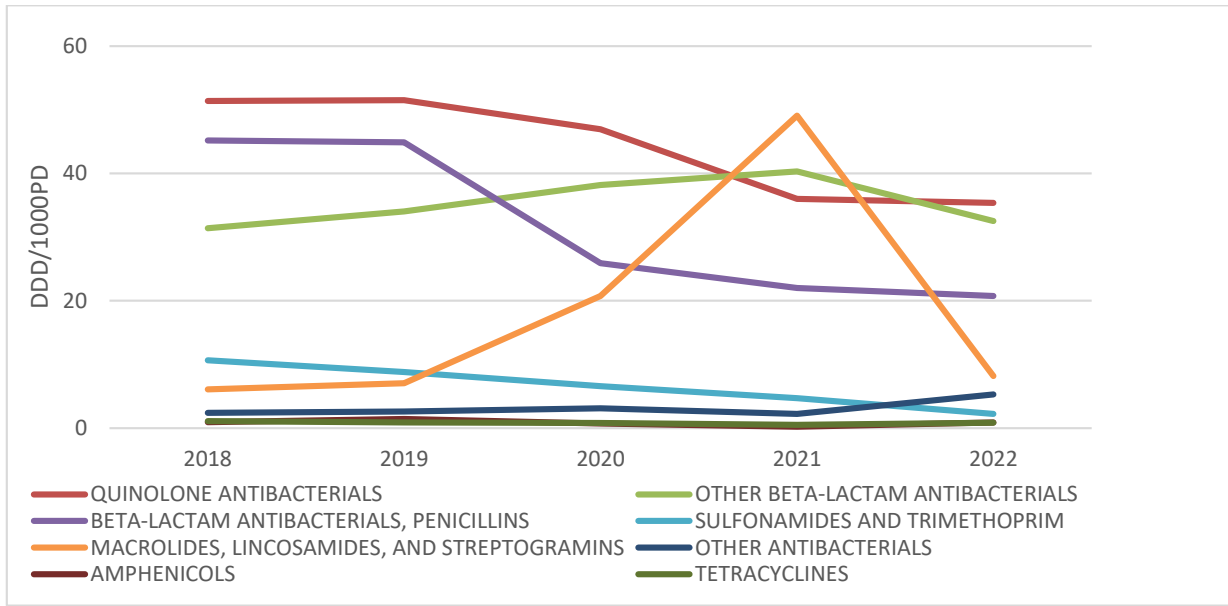


Figure 1. Quantity of antibiotic use at the hospital expressed in DDD/1000PD during the period 2018-2022 based on pharmacological group according to the ATC classification system

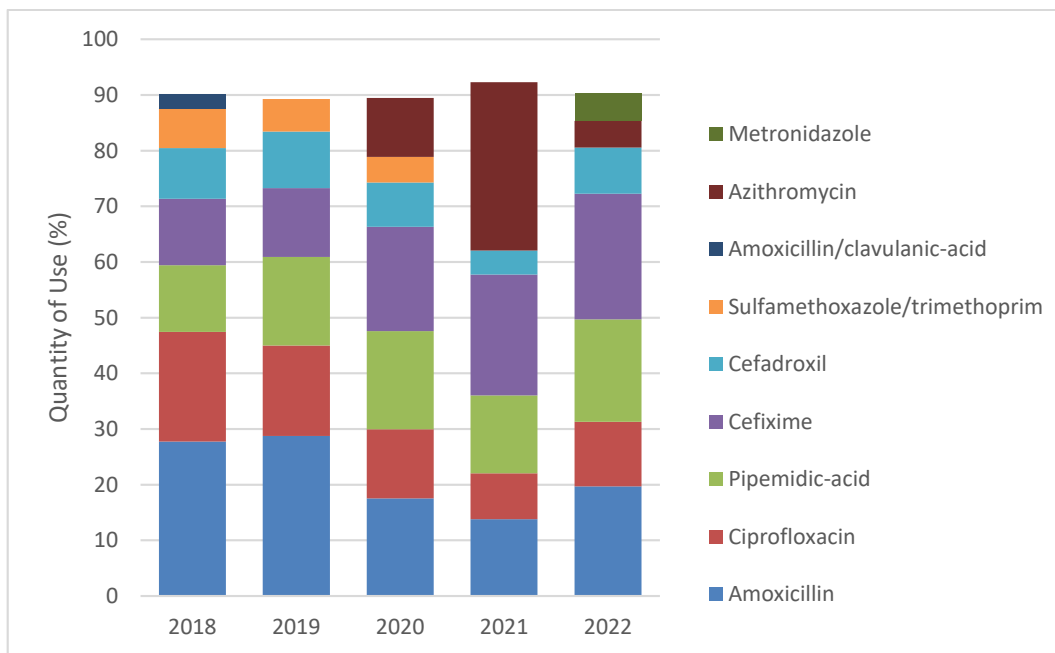


Figure 2. DU90% profiles of antibiotics used for outpatients at the hospital each year during the period of 2018-2022

Compared to other antibiotics in the beta-lactam class, beta-lactams were the second most commonly used in 2018 and 2019, but their usage declined in 2020 (Figure 1). Amoxicillin, which is Access class from both categories, was the most commonly used antibiotic in the beta-lactam class, with an average utilization of 30,41 DDD/1000 PD. The macrolide class of antibiotics, which includes azithromycin, clindamycin, erythromycin, spiramycin, and clarithromycin, was used more frequently in 2020 and 2021 as a result of the beta-

lactam group's decline, with an average utilization of 18,22 DDD/1000 PD. In this investigation, antibiotics belonging to the trimethoprim and sulfonamide classes were found to have an average usage of 6.61 DDD/1000PD. Other antibacterial groups included metronidazole, with an average use of 3.13 DDD/1000PD. This study indicated that the average annual use of antibiotics from the amphenicol and tetracycline classes was less than 2 DDD/1000PD.

Figure 2 depicts the DU profile of 90% annual use of antibiotics during the study period, which reveals that, despite the fact that 19 varieties of antibiotics were used in the hospital, only 6/7 of the 19 types had quantity use in the 90% usage area. These results indicate that approximately 60% of the antibiotic is utilized in the remaining 10%. In addition to being an exceptional clinical review, this profile can also be evaluated from an administration and management perspective to determine the efficiency and efficacy of drug management. Figure 2 also demonstrates that amoxicillin, ciprofloxacin, pipemidic acid, cefixime, and cefadroxil are the five most frequently prescribed antibiotics annually from 2018 to 2022.

Amoxicillin was the most used antibiotic for outpatients at the hospital during the study period, with an average consumption of 22%. Following amoxicillin, cefixime was the second most used antibiotic, with an average consumption of 17.5% during the study period. In contrast with the antibiotic consumption during 2018-2019, azithromycin is included in the segment of DU90% during 2020-2022 and became the most used antibiotic in 2021. Unsurprisingly, the use of azithromycin increased during 2021-2022 as this antibiotic was recommended for the treatment of COVID-19 patients (Oldenburg & Doan, 2020). Infection with the SARS-2 coronavirus has become a focal point of attention throughout 2020, which has influenced the selection of antibiotic therapy by medical professionals (Sinto, 2020). However, subsequent studies did not support the routine use of azithromycin for outpatient SARS, as a single dose of azithromycin compared to placebo did not increase the likelihood of being symptom-free by day 14 (Oldenburg et al., 2021). Overall, the segment of drug utilization 90% (DU90%)

of antibiotics for outpatients at the hospital during the study period was dominated by antibiotics from Watch class according to WHO AWaRe classification. Azithromycin, cefixime, ciprofloxacin, and pipemidic acid, all of which are in the Watch category according to the WHO AWaRe classification, were included in DU90%.

The main aim of this study is to determine the proportion of antibiotic use from the Access class, so the quantity of antibiotic use was then grouped based on the classes defined by WHO and the MoHRI. The usage of each antibiotic is converted into percent and then grouped based on Access, Watch, Reserve and Unclassified classes, and the results are presented in Figures 3 and 4. The primary objective of implementing the AWaRe classification is to mitigate the utilization of antibiotics within the Watch and Reserve categories and, subsequently, enable an increase in the accessibility and utilization of antibiotics from the Access class to surpass 60% of the overall antibiotic consumption (WHO, 2020).

During the study period, consumption of antibiotics from the Access class comprises only 24-50% and 33-71% of total antibiotics consumption for outpatients following WHO and MoHRI AWaRe classification, respectively, as presented in Figure 3. Overall, the utilization of antibiotics from the Access class is lower than the target set by WHO. Consistent with prior research findings (Tomas *et al.*, 2021; Zhussupova *et al.*, 2021), it has been shown that a decline in the utilization of antibiotics from Access class according to WHO AWaRe Classification is subsequently accompanied by a corresponding rise in the consumption of antibiotics from Watch, and even Reserve, class.

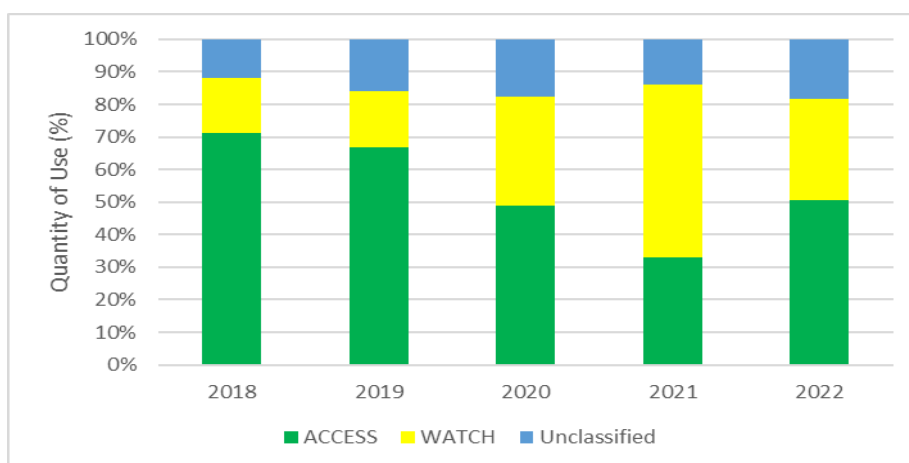


Figure 3. Proportion of the consumption of antibiotics from Access and Watch class for outpatients at the hospital during the period of 2018-2022 according to MoHRI AWaRe Classification

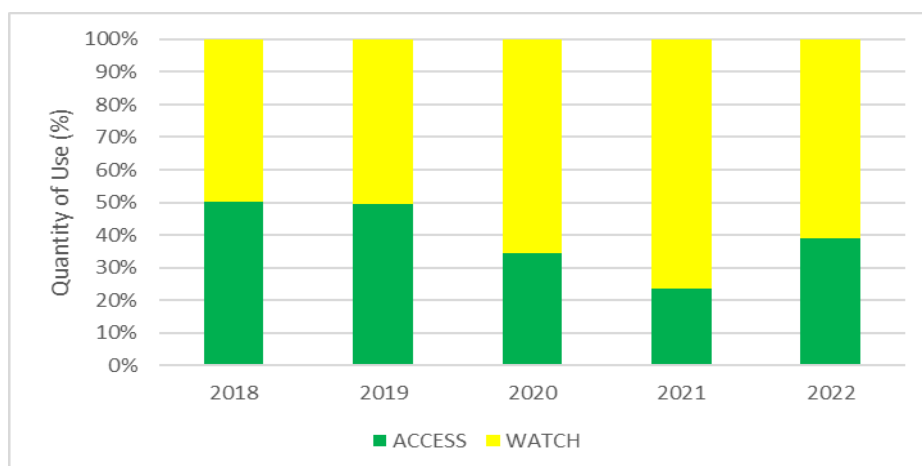


Figure 4. Proportion of the consumption of antibiotics from Access and Watch class for outpatients at the hospital during the period of 2018-2022 according to WHO AWaRe Classification

This study has some limitations, especially regarding the adjustment of antibiotics use with the epidemiological profile of infectious diseases at the hospital. Therefore, results from this study require further follow-up from both the clinical and management aspects. Further clinical research is needed to ensure that the consumption of antibiotics from Watch follows the national guidelines in order to achieve better outcomes without increasing the risk of adverse effects and, importantly, not significantly increasing the risk of developing bacterial resistance.

CONCLUSION

In term of antibiotics agents, antibiotics used for outpatients at the hospital were mostly from Access class. However, in term of quantity, the consumption of antibiotics from Access class still below the target of WHO. This indicates that the implementation of some effective strategies is still needed to achieve the target regarding antibiotics use.

ACKNOWLEDGMENT

Authors would like to thank the pharmacists and staffs at study site as well as the staffs at Master Program of Pharmacy, Universitas Islam Indonesia, for supporting the study.

AUTHOR CONTRIBUTIONS

Conceptualization, S., S. M. G., Y. F. A.; Methodology, S., S. M. G., Y. F. A.; Software S.; Validation, S.; Formal Analysis, S., Y. F. A.; Investigation, Y. F. A.; Resources, Y. F. A.; Data Curation, S., Y. F. A.; Writing - Original Draft, Y. F. A.; Writing - Review & Editing, S., Y. F. A.; Visualization,

S., Y. F. A.; Supervision, S., S. M. G.; Project Administration, S., S. M. G., Y. F. A.; Funding Acquisition, Y. F. A.

FUNDING STATEMENT

This research did not receive any specific grant from funding agencies in the public, commercial, or not for profit sectors.

CONFLICT OF INTEREST

The authors declared no conflict of interest.

REFERENCES

- Apriyanti, Y. F. & Saepudin. (2023). Review: Application of The ATC/DDD Method for Antibiotic Evaluation in Indonesia. *Medical Sains: Jurnal Ilmiah Kefarmasian*; 8; 1323–1344. doi: 10.37874/ms.v8i3.888.
- Assis, D., Madalosso, G., Boszczowski, I. & Piastrelli, F. (2022). 1792. Different Patterns of Antibiotic Use in Different Administrative Categories: An Overview of 10 years (2009/2018) of a Statewide Surveillance Program in Sao Paulo, Brazil. In *Open Forum Infectious Diseases*; 9; 1-10. doi: 10.1093/ofid/ofac492.1422.
- Azyenela, L., Tobat, S. R. & Selvia, L. (2022). Evaluasi Penggunaan Antibiotik di Instalasi Rawat Inap Bedah RSUD M. Natsir Kota Solok Tahun 2020. *Jurnal Mandala Pharmacon Indonesia*; 8; 1–10.
- Alves, P., Rijo, P., Bravo, C., M. M. Antunes, A. & André, V. (2020). Bioactivity of Isostructural Hydrogen Bonding Frameworks Built from Pipemidic Acid Metal Complexes. *Molecules*; 25; 1-14. doi: 10.3390/molecules25102374.

- Dadgostar, P. (2019). Antimicrobial Resistance: Implications and Costs. *Infection and Drug Resistance*; 12; 3903–3910. doi: 10.2147/IDR.S234610.
- Daneman, N., Fridman, D., Johnstone, J., Langford, B. J., Lee, S. M., MacFadden, D. M., Mponponsoo, K., Patel, S. N., Schwartz, K. L. & Brown, K. A. (2023). Antimicrobial Resistance and Mortality Following *E. coli* Bacteremia. *E-Clinical Medicine*; 56; 101781. doi: 10.1016/j.eclinm.2022.101781
- Diah, F. (2022). Rationality of Antibiotics Use with Quantitative and Qualitative Methods at Hospital In Indonesia. *Pharmacology, Medical Reports, Orthopedic, and Illness Details (COMORBID)*; 1; 73–82.
- Dobbyn, D., Zeggil, T., Kudrowich, B. & Beahm, N. P. (2022). Ciprofloxacin Resistances Rates in *Escherichia coli* Across Canada (CREAC): a Longitudinal Analysis 2015–2019. *International Journal of Antimicrobial Agents*; 59; 1-6. doi: 10.1016/j.ijantimicag.2022.106532.
- Feroche, A. T. & Alemu, B. M. (2021). Drug Use Evaluation of Ciprofloxacin at Inpatient and Outpatient Departments of Hiwot Fana Specialized University Hospital, Harar General Hospital and Jagol Hospital in Harar City Advances in Pharmacoepidemiology & Drug Safety. *Population*; 5; 1–5.
- Hollingworth, S. & Kairuz, T. (2021). Measuring Medicine Use: Applying ATC/DDD Methodology to Real-World Data. *Pharmacy*; 9; 1-8. doi: 10.3390/pharmacy9010060.
- Limato, R., Nelwan, E. J., Mudia, M., de Brabander, J., Guterres, H., Enty, E., Mauleti, I. Y., Mayasari, M., Firmansyah, I., Hizrani, M. & Hamers, R. L. (2021). A Multicentre Point Prevalence Survey of Patterns and Quality of Antibiotic Prescribing in Indonesian Hospitals. *JAC-Antimicrobial Resistance*; 3; 1-10. doi: 10.1093/jacamr/dlab047.
- Ministry of Health Republic of Indonesia (MoHRI). (2021). Guidelines for the Use of Antibiotics. Regulation of the Minister of Health of the Republic of Indonesia No 28 of 2021. Jakarta: Ministry of Health Republic of Indonesia.
- Nguyen, N. V., Do, N. T. T., Vu, D. T. V., Greer, R. C., Dittrich, S., Vandendorpe, M., Pham, T. N., Ta, N. T. D., Pham, T. Q., Khuong, V. T., Le, T. T. B., Anh, L. T., Cao, T. H., Trinh, T. S., Nguyen, H. T., Ngo, L. N., Vu, T. T., van Doorn, H. R., Lubell, Y. & Lewycka, S. O. (2023). Outpatient Antibiotic Prescribing for Acute Respiratory Infections in Vietnamese Primary Care Settings by the WHO AWaRe (Access, Watch and Reserve) Classification: An Analysis Using Routinely Collected Electronic Prescription Data. *The Lancet Regional Health - Western Pacific*; 30; 1-12. doi: 10.1016/j.lanwpc.2022.100611.
- Nwobodo, C., Ugwu, D. M. C. O. A., Al-Ouqaili, M. T. S., Chinedu Ikem, J., Victor Chigozie, U. & Saki, M. (2022). Antibiotic Resistance: The Challenges and Some Emerging Strategies for Tackling a Global Menace. *J Clin Lab Anal*, 36; 1-10. doi: 10.1002/jcla.24655.
- Oldenburg, C. E. & Doan, T. (2020). Azithromycin for Severe COVID-19. *The Lancet*; 396; 936–937. doi: 10.1016/S0140-6736(20)31863-8.
- Oldenburg, C. E., Pinsky, B. A., Brogdon, J., Chen, C., Ruder, K., Zhong, L., Nyatigo, F., Cook, C. A., Hinterwirth, A., Lebas, E., Redd, T., Porco, T. C., Lietman, T. M., Arnold, B. F. & Doan, T. (2021). Effect of Oral Azithromycin vs Placebo on COVID-19 Symptoms in Outpatients With SARS-CoV-2 Infection. *JAMA*; 326; 490-498. doi: 10.1001/jama.2021.11517.
- Ranjbar, R., Alam, M. & Antimicrobial Resistance Collaborators. (2022). Global Burden of Bacterial Antimicrobial Resistance in 2019: a Systematic Analysis. *Evidence-Based Nursing (2023)*; 399; 629–655. doi: 10.1016/s0140-6736(21)02724-0.
- Rehman, A., Patrick, W. M. & Lamont, I. L. (2019). Mechanisms of Ciprofloxacin Resistance in *Pseudomonas aeruginosa*: New Approaches to An Old Problem. *Journal of Medical Microbiology*; 68; 1–10. doi: 10.1099/jmm.0.000873.
- Sinto, R. (2020). Peran Penting Pengendalian Resistensi Antibiotik pada Pandemi COVID-19. *Jurnal Penyakit Dalam Indonesia*; 7; 7–9.
- Tomas, A., Pavlović, N., Stilić, N., Horvat, O., Paut-Kusturica, M., Dugandžija, T., Tomić, Z. & Sabo, A. (2021). Increase and Change in the Pattern of Antibiotic Use in Serbia (2010-2019). *Antibiotics*; 10; 1–13. doi: 10.3390/antibiotics10040397.
- WHO. (2020). GLASS Methodology for Surveillance of National Antimicrobial Consumption. WHO: Geneva. <https://iris.who.int/bitstream/handle/10665/336215/9789240012639-eng.pdf?sequence=1>
- WHO. (2022). ATC/DDD Index 2022. https://www.whocc.no/atc_ddd_index/.

- Wilson, A., Mair, T., Williams, N., McGowan, C. & Pinchbeck, G. (2022). Antimicrobial Prescribing and Antimicrobial Resistance Surveillance in Equine Practice. *Equine Veterinary Journal*; 2022; 494–505. doi: 10.1111/evj.13587.
- Xiao, Z. (2023). Antimicrobial Resistance Mechanisms: Using Examples from Gram-Positive and Gram-Negative Bacteria. In G. Royle & S. M. Lipkin (Eds.). *Second International Conference on Biological Engineering and Medical Science (ICBioMed 2022)* SPIE. doi: 10.1117/12.2669646.
- Zhussupova, G., Utepova, D., Orazova, G., Zhaldybayeva, S. & Skvirskaya, G. (2021). Evaluation of Antibiotic Use in Kazakhstan for the Period 2017 – 2019 Based on WHO Access, Watch and Reserve. *Antibiotics*; 10; 1-13. doi: 10.3390/antibiotics10010058.



The Development and Validation of The Indonesian Insulin Adherence Influence Factor Questionnaire (IIAIFQ)

Yuniarti Suryatinah^{1,2}, Umi Athiyah^{3,4}, Adliah Binti Mohd. Ali⁵, Elida Zairina^{3,4,6*}

Master of Pharmaceutical Science Study Program, Faculty of Pharmacy, Universitas Airlangga, Surabaya, Indonesia

²National Research and Innovation Agency, Indonesia

³Department of Pharmacy Practice, Faculty of Pharmacy, Universitas Airlangga, Surabaya, Indonesia

⁴Innovative Pharmacy Practice and Integrated Outcomes Research (INACORE) Group, Universitas Airlangga, Surabaya, Indonesia

⁵Centre of Quality Management of Medicines, Faculty of Pharmacy, Universiti Kebangsaan Malaysia, Kuala Lumpur, Malaysia

⁶Center of Excellence for Patient Safety and Quality, Universitas Airlangga, Surabaya, Indonesia

*Corresponding author: elida-z@ff.unair.ac.id

Submitted: 3 October 2023

Revised: 11 December 2023

Accepted: 18 December 2023

Abstract

Background: Type 2 diabetes mellitus (DMT2) is a metabolic disease due to abnormalities in insulin secretion. Insulin is one of DMT2 therapy. **Objective:** This study aimed to validate a modified the insulin adherence influence factor questionnaire based on the health belief model (HBM) among Indonesian patients with DMT2. **Methods:** The Indonesian insulin adherence influence factor questionnaire (IIAIFQ) was developed based on modified some literature reviews and internal expert discussions. The study included 30 participants aged ≥ 17 y.o years old who had been taking insulin in the previous two months. The questionnaire consists of seven dimensions to measure HBM : perceived susceptibility, perceived severity, perceived benefits, perceived barriers, self-efficacy, cues to action and insulin adherence. **Results:** The construct validity test showed that of the 34 question items in the questionnaire, 10 items were invalid, 24 others were demonstrated valid based on the Pearson Correlation ($>$ table 0.361; $p < 0.05$; loading factor > 0.5). Furthermore, 24 valid items were tested for reliability at a significance level of 0.05, and the results showed that each size had a Cronbach's Alpha > 0.6 with an overall score was 0.858, indicating that all domains in the questionnaire were reliable. **Conclusion:** IIAIFQ based The HBM theory is a valid and reliable instrument for assessing insulin adherence in diabetes mellitus patients.

Keywords: adherence, health belief model, insulin, reliability, validity

How to cite this article:

Suryatinah, Y., Athiyah, U., Ali, A. B. M. & Zairina, E. (2023). The Development and Validation of The Indonesian Insulin Adherence Influence Factor Questionnaire (IIAIFQ). *Jurnal Farmasi dan Ilmu Kefarmasian Indonesia*, 10(3), 369-378. <http://doi.org/10.20473/jfiki.v10i32023.369-378>

INTRODUCTION

Diabetes mellitus (DM) is a non-communicable disease that is a top 10 (ten) cause of death globally. In 2021, DM disease in Indonesia ranked fifth highest globally after China, India, Pakistan, and the United States (International Diabetes Federation, 2021). The results of Basic Health Research show that the prevalence of people aged ≥ 15 years with DM has increased from 6.9% in 2013 to 8.5% in 2018 (Kemenkes RI, 2018).

The International Diabetes Federation estimates that more than 537 million people worldwide suffer from DM, and around 150-200 million are treated with insulin (Masieriek *et al.*, 2022). Insulin therapy is needed when oral antidiabetics in optimal doses cannot improve blood glucose levels and HbA1C values $> 9\%$ with metabolic decompensation conditions (Perkumpulan Endokrinologi Indonesia, 2021a).

In Indonesia, several types of insulin are categorized based on their origin, namely insulin analogues and human insulin. The use of insulin analogues is higher than human insulin (Kehlenbrink *et al.*, 2018). Based on its duration of action, insulin therapy consists of fast-acting, short-acting, intermediate-acting, long-acting, and fixed insulin mix (premixed insulin) (Perkumpulan Endokrinologi Indonesia, 2021b). Adherence to oral drug therapy and insulin therapy influences therapeutic outcomes in diabetic patients. According to the treatment recommendation, good insulin adherence is critical in managing DM therapy. Adherence to insulin therapy is linked to better glycemic control, which lowers the risk of developing microvascular and macrovascular complications and all-cause mortality (Stolpe *et al.*, 2016).

Patients' beliefs about using drugs and their health conditions influence adherence to medication therapy. Individual beliefs include perceptions of susceptibility, severity, benefits, barriers, and self-efficacy. Cues to action also have an impact on compliance (Pakpahan *et al.*, 2021). Adherence to medical regimens extends the health belief model (HBM) implementation (Irwan, 2017).

Based on the literature review, numerous questionnaires assess diabetes mellitus treatment adherence in general and the factors that influence it. The questionnaire about the adherence to insulin used was adapted from the Morisky Medication Adherence Scale (MMAS) (MIAS) (Osborn & Gonzalez, 2016). There was a questionnaire about factors determining insulin adherence like diabetes knowledge, such as the

patient diabetes knowledge questionnaire (PDKQ) and diabetes knowledge questionnaire (DKQ) in the Taiwanese population; a questionnaire about quality of life, such as the Asian diabetes quality of life questionnaire and Indonesian version of the A the audit of diabetes dependent quality of life questionnaire (ADDQoL); and the questionnaire about diabetes mellitus patient behaviour in primary health care service (Hsieh *et al.*, 2022; Lim *et al.*, 2023; Oliveira *et al.*, 2022; Permana *et al.*, 2021; Rooswita *et al.*, 2021; Saputri *et al.*, 2019).

There are only a few questionnaires specific to Indonesian patients with DMT2 with insulin treatment therapy. Fitriani *et al.* (2019) developed an insulin adherence questionnaire based on the health belief model (HBM) only on individual belief or only 5 (five) dimensions. A study was done by compiling personal beliefs and cues to action became 6 (six) dimensions for measuring insulin adherence, and factors determining insulin adherence in Indonesian patients with DMT2 is still limited. This study aimed to develop and validate the insulin adherence influence factor questionnaire based on the health belief model (HBM) among Indonesian patients with DMT2.

MATERIALS AND METHODS

Tools

The Indonesian insulin adherence influence factor questionnaire (IIAIFQ) was developed in the Indonesia language based on literature reviews (Cipolle *et al.*, 2012; Hepler & Strand, 1990; Perkumpulan Edukator Diabetes Indonesia, 2017; Rusmadi *et al.*, 2021; Strachan & Frier, 2013; van der Ven *et al.*, 2003) and expert discussion. This questionnaire consisted of seven dimensions (34 statement items), namely 3 statement items on perceived susceptibility (PSu), 3 statement items on perceived severity (PSv), 5 statement items on perceived benefits (PBe), 6 statement items on perceived barriers (PBa), 4 statement items on perceived self-efficacy (PSE), 3 statement items on cues to action (CA), and 10 statement items on insulin adherence (IA). Assessment of the six dimensions of individual belief used a Likert scale with a score of 5 for the answer "strongly agree", 4 for the answer "agree", 3 for the answer "neutral", 2 for the answer "disagree" and 1 for the answer "strongly disagree". While one dimension of insulin adherence used a Likert scale with ratings of 5 for the answer "always", 4 "often", 3 for the answer "sometimes", 2 for the answer rarely, and 1 for the answer "never."

Method

Study design

This cross-sectional survey was conducted in Banjarbaru City, South Borneo, Indonesia, from March to April 2023. Convenient sampling was employed to select respondents for construct validity and reliability. Ethical approval for this research was received from the Health Research Ethics Committee of Idaman Hospital Banjarbaru City with reference No.RS00122/KEPK-RSDI/02/2023.

The face and content validity test of IIAIFQ was established by an internal research team consisting of pharmacists based on their expertise and credibility in pharmaceutical care. The construct validity test of IIAIFQ was conducted on 30 respondents who visited Nirwana Hospital and Syifa Medika Hospital, Banjarbaru City (Yurdugül, 2008; Yusoff *et al.*, 2021).

Those hospitals were selected by considering the highest number of DMT2 patients who use insulin. The population of the construct validity test in this study were DMT patients who use insulin. The sample were all type 2 diabetes mellitus patients who met the following criteria: aged ≥ 17 years, taking insulin at least in the last 2 months, able to read and hear, and willing to contribute to the study by approving and signing informed consent.

Data collection

Data were collected directly from the respondents via questionnaires when the patients took the medication in the outpatient department at the pharmacy. Data collection techniques include asking respondents a series of questions or writing them down after they were informed about the purpose of the study and consented to participate by signing an informed consent form.

Data analysis

Analysis of the construct validity and reliability results used Jeffrey's Amazing Statistics Program (JASP) application. The construct validity of each statement item can be seen from the Pearson Correlation value using the distribution (table r) at a significance level of 0.05 for a two-way test with r table = 0.361 because of degrees of freedom ($df=N-2=30-2=28$). If the correlation coefficient value equals or exceeds the r table value, then the statement item is considered valid. Then, it was continued with convergent validity; if the loading factor > 0.5 , then the statement is considered valid (Hair *et al.*, 2010). Furthermore, reliability tested each dimension at a significance level of 0.05 by looking at Cronbach's alpha value. The statement is deemed reliable if Cronbach's alpha value is ≥ 0.6 (Sani, 2018).

RESULTS AND DISCUSSION

The demographic characteristics of the respondents can be seen in Table 1. The majority of respondents, or 23 people (76.7%), were patients aged 45-65 years. This aligns with research conducted by Gamayanti *et al.* (2018) at the Internal Medicine Polyclinic of the State General Hospital and Vonna *et al.* (2021) at Dr Zainoel Abidin Hospital in Banda Aceh, who stated that diabetes mellitus patients who use insulin at the most are aged 46-65 years (Gamayanti *et al.*, 2018; Vonna *et al.*, 2021). Another study on people with DMT2 at the Outpatient Pharmacy Installation at ST Elisabeth Hospital in Semarang found that most patients who use insulin were over 45 years (Rukminingsih & Nova, 2021). Based on gender, it can be seen that the majority of respondents in this study (17 people) were male (56.7 %). According to a review, women have a higher prevalence of DMT2 in their youth than men, while men have a higher prevalence in their middle years (Huebschmann *et al.*, 2019). Women patients with DM aged 56-65 years are more susceptible to depression than women patients with DM aged 46-55 years (Fatmawati *et al.*, 2023).

According to Table 1, all respondents used insulin analogue, and the majority of respondents used rapid-acting insulin in the form of Novorapid 100U/mL; as many as 7 seven people (23.3 %) and a combination of long-acting and rapid-acting insulin with the trade name Levemir 100U/ mL + Novorapid 100U/ mL; as many as 7 seven people (23.3 %). This aligns with the findings of Anggraini *et al.* (2020) and Zaim *et al.* (2021), who discovered that the use of insulin analogues is greater than that of human insulin (Anggriani, Rianti, Pratiwi, & Puspitasari, 2020). This is because the risk of hypoglycemia of insulin analogues is lower than human insulin and can be given immediately without paying attention to mealtimes (Fibriani, 2014). The use of a rapid-acting and long-acting insulin combination is in line with research conducted by Adinda *et al.* (2023), which stated that a long-acting and rapid-acting combination is also the most extensively used insulin in Dr Soetomo Hospital, Surabaya (Ayu *et al.*, 2023). The combination of insulin glargine (long-acting insulin) with insulin aspart (rapid-acting insulin) resembles the human body's normal insulin profile because it provides a faster onset of action with a longer duration of action (Kartika *et al.*, 2013).

Table 1. Demographic characteristics of the participants (n = 30)

Demographic	Category	n (%)
Age	< 45 years	4 (13.3)
	45-65 years	23 (76.7)
	> 65 years	3 (10.0)
Sex	Men	17 (56.7)
	Women	13 (43.3)
Education	None	0 (0.0)
	Primary school	1 (3.3)
	Junior high school	4 (13.3)
	Senior high school	13 (43.3)
	D3	2 (6.7)
	D4	0 (0.0)
	Bachelor degree	8 (26.7)
	Master degree	2 (6.7)
	Doctoral	0 (0.0)
Occupation	Unemployment	6 (20.0)
	Retired	4 (13.3)
	Government employees	11 (36.7)
	Self-employed	9 (30.0)
Monthly family income	< IDR 1000000	2 (6.7)
	> IDR 1000000- IDR 2000000	3 (10.0)
	> IDR 2000000- IDR 3000000	6 (20.0)
	> IDR 3000000- IDR 4000000	6 (20.0)
	> IDR 4000000- IDR 5000000	6 (20.0)
Sources of funding for treatment	> IDR 5000000	7 (23.3)
	BPJS/JKN KIS	27 (90.0)
	Private insurance	1 (3.3)
Duration of diabetes mellitus (years, mean ± sd)	Self-pay	2 (6.7)
		4.23 ± 4.5
Comorbidity	None	6 (20.0)
	Allergy	1 (3.3)
	CHF	2 (6.7)
	Dyslipidemia	6 (20.0)
	Hypertension	2 (6.7)
	Maag	1 (3.3)
	CHF + Osteoporosis	1 (3.3)
	Dyslipidaemia + CHF	1 (3.3)
	Dyslipidaemia + Maag	1 (3.3)
	Hypertension + CHF	1 (3.3)
	Hypertension + Dyslipidaemia	1 (3.3)
	Hypertension + Gout	2 (6.7)
	Hypertension + Maag	1 (3.3)
	Hypertension + Sirosis hati	1 (3.3)
	Hypertension + Stroke	1 (3.3)
Maag + Asthma	1 (3.3)	
Hypertension + Dyslipidemia + Gout	1 (3.3)	
Duration of use insulin (months, mean ± sd)		12.5 ± 22.1
Other diabetes medications currently in use	None	17 (56.7)
	Acarbose 100 mg	1 (3.3)
	Glimepiride 2 mg	1 (3.3)
	Glimepiride 3 mg	1 (3.3)
	Metformin 500 mg	5 (16.7)
	Metformin 850 mg	1 (3.3)
	<i>Gliclazide 80 mg</i>	1 (3.3)
	Metformin 500 mg + Glimepiride 2 mg	1 (3.3)
	Metformin 500 mg + Glibenclamide 2.5 mg	1 (3.3)
	Metformin 500 mg + Acarbose 100 mg	1 (3.3)

Table 2. Construct validity for the 34 statements of the IIAIFQ

No	Dimension	Statements	Pearson correlation	r table	Explanation
1	Perceived susceptibility (PSu)	1. I am vulnerable to the risk of blood sugar deficiency when using excessive doses of insulin	0.789	0.361	Valid
2		2. I am vulnerable to infection when using insulin with a syringe that is not replaced	0.853	0.361	Valid
3		3. I am vulnerable to experiencing the risk of swelling of the skin that is injected at the same place continuously	0.790	0.361	Valid
4	Perceived severity (PSe)	1. I feel worried about the condition of my sugar level if I don't adhere to using insulin properly	0.860	0.361	Valid
5		2. I am worried that my health condition will get worse if I don't adhere to using insulin properly	0.922	0.361	Valid
6		3. I am worried about the dangerous condition of the complications of diabetes mellitus	0.831	0.361	Valid
7	Perceived benefits (PBe)	1. I feel the benefit of being obedient to using the correct insulin is that my blood sugar levels are controlled	0.769	0.361	Valid
8		2. I feel that the benefit of adhering to using the correct insulin is that it can prevent complications of blindness	0.946	0.361	Valid
9		3. I feel the benefit of sticking to using the correct insulin is that it can prevent complications of kidney failure	0.915	0.361	Valid
10		4. I feel that the benefit of adhering to using the correct insulin is that it can prevent complications of heart disease	0.938	0.361	Valid
11		5. I feel the benefit of sticking to using the correct insulin is that it can prevent complications of paralysis	0.869	0.361	Valid
12	Perceived barrier (PBa)	1. I feel the fear that insulin will cause pain when injected is an obstacle in sticking to using insulin properly	0.562	0.361	Valid
13		2. I have trouble remembering the schedule for injecting insulin	0.509	0.361	Valid
14		3. I need someone else's help to be able to inject insulin properly	0.488	0.361	Valid
15		4. I find it challenging to buy a refrigerator to store insulin	0.523	0.361	Valid
16		5. I find it challenging to buy insulin because it's expensive	0.789	0.361	Valid
17	Perceived self-efficacy (PSv)	6. I feel uncomfortable with the side effects of insulin	0.605	0.361	Valid
18		1. I feel able to inject insulin properly	0.876	0.361	Valid
19		2. I feel able to inject insulin according to the recommended dose every day	0.895	0.361	Valid
20		3. I feel able to inject insulin when I'm at home even though I'm sick	0.713	0.361	Valid
21		4. I feel able to inject insulin even when I'm outside the house/travelling	0.578	0.361	Valid
22	Cues to action (CA)	1. Information and education from the doctor will be critical to help me take insulin treatment properly	0.319	0.361	Invalid
23		2. Information and education from the pharmacist will be critical to help me take insulin medication correctly	0.940	0.361	Valid
24		3. The support from my family encouraged me to adhere to insulin treatment properly	0.851	0.361	Valid
25	Insulin adherence (IA)	1. I inject insulin according to the dosage recommended by a doctor or health worker	0.361	0.361	Valid
26		2. I inject insulin before eating as directed by a doctor or health worker	0.621	0.361	Valid
27		3. I checked the expiration date of the insulin	0.542	0.361	Valid
28		4. I clean my hands before using insulin	0.744	0.361	Valid
29		5. I removed the protective seal on the needle without touching the needle	-0.044	0.361	Invalid
30		6. I do priming (gas bubble removal) before taking insulin	0.606	0.361	Valid
31		7. I did a cleanup on the location to be injected	0.775	0.361	Valid
32	8. I poked the needle into the skin quickly at a 90-degree angle	0.214	0.361	Invalid	
33	9. I store used insulin at room temperature	0.417	0.361	Valid	
34	10. I store unused insulin in the refrigerator	0.161	0.361	Invalid	

Table 3. Loading factor of convergent validity for IIAIFQ

Dimension	Indicator	Loading Factor
Perceived Susceptibility	PSu1	0,822
	PSu2	0,883
	PSu3	0,729
Perceived Severity	PSv1	0,852
	PSv2	0,922
	PSv3	0,838
Perceived Benefit	PBe1	0,796
	PBe2	0,944
	PBe3	0,910
	PBe4	0,935
	PBe5	0,859
Perceived Barrier	PBa4	0,748
	PBa5	0,798
	PBa6	0,852
Perceived Self Efficacy	PSE1	0,918
	PSE2	0,937
	PSE3	0,665
	PSE4	0,526
Cues to Action	CA2	0,931
	CA3	0,931
Insulin Adherence	IA1	0,870
	IA2	0,901
	IA4	0,553
	IA9	0,797

The construct validity test of the IIAIFQ listed in Table 2 showed that four of the 34 statement items were invalid because the correlation value was less than 0.361, resulting in only 30 statement items being declared valid. The four invalid items were 1) Information and education from a doctor would be critical to help me take insulin medication properly, 2) I removed the protective seal of the needle without touching the needle, 3) I inserted the needle rapidly into the skin at an angle of 90 degrees, and 4) I store unused insulin in the refrigerator.

Providing information to DMT2 patients about the benefits and importance of compliance and the risks of non-adherence is one way to improve adherence to insulin use (Mathew et al., 2022). Item statement no.1 comes from the dimension of cues to action. Item 1 was invalid, which may be due to the results where the majority of 21 people (70%) gave agreed answers. While item statements number 2-4 come from the dimensions of adherence to insulin use. Statements 2-4 are invalid perhaps because the majority of respondents, as many as 29 people (96.7%), answered "always" on item 2, the majority of as many as 27 people (90.0%) answered "always" on statement item 3, and most as many as 13 people (43.3%) answered "always" on the 5th statement item.

There were 30 items of valid statements in IIAIFQ by Pearson's validity analysis, it was then tested for convergent validity, as shown in Table 3. For 24 items of valid statements in IIAIFQ by convergent validity analysis, each dimension was tested for reliability, as shown in Table 4. The reliability test showed that each dimension had a Cronbach's Alpha value greater than 0.6 with an overall score of 0.858 with details for perceived susceptibility of 0.729, perceived severity of 0.841, perceived benefits of 0.927, perceived barriers of 0.711, perceived confidence of 0.757, cues to action by 0.844, and adherence to insulin use by 0.645. This means that all dimensions in the questionnaire are declared reliable.

Several studies on medication therapy adherence have been carried out using the Health Belief Model (HBM) theoretical approach. Fitriani (2019) conducted insulin treatment adherence research using a questionnaire that measures adherence to insulin treatment therapy from the five dimensions of HBM theory: perceived vulnerability, perceived severity, perceived benefits, perceived barriers, and perceived self-efficacy (Fitriani, 2019). This aligns with research conducted by Hidayati *et al.* (2020), which only included these five dimensions to analyze behavioural factors that affect adherence to medication therapy in gout patients (Hidayati *et al.*, 2020).

Table 4. Reliability for IIAIFQ

Dimension	Cronbach's alpha coefficient	Standard coefficient	Explanation
Perceived susceptibility (PSu)	0.729	0.60	Reliable
Perceived severity (PSv)	0.841	0.60	Reliable
Perceived benefits (PBe)	0.927	0.60	Reliable
Perceived barrier (PBa)	0.711	0.60	Reliable
Perceived self-efficacy (PSE)	0.757	0.60	Reliable
Cues to action (CA)	0.844	0.60	Reliable
Insulin adherence (IA)	0.645	0.60	Reliable
All dimension	0.858	0.60	Reliable

Research conducted by Fithri *et al.* (2021) also included these five dimensions with an additional dimension, namely perceived threat, in a questionnaire to assess factors that affect medication adherence in elderly patients with hypertension (Fithri *et al.*, 2021). In this study, the questionnaire was made to measure six dimensions of the HBM theory: perceived vulnerability, perceived severity, perceived benefits, perceived barriers, perceived self-efficacy, and cues to action. This aligns with previous research conducted by Rusmadi *et al.* (2021), which also included the six dimensions of the HBM theory in the medication adherence questionnaire in elderly patients with hypertension (Rusmadi *et al.*, 2021). The six dimensions of the HBM theory also measure self-care practices and associated factors among diabetic patients in Gondar City (Melkamu *et al.*, 2021).

Another perspective studies on diabetes mellitus medication adherence have been carried out using the Theory of Planned Behavior (TPB) approach. Oliveira *et al.* (2022) verified the content validity of questions of an insulin adherence questionnaire in outpatients DMT2 from the four dimensions of TPB: intention, attitude, perceived norm, and perceived control (Oliveira *et al.*, 2022). This aligns with previous research that included these four dimensions that affect antidiabetic medication adherence (Wu & Liu, 2016; Zomahoun *et al.*, 2016).

The instrument or questionnaire designed for Indonesian DMT2 patients and specific to analyzing diabetes treatment by insulin pen based on health behaviour theory distinguishes this study from others. This questionnaire measures the six dimensions of the HBM theory: perceived vulnerability, perceived severity, perceived benefits, perceived barriers, perceived self-efficacy and cues to action. Previous research did not include cues to action dimensions (Fitriani, 2019). The limitations of this study were due to the distribution of questionnaires carried out in two private hospitals in Banjarbaru City, so each respondent had different health service experiences. It affected the respondent's experience regarding cues to action related

to the role of health workers in the treatment of DM, especially the use of insulin. This questionnaire is less suitable when applied to research conducted at only one health facility. More research may be needed to test this questionnaire in a larger, more representative sample and only at one health facility to appropriately depict insulin adherence behaviour in that area. In order to create a comprehensive questionnaire, other approaches such as factor analysis for concept validity, known group validity, split half or test-retest reliability must be incorporated into the validity and reliability study.

CONCLUSION

IIAIFQ is a valid and reliable tool for assessing the factors that influence insulin adherence in Indonesian patients with DMT2 based on the HBM.

ACKNOWLEDGMENT

The authors would like to thank the Director of Nirwana Hospital, the Director of Syifa Medika Hospital, fellow hospital pharmacy installation employees who assisted in the research, the Ministry of Health of the Republic of Indonesia, which funded this study, and Ayunina Rizky Ferdina who helped in this article.

AUTHOR CONTRIBUTIONS

Conceptualization, Y. S., U. A., E. Z., A. M.A.; Methodology, Y. S., U. A., E. Z., A. M. A.; Software, Y. S.; Validation, Y. S., U. A., E. Z., A. M. A.; Formal Analysis, Y. S., U. A., E. Z.; Investigation, U. A., E. Z., A. M. A.; Resources, Y. S.; Data Curation, Y. S.; Writing - Original Draft, Y. S.; Writing - Review & Editing, Y. S., U. A., E. Z., A. M. A.; Visualization, Y. S., E. Z.; Supervision, U. A., E. Z., A. M. A.; Project Administration, Y. S.; Funding Acquisition, Y. S.

FUNDING STATEMENT

This research did not receive any specific grant from funding agencies in the public, commercial, or not for profit sectors.

CONFLICT OF INTEREST

The authors declared no conflict of interest.

REFERENCES

- Ayu, A., Rahadini, D., Murtini, S. & Soehita, S. (2023). Insulin Therapy in T2DM Patients in Diabetes Outpatient Clinic, Dr. Soetomo General Academic Hospital, Surabaya, Indonesia. *Majalah Biomorfologi (Biomorphology Journal)*; 33; 38–43. Retrieved from <https://doi.org/10.20473/mbiom.v33i1.2023.38-43>.
- Cipolle, R. J., Strand, L. M., & Morley, P. C. (2012). Chapter 5: Drug Therapy Problems. *Pharmaceutical Care Practice: The Clinician's Guide*. Chicago: McGraw-Hill Medical.
- Fatmawati, F., Suswani, A. & Nurlina, N. (2023). Comparison of the Rate of Depression in Early and Late Elderly Women with Diabetes Mellitus. *Jurnal Penelitian Pendidikan IPA*; 9; 5329–5332. Retrieved from <https://doi.org/10.29303/jppipa.v9i7.3658>.
- Fibriani, R. (2014). Diabetes Mellitus dan Terapi Insulin. *Forum Penunjang*; 1; 1–8.
- Fithri, R., Athiyah, U. & Zairina, E. (2021). The Development and Validation of the Health Belief Model Questionnaire for Measuring Factors Affecting Adherence in the Elderly with Hypertension. *Journal of Basic and Clinical Physiology and Pharmacology*; 32; 415–419. Retrieved from <https://doi.org/10.1515/jbcpp-2020-0459>
- Fitriani, Y. (2019). Analisis Faktor Yang Mempengaruhi Kepatuhan Pasien Diabetes Melitus Dalam Penggunaan Insulin Yang Benar Dengan Pendekatan Teori Health Belief Model (HBM) (Studi di RS PHC Surabaya). *Tesis*; Universitas Airlangga, Surabaya.
- Gamayanti, V., Ratnasari, N. L. M. N. & Bhargah, A. (2018). Pola Penggunaan Insulin Pada Pasien Diabetes Mellitus Tipe 2 di Poli Penyakit Dalam RSU Negara Periode Juli – Agustus 2018. *Intisari Sains Medis*; 9; 68–73. <https://doi.org/10.1556/ism.v9i3.306>.
- Hair, J. F., Black, W. C., Babin, Ba. J. & Anderson, R. E. (2010). *Multivariate Data Analysis (7th ed.)*. New York: Pearson. <https://doi.org/10.3390/polym12123016>.
- Hepler, C. D. & Strand, L. M. (1990). Opportunities and Responsibilities in Pharmaceutical Care. *American Journal of Hospital Pharmacy*; 47; 533–543. Retrieved from <https://doi.org/10.1093/ajhp/47.3.533>.
- Hidayati, I. R., Damayanti, D. A. & Pristianty, L. (2020). Analysis of Behavioral Factors on Medications in Gout Patients with Health belief Model Theory. *Journal of Global Pharma Technology*; 12; 79–84.
- Hsieh, M. H., Chen, Y. C., Ho, C. H. & Lin, C. Y. (2022). Validation of Diabetes Knowledge Questionnaire (DKQ) in the Taiwanese Population — Concurrent Validity with Diabetes-Specific Quality of Life Questionnaire Module. *Diabetes, Metabolic Syndrome and Obesity*; 15; 2391–2403. Retrieved from <https://doi.org/10.2147/DMSO.S369552>.
- International Diabetes Federation. (2021). *IDF Diabetes Atlas 10th Edition*. Diabetes Research and Clinical Practice (Vol. 102). Brussels: International Diabetes Federation. Retrieved from <https://doi.org/10.1016/j.diabres.2013.10.013>.
- Irwan. (2017). *Etika dan Perilaku Kesehatan*. Yogyakarta: CV Absolute Media.
- Kartika, I. G. A., Lestari, A. A. & Swastini, D. A. (2013). Perbandingan Profil Penggunaan Terapi Kombinasi Insulin pada Pasien Diabetes Mellitus Tipe 2 di Unit Rawat Inap Rumah Sakit Umum Pusat Sanglah. *Jurnal Farmasi Udayana*; 2; 62–69.
- Kehlenbrink, S., McDonnell, M. E., Luo, J. & Laing, R. (2018). *Review of the Evidence on Insulin and Its Use in Diabetes*. Amsterdam: Health Action International.
- Kemendes RI. (2018). *Laporan Nasional RISKESDAS 2018 Kementerian Kesehatan RI*. Jakarta: Kementerian Kesehatan Republik Indonesia. Retrieved from http://labdata.litbang.kemkes.go.id/images/download/laporan/RKD/2018/Laporan_Nasional_RKD_2018_FINAL.pdf.
- Lim, P. C., Rajah, R., Lim, Y. L., Kam, J. L. H., Wong, T. Y., Krishnanmurthi, V., ... Zainal, H. (2023). Development and Validation of Patient Diabetes Knowledge Questionnaire (PDKQ). *Journal of Pharmaceutical Policy and Practice*; 16; 1–10. <https://doi.org/10.1186/s40545-023-00631-3>.
- Masierek, M., Nabrdalik, K., Janota, O., Kwiendacz, H., Macherski, M. & Gumprecht, J. (2022). The Review of Insulin Pens—Past, Present, and Look to the Future. *Frontiers in Endocrinology*; 13; 1–23. <https://doi.org/10.3389/fendo.2022.827484>.

- Melkamu, L., Berhe, R., & Handebo, S. (2021). Does Patients' Perception Affect Self-Care Practices? The Perspective of Health Belief Model. *Diabetes, Metabolic Syndrome and Obesity*; 14; 2145–2154. Retrieved from <https://doi.org/10.2147/DMSO.S306752>.
- Oliveira, M. K. de M., Kaizer, U. A. de O., Jannuzzi, F. F., Gallani, M. C., Alexandre, N. M. C., Cornélio, M. E., ... Rodrigues, R. C. M. (2022). Content Validity of a Questionnaire Based on the Theory of Planned Behavior to Assess the Psychosocial Determinants of Insulin Adherence. *Value in Health Regional Issues*; 29; 76–85. Retrieved from <https://doi.org/10.1016/j.vhri.2021.08.007>.
- Osborn, C. Y. & Gonzalez, J. S. (2016). Measuring Insulin Adherence Among Adults with Type 2 Diabetes. *Journal of Behavioral Medicine*; 39; 633–641. Retrieved from <https://doi.org/10.1007/s10865-016-9741-y>.
- Pakpahan, M., Siregar, D., Susilawaty, A., Tasnim, Mustar, Ramdany, R., ... M, M. (2021). Promosi Kesehatan & Perilaku Kesehatan. (R. Watrianthos, Ed.). Medan: Yayasan Kita Menulis Sumatera Utara.
- Perkumpulan Edukator Diabetes Indonesia. (2017). Pedoman Teknik Menyuntik Insulin Indonesia: The Indonesian Recommendations for Best Practice in Insulin Injection Technique. Jakarta: Perkumpulan Edukator Diabetes Indonesia.
- Perkumpulan Endokrinologi Indonesia. (2021a). Pedoman Pengelolaan dan Pencegahan Diabetes Melitus Tipe 2 Dewasa di Indonesia. PERKENI. Jakarta: PB PERKENI. Retrieved from www.ginasthma.org.
- Perkumpulan Endokrinologi Indonesia. (2021b). Pedoman Petunjuk Praktis Terapi Insulin Pada Pasien Diabetes Mellitus 2021. Jakarta: PB PERKENI.
- Permana, H., Liem, M. V. & Soetedjo, N. N. M. (2021). Validation of the Indonesian Version of the Asian Diabetes Quality of Life Questionnaire. *Acta Medica Indonesiana*; 53; 143–148.
- Rooswita, P. A., Nita, Y., Zairina, E., Nugraheni, G. & Libriansyah, L. (2021). Linguistic Validation of Indonesian Version of the Audit of Diabetes-Dependent Quality of Life Questionnaire. *Jurnal Farmasi Dan Ilmu Kefarmasian Indonesia*; 8; 293. Retrieved from <https://doi.org/10.20473/jfiki.v8i32021.293-300>.
- Rusmadi, N., Pristianty, L. & Zairina, E. (2021). Validitas dan Reliabilitas Kuesioner Kepatuhan Pengobatan Pasien Lansia dengan Hipertensi berdasarkan Teori Health Belief Model. *Jurnal Sains Farmasi & Klinis*; 8; 60-68. Retrieved from <https://doi.org/10.25077/jsfk.8.1.60-68.2021>.
- Sani K, F. (2018). Metodologi Penelitian Farmasi Komunitas Dan Eksperimental (1st ed.). Yogyakarta: Deepublish.
- Saputri, G. Z., Akrom, D. H. & Okta M. S. (2019). Validation of Diabetes Mellitus Patient Behavior Questionnaire in Primary Health Care Service. *International Journal of Public Health Science*; 8; 461–466. Retrieved from <https://doi.org/10.11591/ijphs.v8i4.18348>.
- Stolpe, S., Kroes, M. A., Webb, N. & Wisniewski, T. (2016). A Systematic Review of Insulin Adherence Measures in Patients with Diabetes. *Journal of Managed Care and Specialty Pharmacy*; 22; 1224–1246. Retrieved from <https://doi.org/10.18553/jmcp.2016.22.11.1224>.
- Strachan, M. W. & Frier, B. M. (2013). Insulin Therapy: a Pocket Guide. Springer London Heidelberg New York Dordrecht. Retrieved from <https://doi.org/10.1002/edn.231>.
- van der Ven, N. C. W., Weinger, K., Yi, J., Pouwer, F., Adèr, H., van der Ploeg, H. M., & Snoek, F. J. (2003). The Confidence in Diabetes Self-Care Scale. *Diabetes Care*; 26; 713–718. Retrieved from <https://doi.org/10.2337/diacare.26.3.713>.
- Vonna, A., Marlinda, M. & Suryawati, S. (2021). Evaluasi Pengetahuan dan Keterampilan Pasien Diabetes Melitus Tipe 2 Dalam Penggunaan Insulin Pen. *Sel Jurnal Penelitian Kesehatan*; 8; 106–116. Retrieved from <https://doi.org/10.22435/sel.v8i2.5496>.
- Wu, P. & Liu, N. (2016). Association Between Patients' Beliefs and Oral Antidiabetic Medication Adherence in a Chinese Type 2 Diabetic Population. *Patient Preference and Adherence*; 10; 1161–1167. Retrieved from <https://doi.org/10.2147/PPA.S105600>.
- Yurdugül, H. (2008). Minimum Sample Size for Cronbach'S Coefficient Alpha: a Monte-Carlo Study. *Journal of Education*; 35; 397–405.
- Yusoff, M. S. B., Arifin, W. N. & Hadie, S. N. H. (2021). ABC of Questionnaire Development and Validation for Survey Research. *Education in Medicine Journal*; 13; 97-108. Retrieved from <https://doi.org/10.21315/EIMJ2021.13.1.10>.
- Zomahoun, H. T. V., Moisan, J., Lauzier, S., Guillaumie, L., Grégoire, J. P. & Guénette, L. (2016). Predicting Noninsulin Antidiabetic Drug

Adherence Using a Theoretical Framework Based on the Theory of Planned Behavior in Adults with Type 2 Diabetes. *Medicine (United States)*; 95; 1–

10. Retrieved from <https://doi.org/10.1097/MD.0000000000002954>.



Protective Factor Evaluation of Purslane (*Portulaca grandiflora*) Magenta Flower Variety Herbs Extract Cream Formula

Bida Cincin Kirana*, Erlien Dwi Cahyani, Antonius Budiawan

Department of Pharmacy Diploma III, Vocational Faculty, Universitas Katolik Widya Mandala Surabaya, Indonesia

*Corresponding author: bida.cincin.kirana@ukwms.ac.id

Submitted: 26 June 2023

Revised: 10 December 2023

Accepted: 19 December 2023

Abstract

Background: Indonesia is an equatorial country that is rich in sunlight all year. UV light is divided into three wavelength groups: UV-A (320-400nm), UV-B (280-320nm), and UV-C (100-290nm). Intracellular chromophores in skin cell membranes such as riboflavin, porphyrin, nicotinamide, and enzymes will absorb the UV-A light. The UV-B light penetrates the dermis layer and causes DNA structure changes, which lead to wrinkles and a rising risk of skin cancer. Premature skin aging and skin cancer can be prevented with sunscreen preparation containing compounds that can protect the skin from UV radiation. Flavonoid is one of the purslane (*Portulaca grandiflora*) active metabolites that have the potency to be developed as sunscreen. **Objective:** This research aimed to determine the ability of purslane (*Portulaca grandiflora*) magenta flower variety herbs extract cream as a sunscreen as indicated by the %Te, %Tp, and Sun Protective Factor value. **Methods:** This research was an experimental study with various purslane magenta flower variety herbs extract cream formulas that were tested for their %Te, %Tp, and SPF value with a UV-Vis spectrophotometer. **Results:** The sunscreen cream preparation with 2.5% of purslane (*Portulaca grandiflora*) magenta flower variety herb extract had %Te, %Tp, and SPF values of $25.86 \pm 2.41\%$, $36.05 \pm 2.82\%$, and 3.97 ± 0.35 respectively. At the same time, preparations with 5% concentration of extract had %Te, %Tp, and SPF values of $8.23 \pm 0.86\%$, $16.65 \pm 0.92\%$, and 8.03 ± 0.38 , respectively. **Conclusion:** The sunscreen activity of all extract concentration creams was significantly different compared to the negative control (cream base) in all parameters. Flavonoids are the compounds responsible for the sunscreen activity of purslane extract.

Keywords: cream, magenta, *Portulaca grandiflora*, purslane, sun protective factor

How to cite this article:

Kirana, B. C., Cahyani, E. D. & Budiawan, A. (2023). Protective Factor Evaluation of Purslane (*Portulaca grandiflora*) Magenta Flower Variety Herbs Extract Cream Formula. *Jurnal Farmasi dan Ilmu Kefarmasian Indonesia*, 10(3), 379-385. <http://doi.org/10.20473/jfiki.v10i32023.379-385>

INTRODUCTION

One of the energy sources needed by living creatures is sunlight because of its involvement in every stage of the living process. For example, it is vitamin D generation. Otherwise, sunlight overexposure also has a negative effect.

Sunlight radiation consists of infrared light (wavelength > 760 nm), visible light (400-760 nm), and UV (ultraviolet) light consisting of UV-A (320-400 nm), UV-B (290-320 nm), as well as UV-C (200-290 nm) (Limpiangkanan & Limpiangkanan, 2010). UV-A and UV-B rays are radiation from sunlight that reaches the earth's surfaces and has an impact on the skin (Wang *et al.*, 2008). The UV-A light that reaches the skin surface will be absorbed by intracellular chromophores in cell membranes such as riboflavin, porphyrin, nicotinamide, and enzymes. This causes oxidative stress, whereas Reactive Oxygen Species (ROS) production overwhelms the natural skin antioxidant mechanism, leading to a decrease in collagen production and wrinkle appearance (Gagnani *et al.*, 2014). The UV-B light that reaches the skin will penetrate the dermis layer and cause DNA structure changes, which lead to wrinkles and rising skin cancer risk (Matsuda *et al.*, 2013).

Indonesia is a country in the equatorial area with an abundance of sunlight, which leads to high premature skin aging and skin cancer risk. Premature skin aging and skin cancer can be prevented with sunscreen preparation containing compounds that can protect the skin from UV radiation. The ability to protect skin from sunlight exposure is shown by erythema transmission percentage (%Te), pigmentation transmission percentage (%Tp), and Sun Protective Factor (SPF). Commonly, plants rich in flavonoids have a high SPF value because of their chromophore chemical structure capable of absorbing UV light radiation energy (Saewan & Jimtaisong, 2013). Besides that, flavonoids also have antioxidant activity to prevent oxidative stress so that premature skin aging and cancer risk can be prevented (Chen *et al.*, 2012).

Purslane is a plant that has been studied for its health benefits because of its various secondary metabolites. Flavonoid is one of the purslane active metabolites that have the potency to develop as sunscreen. Purslane *Portulaca grandiflora* magenta flower variety has higher levels of flavonoids compared to other varieties, making it suitable to be developed as a sunscreen (Budiawan *et al.*, 2023).

Cream is a topical preparation with a semi-solid emulsion system. This preparation is easy to use and gives a comfortable feeling in its application. In

addition, with the right cream consistency, the extracts in sunscreen can stick long enough and provide sufficient time for the flavonoid compounds to be absorbed by the skin, providing a maximum sun protection effect.

MATERIALS AND METHODS

Materials

Fresh purslane (*Portulaca grandiflora*) magenta flower variety herb was obtained from Madiun regency, East Java, Indonesia. Ethanol 96% was used the extraction process. Ceto stearyl alcohol, stearic acid, cetyl alcohol, methylparaben, propylparaben, tween 80, and aqua destilata were used to make cream base preparation. Magnesium powder, HCl 2N, C₂H₅OH, NH₃, CHCl₃, Dragendorff, Mayer, Bouchardat, FeCl₃, H₂SO₄ concentrate, and methanol pro analysis were used as reagents.

Tools

Tools used in this experiment were Spectrophotometer UV-Vis (JaSCO V-730), rotary evaporator, water bath, analytical balance, and glassware (pyrex).

Method

Extract preparation

Two hundred grams of dried purslane (*Portulaca grandiflora*) magenta flower variety herb was extracted with maceration method using 500 mL ethanol 96% for five days. The dregs were re-macerated using the same solvent for another five days. The first and second filtrates were then mixed and thickened with a rotary evaporator at 40°C until one-third of the volume was remaining. The thickened filtrates were then dried in the oven at 50°C for 24 hours until thick extract was obtained.

Phytochemical screening

1. Flavonoids Identification

Half a gram of purslane (*Portulaca grandiflora*) magenta flower variety extract was dissolved into water and transferred into a test tube. Magnesium metal and five drops of HCl 2N were added into the tube, and then the mixture was heated for 5-10 minutes. After filtration, the filtrate waited until it cooled down and was added with amil alcohol and then shaken hard. The reaction was positive if a red color formed in the amil alcohol layer (Harbone, 1987; Hanani, 2017).

2. Alkaloid Identification

Half a gram of purslane (*Portulaca grandiflora*) magenta flower variety extract was basified with 1 mL of ammonia, then chloroform was added and crushed vigorously. The chloroform liquid was filtered, the

filtrate was placed in a test tube, 2 N HCl was added, the mixture was shaken, and then left to separate. In a separate test tube: Filtrate 1: As much as one drop of Dragendorff reagent solution is dropped into the filtrate, the presence of alkaloids is indicated by the formation of precipitate or turbidity that is coloured brown. Filtrate 2: As much as one drop of Mayer's reagent solution is dripped into the filtrate, the presence of alkaloids is indicated by the formation of a white precipitate or turbidity. Filtrate 3: As a blank or negative control (Harbone, 1987; Hanani, 2017).

3. Saponin Identification

Half a gram of purslane (*Portulaca grandiflora*) magenta flower variety extract was put in a test tube, added hot water and cooled, then shaken for 10 seconds, a stable foam will form in less than 10 minutes, 1-10 cm high, and with the addition of 1 drop of HCl The 2N foam was persistence which indicated the presence of saponins (Harbone, 1987; Hanani, 2017).

4. Tannin Identification

Half a gram of purslane (*Portulaca grandiflora*) magenta flower variety extract was put into a test tube and reacted with FeCl₃ 1% solution. The extract contains tannins if a green-black or dark-blue color was formed (Harbone, 1987; Hanani, 2017).

5. Terpenoid Identification

Half a gram of purslane (*Portulaca grandiflora*) magenta flower variety extract was put into a test tube and added with chloroform and H₂SO₄ concentrated. The extract would contain terpenoids if a brown colour was formed (Harbone, 1987; Hanani, 2017).

Cream preparation

The preparation of this research cream was based on the Arisca (2018) with minor modifications. Each material was measured and the oil phase (ceto stearyl alcohol, cetyl alcohol, stearic acid, and propylparaben) was mixed. The water phase (tween 80 and methylparaben) was mixed. Both phases were heated at 80°C with a water bath until dissolved. Cream preparation was done by adding the hot water phase to

the hot oil phase and the mixture stirred at 12500 rpm until a cold cream base formed. The purslane (*Portulaca grandiflora*) magenta flower variety herb extract was added to the cream base and stirred at 20 rpm until a homogeneous cream was formed (Table 1).

Sunscreen activity test

The sunscreen activity test was carried out by determining the SPF value in vitro using the UV-Vis spectrophotometry method. The purslane magenta flower variety herbs extract cream was dissolved into methanol pro analysis to obtain a 1000 ppm concentration of test solution. After that, the test solution transmission was read at 292.5–372.5 nm wavelength (every 5 nm interval). The amount of erythema flux that was transmitted by the sunscreen agent (Ee) is calculated by the formula: $E_e = \sum T.F_e$ while the pigmentation flux is calculated by the formula: $E_p = \sum T.F_e$. %Te and %Tp value calculated by formula $\%T_e = E_e / \sum E_e$ and $\%T_p = E_p / \sum E_p$, where T= Transmition value, Fe=a constant of flux erythema, Fp= a constant of flux pigmentation (Cumpelick, 1927). SPF value measurement was done by reading the test solution absorbance at 290-320 nm wavelength with 5 nm interval (Mansur *et al.*, 1986; Mishra *et al.*, 2012) (Table 2). SPF was obtained using the formula:

$$SPF = CF \times \sum_{290}^{320} EE \times I \times Abs$$

Where: CF: correction factor, EE: erythema effect spectrum, I: light intensity spectrum, Abs: sample absorbance.

Table 2. Value of EE x I

λ (nm)	EE x I
290	0.015
295	0.0817
300	0.2874
305	0.03278
310	0.1864
315	0.0839
320	0.018

Table 1. Purslane magenta flower variety herb extract cream formula

Ingredients	Negative Control Formula (%)	2,5% Extract Formula (%)	5% Extract Formula (%)
Ceto stearyl alcohol	7	7	7
Stearic acid	7	7	7
Cetyl alcohol	6	6	6
Nipagin	0.15	0.15	0.15
Nipasol	0.05	0.05	0.05
Purslane extract	-	2.5	5
Tween 80	0.5	0.5	0.5
Aqua destilata ad	100	100	100

Table 5. %Te value of cream preparation

Replication	Negative Control (Cream Base)	Value of %Te (%) 2.5% Extract	5% Extract
I	97,56	27,36	8,97
II	90,28	23,08	8,44
III	93,06	27,14	7,29
Mean	93,64 ± 3,67	25,86 ± 2,41	8,23 ± 0,86

Data analysis

The %Te, %Tp, and SPF values were analyzed statistically using a one-way ANOVA analytical method with $\alpha = 0.05$ and followed by a post hoc test.

RESULTS AND DISCUSSION

Fresh purslane (*Portulaca grandiflora*) magenta flower variety herb dried and extracted using maceration method until 5.51 gram thick extract was obtained with 10.64% yield (Table 3).

The next step was qualitative phytochemical identification of the obtained extract. The phytochemical screening result is explained in Table 4.

Table 3. Purslane (*P. grandiflora*) magenta flower variety herb extract yield

Simplicia	Powder weight (g)	Extract weight (g)	Yield (%)
Purslane magenta flower variety herb	51.78	5.51	10.64

Table 4. Purslane (*P. grandiflora*) magenta flower variety herb extract phytochemical screening

Test	Reagent	Result
Flavonoid	Mg powder + HCl 2N + C ₂ H ₅ OH	+
Alkaloid	NH ₃ +CHCl ₃ +HCl 2N+ Dragendorff/ Mayer/Bouchardat	+
Saponin	Foam test	+
Tannin	FeCl ₃	+
Terpenoid	H ₂ SO ₄ concentrate + CHCl ₃	+

The purslane extract was used as an active ingredient in cream preparation with 2.5% and 5% concentration variations. Cream preparation was chosen because it has benefits such as being easy to use, comfortable, and easy to wash with water. The cream also has various functions as a drug carrier, skin emollient, and protection from different interferences, including sunlight.

Sunscreen preparation could contain active ingredients in an inorganic compound (reflect UV radiation) and an organic compound (absorb UV radiation). The purpose of sunscreen application is not only to protect the skin from UV rays exposure, which can trigger negative effects, but also it's expected to inhibit ROS formation, which triggers gene mutations, premature aging, and carcinogenic effects in the long term. Therefore, active antioxidant compounds that can help increase the physical activity of sunscreen are needed in sunscreen preparations. Purslane (*Portulaca grandiflora*) magenta flower variety herb extract contains various secondary metabolites and has antioxidant activity (Addor *et al.*, 2022).

The cream sunscreen activity is determined from the percentage of erythema transmission (% Te), the percentage of penetration transmission (% Tp), and the Sun Protective Factor (SPF) value (Table 5).

The percent erythema transmission value (%Te) describes the amount of UV rays exposure from the sun that hits the skin after using sunscreen, which causes erythema (redness) on the skin (Chen *et al.*, 2012). The lower the % Te value, the better the sunscreen protection to prevent erythema. Based on Table 5, the highest %

Te was in the negative control (preparation basis), which was 93.64 ± 3.67%, followed by preparations containing 2.5% extract, which was 25.86 ± 2.41%, and the lowest was the preparation with 5% extract, which was 8.23 ± 0.86%. Based on the statistical test results, it showed that there was a significant difference in the % Te value both in the negative control preparations with 2.5% and 5% extract. This indicates that the extract concentration determines the erythema transmission value of sunscreen preparations.

The percentage value of pigmentation transmission (% Tp) describes the amount of exposure to UV rays from the sun that hits the skin after using sunscreen, which causes pigmentation of the skin. As with % Te, the lower % Tp value indicates better protection of sunscreen against pigmentation on the skin.

Table 6. %Tp value of cream preparation

Replication	Negative Control (Cream Base)	Value of %Tp (%) 2.5% Ekstrak	5% Extract
I	98.29	36.69	17.46
II	91.49	32.96	16.83
III	95.66	38.49	15.65
Mean	95.15 ± 3.43	36.05 ± 2.82	16.65 ± 0.92

Table 7. SPF value of cream preparation

Replication	Negative Control (Cream Base)	Value of SPF 2.5% Ekstrak	5% Extract
I	0.18	3.84	7.83
II	0.16	3.71	8.47
III	0.19	4.37	7.79
Mean	0.18 ± 0.02	3.97 ± 0.35	8.03 ± 0.38

Based on Table 6, shows that the highest % Tp was in the negative control (preparation basis), which was 95.15 ± 3.43 , followed by preparations containing 2.5% extract, which was 36.05 ± 2.82 , and the lowest is a preparation with 5% extract, namely 16.65 ± 0.92 . Based on the results of statistical tests, there was a significant difference in % Tp value in the negative control, preparations with 2.5%, and 5% extract with a $p > 0.05$. This shows that the extract concentration in preparation determines the pigmentation transmission value of the sunscreen preparation.

The SPF value states how many times the skin's natural resistance is multiplied so that it is safe in the sun without experiencing sunburn¹⁶. Based on the test result, the SPF value also shows an increasing trend with increasing extract concentration in the preparation. Based on Table 7, it can be seen that the lowest SPF value was in the negative control (preparation base), which was 0.18 ± 0.02 , followed by preparations containing 2.5% extract, which was 3.97 ± 0.35 , and those having the highest was the preparation with 5% extract, namely 8.03 ± 0.38 . Based on the results of statistical tests, it showed that there was a significant difference in the SPF value in the negative control, preparations with extracts of 2.5%, and 5% with $p > 0.05$. This shows that the extract concentration determines the SPF value of the sunscreen preparation.

Based on these results, a cream preparation containing 5% purslane herb extract had a higher % Te and % Tp value compared to preparations containing 2.5% purslane herb extract. At the % Tp value, both preparations showed the maximum protection, which was in the sunblock category, while based on % Te, the protection was still in the tanning and suntan categories (Kasitowati *et al.*, 2021). To obtain better protection

based on the % Te value, a higher extract content is needed in the preparation.

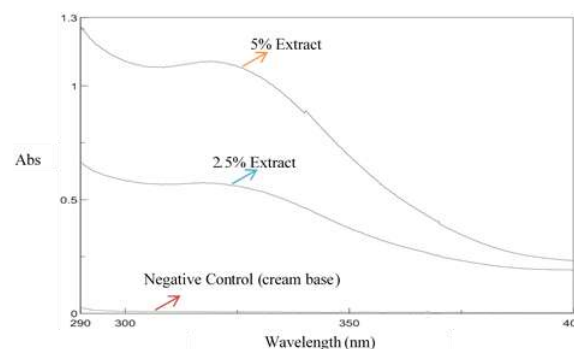


Figure 1. Absorbance spectra at 290-400 nm wavelength of cream preparation

The potential for sunscreen activity can be expressed through the value of the Sun Protective Factor (SPF). The SPF value is determined from the absorption results of the preparation at UV wavelengths between 290 – 400 nm (Figure 1). Based on the research results, it was obtained that the SPF values of cream preparations containing 2.5% and 5% purslane herb extract were 3.97 ± 0.35 and 8.03 ± 0.38 , respectively. Both of these SPF values are less than 12, which is in the minimal protection category. This SPF value is not optimal for providing protection because, with an SPF value of less than 15, protection is only given for 1.5 hours (Buso *et al.*, 2017).

Statistical tests were carried out to determine whether there were differences in sunscreen activity in each preparation. Based on statistical tests using one-way ANOVA, a significance value of < 0.05 was obtained for both the %Te, %Tp, and SPF values. This means that the purslane herb extract concentration in preparation determines the sunscreen activity. The

higher the extract concentration in the preparation, the better the sunscreen protection will be.

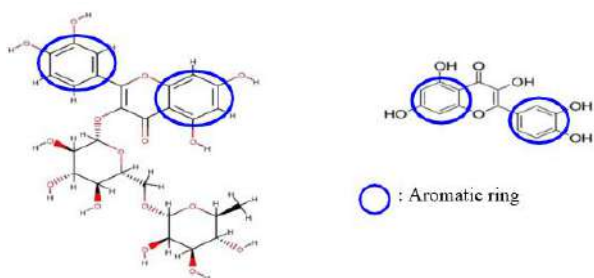


Figure 2. Structure of flavonoid A: rutin, B: quercetin (Ganeshpurkar *et al.*, 2017; El-Saber Batiha *et al.*, 2020)

Flavonoids are compounds contained in purslane herb extracts that are thought to have sunscreen activity (Cahyani *et al.*, 2022). Flavonoids can absorb energy at UV light wavelengths because they have covalent bonds in their structure. Flavonoids can absorb energy at a wavelength of 240-290 nm, and flavonoids that have conjugated covalent bonds can absorb at a wavelength of up to 550 nm (He *et al.*, 2021). The Magenta flower variety purslane herb contains the and most significant amount of flavonoids compared to other variants. Therefore, this study used extracts from the purslane herb with the magenta flower variant. Flavonoids contained in purslane (*Portulaca grandiflora*) herb are rutin, quercetin, and isoquercetin compounds (Husein *et al.*, 2021). Flavonoids have at least two aromatic rings with a basic carbon skeleton consisting of 15 C atoms forming C6-C3-C6 (Figure 2) (Julianto, 2019).

CONCLUSION

The sunscreen cream preparation with 2.5% of purslane (*Portulaca grandiflora*) magenta flower variety herb extract had %Te, %Tp, and SPF values of $25.86 \pm 2.41\%$, $36.05 \pm 2.82\%$, and 3.97 ± 0.35 respectively. In comparison, preparations with 5% concentration of extract had %Te, %Tp, and SPF values of $8.23 \pm 0.86\%$, $16.65 \pm 0.92\%$, and 8.03 ± 0.38 , respectively. The sunscreen activity of all extract concentration creams was significantly different compared to the negative control (cream base) in all parameters. Flavonoids are the compounds responsible for the sunscreen activity of purslane (*Portulaca grandiflora*) magenta flower variety herb extract.

AUTHOR CONTRIBUTIONS

Conceptualization, B. C. K., E. D. C., A. B.; Methodology, B. C. K., E. D. C.; Software, E. D. C., A. B.; Validation, B. C. K., E. D. C.; Formal Analysis, B.

C. K., A. B.; Investigation, E. D. C., A. B.; Resources, B. C. K.; Data Curation, B. C. K.; Writing - Original Draft, B. C. K., E. D. C., A. B.; Writing - Review & Editing, A. B.; Visualization, E. D. C.; Supervision, B. C. K.; Project Administration, B. C. K.; Funding Acquisition, B. C. K.

FUNDING STATEMENT

This research did not receive any specific grant from funding agencies in the public, commercial, or not for profit sectors.

CONFLICT OF INTEREST

The authors declared no conflict of interest.

REFERENCES

- Addor, F. A. S. A., Barcaui, C. B., Gomes, E. E., Lupi, O., Marçon, C. R. & Miot, H. A. (2022). Sunscreen Lotions in the dermatological prescription: review of concepts and controversies. *Anais Brasileiros de Dermatologia*; 97(2); 204–222. doi: 10.1016/j.abd.2021.05.012
- Arisca, H. (2018). Uji Aktivitas Antioksidan Ekstrak Angkak dan Formulasinya dalam Sediaan Krim yang Diuji Daya Penetrasi dan Keamanan pada Kelinci. *Skripsi*; Universitas Setia Budi Surakarta.
- Budiawan, A., Purwanto, A., Puradewa, L., Cahyani, E. D. & Purwaningsih, C. E. (2023). Wound Healing Activity and Flavonoid Contents of Purslane (*Portulaca grandiflora*) of Various Varieties. *RSC Advances*; 13; 9871-9877. doi: 10.1039/D3RA00868A.
- Buso, P., Radice, M., Baldisserotto, A., Manfredini, S., & Vertuani, S. (2017). Guideline for The Development of Herbal-Based Sunscreen. London: IntechOpen. doi: 10.5772/intechopen.72712.
- Cahyani, E. D., Budiawan, A. & Puradewa, L. (2022). Sunscreen Activity of Soursop Seeds Extract. *Strada Journal of Pharmacy*; 4; 23-26
- Chen, L., Hu, J. Y. & Wang, S. Q. (2012). The Role of Antioxidants in Photoprotection: A Critical Review. *Journal of the American Academy of Dermatology*; 67; 1013–1024. doi: 10.1016/j.jaad.2012.02.009.
- Cumpelick, B. (1927). Analytical Procedures and Evaluation of Sunscreens. *Journal of the Society of Cosmetics Chemists*; 23; 333–345.
- El-Saber Batiha, G., Beshbishy, A. M., Ikram, M., Mulla, Z. S., Abd El-Hack, M. E., Taha, A. E., Algammal, A. M. & Ali Elewa, Y. H. (2020). The

- Pharmacological Activity, Biochemical Properties, and Pharmacokinetics of the Major Natural Polyphenolic Flavonoid: Quercetin. *Foods*; 9; 1-16. doi: 10.3390/foods9030374.
- Ganeshpurkar, A. & Saluja, A. K. (2017). The Pharmacological Potential of Rutin. *Saudi Pharmaceutical Journal*; 25; 149–164. doi: 10.1016/j.jsps.2016.04.025.
- Graghani, A., Cornick, S. Mac, Chominski, V., Ribeiro de Noronha, S. M., Alves Corrêa de Noronha, S. A. & Ferreira, L. M. (2014). Review of Major Theories of Skin Aging. *Advances in Aging Research*; 3; 265–284. doi: 10.4236/aar.2014.34036.
- Hanani, E. (2017). Analisis Fitokimia. Jakarta: Buku Kedokteran EGC.
- Harbone, J. (1987). Metode Fitokimia Edisi Kedua. Padmawinata K. Soediro I. penerjemah. Terjemahan dari Phytochemical Methods. Bandung: ITB.
- He, H., Li, A., Li, S., Tang, J., Li, L., & Xiong, L. (2021). Natural Components in Sunscreens: Topical Formulations with Sun Protection Factor (SPF). *Biomedicine and Pharmacotherapy*; 134; 1-11. doi: 10.1016/j.biopha.2020.111161.
- Husein, S. G., Sundalian, M. & Husna, N. (2021). Review: Component Analysis of Purslanes Chemicals Compound (*Portulaca oleraceae* L. and *Portulaca grandiflora* Hook.). *Jurnal Sains dan Kesehatan*; 3; 317–327.
- Julianto, T. S. (2019). Fitokimia: Tinjauan Metabolit Sekunder dan Skrining Fitokimia. Yogyakarta: Universitas Islam Indonesia.
- Kasitowati, R., Wahyudi, A., Asmara, R., Aliviyanti, D., Iranawati, F., Panjaitan, M. A. P., Pratiwi, D. C. & Arsad, S. (2021). Identification Photoprotective Activity of Marine Seaweed: *Eucheuma sp.* *International Conference on Biotechnology and Food Sciences*; 679; 1–5. doi: 10.1088/1755-1315/679/1/012014.
- Limpiangkanan, W. & Limpiangkanan, W. (2010). Special Article: Photo-aging: A Literature Review. *Journal of the Medical Association of Thailand*; 93; 753–757.
- Mansur, J. S., Breder, M. N., Mansur, M. C. & Azulay, R. D. (1986). Determination of Sun Protective Factor by Spectrophotometry. *An Bras Dermatol*; 61; 121–124.
- Matsuda, M., Hoshino, T., Yamakawa, N., Tahara, K., Adachi, H., Sobue, G., Maji, D., Ihn, H. & Mizushima, T. (2013). Suppression of UV-Induced Wrinkle Formation by Induction of HSP70 Expression in Mice. *Journal of Investigative Dermatology*; 133; 919–928. doi: 10.1038/jid.2012.383.
- Mishra, A. K., Mishra, A. & Chattopadhyay, P. (2012). Assessment of In Vitro Sun Protection Factor of *Calendula officinalis* L. (*asteraceae*) Essential Oil Formulation. *Journal of Young Pharmacists*; 4; 17–21. doi: 10.4103/0975-1483.93575.
- Saewan, N. & Jimtaisong, A. (2013). Photoprotection of Natural Flavonoids. *Journal of Applied Pharmaceutical Science*; 3; 129–141. doi: 10.7324/JAPS.2013.3923.
- Wang, S. Q., Stanfield, M. S. & Osterwalder, U. (2008). In Vitro Assessment of UV A Protection by Populer Sunscreen Available in the United States. *Journal of America Dermatology*; 59; 934- 942.



Green Tea Dregs (*Camellia sinensis* (L.) Extraction Method Effect on *Cutibacterium acnes* and Development of Spot Cream

Maria Odelia Vania Arief¹, Caroline Lieanto¹, Jessica Mei Sabani¹, Purwanto^{2*}

¹Undergraduate student, Faculty of Pharmacy, Universitas Gadjah Mada, Yogyakarta, Indonesia

²Department of Pharmaceutical Biology, Faculty of Pharmacy, Universitas Gadjah Mada, Yogyakarta, Indonesia

*Corresponding author: purwanto_fa@ugm.ac.id

Submitted: 31 August 2023

Revised: 12 December 2023

Accepted: 20 December 2023

Abstract

Background: Acne is a prevalent skin health problem experienced by teenagers and adults. Green tea is one of the plants that can be used to treat acne. Green tea dregs contain catechins, which have antibacterial activity that causes acne. **Objective:** This study aims to determine the antibacterial activity of green tea dregs extract against *Cutibacterium acnes* bacteria. **Methods:** This study used two brewing time variations and three green tea dregs with maceration variations. The obtained extract was then analyzed for its catechin content using the total phenolic test. Section, which has a high phenolic content, was then tested for its activity against *Cutibacterium acnes* bacteria using the microdilution method to obtain the MIC₅₀ value. The extract with a brewing time of 2 minutes and the ultrasonic-assisted extraction maceration method had the highest MIC₅₀ value of 8.586 mg/mL. The MIC₅₀ value references extract concentrations used in acne spot cream formulations. The cream obtained after the stability test is semisolid, brown, and smells like tea. Spot cream is also homogeneous and meets the pH range in cosmetic preparations of 5.5. However, the viscosity of spot cream decreased significantly after storage to 4546 cPoise from 8106 cPoise. The decrease in the viscosity of the cream was caused by the catechin content in green tea dregs extract, which is acidic, thus reducing the effectiveness of the emulsifier in the form of triethanolamine, which is alkaline. The decrease in viscosity of the cream also caused the spreadability of the cream to increase and the stickiness of the cream to decrease.

Keywords: acne spot cream, brewing time, catechin, *Cutibacterium acnes*, green tea dregs

How to cite this article:

Arief, M. O. V., Lieanto, C., Sabani, J. M. & Purwanto. (2023). Green Tea Dregs (*Camellia sinensis* (L.) Green Tea Dregs (*Camellia sinensis* (L.) Extraction Method Effect on *Cutibacterium acnes* and Development of Spot Cream. *Jurnal Farmasi dan Ilmu Kefarmasian Indonesia*, 10(3), 386-394. <http://doi.org/10.20473/jfiki.v10i32023.386-394>

INTRODUCTION

Acne is a common condition in which there is an overproduction of oil in the skin that leads to clogging the hair follicles. Clogged hair follicles lead to inflammation of skin pores, which is characterized by red discoloration of the skin as well as small pus-filled bumps that are known as pimples (Aslam *et al.*, 2015). *Cutibacterium acnes* is present in the fatty acids of sebum secreted by sebaceous glands in skin follicles and produces lipases that facilitate the breakdown of sebum-free short-chain fatty acids that are pro-inflammatory (McLaughlin *et al.*, 2019).

Because of this reason, *C. acnes* is a common bacteria that is chosen in the case of antiacne activity analysis of a drug. Clinical and laboratory studies in the last 20 years reported that many natural ingredients are potent antiacne agents.

One of the natural ingredients that is widely used in the treatment of acne is green tea. According to research from Peluso & Serafini (2017), green tea has more substantial antioxidant potential than black tea and oolong tea. These antioxidant properties are attributed to the catechin content in green tea. Catechins are likely and efficacious in treating acne as they have apoptotic, sebo-suppressive, anti-inflammatory, and antibacterial effects against *C. acnes* (Yoon *et al.*, 2013).

Indonesians have long used green tea dregs as a facial beauty treatment. According to Soetjipto *et al.* (2012), green tea dregs still have antioxidant and polyphenol activity. Green tea dregs help brighten the skin, overcome acne, remove panda eyes, and soothe the skin. Green tea waste as an antiacne is commonly used as a mask. The green tea dregs mask is left to dry and rinse with water.

Based on this phenomenon, researchers are interested in knowing the potential of green tea dregs as an antiacne agent. Two variables will be tested in this study: tea brewing time and the extraction method of brewed tea dregs. Brewing time will significantly affect the content of dissolved chemicals, colour intensity, and aroma of the tea to be consumed.

The extraction method used in this study is maceration with several modifications, that are maceration at room temperature, maceration at 60°C (digestion), and maceration with ultrasonic-assisted extraction. Acne patch cream preparation was chosen to treat acne to obtain local effects in drug delivery to the skin layer, especially on problem skin (Rai *et al.*, 2019).

MATERIALS AND METHODS

Materials

Green tea (Brand A), technical ethanol (Bratako), distilled water, Na₂CO₃ (Merck), Folin reagent (Merck), Brain Heart Infusion media (Merck), *Cutibacterium acnes* bacteria, 96 well microplates (Iwaki), blue tip (Socorex), yellow tip (Socorex), white tip (Socorex), stearic acid, glycerin, propylparaben, methylparaben, triethanolamine, cetyl alcohol, and pH stick (Merck).

Tools

Analytical scales (Mettler Toledo AL204), flannel cloth, oven (Memmert), hot plate, autoclave (Hirayama Hiclave HVE-50), incubator (Sakura, Japan), laminar airflow (Nuair Airegard NU-126-400E), Bunsen burner, micropipette (Socorex), microplate reader (AMR-100-Allsheng), vortex (Thermo Scientific), mortar, stamper, overhead stirrer (IKA) and Brookfield viscometer (Lamy Rheology B One Plus).

Method

Determination of green tea leaf

Determination of green tea leaf (*Camellia sinensis* (L.) O. Kuntze) used in this study was carried out at the Cell Biology-Microbiology Laboratory, Department of Pharmaceutical Biology, Gadjah Mada University.

Brewing and preparation of dry dregs

Green tea leaves were weighed as much as 300 g and then brewed using 1000 mL of distilled water at 100°C for 2 minutes and 5 minutes. The brewed green tea was then filtered by a flannel cloth until the water was drained. The green tea dregs were then dried in an oven at 50°C for 1x24 hours until completely dry. The dried material was then pulverized by a mortar and stamper.

Extraction

Extraction optimization was carried out on tea grounds in three extraction methods, namely cold maceration for 3x24 at room temperature, maceration with digestion for 6 hours at 60°C using a water bath, and maceration with ultrasonic-assisted extraction (UAE) for 30 minutes at room temperature by an ultrasonic chamber. The weight of dry tea leaf dregs for one maceration was 75 grams. Ethanol with 70% concentration is used as a solvent because it is polar and can attract polyphenolic compounds in green tea pulp, which are opposite in nature. In addition, ethanol has a low boiling point, which is 79°C, so it requires less heat for the concentration process. The ratio of the weight of the dry tea leaf dregs to the volume of the liquid was 1:7 *b/v*. Filtration was carried out to separate the filtrates and

residue. The filtrates were then evaporated in a water bath at 60°C until a slightly thick extract was obtained and then dried by the freeze-drying method.

Total phenolic test with folin-ciocalteau colorimetric method

The Folin-Ciocalteau colourimetric method is based on the chemical reduction of the reagent, a mixture of tungsten and molybdenum oxide based on the method (Singleton *et al.*, 1999). The content of total phenolic compounds in the extract was expressed as gallic acid equivalents (mg/g extract) based on the regression equation of the gallic acid calibration curve. Sample solution (150 uL) and gallic acid standard solution (0, 25, 50, 75, 100, 150, 175, and 200 uL) were pipetted into test tubes. Distilled water was added to 4 mL and 250 uL Folin-Ciocalteau. The mixture was then shaken until homogeneous. After standing for 8 minutes, 750 ul of 20% Na₂CO₃ was added and homogenized. The mixture was then allowed to stand for 2 hours at room temperature. The absorbance was measured at a wavelength of 749 nm. The measurement was repeated in triplicate to obtain the phenol content as gallic acid equivalent (mg GAE/g sample).

Antibacterial activity test by microdilution method

C. acnes from glycerol stock was streaked on sterile Brain Heart Infusion (BHI) medium in a petri dish and incubated at 37°C for 24 hours under anaerobic conditions in a jar incubator. To prepare the starter, one tip of the *C. acnes* culture was inoculated in 5 mL of Brain Heart Infusion Broth (BHIB) media in a test tube aseptically, then vortexed and incubated at 37°C for 2

hours. The bacterial suspension was standardized using a spectrophotometer at a wavelength of 600 nm to obtain an OD of 0,08 – 0,13, which is equivalent to 1,5 x 10⁸ CFU/mL (CSLI, 2017). The antibacterial activity test was carried out by microdilution method in BHI media with varying concentrations of green tea dregs extract of 3 mg/mL, 5 mg/mL, and 10 mg/mL in 1% DMSO solution. A mixture of 5 µL of *C. acnes* bacteria suspension, 50 µL of extract, and 145 µL of BHI media were pipetted into the wells as treatments and replicated three times. The negative control consisted of 145 µL of BHI media, 5 µL of bacterial suspension, and 50 µL of 1% DMSO. The inhibition calculation used the following formula (CLSI, 2017).

$$\%Inhibition = \frac{(Negative\ control\ absorbance - Treatment\ absorbance)}{Negative\ control\ absorbance} \times 100\%$$

Acne spot cream formulation

The formulation of green tea dregs extract spot cream preparation refers to the formula optimization results of Karmilah & Musdalipah (2018), with minor modifications, which can be seen in Table 1 (Arief, 2023).

Physical stability test of cream preparation

The stability test conducted in this study was an accelerated stability test by a climatic chamber for one month with a temperature of 40°C ± 2°C and RH 75% ± 5% and testing intervals every one week (CSLI, 2012). Tests that are conducted every week include organoleptic, homogeneity, viscosity, pH, spreadability, and adhesion tests, as seen in Table 2.

Table 1. The formula of green tea dregs extract spot cream (Karmilah & Musdalipah (2018)). The amount of extract was performed based on the MIC50 value of microdilution analysis

Composition	Cream Formula (%)		Usability
	Control	Extract	
Stearic acid	10	10	Oil base
Glycerin	10	10	Humectants
Cetyl alcohol	3	3	Oil base
Liquid paraffin	2	2	Emollients
Triethanolamine	1	1	Emulgator
Green tea dregs extract	-	0,9	Active substance
Methylparaben	0,2	0,2	Preservatives
Propylparaben	0,05	0,05	Preservatives
Distilled water	ad 100	ad 100	Solvents

Table 2. Test methods are conducted every week in the physical stability test of cream preparation. Each test was performed in triplicate

Tests	Test methods
Organoleptic test	The organoleptic test was carried out by observing the physical appearance of the preparation consisting of shape, colour, and odour (Saryanti <i>et al.</i> , 2019).
Homogeneity test	The homogeneity test was conducted by weighing 0.1 g of cream and then applying it evenly to the glass object. The cream preparation must be homogeneous, characterized by absence of coarse particles that appear in the preparation (Saryanti <i>et al.</i> , 2019).
Viscosity test	Viscosity measurements were carried out at 25°C using a Brookfield viscometer, namely by installing spindle No. 6 on the device and then dipping it into the preparation to a specific limit and setting a speed of 100 rpm for 15 seconds (Saryanti <i>et al.</i> , 2019).
pH test	The pH measurement was carried out using a Merck brand pH stick. The pH tolerance range of the cream ranges from 4.0-7.5 (Saryanti <i>et al.</i> , 2019).
Spreadability test	A 0.5 g of cream preparation was placed on a glass on a millimetre block of paper. The glass was then covered with another transparent glass and left for 1 minute to obtain the diameter of the spread. Next, a load of 50 g to 250 g was added to the glass every 1 minute, and the diameter of the spread formed was observed. The cream preparation is expected to spread readily and evenly.
Adhesive test	A 0.5 g of cream preparation is placed on a glass object marked 4 x 2 cm. Another object glass is placed on top of the preparation and given a load of 1 Kg for 5 minutes. The test glass was placed on the test device and given a load of 80 grams. The load that has been installed is dropped, and the time until the two glass objects are released after the load is dropped is recorded.

Data analysis

Data analysis was carried out using SPSS version 20.0. The obtained data were then analyzed for normality. The normality test ensures that the research data comes from a population with a normal distribution. The normality test was conducted by Saphiro-Wilk with a confidence level of 95%. If the significance value of p-value > 0.05, it can be said that the data is normally distributed and vice versa (Rohman, 2014). Normally distributed data were tested for significance with One-Way ANOVA with a 95% confidence level.

RESULTS AND DISCUSSION

Brewing brand A green tea for 2 and 5 minutes at 100°C was chosen because it is the time and temperature commonly used by the public. In addition, 100°C produces the highest catechin content compared to 70°C and 85°C (Chadijah & Qaddafi, 2021). After brewing, the green tea was drained by a flannel cloth, then arranged on a tray, and dried in an oven at 50°C for 1x24 hours. The temperature of 50°C was chosen because catechins are not resistant to high heat and will degrade at 98°C (Vuong *et al.*, 2011). The code of variation of brewing time and extraction method can be seen in Table 3.

Table 3. Brewing time variation code and extraction method

Code	Brewing time	Extraction method
2A	2 minutes	Cold maceration
2B	2 minutes	Maceration with digestion
2C	2 minutes	Maceration with ultrasonic-assisted extraction (UAE)
5A	5 minutes	Cold maceration
5B	5 minutes	Maceration with digestion
5C	5 minutes	Maceration with ultrasonic-assisted extraction (UAE)

The drying of green tea dregs macerate was carried out using the vacuum freeze-drying method. This method is drying materials by reducing the ambient temperature pressure to allow sublimation, transferring the solid phase to the gas phase without going through the liquid phase. This method is used because it can dry materials without heating, thereby reducing product damage due to high temperatures, and the dried product has an attractive physical shape.

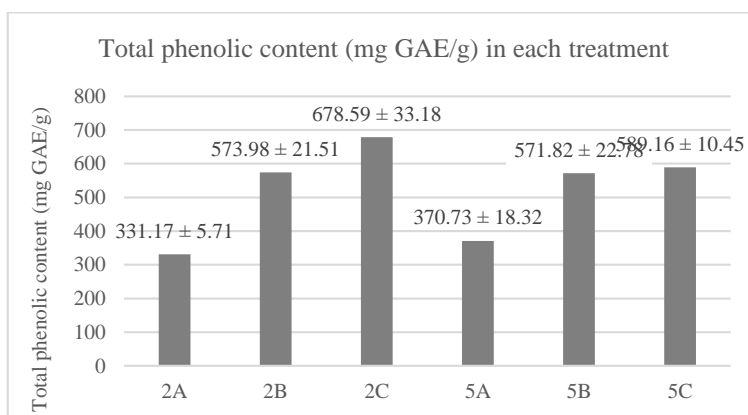


Figure 1. Total phenolic content (mg GAE/g) in each treatment. Each sample was performed in triplicate

Percent extract yield (Table 4) was obtained by calculating the ratio of the tea dregs extract produced's dry weight to the raw material used multiplied by 100%. The extract obtained is brownish green, smells typical of tea, and tastes like chelate. The yield of green tea dregs extract ranges from 12.56 - 20.99%. Green tea dregs extract yield with a brewing time of 2 minutes is greater than 5 minutes, following the theory that the faster the brewing time, the more compounds are left in the dregs.

Table 4. The yield of green tea dregs extracts of each treatment

Brewing time	Extraction method	Mass of extract (gram)	Extract yield (%)
2 minutes	Cold maceration	9.76	13.02
	Maceration with digestion	15.74	20.99
	Maceration with UAE	15.07	20.09
5 minutes	Cold maceration	9.42	12.56
	Maceration with digestion	12.81	17.08
	Maceration with UAE	11.95	15.93

The extract was then tested for total phenolic content by a colourimetric method. The maximum wavelength of gallic acid was determined by measuring a gallic acid solution with a concentration of 150 ppm in the wavelength range of 400 - 800 nm with a UV-Vis spectrophotometer. The maximum wavelength obtained was 749 nm. The maximum wavelength is needed because it will provide optimal absorption of phenolic compounds with high sensitivity. Gallic acid reacts with the Folin-Ciocalteu reagent in an alkaline atmosphere to produce a blue colour, indicating the presence of

phenolic compounds. The more intense the blue colour formed, the greater the concentration of phenolic ions formed.

The absorbance of the gallic acid solution obtained is made in the form of a standard curve and the equation $y = 0.0041x + 0.003$ and R^2 0.998, which can be concluded that the data obtained is linear. The eligibility requirements for acceptable analytical methods for the correlation coefficient (R) of the range 0.996 - 1 will be used to determine the total phenolic content of green tea dregs extract. Measurement of total phenolic compounds was made as many as three replicates for precision purposes with phenol content obtained as gallic acid equivalent (mg GAE/g sample) as attached in Figure 1.

Based on Figure 1., the average total phenolic content of green tea dregs extract was 331,17 mg GAE/g in treatment 2A; 370,73 in treatment 5A; 573,98 in treatment 2B; 571,82 in treatment 5B; 678,59 in treatment 2C; and 589,16 in treatment 5C. The highest total phenolic test results were obtained in the 2C extract of 0,679 mg GAE/g, which means that every 1 gram of sample contained 0,679 mg gallic acid equivalent.

Furthermore, data analysis carried out by SPSS indicated that the data is customarily distributed and homogeneous. However, the significance of 0,00 was obtained after the One-Way ANOVA test so it can be concluded that there is a significant difference between the average total phenolic content in each treatment code. The homogeneous subset posthoc test found that green tea dregs' average total phenolic content was grouped into three subsets. In subset 1, there are treatment codes 2A and 5A; in subset 2, there are treatment codes 2B, 5B, and 5C. In subset 3, there is only treatment code 2C.

So, the highest average total phenolic is the sample with treatment code 2C of 0,679 mg GAE/g. The

average total phenolics of samples with treatment codes 2B, 5B, and 5C were not significantly different. The insignificant difference between the average total phenolic content of samples brewed for 2 and 5 minutes in each maceration treatment was due to the narrow difference between the brewing times. The significant differences between the mean total phenolic content of cold macerated green tea dregs, maceration with digestion, and UAE maceration were due to temperature and ultrasonication. Maceration with digestion and UAE did not significantly differ in the average total phenolic content because both maceration processes can increase the solubility of the extracted active substances, whereas in the ultrasonication methods, there is an agitation that helps the diffusion process of active ingredients.

Only the two subsets with the highest phenolic content were then tested for antibacterial activity using the microdilution method because they were considered to have better antibacterial activity against *C. acnes* bacteria. Therefore, the antibacterial activity test was conducted on samples with treatment codes 2B, 2C, 5B, and 5C.

The bacterial suspension was standardized by a spectrophotometer at a wavelength of 600 nm to obtain an OD of 0,08 – 0,13. This OD was chosen because the bacteria are in the exponential phase in this range (Martins *et al.*, 2011). The incubation time of 18 hours was determined because it follows CLSI (2012) guidelines, which are 18-24 hours. The incubation temperature of 37°C was chosen because it corresponds to the optimum temperature for bacterial growth (Tellu *et al.*, 2019). Meanwhile, concentrations of 3 mg/mL, 5 mg/mL, and 10 mg/mL were selected based on preliminary tests that fall into the range required to obtain the MIC₅₀ value.

The amount of bacterial inhibition was obtained from turbidity readings using a microplate reader at OD 600 nm. The wavelength of 600 nm was chosen because it only measures the level of light scattering caused by bacteria in a culture and does not absorb bacterial growth media, which impacts increasing absorbance (Martins *et al.*, 2011). The absorbance obtained was then compared with the absorbance of the negative control to determine the inhibitory value of the extract against *C. acnes* bacteria, and the data attached in Table 5 was obtained.

Based on Table 5, it is known that the highest antibacterial potential is 2C code with a MIC₅₀ value of 8,958 mg/mL. This value means that the extract concentration needed to inhibit 50% bacterial growth is 8,958 mg/mL. The order of antibacterial activity in the

four samples from the highest is 2C with an MIC₅₀ value of 8,958 mg/mL; then 2B at 9,060 mg/mL; 5B at 9,091 mg/mL, and the lowest 5C at 9,189 mg/mL.

Table 5. Percent inhibition and MIC₅₀ value of each treatment. Only samples with maceration treatment B and C were tested for their MIC because of high phenolic content

Sample	Concentration	Percent inhibition	MIC ₅₀ value
2B	3 mg/mL	30.304	9.060
	5 mg/mL	39.746	
	10 mg/mL	52.294	
2C	3 mg/mL	32.086	8.958
	5 mg/mL	39.834	
	10 mg/mL	52.683	
5B	3 mg/mL	28.221	9.091
	5 mg/mL	39.552	
	10 mg/mL	51.518	
5C	3 mg/mL	29.827	9.189
	5 mg/mL	38.281	
	10 mg/mL	52.171	

Furthermore, data analysis carried out by SPSS indicated that the data is homogeneous. However, the significance of 0.960 was obtained after the One-Way ANOVA analysis, so it can be concluded that there is no significant difference between the MIC₅₀ values in each treatment code.

The insignificant difference between the MIC₅₀ values in each treatment is associated with the average total phenolic content, which is also not significantly different. Not all phenolic compounds contained in the extract have activity against *C. acnes*. Green tea contains phenolic compounds in the form of catechins, epicatechins, epicatechin gallate, epigallocatechin gallate, gallic acid, teaflavin, and Gallocatechin (Khan & Mukhtar, 2019). In addition, the MIC₅₀ value of green tea dregs extract against *C. acnes* obtained was not potent because it was more than 100 µg/mL. The low potency of the material in this investigation could be attributed to a brief maceration treatment lasting approximately 2-5 minutes. Another possibility is the usage of waste. Tea dreg means there is a previous process (maceration for drinking purposes) before maceration to get a sample for antibacterial purposes. In addition, low-quality green tea is used. According to research by Koch *et al.* (2018), the quality of green tea affects the catechin content contained in the extract, where the highest catechin content was obtained in green tea samples from Japan.

The stability of pharmaceutical preparations is defined as the ability of a preparation in a specific packaging system to maintain physical, chemical, microbiological, and pharmacological specifications during storage and application. The stability test used in this study was an accelerated stability test for one month in a climatic chamber with a temperature of $40^{\circ}\text{C} \pm 2^{\circ}\text{C}$ and RH $75\% \pm 5\%$ and a testing interval of one week. The cream preparation in each replication has a distinctive smell of tea and a brown colour derived from green tea dregs extract. It is homogeneous, which is characterized by the absence of coarse particles and even color visible in the preparation. The cream preparation in each replication also has the same pH of 5.5. This value shows that the preparation is stable both before and after storage with an accelerated stability test.

However, the cream preparation viscosity decreased after storage with accelerated stability (Figure 2). This decrease in value probably can be caused by increasing storage temperature and absorption of water from the surrounding environment by moisture-absorbing ingredients in the formula, such as glycerin. Furthermore, the acidic green tea dregs extract lowers the efficiency of the alkaline triethanolamine, making the preparation thinner.

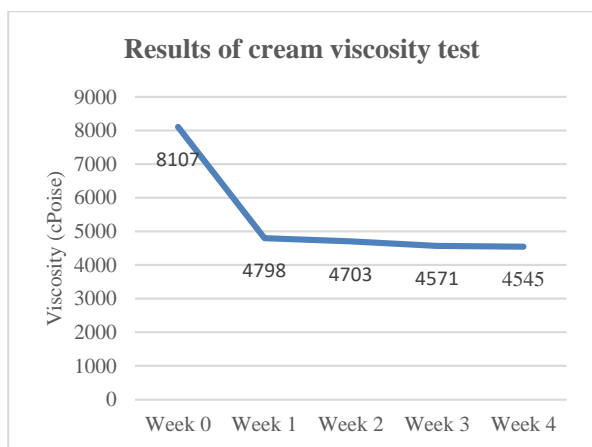


Figure 2. Results of cream viscosity test

The significance of 0,00 was obtained after the homogeneity test so that the One-Way ANOVA analysis could not be carried out and replaced with the non-parametric Kruskal-Wallis test and obtained the results of cream viscosity in week four was not significantly different from weeks 2 and 3, but significantly different from weeks 0 and 1. The cream viscosity of week 3 was not significantly different from week two but significantly different from weeks 0 and 1. On the other parameter, spreadability testing on cream preparations

increased after storage with accelerated stability (Figure 3). The increase in spreadability was due to the decreased viscosity of the cream after stability testing.

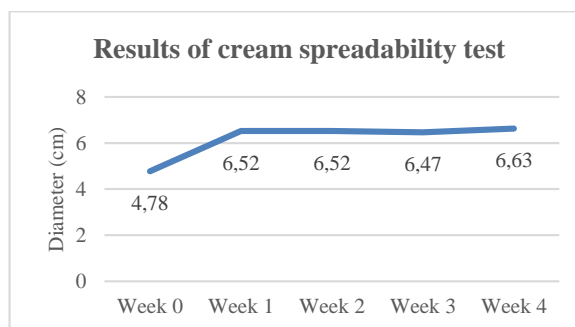


Figure 3. Results of cream spreadability test

A significance of 0,00 was obtained after the one-way ANOVA analysis, so it can be concluded that there is a significant difference between the averages of each week. In the homogeneous subset posthoc test, it was found that the spreadability of the total cream was grouped into three subsets. In subset 1, there is only week 0. In subset 2, there are weeks 1, 2, and 3 (not significantly different). So, the spreadability of green tea dregs extract cream in week 0 experienced a static increase in weeks 1, 2, and 3. Then, increase again in week 4.

Testing the adhesion of the cream preparation showed a decrease after storage with accelerated stability (Figure 4) due to the viscosity of the cream, which decreased after stability testing. A significance of 0,00 was obtained after po analysis, so it can be concluded that there is a significant difference between the means of each week. In the homogeneous subset post-hoc test, it was found that the stickiness of the patch cream was grouped into three subsets. In subset 1, there is only week 4. In subset 2, there are weeks 1, 2, and 3 (not significantly different). So, the adhesion of green tea pulp extract cream in week 0 experienced a static decrease in weeks 1, 2, and 3. Then, it decreased again in week 4.

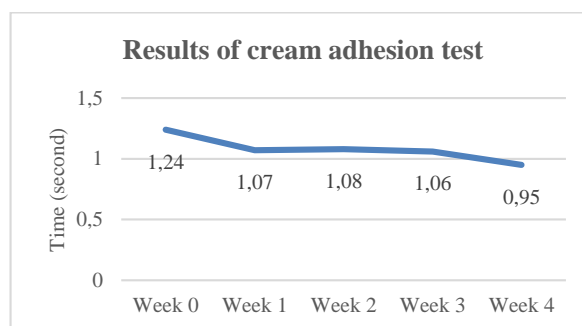


Figure 4. Results of cream adhesion test

CONCLUSION

Green tea dregs have activity against acne-causing *Cutibacterium acnes* bacteria. However, there was no significant difference between green tea brewing time for 2 and 5 minutes in obtaining catechin content in green tea dregs due to the narrow time difference. In addition, there is no significant difference between maceration with digestion and UAE in obtaining catechin content in green tea dregs. In the development of the spot cream dosage form, the cream had a stable characteristic during the accelerated stability test.

ACKNOWLEDGMENT

The authors are grateful to the Department of Pharmaceutical Biology and Pharmaceutics, Faculty of Pharmacy, Gadjah Mada University and staff who assisted in providing places and facilities during the research.

AUTHOR CONTRIBUTIONS

Conceptualization, M. A., P.; Methodology, M. A., P.; Validation, M. A., P.; Formal Analysis, M. A., C. L., J. M., P.; Investigation, M. A., C. L., J. M., P.; Resources, M. A., C. L., J. M., P.; Data Curation, M. A., P.; Writing - Original Draft, M. A., P.; Writing - Review & Editing, M. A., C. L., J. M., P.; Visualization, P.; Supervision, M. A., P.; Project Administration, P.; Funding Acquisition, M. A., P.

FUNDING STATEMENT

This research did not receive any specific grant from funding agencies in the public, commercial, or not for profit sectors.

CONFLICT OF INTEREST

The authors declared no conflict of interest.

REFERENCES

Arief, M. (2023). Pengaruh Metode Ekstraksi Ampas Teh Hijau (*Camellia sinensis* (L.) O. Kuntze) dan Aktivitasnya terhadap *Propionibacterium acnes* dalam Sediaan Krim Totol. *Skripsi*; Fakultas Farmasi UGM, Yogyakarta.

Aslam, I., Fleischer, A. & Feldman, S. (2015). Emerging Drugs for the Treatment of Acne. *Expert Opinion on Emerging Drugs*; 20; 91–101.

Chadajah, S. & Qaddafi, M. (2021). Optimalisasi Suhu dan Waktu Penyeduhan Daun Teh Hijau (*Camellia sinensis* L.) P+3 terhadap Kandungan Antioksidan Kafein, Katekin dan Tanin.

Bencoolen Journal of Pharmacy; 1; 59–65. doi: 10.33369/BJP.V1I1.15596.

- CSLI. (2012). *Methods for Dilution Antimicrobial Susceptibility Tests for Bacteria That Grows Aerobically* (9th ed.). Wayne: Clinical and Laboratory Standards Institute.
- CSLI. (2017). *Performance Standards for Antimicrobial Susceptibility Testing* (27th ed.). PA: Clinical and Laboratory Standards Institute.
- Karmilah, K., & Musdallipah, M. (2018). Formulasi Krim Antijerawat Ekstrak Ampas Teh Hijau (*Camellia sinensis* L.). *Jurnal Insan Farmasi Indonesia*; 1; 26–33.
- Khan, N. & Mukhtar, H. (2019). Tea Polyphenols in Promotion of Human Health. *Nutrients*; 11; 1-16. doi: 10.3390/NU11010039.
- Koch, W., Kukula-Koch, W., Komsta, L., Marzec, Z., Szwerc, W. & Gloniak, K. (2018). Green Tea Quality Evaluation Based on Its Catechins and Metals Composition in Combination with Chemometric Analysis. *Molecules: A Journal of Synthetic Chemistry and Natural Product Chemistry*; 23; 1-19. doi: 10.3390/MOLECULES23071689.
- Martins, I., Cortes, J., Munoz, J., Moreno, M., Ramos, M., Clemente-Ramos, J., Duran, A. & Ribas, J. (2011). Differential Activities of Three Families of Specific Beta(1,3)Glucan Synthase Inhibitors in Wild-Type and Resistant Strains of Fission Yeast. *The Journal of Biological Chemistry*; 286; 3484–3496. doi: 10.1074/JBC.M110.174300.
- McLaughlin, J., Watterson, S., Layton, A.M., Bjourson, A.J., Barnard, E. & McDowell, A. (2019). *Cutibacterium Acnes* and *Acne Vulgaris*: New Insights from the Integration of Population Genetic, Multi-Omic, Biochemical and Host-Microbe Studies. *Microorganisms*; 7; 1-29.
- Peluso, I. & Serafini, M. (2017). Antioxidants from Black and Green Tea: from Dietary Modulation of Oxidative Stress to Pharmacological Mechanisms. *British Journal of Pharmacology*; 174; 1195–1208. doi: 10.1111/BPH.13649.
- Rai, P., Poudyl, A., & Das, S. (2019). Pharmaceutical Creams and Their Use in Wound Healing: A Review. *Journal of Drug Delivery and Therapeutics*; 9; 907–912. doi: 10.22270/JDDT.V9I3-S.3042.
- Rohman, A. (2014). *Statistika dan Kemometrika Dasar dalam Analisis Farmasi*. Yogyakarta: Pustaka Pelajar.

- Saryanti, D., Setiawan, I. & Safitri, R. (2019). Optimasi Asam Stearat dan Tea pada Formula Sediaan Krim Ekstrak Kulit Pisang Kepok (*Musa paradisiaca* L.). *Jurnal Riset Kefarmasian Indonesia*; 1; 225–237. doi: 10.33759/JRKI.V1I3.44.
- Singleton, V. L., Orthofer, R., and Lamuela-Raventós, R. M. (1999). Analysis of Total Phenols and Other Oxidation Substrates and Antioxidants by Means of Folin-Ciocalteu Reagent. *Methods Enzymol*; 299; 152–178.
- Soetjipto H., Martono, Y. & Setiawan T. H. (2012). Potensi Pemanfaatan Ekstrak Ampas Teh Hijau Fraksi Etil Asetat Sebagai Agensia Antibakteri. Seminar Nasional Kimia dan Pendidikan Kimia IV, Universitas Negeri Yogyakarta.
- Tellu, F., Sunarto & Utami, E. (2019). Aktivitas Antibakteri Ekstrak Etil Asetat Kulit Buah Manggis (*Garcinia Mangostana* L.) terhadap *Propionibacterium acnes*. *Acta Pharmaciae Indonesia*; 7; 58–67. doi: 10.5281/ZENODO.3707175.
- Vuong, Q., Golding, J., Stathopoulos, C., Nguyen, M. & Roach, P. (2011). Optimizing Conditions for the Extraction of Catechins from Green Tea Using Hot Water. *Journal of Separation Science*; 34; 3099–3106. doi: 10.1002/JSSC.201000863.
- Yoon, J., Kwon, H., Min, S., Thiboutot, D., & Suh, D. (2013). Epigallocatechin-3-gallate Improves Acne in Humans by Modulating Intracellular Molecular Targets and Inhibiting *P. acnes*. *Journal of Investigative Dermatology*; 133; 429–440. doi: 10.1038/jid.2012.292.